University of Reading

Exploring the mechanistic rationale of plant-pollinator communication disruption by ozone

Degree of Doctor of Philosophy

School of Agriculture, Policy and Development

Matthew Kaan Alkan

January 2021

Declaration

I confirm that this is my own work and the use of all material from other sources has been properly and fully acknowledged.

Matthew Kaan Alkan

Abstract

In recent years pollinator populations have been declining worldwide, while concurrently tropospheric ozone concentrations have been increasing. It has been shown that plant-pollinator communication is partially mediated by volatile organic compound (VOC) based communication and this communication method is susceptible to perturbation as a result of ozone exposure. However, to date, no single study has investigated the individual mechanisms that cause the perturbation of VOC based communication in isolation of each other. This thesis tested and or modelled the effect of several of these mechanisms on the antennal electrophysiological responses of *Apis mellifera* in isolation, namely: i) VOC blend ratio alteration, ii) VOC degradation product formation, and iii) Secondary organic aerosol (SOA) formation.

Testing and/or modelling was conducted under two landscape-scale scenarios, applying a literature derived average foraging distance for *A. mellifera* of 400m when undertaking comparisons. Modelling demonstrated that, under these modelling parameters, alterations in VOC blend ratio as a result of ozone pollution may cause large changes in electrophysiological response for some compounds with minor changes for others. Several VOC degradation products were identified and elicited statistically significant electrophysiological antennal responses. While it was demonstrated that each of the VOCs tested was capable of forming SOA as a result of their reaction with ozone, exposure of *A. mellifera* antennae to SOA did not cause a statistically significant change in antennal electrophysiological response to two stimuli during or after SOA exposure. It was also observed that any effects of these mechanisms were likely to be greater under an ozone excess landscape scenario which may be akin to a small group of flowers in an open landscape. This work has not only shown the potential of differing mechanisms to contribute to VOC communication perturbation, thus allowing for the synthesis of further work to characterise the most at-risk plant-pollinator interactions but has also highlighted the effect that landscape may have on these interactions.

Dedication

This PhD has been a huge undertaking and has taken in excess of four years of my life. Lots has happened in this time and many people have come and gone so I cannot mention everyone here; however, I would like to especially thank my supervisors; Dr Robbie Girling, Dr John Mckendrick and Dr Christian Pfrang for their guidance and support in facilitating this project. I would also like to thank all of my fellow PhD students, all the administrative staff and all the technical staff I have met and worked with across the University of Reading and beyond and I wish them all the best in their future endeavours. Without the support of all of these people combined, and them consistently going the extra mile, I would not have been able to conquer the logistical and practical challenges that have faced me during the PhD.

On a personal note, I would like to thank Amanda, Jill, Harley and all the rest of my family for their understanding and guidance that without which, this thesis would have never been written. They have been there to reassure me and make me smile on tough days which has proved invaluable.

I would also like this thesis to serve as a reminder that, if you work hard enough, you can do anything regardless of your background and never doubt yourself. You CAN do this.

Acknowledgements

I would like to gratefully acknowledge funding provided by NERC in the form of a SCENARIO DTP Studentship (Award Ref: NE/L002566/1).

Contents

Chapter 1: General introduction

1.1 Pollination as an ecosystem service

Humans are dependent upon the environment in which they live to be able to sustain, grow and reproduce. The benefits the environment provides have been described as a set of "services" provided by the ecosystem to which a monetary benefit may be attributed. These are commonly termed "ecosystem services", generally defined as the benefits that nature provides to humans; however, several definitions have been coined by various authors (for a review of definitions see Nahlik et al. (2012)). Four subcategories of ecosystem service were defined by the millennium ecosystem assessment (Sarukhán et al. 2005) including; provisioning services (the products obtained from ecosystems such as food and fresh water), regulatory services (climate regulation, pollination and air quality regulation), supporting services (water cycling, nutrient cycling, soil formation) and cultural services (recreation and heritage).

An extensively studied example of an ecosystem service is pollination. Pollination can take place as a result of wind pollination or pollination by an organism, for example by insects or mammals (Willmer 2011). A plant's reliance on wind pollination versus insect pollination can vary significantly between plant species and even between two species of the same genus. This has been demonstrated by Peeters and Totland (1999) who showed that *Salix herbacea* L. produces a higher seed set under wind pollination conditions (wind pollination contributes to 57% of total seed set), while the closely related *Salix myrsinites* L. produces a higher seed set under organism pollination conditions (organism pollination contributes to 98% of total seed set).

Seventy-eight percent of all crop species used by humans as a food source rely upon insect pollination and 87.5% of global flowering plants also rely upon insect and other animal pollination (Ollerton et al. 2011). Pollination has also been shown to increase oilseed rape (*Brassica napus* L.) seed yield, weight and thus market value which indicates the key economic role that insect pollination can play (Bommarco et al. 2012). Insect pollination contributes significantly to regional economies, for example, it was estimated to contribute $358 million every year to the south African western cape deciduous fruit industry (Allsopp et al. 2008) while contributing in the region of $127-$152 billion to the global economy (Bauer and Sue Wing 2016).

1.2 Declines in pollinator populations

Pollinators such as the bumblebee (*Bombus terrestris* L.) have been declining in numbers over the last century with a 59% reduction in wild colonies reported in north America in 2005 versus 1947 (Potts et al. 2010). Managed colonies of *Apis mellifera*, L. have also shown an increase in the prevalence of colony collapse in recent years, thus placing a greater economic cost on colony owners

to maintain numbers (Kluser and Peduzzi 2007). Further to this, up to 50% of all wild bee species in several European countries are listed as critically endangered (Nieto et al. 2014) and over the last 20 years, a 71% decrease in butterfly species has been observed (Kluser and Peduzzi 2007).

These declines come at a time when pollination services are required more than ever with a threefold increase in demand for insect pollination of crops since 1961 (Aizen and Harder 2009). If this demand is not met, then it is likely that crop shortages may occur (Gallai et al. 2009) and, although wind-pollinated crops can provide sufficient calorific intake, human health may suffer as a result of decreases in intake of micronutrients such as vitamins and antioxidants, which are provided by insect-pollinated crops (Eilers et al. 2011).

1.2.1 Causes of pollinator population declines

Many theories have been proposed to explain the declines in global pollinator populations including; changes in land use and agricultural practices (such as the use of pesticides), the introduction of invasive alien species to the ecosystem and climate change (Kluser and Peduzzi 2007; Potts et al. 2010; Jepsen et al. 2015).

Intensification of agriculture has facilitated feeding of the world's ever-expanding population, but this has caused several changes in the way that land is managed (Jepsen et al. 2015) with a move towards; increases in monoculture, fragmentation of habitats and high use of agrochemicals (Steffan-Dewenter and Westphal 2008). Habitat fragmentation has been shown to have the greatest impact on higher trophic levels and food/habitat specialists (Tscharntke and Brandl 2004) and thus, has contributed to decreases in the diversity and abundance of pollinators. These decreases in pollinator diversity and abundance also have negative impacts on the reproductive success of plants, thus decreasing the total number of nectar and pollen sources available to pollinators (Kohler et al. 2008). These reductions in the number of food sources as a result of pollinator declines cause further reductions to pollinator numbers, thus creating a downward spiral of pollinator numbers and plant diversity.

The adoption of monoculture has also been detrimental to pollinators in other ways. The lack of diversity of nectar and pollen not only reduces the nutritional content ingested by pollinators (Alaux et al. 2010), thus making them more susceptible to both pesticide and pathogen stressors (Dolezal and Toth 2018), but also makes the supply of nectar and pollen more susceptible to collapse as a result of stressors on the nectar and pollen producers (Baude et al. 2016).

The introduction of alien species may also lead to pollinator declines by either directly placing pressure on native species for limited resources or as a result of predating native species. For example, the western yellow jacket wasp (*Vespula pensylvanica* Saussure) which was introduced to Hawaii has predated native bees as well as dominated and defended nectar resources (Hanna et al.

2013). This has increased pressure on all pollinators but particularly on Hawaii's native bee species as they tend to be specialists (Wilson and Holway 2010).

Alien species are also capable of introducing foreign pathogens and parasites, to which local species may not show resistance. The parasitic mite *Varroa destructor* Anderson & Trueman is a well-known example of an alien species that has spread across the world (Schroeder and Martin 2012). Initially confined to afflicting the Asiatic honeybee (*Apis cerana* J. Fabr.), it has spread to other species, such as the western honeybee (*A. mellifera*). Western honeybees are farmed commercially all over the world and global trade of hives has facilitated the spread of the varroa mite (Brettell and Martin 2017). By itself, the varroa mite requires large numbers to kill a mature honeybee colony; however, the varroa mite can act as a vector for the deformed wing virus (DWV) pathogen which if transmitted can result in the death of a colony (Carreck et al. 2010).

It has also been shown that DWV has been able to act unchallenged as a result of the use of insecticides such as neonicotinoids which have been shown to act as immunosuppressants in honeybees (Di Prisco et al. 2013). It has also been shown that, upon extended consumption of food laced with several commonly used neonicotinoids at field-relevant doses, *A. mellifera* has been shown to exhibit reduced motor function (Williamson et al. 2014) while bumblebee (*B. terrestris*) colonies showed an 85% reduction in queen production (Whitehorn et al. 2012). Kessler et al. (2015) also showed that both *A. mellifera* and *B. terrestris* show a preference for food laced with neonicotinoids at nectar relevant concentrations, which is likely to compound the detrimental effects of neonicotinoids.

From the evidence presented, it is clear that no one factor is likely to be solely responsible for the decline in pollinator numbers and instead many factors are working in combination to cause the observed decline. The interlinking of factors has been explored in depth by several authors (Potts et al. 2010; Vanbergen et al. 2013; Goulson et al. 2015) and illustrates the sheer interconnectivity of these stressors and how they must be understood in unison and not in isolation.

1.2.2 Pollinator population declines – climate change

Climate change is hypothesised to be the result of increased levels of air pollutants, such as increased emission of carbon dioxide (CO_2) as a result of anthropogenic activities such as the burning of fossil fuels and increased emissions of methane as a result of landfill and beef production (Gifford et al. 2011). Climate change has been hypothesised to be exacerbating the effects of stressors upon bee populations (Potts et al. 2010).

Changes to the earth's climatic cycle are altering seasonal weather conditions (Millar et al. 2017), thus the flowering periods of plants may change (Wolkovich et al. 2012) potentially causing asynchrony between flowering periods and pollinator life cycles (Hegland et al. 2009). The potential

change in flower diversity and flowering time may affect food resource (pollen and nectar) availability for pollinators, which could result in declines in pollinator populations. This would further reduce the rate of pollination, thus reducing the viability of plants that require pollination and thus food resource availability, creating a negative feedback loop. As a result of these hypothesised changes in plant abundancies, it has been hypothesised that specialist pollinators may suffer the greatest effects from climate change as they are unable to alter their host plants in reaction to these changes (Carvalheiro et al. 2013).

Increased temperatures as a result of climate change have also been hypothesised to be causing species migration towards colder climates (Loarie et al. 2009; Kerr et al. 2015). This disproportionately affects species diversity because, species that can migrate and maintain optimum climatic conditions may thrive, while species that cannot rapidly migrate may suffer as a result of changes in climatic conditions (Thomas et al. 2006). This migration of species is likely to introduce alien species to environments, potentially further exacerbating the stresses on resident species by increasing competition for food resources, increasing predation of native species by alien species and introducing pathogens to which native species may not be able to defend against (Schweiger et al. 2010; Vanbergen et al. 2018).

1.3 Air pollution

1.3.1 Structure of the atmosphere

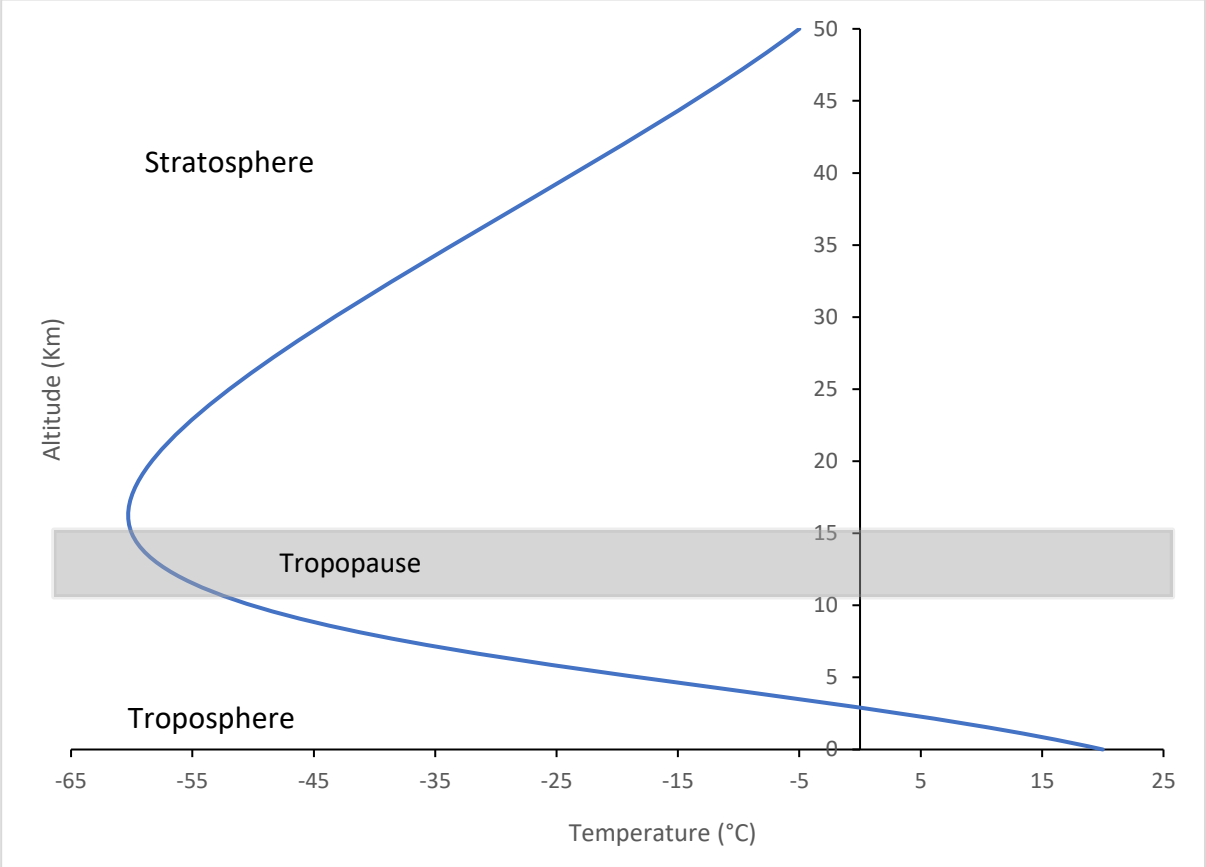

Figure 1.1 – Cross-section of earth's atmosphere contrasting altitude and mean temperature. Based upon Holloway and Wayne (2010).

The atmosphere consists of multiple layers, each with distinct attributes (Figure 1.1). The troposphere extends from sea level to ca.10Km, depending on latitude, and sees a gradual decrease in temperature as altitude is gained until the tropopause is reached. The tropopause is a cold layer of the atmosphere and as such molecular transport through the tropopause is very slow and it; therefore, acts as a permeable transport barrier between the troposphere and stratosphere. As altitude continues to increase the stratosphere is reached and temperature increases as a result of the absorption of ultraviolet radiation by stratospheric ozone. This existence of the tropopause means chemical processes in the stratosphere and troposphere are usually considered to be discrete entities (Holloway and Wayne 2010) and as such the work discussed in this thesis will focus on the troposphere.

1.3.2 Atmospheric pollution and its sources

The definition of a pollutant is disputed; however, it may be broadly classed as any chemical species emitted that causes undesirable effects on the environment in either its entirety or as a result of the amount of the chemical emitted (United nations 1997). Modelling the impact of atmospheric

pollutants on the environment is complex because a range of factors need to be considered, such as the rates of emission and rates of deposition of the original pollutant, as well as the potential for the pollutant to undergo atmospheric chemical reactions and form secondary pollutants which themselves will have differing effects on the environment.

Biogenic sources of air pollution are often caused by serious environmental events such as volcanic eruptions or wildfires releasing pollutants such as sulphur dioxide (SO_2) and soot into both the troposphere as well as the stratosphere (Hobbs 2000). Further to this, biological volatile organic compound (VOC) emissions, such as emission of α-pinene from pine trees, account for a large proportion of atmospheric pollutants, with biological emission totalling between 700 and 1000 Gigatons annually (Laothawornkitkul et al. 2009) and anthropogenic emissions totalling 0.11 Gigatons (Piccot et al. 1992).

Anthropogenic air pollution is caused by several activities such as manufacturing, intensive agriculture and the burning of fossil fuels and, while globally the quantities released may be lower than those of biogenic emissions (Guenther et al. 1995), locally anthropogenic emissions may be greater than biogenic emissions (Gentner et al. 2014). Air pollution as a result of land-use change to intensive agriculture has led to increased emissions, such as ammonia (NH_3), nitrous oxides (NO_X) and particulate matter (PM) (Aneja et al. 2008) with changes in the types and levels of VOCs emitted (Lathière et al. 2006). Fossil fuel use produces several types of air pollutants such as PM, CO_2, SO_2 as well as NO_X, which is a term used to describe both nitric oxide (NO) and nitrogen dioxide (NO_2). As with many atmospheric pollutants, NO_X may be emitted from both anthropogenic sources such as fossil fuel combustion as well as biogenic sources such as wildfires, soil emissions and as a result of the interconversion of other pollutants in the atmosphere (Holloway and Wayne 2010).

1.3.3 Tropospheric oxidants

NO_x emissions are a key source of tropospheric oxidants and once in the troposphere, may be interconverted in combination with other atmospheric species into atmospheric oxidants (Hobbs 2000). The three main atmospheric oxidants in the troposphere in order of reactivity from highest to lowest are hydroxyl radicals (OH), nitrate radicals (NO_3) and ozone (O_3) (Holloway and Wayne 2010). None of these species are directly emitted to the atmosphere but are formed by the reaction of directly emitted pollutants, such as nitrogen oxides (NO_x) within the atmosphere. The primary reaction pathways by which these oxidants form in the troposphere are as follows.

Tropospheric ozone is produced by the reaction of molecular oxygen radicals, produced by the photodissociation of nitrogen dioxide (NO_2), with oxygen (O_2). Production is strictly limited to the day due to its dependence on the photodissociation of nitrogen dioxide (Equation 1.1).

$$\dot{N}O_2 + h\nu \longrightarrow O^{\cdot}(^3P) + \dot{N}O$$

$$O^{\cdot}(^3P) + O_2 + M \longrightarrow O_3 + M$$

Equation 1.1 – Production of tropospheric ozone from NO_2, M = Third body to remove excess energy, normally N_2 or O_2, ^3P = electron configuration in an excited state. (Holloway and Wayne 2010)

OH radicals are primarily produced in the troposphere according to equation 1.2 and rely upon sunlight to enable the formation of the excited $O(^1D)$ oxygen which has sufficient energy to react with water**.** (Stone et al. 2012). The rate of hydroxyl (OH) radical formation is stifled by the sparsity of water in comparison to O_2 or N_2 and thus, most $O(^1D)$ oxygen is quenched before producing hydroxyl (OH) radicals.

$$O_3 + h\nu \longrightarrow O^{\cdot}(^1D) + O_2$$

$$O^{\cdot}(^1D) + H_2O \longrightarrow 2\dot{O}H$$

Equation 1.2 – Reaction for the photocatalytic production of OH radicals in the troposphere, ^1D = electron configuration in an excited state. (Holloway and Wayne 2010)

NO_3 radicals are formed by the relatively slow reaction (Monks 2005) of NO_2 with O_3 (Equation 1.3).

$$\dot{N}O_2 + O_3 \longrightarrow \dot{N}O_3 + O_2$$

Equation 1.3 – Production of nitrate radicals (Holloway and Wayne 2010; Dillon and Crowley 2018)

However, nitrate radical (NO_3) is photolabile and thus, during the day, is photolyzed (Equation 1.4) back to nitrogen oxide (NO) and nitrogen dioxide (NO_2).

$$\dot{N}O_3 + h\nu \longrightarrow \dot{N}O_2 + O^{\cdot}(^3P)$$

$$\dot{N}O_3 + h\nu \longrightarrow \dot{N}O + O_2$$

Equation 1.4 – Photolysis of NO_3, ^3P = electron configuration in an excited state. (Holloway and Wayne 2010; Dillon and Crowley 2018).

1.3.4 Characteristics of key tropospheric oxidants

The three primary atmospheric oxidants have different properties and abundancies in the troposphere which influences the reaction characteristics of these oxidants (Table 1.1).

Table 1.1 – Comparison of characteristic reaction properties of ozone (O_3), nitrate (NO_3) and hydroxyl radicals (OH).

	Ozone (O_3)	Nitrate (NO_3)	Hydroxyl (OH)
Order of rate constant (cm^3 $molecule^{-1}$ s^{-1}) [a]	$X10^{-17}$	$X10^{-13}$	$X10^{-10}$
General tropospheric concentrations [b]	10-100ppb	10-0.1 ppt	0.1-0.001ppt
Reaction mechanism	Addition only	Addition/Abstraction	Addition/Abstraction
Diurnal peak	Day	Night	Day

[a] Order of rate constants determined for reaction with Z-3-hexenol (Atkinson et al. 1995)
[b] Typical concentrations taken from modelling by (Bey et al. 1997)

OH shows the fastest rate of reaction while ozone shows the slowest rate of reaction. This is reflected in the general tropospheric concentrations observed, with OH having the lowest concentration, because it is consumed rapidly after production, while ozone has the highest concentration, taking the longest time to be consumed after production and thus, is persistent throughout the diurnal cycle. The diurnal variation of the three oxidants illustrates the reliance of OH and ozone on light to drive their formation reactions and the photolabile nature of NO_3.

OH and NO_3 radicals both undergo two types of chemical reaction pathways namely addition to a double bond and hydrogen abstraction, while ozone is only able to undertake the addition mechanism (Figure 1.2). Abstraction is generally slower than the addition reaction (Gao et al. 2014).

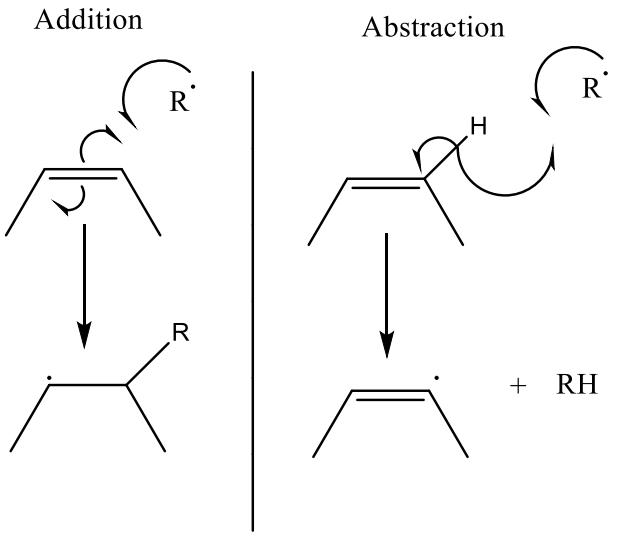

Figure 1.2 – Generalised abstraction and addition reaction mechanisms (Gao et al. 2014)(Atkinson et al. 2007)

The reaction of atmospheric oxidants with molecules consumes the original molecule, thus creating new and more highly oxidised molecules. Both the destruction of the original molecule as well as the creation of the two new molecules is likely to impact the usual biological functioning of the original molecule.

1.3.5 Trends in tropospheric ozone concentration

Ozone is not directly emitted to the troposphere but is produced as a result of the interconversion of directly emitted precursors (such as NO_x, see Equation 1.1) and thus, trends in NO_x concentrations give rationale to trends in ozone concentrations. NO_X emissions in the UK have shown a steady decrease from over 3 million tonnes of NO_x in 1990 to 823,000 tonnes in 2018 through the introduction of various policy measures intended to curb emissions from farming, transport and manufacturing (Department for rural affairs 2018). However, emissions of NO_x in developing nations have shown increases in previous decades thus, giving a roughly constant global level of NO_x emissions despite regional declines (Miyazaki et al. 2017).

Due to the net steady global emission of NO_x, concentrations of ozone have been forecast to increase over the coming century with peak summer ozone concentration being ca.40ppb over Eurasia in the early 2000's rising to peaks of ca.70ppb by 2100 (Jaffe and Ray 2007; Sitch et al. 2007). However, as a result of changes in weather patterns due to climate change, ozone transport within the troposphere and from the stratosphere to the troposphere may be altered causing marked decreases in ozone in some regions and conversely marked increases in others (Akritidis et al. 2019; Lu et al. 2019). These trends are therefore uneven with some regions being more affected by tropospheric ozone despite local and national changes to combat emissions, thus highlighting the need to explore ways to directly mitigate the impacts of ozone.

1.3.6 Effects of tropospheric ozone on human health and the environment

Research on the health effects of tropospheric ozone on humans is abundant. For example, it has been shown to directly affect human health by causing symptoms such as decreased lung function and eye irritation (Kampa and Castanas 2008). Lung function is decreased because ozone directly attacks lung lining fluid thus, reacting with proteins in the fluid and producing secondary oxidation products, which have the potential to be absorbed into the body and cause cellular stress reactions (Kelly 2003). The effects of ozone exposure have been shown to be most prevalent in females and older individuals (Bell et al. 2014) with deaths attributable to ozone predicted to increase over the coming century as tropospheric ozone levels rise (Silva et al. 2017).

Human health may also be indirectly affected by increases in tropospheric ozone as a result of decreases in crop yield and quality reducing the nutritional value of the average diet (Gimeno et al. 2004; Black et al. 2007). Blanco-Ward et al. (2021) showed that ozone causes reductions in grapevine (*Vitis vinifera*, L.) yield and polyphenol content by 20-31% and 15-23% respectively while Wilkinson et al. (2012) showed that wheat crop yield may be reduced by up to 15%. Wilkinson *et al.* (2012) hypothesised that reductions in crop yield and quality may be a result of leaf injury, stomatal closure, and diversion of resources from crop growth to antioxidant synthesis (Loreto and Velikova 2001; Bindi et al. 2002; Black et al. 2007; Li et al. 2021).

The effects on the broader environment, and thus human health may also be profound. It is hypothesised that increases in tropospheric ozone favour species that can withstand ozone stress, thus decreasing species richness and exacerbating the effect of pests or disease both affecting species diversity and food availability (Martínez-Ghersa et al. 2017). The effect of increased ozone on a plant's ability to respond to herbivores, and thus its overall fitness, has been evidenced by several authors. Duque et al. (2019) showed that, as a result of prolonged exposures to high (120ppb) ozone concentrations, cabbage moth (*Pieris brassicae* L.) showed a 49% reduction in oviposition (egg-laying) but an increased egg survival rate on wild mustard plants (*Sinapis arvensis* L.). This is also concurrent with the observation that alder leaf beetle larvae (*Agelastica coerulea* L.) that were fed with Japanese white birch leaves (*Betula platyphylla* Sukachev) that had been exposed to increased ozone, showed an increased rate of feeding and shorter life cycles (Vuorinen et al. 2004). Ozone exposure has also been shown to accelerate flowering in wild mustard (*Sinapis arvensis*) which potentially causes desynchronization between flowering events and pollinator activity (Duque et al. 2021).

It is clear that the mechanisms by which increases in tropospheric ozone concentration may affect human health directly and the environment, as well as the interactions between the environment and human health, are complex. Further research is emerging to suggest that this pollutant may have further negative impacts on the environment and thus human health by altering the VOC chemical cues that many organisms rely upon for communication.

1.4 VOC communication in the environment

Information exchange is key to enabling and enhancing interactions between organisms and has been shown to be mediated by several different senses, often working in unison, such as smell, vision and hearing (Fischer et al. 2001; Leonard and Masek 2014).

Smell is mediated by chemical release and detection and is sometimes termed VOC communication (Wright and Schiestl 2009). Any chemical that mediates these interactions may be described as a semiochemical and can take a wide variety of chemical structures (Figure 1.3). For example, female lepidopteran sex pheromones (such as (Z)-9-Tetradecenyl acetate) are commonly a long linear carbon chain with primary alcohol, aldehyde or acetate functionality often showing low vapour pressures and thus, low levels of volatility (Birch and Haynes 1982; Pichersky et al. 2006; De Bruyne and Baker 2008). In contrast, the top five most common floral VOCs (such as myrcene, Table 1.2) show smaller chain or ring-like molecules, often showing a high level of volatility (Dudareva et al. 2004; Knudsen et al. 2006).

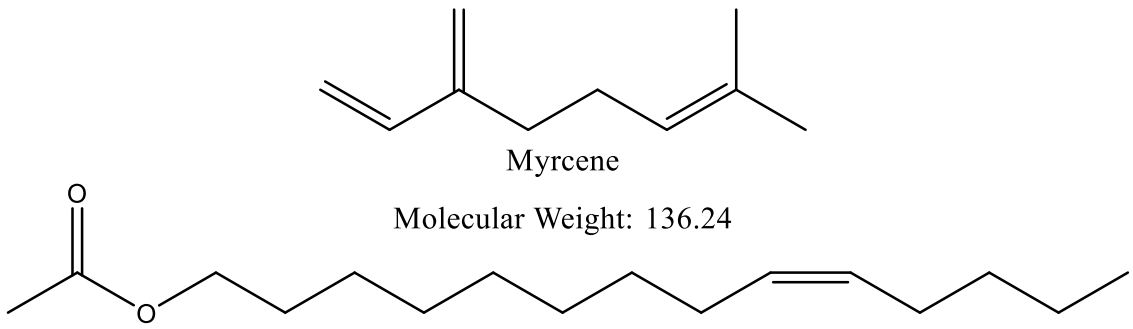

Figure 1.3 – Comparison of the structures of the floral VOC Myrcene and the moth pheromone component Z-tetradecenyl acetate (Z9-14:Ac)

Table 1.2- Comparison of vapour pressure in torr of moth pheromones with the 5 most common floral VOC's (Knudsen et al. 2006). [a] Olsson et al. (1983), [b](NCBI), [c](RSC chemspider).

Moth pheromones		Common floral VOCs	
Compound	Vapour pressure (torr)	Compound	Vapour pressure (Torr)
10:Ac	0.0424[a]	Limonene	1.55[b]
Z3-10:Ac	0.0507[a]	(E)-Ocimene	1.6[c]
Z5-10:Ac	0.0518[a]	Myrcene	2.09[b]
Z7-12:Ac	0.0067[a]	Linalool	0.16[b]
Z9-14:Ac	0.0012[a]	α-Pinene	4.75[b]

Nomenclature has been devised for semiochemicals to classify them into subcategories as a result of their function within the environment.

1.4.1 Intraspecific semiochemicals

Intraspecific semiochemicals may be generally defined as "substances which are secreted to the outside world by an individual and received by a second individual of the same species in which they release a specific reaction, for example, a definite behavioural or developmental process"(Sbarbati and Osculati 2006). By this definition, intraspecific semiochemicals may also be termed pheromones. The term pheromone is well known but it is often considered that all pheromones function as sexual attractants when in fact there are several subclasses of pheromones such as aggregation pheromones, sex pheromones and trail marking pheromones.

1.4.1.1 Sex pheromone

These pheromones mediate behaviour to increase the chance of mating. Within this, sex pheromones can be further sub-categorised into mate location attractant pheromones which elicit long-range searching behaviours, and courtship pheromones, which elicit courtship behaviours at short ranges (Borges et al. 1987). An example of compounds acting as sex pheromones are (Z)-7-Dodecen-1-yl acetate and (Z)-7-dodecen-1-ol which have been shown to be a two-component sex pheromone for Silver Y moth (*Autographa gamma*, L.) (Tóth et al. 1983).

1.4.1.2 Aggregation pheromone

These pheromones are released to alter the density of individuals within the vicinity of the pheromone source. The use of 2-methyl-3-buten-2-ol by bark beetle of Eurasia (*Ips typographus* L.) is an example of using aggregation pheromones to not only

launch an attack on host trees but also to regulate conspecific densities (Schlyter et al. 1987).

1.4.1.3 Trail marking pheromone

These pheromones allow organisms to easily follow each other, often to a source of resources. An example of this is 4-methlpyrolle-2-carboxylate which has been identified as a component of the trail marking pheromone used by the Texas leaf-cutting ant (*Atta texana* Buckley) (Tumlinson et al. 1972). It is predicted to have a low volatility (RSC ChemSpider) and thus, be adapted to be persistent in the environment.

1.4.1.4 Alarm pheromone

These pheromones initiate defensive responses of other individuals in the vicinity of the pheromone source. For example, 2-heptanone has been identified as an alarm pheromone of the Texas leaf-cutting ant (*Atta texana*) (Andryszak et al. 1990) and is predicted to have a high volatility (RSC ChemSpider) and thus be adapted to rapid vaporisation and dissemination to conspecifics in the locality of its emission.

Intraspecific communication using pheromones is key to the efficient running of large colonies of social insects. Slessor et al. (2005) review several uses of pheromones within an *A. mellifera* colony; isopentyl acetate is used as a defence pheromone within the colony to elicit stinging actions, the nasonov pheromone (a mixture of several compounds) acts as an aggregation pheromone to initiate swarming behaviour and retinue pheromone acts as a sex pheromone attracting drones to the queen during her mating flight. Similarly, pheromones are used in ant colonies with functions such as trail marking and alarm (Jackson and Morgan 1993).

Intraspecific communication of plants has been documented to take place either via VOC emission or via common mycorrhizal networks. Zakir et al. (2013) found that upon exposure to VOCs produced by herbivory of cotton leaf worm (*Spodoptera littoralis* Boisduval) on cotton plants (*Gossypium hirsutum* L.), undamaged conspecifics became less attractive to oviposition (egg-laying) by cotton leaf worm. Song et al. (2010) found that on infection of tomato plant (*Lycopersicon esculentum* L.) with *Alternaria solani*, conspecifics connected via the common mycorrhizal network had a greater expression of defence enzymes.

1.4.2 Interspecific semiochemicals

If VOCs are used to facilitate communication between two different species, they are termed allelochemicals and can be classified into three categories.

1.4.2.1 Kairomone

The allelochemical is advantageous to the odour receiver and disadvantageous to the emitter (Ruther et al. 2002). For example, a herbivore such as oak buprestid (*Agrilus biguttatus* J.Fabr.) utilising vegetative VOCs from English oak (*Quercus robur* L.) to find host plants to feed on (Vuts et al. 2016).

1.4.2.2 Allomone

The allelochemical is disadvantageous for the odour receiver and is advantageous to the emitter (Dicke and Sabelis 1988). For example, tobacco plants (*Nicotiana tabacum* L.) release VOCs that are highly repellent to female moths which would normally oviposit upon the tobacco and the larvae would subsequently eat its leaves (*Heliothis virescens* J. Fabr.) (De Moraes et al. 2001).

1.4.2.3 Synomone

The allelochemical benefits both the producer and receiver (Dicke and Sabelis 1988). For example, the utilisation of floral VOCs by a pollinator such as the Silver Y moth (*Autographa gamma* L.) to pollinate a plant such as a butterfly orchid (*Platanthera bifolia* L.) (Plepys et al. 2002).

Insect-plant signalling provides a model for several examples of interspecific signalling. Vegetatively released VOCs can function in a kairomonal context as it has been shown by several authors that pests use vegetative VOCs to successfully locate plants for feeding as well as laying of eggs (oviposition) that will hatch and feed (Kessler and Baldwin 2001; Bruce et al. 2005). Vegetative VOCs may also function in an allomonal context as it has been shown that VOCs produced as a result of herbivory may either repel conspecific herbivores or decrease the rate of oviposition upon infested plants (Ružička 1997; Mutyambai et al. 2016). Vegetative VOC's may also function in a synomonal context, where parasitoids may utilise vegetative VOCs often produced as a result of herbivory, to locate hosts to oviposit in and thus benefit both the plant and the parasitoid (Holopainen and Gershenzon 2010) which is exemplified by the attraction of the parasitoid *Exorista japonica* L. to herbivore-induced VOCs from corn (*Zea mays*, L.) plants (Ichiki et al. 2008).

Synomonal use of floral VOCs is key to pollination, floral VOCs are released by flowers and detected by pollinators (Jürgens et al. 2014). VOCs are used in conjunction with visual cues such as colour, shape and size to determine the location of plants (Schiestl 2015a) and it has been shown by Raguso and Willis (2002) that, while tobacco hornworm moth (*Manduca sexta* L.) showed attraction to both

the visual and olfactory components of evening primrose (*Oenothera neomexicana*, L.) only in unison was proboscis extension observed. An increase in attraction of German wasp (*Vespula germanica* J.Fabr.) to common ivy (Hedera helix, *L.*) was also seen when visual and olfactory components were presented in unison (Lukas et al. 2020). However, that the interplay between these cues is poorly understood and visual cues are only likely to be effective at short ranges (Burger et al. 2010).

Plants have developed the ability to alter the timing, composition and emission rate of VOCs so as to elicit visitation by the most effective pollinators which further shows the importance of VOC emissions for pollination. This has been demonstrated by Raguso (2008) using a white petunia (*Petunia axillaris* Britton, Sterns & Poggen*)*-Tobacco hornworm (*M. sexta* L.*)* system, showing that the composition of the emissions from *P. axillaris* exhibited diurnal variation, but that the night time emissions were more attractive to the night-active *M. sexta* moth. It has also been shown that plants can regulate levels of pollination by altering the VOCs they emit once pollination has occurred (Proffit et al. 2018).

1.4.3 VOC blends

VOCs are rarely emitted in isolation and are usually emitted in unique combinations and ratios of chemicals which are often referred to as blends. Blends allow receivers to both locate resources as well as transfer encoded information from resource to receiver (Wright and Schiestl 2009; Girling et al. 2013). Blends are unique to each emission source with differing compositions and thus, are used for resource discrimination. Bertrand et al. (2006) showed that the blend emitted by the related flowers *Brunfelsia australis*, L. and *Brunfelsia pauciflora* Cham. & Schldtl. are both quantitatively and qualitatively different even though they have similar physical characteristics. Further to this, it has been shown that the parasitoid wasp *Cardiochiles nigriceps* Viereck can use differences in herbivore induced VOCs to discriminate between infestations of its host *Heliothis virescens* J. Fabr. and non-host *Helicoverpa zea* Boddie. caterpillars on several different crops such as tobacco, maize and cotton (De Moraes et al. 1998).

The importance of blend composition has been evidenced by Webster et al. (2010) who found that black bean aphid, *Aphis fabae*, Scopoli , produced different behavioural responses to physiologically relevant doses of VOCs emitted by its host, *Vicia faba*, L., when presented in isolation as opposed to presentation in unison. The importance of blend ratio has been evidence by Riffell et al. (2014) who used a sacred datura plant (*Datura wrightii* Regel) and Tobacco hornworm moth (*M. sexta*) system and noted that by increasing the concentration of benzaldehyde in the datura blend (through the addition of benzaldehyde as a background VOC to the full datura flower odour blend), odour tracking ability was significantly reduced even though blend composition was constant.

There is much debate as to the underlying mechanisms that allow resource discrimination using VOCs to take place; however, for the specific case of plant-insect interactions two major hypotheses have been suggested as summarised by Bruce et al. (2005): 1) blends contain certain VOCs that are not produced by unrelated species, thus allowing for species discrimination, and 2) blends are formed of ubiquitous VOCs and species discrimination is as a result of different combinations and ratios of these compound.

Olfactory systems detect blends by having antennae covered in sensilla which respond to VOC stimuli and send nerve impulses for processing in the brain (for further information see section 2.5.6). Thus, on a physiological level, it may be suggested that if discrimination took place solely as a result of species-specific VOCs, antennae would only contain VOC specific sensilla. Further to this, it may also be hypothesised that specialists would only require very few types of VOC specific sensilla while generalists would require multiple and thus, given the finite space on an antenna, generalists may show lower electrophysiological responses than specialists to equivalent stimuli.

The presence of species-specific sensilla has been noted by (Nottingham et al. 1991) who found isothiocyanate tuned sensilla (almost exclusively produced by *Brassicae* species (Knudsen et al. 2006)) on the antennae of *Brevicoryne brassicae* L. The presence of generalist sensilla has been evidence by Raguso and Light (1998) who showed that *Hyles lineata* J. Fabr. (generalist) and *Sphinx perelegans* Edwards (specialist) show comparable electroantennography (EAG) responses to floral VOCs derived from fairy fan (*Clarkia breweri* Greene) flowers.

The theory that generalist sensilla are the dominant type of sensilla is also evidenced by the ability of blend receivers to adapt to changes in VOC blend composition. Blend composition has been shown to subtly change depending on environmental factors affecting the emitter such as weather, drought conditions, flowering period, time of day and sunlight level (Dudareva et al. 2004). Insects plasticity to these changes has been demonstrated in many species for example; the grapevine moth (*Lobesia botrana* Denis & Schiffermuller) was shown to respond to an altered synthetic lure (Tasin et al. 2007) and Mas et al. (2020) who used honey bee (*A. mellifera*) to show that insects may change their preference for VOCs as a result of learning, thus, allowing them to adapt to the most abundant food source.

The presence of isothiocyanate detectors supports the theory that unique compounds play a role in resource discrimination; however, the lack of difference in olfactory system responses between specialist and generalist herbivores suggests that the blend ratio of ubiquitous VOCs is important. This meeting point of both theories is demonstrated by (Carey et al. 2010) who demonstrated that both generalist, as well as specialist sensilla, are present on *Anopheles gambiae* Giles antenna.

The ability to show plasticity and to even learn and associate new odours points to not only the presence of generalist sensilla but also that much of the blend processing must take place beyond the sensilla in the central nervous system (CNS) of the insect. Generalisation, where a learnt behaviour is applied to a different but sufficiently similar stimulus, is an example of how insects achieve plasticity when utilising VOC blends (Shepard 1987). Such generalisation of blend components seems to be non-linear, for example if you consider two odours (A and B), the generalisation from odour A to B not necessarily being as strong as from odour B to A (Guerrieri et al. 2005). The reasons for this is not currently known; however, it may be as a result of "overshadowing" of the original odour where, when learning floral odours, one VOC component of the floral blend is often learnt better than the others (Getz and Smith 1987; Smith 1998). Overshadowing has been shown to be apparent experimentally by Tasin et al. (2007) who showed grapevine moth (*L. botrana*) responded similarly to a blend of three components formed from a broader ten component blend.

Behavioural experiments have shown that generalisation seems to be more prominent at lower concentrations as Wright et al. (2005) showed that *A. mellifera* displayed a greater ability to discriminate between four snapdragon (*Antirrhinum majus* L.) cultivars as the number of flowers increased.

Behavioural responses to blend concentration have also been shown to be both plastic and also important for resource discrimination. Ditzen et al. (2003) showed that the concentration of VOC blends are important with bees selecting the learnt concentration of stimuli from an array of higher and lower concentrations. However, generalisation of concentration (and thus plasticity) has also been shown. Oriental fruit moth (*Cydia molesta* Busck) showed no change in attraction relative to a synthetic VOC blend derived from the leaves of its peach tree (*Prunus persica* L.) host plant up to a 100x increase in benzonitrile concentration (Najar-Rodriguez et al. 2010). This shows that the level of behavioural plasticity with regards to concentration is species specific.

Behavioural responses to VOC blends are also plastic with regard to the physiological state of the receiver organism (age, mating status or feeding state) (Gadenne et al. 2016). Saveer et al. (2012) showed that, unmated cotton leafworm (*Spodoptera littoralis*, Boisduval) females were strongly attracted to lilac flowers (*Syringa vulgaris*, L.). Post mating, attraction to floral odour was abolished and attraction was instead seen to the larval host plant cotton (*Gossypium hirsutum*, L.). Edgecomb et al. (1994) showed that fruit fly (*Drosophila immigrans* Sturtevant) increased its feeding behaviour as a result of 72 hours of starvation.

1.4.4 VOC plumes

It is important to not only understand the characteristics of a VOC emission but also how it moves within the environment post emission. On emission from a source, VOCs are carried by both wind as well as molecular diffusion away from the emission point thus creating a "plume" of molecules (Atema 1996). Due to climatic conditions such as turbulence, obstacles and wind speed variation, the plume does not form a homogeneous, ordered structure but instead shows a meandering and unique pattern (Koehl 2006). Insects are tasked with being able to navigate these plumes and do so with both physiological and behavioural adaptions.

Plumes may be thought of as a series of "packets" that disperse from the emission point (Murlis and Jones 1981). Insects can discriminate between these packets as a result of both the concentration as well as the composition of these packets (Beyaert and Hilker 2014; Riffell et al. 2014; Terry et al. 2014). Further to this, packets originating from differing plumes will be encountered at differing time points and thus this adds a further method of odour discrimination (Nikonov and Leal 2002).

To encounter a plume, insects have been shown to use differing search strategies that vary by stimulus type and insect species (Cardé et al. 2012). Zanen et al. (1994) used hungry fruit fly (*D. immigrans*) to show that while searching for food, for winds that varied less than ca.60°, flying at right angles to the wind direction was the strategy of choice while when winds varied more than ca.60°, flight parallel to the time-averaged wind direction was chosen. In contrast, Cardé et al. (2012) undertook studies with male bog holomelina moth (*Virbia lamae* Freeman) which, in search of pheromone plumes showed no directional preference with respect to wind direction. Reynolds et al. (2007) used male turnip moths (*Agrotis segetum* Micheal) and found that upwind flight was the predominant search strategy in response to sex pheromones.

Upon incidence with a plume odour packet, insects turn upwind and surge forward for a set amount of time at which point, if no packets have been encountered, "casting" from side to side is initiated again until a further packet is encountered (Cardé and Willis 2008).

Some authors have postulated the idea of "odour switching" which may be summarised as; if a plume indicating a low chance of task success e.g., a parasitoid following plant VOCs from a plant in which its host is normally found, is encountered then this plume is followed. However, if a higher priority plume is encountered such as pheromone of the parasitoid host is encountered then this plume is preferentially followed (Beyaert and Hilker 2014).

1.5 Disruption of VOC communication by atmospheric oxidants

As illustrated above, VOC communication between organisms within the environment is both ubiquitous and complex. In section 1.3.6 the negative effects of oxidising atmospheric pollutants on human health and the environment were illustrated; however, recent evidence suggests that these

pollutants may also negatively affect VOC communication (McFrederick et al. 2009; Pinto et al. 2010). To date, attention has primarily been focused on ozone as a result of its atmospheric prominence (see section 1.3.4), the depth of research on its chemistry and its ease of use during experimental work. As a result of this, only the effects of ozone on VOC communication will be reviewed in this chapter.

1.5.1 Interaction of ozone with selected VOC blend components

The molecular basis for the disruption of VOC communication as a result of exposure to ozone is the reaction of ozone with unsaturated VOC blend components (Figure 1.4). While not all VOCs emitted by organisms such as plants and insects in the environment are of an unsaturated nature, of the 12 most commonly emitted floral VOCs in nature eight are unsaturated and thus, are susceptible to undergo a reaction with ozone (Knudsen et al. 2006).

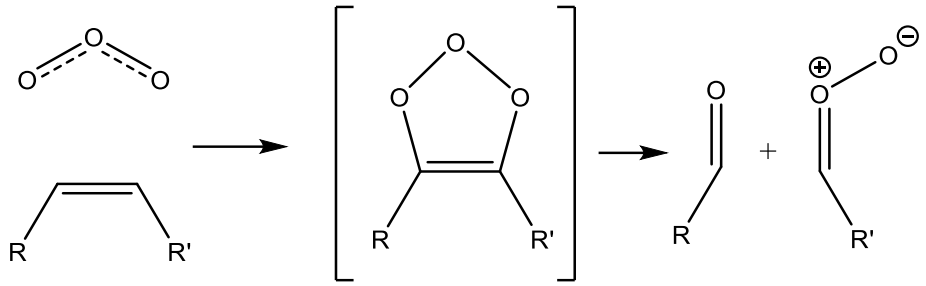

Figure 1.4 – Generic mechanism for the reaction of ozone at a Carbon-Carbon double bond (C=C) adapted from Monks (2005). [] = Transition state.

As a result of the reaction, the original VOC is degraded into new more highly oxidised compounds thus, decreasing the quantity of the original VOC in the atmosphere and potentially perturbing the overall blend ratio.

Furthermore, reaction products are formed which will have a greater degree of oxidation and thus, greater viscosity and lower volatility. This allows for condensation to occur, either on fine-scale particulates in the air or intermolecular condensation, thus forming secondary organic aerosol (SOA) particles (Robinson et al. 2007). SOA particles size (ca.1-100nm (Shrivastava et al. 2017)) is dictated by several factors such as humidity, the presence of seed particles and the gaseous molecule the SOA is formed from (Jonsson et al. 2008; Von Hessberg et al. 2009; Lambe et al. 2015); however, they are larger than gaseous molecules (ca.0.1-1nm) (Witherspoon and Saraf 1965). SOA particles tend to grow in size post-reaction as a result of further condensation of volatile molecules (Poulain et al. 2010) as well as coalescence of smaller particles (Pajunoja et al. 2014).

SOA formation has the potential to affect levels of cloud formation, thus altering the earth's climate which in turn affects the ecosystem (Stevens and Feingold 2009; Shrivastava et al. 2017). The exact effects of SOA on organisms remains unclear; however, it is hypothesised by Holopainen et al. (2017) that SOA may have wide-ranging effects such as altering leaf emissions, reducing rates of

photosynthesis (as a result of leaf deposition), and affecting root systems (as a result of soil leaching). What is known, however, are the damaging effects of sub-micron particles, such as SOA, on human health which have been shown to cause lung inflammation and cellular damage (Xing et al. 2016) and thus, it may be inferred that the effect of SOA particles on other living organisms may also be negative.

It may also be surmised that any potential effects of ozone upon the environment are likely to become more pronounced as a result of global warming (see section 1.3.5).

1.5.2 Experimental examples of VOC communication degradation

As a result of the theory that increases in the concentration of atmospheric oxidants may negatively affect VOC communication, experimental work has been undertaken by several authors to investigate this hypothesis more broadly using several different ecological systems.

Blande et al. (2010) measured changes in extrafloral nectar secretion to show that, as a result of increased tropospheric ozone concentrations (>80ppb), lima bean (*Phaseolus lunatus* L.) plants infested with spider mite (*Tetranychus urticae* Koch) invoked defence responses in uninfested conspecifics at lesser distances than that seen under clean air conditions. Fuentes et al. (2013) showed using Y tube olfactometer experiments that, under increased levels of ozone pollution (>80ppb), striped cucumber beetle (*Acalymma vittatum* J.Fabr.) was unable to locate flowers of its host plant Buffalo gourd (*Cucurbita foetidissima* Kunth) and instead moved randomly. Arndt (1995) used behavioural assays to show that fruit fly fruit fly (*D. immigrans*) aggregation pheromone that had been pre fumigated with ozone showed a lower rate of aggregation as opposed to the non-fumigated sample. GC-MS testing of the aggregation pheromone also showed qualitative changes in the chemical composition of the fumigated pheromone sample relative to the unfumigated sample. Cook et al. (2020) showed using a wind tunnel assay that hawkmoth (*M. sexta*) showed shorter foraging times on fake flowers emitting an ozone degraded floral blend from sweet tobacco (*Nicotiana alata* F.) relative to fake flowers emitting an undegraded floral blend. Girling et al. (2013) showed, using an oilseed rape (*B. napus*) Western honeybee (*A. mellifera*) system, that an oilseed rape floral blend degraded by NO_x provoked a reduced proboscis extension reflex (PER) in honeybees trained to the undegraded blend. Farré-Armengol et al. (2016) showed using flight arena behavioural experiments that buff-tailed bumblebee (*B. terrestris*) preferred the undegraded floral blend of black mustard (*Brassica nigra* L.) as opposed to a floral blend that had been mixed with ozone (120ppb).

In combination, these studies indicate that the presence of increased levels of atmospheric oxidants negatively affects VOC communication of several different ecological interactions. Ozone has been shown to affect several different facets of the plant-pollinator communication system.

1.5.3 Theorised mechanisms of VOC communication disruption by ozone

Jürgens and Bischoff (2017) have proposed a series of mechanisms by which ozone can disrupt VOC communication namely:

1) Stress as a result of ozone exposure may change plant VOC emission profiles.
2) Ozone may react with VOC blend components, thus altering the ratio of VOC blend components which may then alter blend recognition/perception by the receiver.
3) Ozone pollutants may react with VOC blend components and thus create new compounds, which may alter blend recognition/perception by the receiver.

In addition, I propose the further disruption mechanism of:

4) Oxidative pollution and related degradation products may damage or impair an insect's blend perception system

The literature evidence for each hypothesis is presented below.

Stress as a result of exposure to oxidising pollutants may change plant VOC emission profiles

It has been shown for several species that plants exposed to increased levels of tropospheric ozone exhibit changes in both their rate of VOC emissions and the composition of the VOCs they emit, thus altering the emitted VOC blend (Blande et al. 2015).

With respect to vegetative VOC emissions, Pinto et al. (2007) showed that under both 60ppb and 120ppb ozone, both Lima bean (*Phaseolus lunatus* L.) and cabbage (*Brassica oleracea* L.) showed changes in vegetative blend composition, with the extent of the changes in emission being correlated to increases in ozone concentration. Blande et al. (2010) also showed quantitative changes in the vegetative VOC profile produced by lima bean as a result of 80ppb ozone. Furthermore, Himanen et al. (2009) demonstrated that upon exposure to 100ppb ozone, oilseed rape (*B. napus*) showed reductions in its total terpene emission and changes in the ratios of the VOC components of the emitted vegetative blend.

For floral emissions, Saunier and Blande (2019) demonstrated that on exposure to elevated ozone concentrations at both 80 and 120ppb, no statistically significant change in total floral VOC emissions were seen for any of the four Brassicaceae species tested: *Sinapis alba* L., *Sinapis arvensis* L., *B. napus* and *B. nigra*. Further work (Brosset et al. 2020a, b) using similar methods and specimens to that used by Saunier and Blande (2019), has since also found a lack of a statistically significant change in total floral VOC emissions but found qualitative changes in floral emission composition upon exposure to increased levels of ozone (80ppb).

It is clear from the literature above that a change in VOC emissions of plants as a result of increased levels of ozone is seen across a number of plant species and that atmospherically relevant ozone concentrations of 80ppb (Wilkinson et al. 2012) can cause these changes.

It is possible that alterations to plant VOC emission profiles as a result of ozone stress may affect the ability of insects to recognise their host plants. It has been hypothesised that alterations to a blend as a result of ozone stress may be similar to that seen as a result of pest infestation (Vuorinen et al. 2004) and it has been shown by Kessler et al. (2011), using a Peruvian tomato (*Solanum peruvianum* L.) model, that upon herbivory a lower rate of pollination is seen thus, reducing the ability of a plant to reproduce. Further to this, the work of Brosset et al. (2020) showed that changes in vegetative emission profiles as a result of ozone exposure are more pronounced in wild plants as opposed to their closely related cultivated strains which would thus mean, wild plants seeing lower levels of pollination relative to cultivated strains and thus an effect upon plant biodiversity.

When experimentally testing the effect of changes in VOC profile upon host plant finding, it is often hard to distinguish between the alteration to the ratio of blend constituents emitted by the plant and degradation of the blend post emission but before collection. To the knowledge of the author, no study has managed to test the effect of ozone induced changes in VOC profile directly while fully removing any changes to the blend as a result of blend degradation post emission.

<u>Oxidising pollutants may react with VOC blend components and thus, alter the ratio of VOC blend components which may alter blend recognition</u>

The potential effects of degradation of blend components upon blend ratio, and thus the efficacy of VOC communication, has been illustrated by several authors. McFrederick et al. (2008) modelled the effect of several realistic air pollutant scenarios of mixtures of ozone, nitrate radicals (NO_3) and hydroxyl radicals (OH) upon a model floral blend. It was illustrated that the concentration of individual blend components reduced with increasing distance from the point of emission at differing rates and thus, both the blend ratio and intensity are likely to be altered. It was hypothesised that as a result of this alteration to the blend concentration, composition and ratio, under polluted air conditions, VOC communication may be less effective.

This hypothesis has begun to be explored experimentally by several authors. Farré-Armengol et al. (2016) exposed the floral blend produced by black mustard plants (*B. nigra*) to ozone (120ppb and sampled at various distances. Quantitative changes in blend ratio were recorded upon mixing with ozone with the severity of the changes to the blend ratio increasing with distance. Subsequent behavioural experiments in a flight arena in which a buff-tailed bumblebee (*B. terrestris*) was given the choice between an undegraded floral blend of black mustard or a blend that had been mixed with ozone (120ppb) and been allowed to react for several seconds. Li et al. (2016) showed that, upon reaction with ozone at two different mixing ratios (100ppb, 50ppb), there was a statistically significant change in cabbage plant (*B. oleracea*) VOC emission post reaction. Subsequent behavioural testing in a Y-tube olfactometer assay and showed that diamond back moth (*Plutella xylostella* L.) preferred a blend that had not been exposed to ozone.

While these papers start to explore the effect of ozone degradation of VOC blend components and how these changes affect the attractiveness of a blend, they have not fully separated the effects of changes in VOC blend ratio from the effects of the formation of gaseous reaction products and SOA.

Oxidising pollutants may react with VOC blend components and thus, create new compounds which may alter blend recognition

Upon the reaction of VOC blend components with ozone, reaction products are formed (Monks 2005). The effect of individual blend degradation products on the perception of a blend has been hypothesised to either enhance, mask or have no effect on the attractiveness of the blend (Schröder and Hilker 2008; Wilson et al. 2015). To date, there has been much work regarding the effects of introducing third party VOCs on blend perception, although little work regarding the effect of blend degradation product formation.

Blend enhancement as a result of the addition of VOCs has been shown by Mozuraitis et al. (2002) who showed that the addition of Germacrene to a behavioural study chamber increased both attraction and oviposition of tobacco budworm (*H. virescens*) on tobacco (*Nicotiana tabacum* L.).

An early example of blend masking was demonstrated by (Thiery and Visser 1987) who showed that potato beetle (*Leptinotarsa decemlineata* Say) exhibited a lower preference for undamaged potato plants (*Solanum tuberosum* L.) when the odour was mixed with that of wild tomato plant (*Lycopersicon hirsutum* F.), thus inferring that the VOCs of *L. hirsutum* may be masking the VOCs of *S. tuberosum*. Lawson et al. (2017) provided further support for blend masking by showing that, upon introduction of chemical noise in the form of plant essential oils to a flight arena, bumble bees (*B. terrestris*) were less able to discriminate between rewarding and non-rewarding flowers in comparison to a chemically pure environment, which is indicative of the essential oils masking the blends.

Riffell et al. (2014) showed both neutral and masking roles for VOCs by using a sacred datura plant (*D. wrightii*) - Tobacco hornworm moth (*M. sexta*) system in combination with antennal lobe excitation measurements. Upon addition of ethyl sorbate to the plume (a molecule chemically dissimilar to those present in the *D. wrightii* plume), no difference in odour tracking ability was seen. Upon addition of a background of benzaldehyde and geraniol separately (VOCs present in datura blends) as a background VOC, odour tracking ability was significantly reduced. Similar results were also seen when the plume from *D. wrightii* was mixed with the blend produced by creosote bush plants (*Larrea tridentata* Coville). The work of Riffell et al. (2014) pushes our understanding of the effects of VOCs on blend perception by providing evidence that chemically dissimilar VOCs may not affect the perception of a blend thus, allowing for forecasting regarding the effect of a reaction product on blend perception by a receiver.

The effect of VOC degradation products upon chemical signalling has begun to be explored although to date this has rarely been undertaken in isolation of the other facets of blend degradation such as alterations to blend ratio and SOA formation. Li et al. (2016) investigated the attraction of *P. xylostella* to the ozone degraded vegetative blend of *B. oleracea*; however, the other facets of blend degradation were not isolated from the formation of reaction products during this experiment. Farré-Armengol et al. (2016) tested the behavioural preference of *B. terrestris* to a degraded *B. nigra* blend during a flight chamber study and showed a lower behavioural preference for the degraded floral blend. Once again, the other facets of blend degradation were not isolated from the formation of reaction products during this experiment. It is also of note that while both Li et al. (2016) and Farré-Armengol et al. (2016) noted changes to blend ratios as a result of ozone exposure, neither explicitly characterised the resulting blend degradation products. Mofikoya et al. (2020) used artificial *B. oleracea* leaves (glass microscope slide coated in epicuticular leaf extracts) that had been exposed to α-pinene reaction products for 24 hours to test for alterations in the oviposition of *P. xylostella*. A reduction in oviposition was seen, thus indicating a repellent effect of degradation products in isolation of other facets of blend degradation.

The work of Mofikoya et al. (2020) brings the first study where the effects of degradation products are observed in isolation of alterations in blend ratio. However, the work did not identify the effect of degradation products produced from the emitted VOC blend but from an atmospherically prominent VOC (α-pinene) instead and did not account for the potential effects of SOA formation. There is thus, novelty in identifying the effect of degradation products directly produced from an emitted VOC blend in complete isolation of other effects of blend degradation. There is also further novelty in using a plant-pollinator system to verify if the effects seen using a plant-ovipositor system are translatable.

<u>Oxidative pollution and related degradation products may damage or impair an insect's blend perception system</u>

Insect olfactory systems are highly complex and rely upon several key components to operate effectively (see section 2.4.8). On approach to an antenna, molecules are fed into pores with the assistance of cuticular hydrocarbons which are of a fatty acid, apolar nature (Steinbrecht 1997). In species examined to date, these hydrocarbons have primarily been of an unsaturated nature meaning that they are repellent to attack by ozone (Böröczky et al. 2008); however, if some species possess unsaturated cuticular compounds, they may be attacked by ozone and their function potentially degraded. Once within the pore, molecules bind to olfactory binding proteins (OBP) to become soluble and allow them to diffuse through the lymph and attach to the dendritic nerve. It is, therefore, possible that if odorant-binding proteins possess bases that are of an unsaturated nature then may be attacked and degraded by ozone (Iriti and Faoro 2008).

Dötterl et al. (2016) undertook electroantennography (EAG) experiments to explore the effect of ozone exposure on the ability of western honeybee (*A. mellifera*) to physiologically respond to selected stimuli. The experiment found that ozone had a compound specific effect, significantly reducing physiological response to certain compounds and thus, suggesting that olfactory systems are indeed susceptible to attack by oxidative pollutants. A reduction in olfactory response to stimuli as a result of prior ozone exposure has also been observed by Vanderplanck et al. (2021). Both bumblebee (*B. terrestris*) and fig wasp (*Blastophaga psenes*, L.) showed reduced antennal responses to synthetic stimuli during EAG experiments and reduced behavioural preference for stimuli in comparison to a clean air control during dual choice behavioural experiments. It is clear that ozone perturbs olfactory functioning on a physiological and behavioural level, however, the exact method by which ozone impairs physiological response, and thus the cause of specificity was unable to be elucidated.

When ozone reacts with a blend, gas-phase products are produced that have the ability to condense and form secondary organic aerosol (SOA) particles (Chen and Hopke 2009) and have been shown to account for in excess of 25% of all reaction products (Tasoglou and Pandis 2015). SOA has been directly shown to cause damage to human lung cells (Xing et al. 2016); however, the interaction of SOA particles with an insect's olfactory system is unknown but it is hypothesised that SOA particles may either enter or block the antennal pore kettle or perturb the functioning of the cuticle.

Direct experimental work exploring the effect of SOA on antennal functioning in isolation of other ozone degradation related factors has been scarce to date. Literature to date such as the work detailed in sections 1.5.3 (Li et al. 2016; Farré-Armengol et al. 2016; Mofikoya et al. 2020) has explored the combined effects of ozone degradation upon VOC blends which include; alteration in blend ratio, formation of reaction products and formation of SOA and found that a significant change in behaviour is seen. As with the other sections highlighted, the lack of studies looking at the mechanisms of ozone degradation upon VOC blends in isolation of each other provides a knowledge gap which will be vital in understanding the risks that ozone degradation may pose to VOC based communication.

1.5.4 Potential for circumvention of blend degradation

Although it may be seen from section 1.5.2 that ozone has been experimentally shown to perturb VOC communication, novel work by Cook et al. (2020) has shown that, under certain conditions, this perturbation may potentially be mitigated as a result of insect plasticity (see section 1.4.3). It was shown that hawkmoth (*M. sexta*) was able to, in the absence of a nectar reward, adapt to an ozone degraded sweet tobacco (*N. alata*) floral blend, thus potentially circumventing blend degradation. However, it is hypothesised that this learning was due to the hawkmoth's previous association of the host plant visual cue with a nectar reward, thus in the presence of a degraded blend, the hawkmoth

utilised the previously learnt visual cue and then began to associate the degraded blend with the subsequent nectar reward. This learning methodology relies on the presence of a visual cue for an initial learning stage thus, limiting the effective range of plant-pollinator communication and reducing pollination efficiency. It is also conceivable that if the degraded blend, or a VOC within the locality of the degraded blend, has a repellent effect on the pollinator then the nectar reward learning association may not be achieved, thus meaning the effect of ozone pollution on emitted blend may not be able to be mitigated.

While this work is interesting it is still not considered that this learning behaviour is sufficient to fully mitigate the effect of blend degradation and this novel work is presented for completeness.

1.6 Conclusions

Pollinators have been shown to be key to human health and wellbeing with 78% of foods requiring insect pollination (Ollerton et al. 2011); however, it has been demonstrated that pollinator numbers are decreasing for several reasons including land use change, the introduction of invasive species and the use of pesticides. At the same time, levels of anthropogenically emitted tropospheric oxidants such as ozone have been rising and has been shown to affect human health but also the wider environment. VOC based chemical communication has been shown to be ubiquitous in the environment; however, it has been demonstrated to be susceptible to perturbation by atmospheric oxidants. It is thus hypothesised that perturbation of VOC communication by increased levels of tropospheric oxidants may potentially be contributing to pollinator declines.

Several theories have been proposed as to the mechanisms by which tropospheric oxidants may be perturbing VOC communication such as; 1) alteration of VOC blend emissions from plants due to ozone stress, 2) degradation of VOC blends may alter blend ratios, thus altering blend perception, 3) degradation of VOC blends may produce products which alter blend perception, 4) oxidants may directly, or indirectly by forming oxidation products such as SOA, alter the functioning of the blend receivers olfactory system.

While the alteration of VOC blend emissions due to ozone stress has been extensively studied in isolation, the other mechanisms have generally been studied in unison. This thesis aims to use both experimental and modelling methods to isolate and attempt to quantify the effects of ozone degradation on the differing aspects of ozone-initiated blend degradation. A model system, hypothesis and thesis plan will now be presented to set out how this knowledge gap will be addressed.

1.7 Model system

To undertake this work, a model plant-pollinator system consisting of oilseed rape (*B. napus*) and western honeybee (*A. mellifera*) was chosen.

Brassica napus was selected as the model plant species for this study due to the well-characterised nature of its floral VOC emission profile as well as its prominence in British agriculture. The VOCs used in this study were Z-3-hexenol, Z-3-hexenyl acetate, 3-carene, 1-undecene and 1-dodecene and the rationale regarding their selection may be viewed in section 2.1. *Apis mellifera* was selected as the model insect as it is known to pollinate *B. napus* and as such is likely to be able to detect the floral VOC organic compounds used in the model study (Blight et al. 1997; Garratt et al. 2014; Lusebrink et al. 2015). *Apis mellifera* has also been used widely in previous electroantennography (EAG) experiments (Luo et al. 2013; Dötterl et al. 2016; Mas et al. 2020).

Ozone was selected as the tropospheric oxidant due to the wealth of literature regarding its reaction mechanism with unsaturated VOCs, its prominence during the day (Dickerson et al. 1982) when both pollinator activity (Vicens and Bosch 2000) and VOC emissions (Pio et al. 2005) are at their maxima and safety concerns regarding the experimental use of other common atmospheric oxidants.

1.8 Hypothesis

This work aims to provide evidence to test three key hypotheses which will each expand the understanding of how ozone degradation of blend components may affect a receiver's ability to physiologically detect a model blend. It is hypothesised that:

- On a relevant spatial scale, as a result of exposure to ozone, emitted oilseed rape floral blend components that are unsaturated will reduce in concentration, thus altering the overall blend ratio. The reductions in VOC concentration will alter the physiological response of *A. mellifera* to components of the VOC blend in a non-uniform manner with varying levels of physiological response over distance.
- Products resulting from the ozonolysis of VOCs present in the floral blend of oilseed rape will be able to be physiologically detected by *A. mellifera*.
- On a relevant spatial scale, SOA will have the potential abundance and size range to interact with antennal sense organs and thus, cause a reduction in the physiological ability of *A. mellifera* to detect VOCs.
- The effects of ozone degradation may vary between ozone excess and VOC excess landscape scenarios.

1.9 Thesis outline

To address the four hypotheses above, three experiments were conducted.

In chapter three I addressed the first hypothesis. Due to the complexity of presenting reductions in floral blend component concentrations in isolation of other degradation effects, a novel modelling approach was undertaken. Initially, simple atmospheric modelling which utilised literature derived rate constant values was undertaken to characterise how the concentration of individual VOCs change over distance as a result of ozone degradation under both ozone excess and VOC excess scenarios. Dose-response electroantennography (EAG) experiments were subsequently undertaken to ascertain how the electrophysiological response of *A. mellifera* antennae to individual VOCs changes as concentration is altered. The two data sets were then combined to create two final models that describe how the electrophysiological response of *A. mellifera* to each of the model VOCs changes over distance as a result of ozone degradation under both ozone excess and VOC excess scenarios.

In chapter four I addressed the second hypothesis using a mixture of experiments to ascertain degradation products and their electrophysiological activity. Initially, gas phase ozonolysis experiments were undertaken under both VOC excess and ozone excess conditions to characterise ozone induced degradation products by exposing reactive blend VOCs to ozone in isolation. Further experiments were then conducted that exposed a synthetic blend of the VOCs to ozone and characterised the resulting reaction products to identify any possible side reactions. Identified products, where available, were then used in EAG experiments to test their ability to invoke an electrophysiological response.

In chapter five I addressed the third hypothesis by using a mixture of experiments to ascertain SOA characteristics as well as their effects on the physiological response of an antenna to stimuli. Initially, experiments used a scanning mobility particle sizer (SMPS) to determine both the yield of SOA particles as well as SOA particle size over time for all model VOCs in isolation under both ozone excess and VOC excess conditions. EAG-treatment experiments were then undertaken to ascertain the effect of not only SOA, but also components within the SOA reaction mixture such as unreacted VOC and ozone, upon the physiological ability of *A. mellifera* to detect two VOC stimuli.

Chapter 2 – Experimental model, systems and approach

2.1 Rationale for chosen model and conditions

2.1.1 Establishment of plant-pollinator model system

The model plant to be used in this thesis was selected by initially consulting Knudsen et al. (2006), which reviews literature that has identified plant volatile organic compound (VOCs) emissions from various plant species. Refinement took place by considering the potential plants against three criteria namely: the plant must be known to be organism pollinated, the plant must be easy to grow in a UK climate and the plant must have had its VOCs characterised by several groups. As a result of this search, oilseed rape (*Brassica napus* L.) was chosen and 34 unique floral emitted VOCs were identified in the literature which are displayed in Table 2.1 (Evans and Allen-Williams 1992; Jakobsen et al. 1994; Blight et al. 1997). A shortlist of VOCs to be used in this work was then created by comparing the VOCs against three criteria namely; the presence of a Carbon-Carbon double bond (C=C) (so as to allow reaction with ozone), commercial availability as of January 2017, conflicts with the PDRA project running in parallel to this work which was based upon the 10 most commonly emitted floral VOCs according to Knudsen et al. (2006).This produced a shortlist of 6 VOCs as displayed in Table 2.2 namely; α-Terpinene, 1-undecene, 1-dodecene, 3-carene, Z-3-hexenol and Z-3-hexenyl acetate.

Due to time constraints, only 5 VOCs could be studied and thus the prevalence of the VOCs in the environment according to Knudsen et al. (2006), was considered in addition to the presence of literature data regarding SOA yield and reaction products. Due to their prevalence in the environment 3-carene, Z-3-hexenol and Z-3-hexenyl acetate were chosen. Due to the large amount of data already present in the literature for α-Terpinene, 1-undecene and 1-dodecene were instead chosen for study during this thesis as they add utility to the project by producing novel data that may be utilised by both this project and the wider scientific community.

Table 2.1 – List of all identified *Brassica napus* floral VOCs present in Knusden *et al.* (2006) combined with information regarding; the presence of carbon-carbon double bond (C=C), commercial availability in the UK as of January 2017 and conflict with work being undertaken by the project PDRA.

VOC	reference	Contains nonaromatic C=C?	Commercially available?	PDRA studying?
benzaldehyde	1,2	N	Y	N
α-pinene	1,2,3	Y	Y	Y
α-terpinene	1	Y	Y	N
Phenylacetaldehyde	1,2	N	Y	N
benzyl alcohol	1	N	Y	N
p-cymene	1	N	y	N
limonene	1,2,3	Y	Y	Y
1,8-cineole	1,3	N	Y	N
2-nonanone	1	N	Y	N
linalool	1,2,3	Y	Y	Y
2-phenylethanol	1,2	N	Y	N
1-undecene	1	Y	Y	N
1-dodecene	1	Y	Y	N
methyl salicylate	1	N	Y	N
3-carene	1,3	Y	Y	N
(E,E)-α-farnesene	1,2,3	Y	N	Y
caryophyllene	2	Y	N	Y
cedrene	2	Y	N	N
myrcene	2,3	Y	Y	Y
E-β-ocimene	2	Y	N	Y
perillene	2	Y	N	N
β-pinene	2,3	Y	Y	Y
sabinene	2,3	Y	N	N
Z-3-hexenol	2	Y	Y	N
Z-3-hexenyl acetate	2	Y	Y	N
4-methoxybenzaldehyde	2	N	Y	N
nonane	3	N	Y	N
3-thujene	3	Y	N	N
decane	3	N	Y	N
undecane	3	N	Y	N
dodecane	3	N	Y	N
tridecane	3	N	Y	N
tetradecane	3	N	Y	N

[1] (Blight et al. 1997) [2](Evans and Allen-Williams 1992) [3](Jakobsen et al. 1994)

Table 2.2 – Shortlist of VOCs from Table 2.1 providing information regarding the abundance of the production of VOCs across taxonomic groups as well as the presence of reaction product or SOA yield studies in the literature.

VOC	Number of taxonomic groups that produce VOC in floral odour according to Knudsen et al. (2006).	Reaction product studies in literature?	SOA yield studies in literature?
α-Terpinene	14	Y	Y
1-undecene	2	N	N
1-dodecene	2	N	N
3-carene	26	Y	Y
Z-3-hexenol	42	Y	Y
Z-3-hexenyl acetate	38	Y	Y

Apis mellifera L. was chosen as the model pollinator for this thesis due to its widespread importance as a crop pollinator, with 80% of global crop pollination services attributed to *A. mellifera* (Carreck and Williams 1998), as well as being a known pollinator of *B. napus* (Garratt et al. 2014). Further to this, due to its importance as a pollinator, *A. mellifera* has been the subject of intensive research in the scientific literature and has had its suitability for electroantennography (EAG) experiments previously demonstrated (Wright and Smith 2004; Luo et al. 2013; Dötterl et al. 2016).

2.1.2 Establishment of atmospherically relevant modelling scenarios

Varying landscapes are seen throughout the UK such as wetland, grassland, arable and forest (Ostle et al. 2009) each with its own differing traits such as its propensity to generate ozone (Jiang et al. 2008). As such, this work aims to construct two extreme reactant scenarios (ozone excess/VOC excess) that could conceivably occur in nature and explore the impact of ozone degradation on VOC based communication under these two extreme scenarios.

The first scenario considered was of a single flower occurring in a landscape containing few other floral resources, for example a single oilseed rape plant occurring in a field of wheat (wheat is self-pollinated and thus unlikely to release floral VOC (Okada et al. 2018)), releasing floral VOCs into a continuous wind. The concentration of the floral VOC emissions may be estimated by using literature values for release rates of emission (Jakobsen et al. 1994), which are in the order of 5ng floret^{-1} hour^{-1} or 0.013 part per trillion (ppt). The background daytime concentration of tropospheric ozone (O_3) at ground level is ca. 20-60 part per billion (ppb) (Jaffe and Ray 2007) and thus, it may be seen that the

O_3 concentration is many times larger than that of the VOC emission concentration and may be termed an ozone excess situation (Figure 2.1A).

A second scenario is that of a sampling point in the middle of a field of flowers on an overcast day with a very light wind which may be representative of an agricultural field or woodland. The emitted floral VOCs may accumulate in the vicinity of the field and thus, it is feasible that floral VOC concentration levels may surpass that of background O_3 levels (Figure 2.1B). This reactant scenario has been indicated to be plausible with experimental measurements such as that of Acton et al. (2016), who measured 4m above a tree canopy at a wind speed of 6m/s, showing that ambient mixing ratios of isoprene may be as high as 4.79ppb. In isolation this is not proof of a situation where VOC concentration is greater than ozone concentration; however, Aylor et al. (1993) showed that wind speed at lower levels and within tightly cropped areas has been shown to decrease exponentially thus, highlighting that at the low heights that an insect flies, the mixing ratios highlighted by Acton et al. (2016) may be even greater. When considering this scenario, it is of note; however, that as the distance from the flower increases, floral VOC concentration will steadily decrease as a result of diffusion, potentially leading to an O_3 dominant situation. However, the distances for this reduction to take place could be significant because the effects of diffusion are thought to be negligible due to the fact that the time required for molecules to travel through a fluid by diffusion increases as the square of the distance travelled (Vogel 1994; Koehl 2006). Both scenarios are illustrated graphically in Figure 2.1.

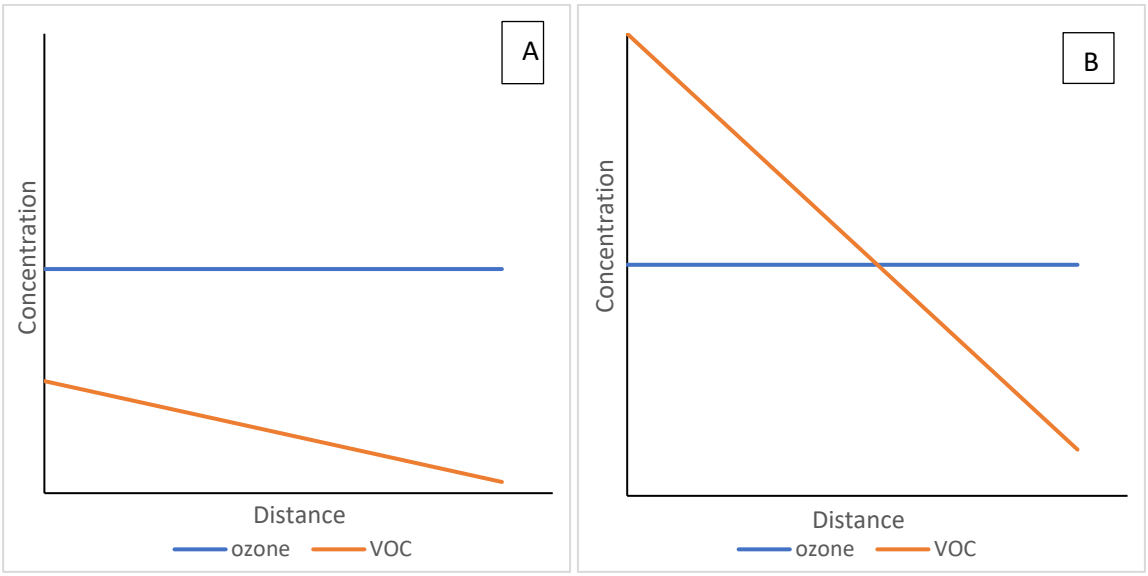

Figure 2.1 – Graphical comparison of how O_3 and VOC concentrations may evolve over distance under a single floral VOC emitter, high wind speed scenario (A, ozone excess) and a multiple floral VOC emitter, low windspeed scenario (B, VOC excess). Not to scale.

Concentrations in the part per million (ppm) range were used during this experiment which does not reflect the ppb and ppt concentrations generally seen in the environment (Bey et al. 1997; Acton et

al. 2016). Part per million concentrations were used as opposed to the more environmentally relevant concentrations due to the sensitivity of the equipment used in this experiment not ranging as low as the ppb and ppt region (TSI 2007).

For the O_3 excess scenario, a 4x excess was chosen because this was consistent with literature standards and was the maximum achievable concentration using an O_3 trap "reservoir" on the ppm scale. Literature sources use various excesses of O_3 ranging from 10x (Tasoglou and Pandis 2015) to 3x (Griffin et al. 1999). For the VOC dominant scenario, a 3x VOC excess was chosen because this was the maximum excess achievable when using a cyclohexane scavenger on the ppm scale.

A wind speed of $1ms^{-1}$ was chosen because it is smaller than the literature derived maximum wind speeds at which pollinators will fly ($6ms^{-1}$, Vicens and Bosch (2000), $<2.5ms^{-1}$, Primack and Inouye (1993)) as well as being concurrent with the wind speed of $1ms^{-1}$ at 2m height used in a related study by Fuentes et al. (2016).

There is significant discussion in the literature regarding the distances at which floral VOCs are used by bees for location of floral resources. A proxy for this distance may be the recorded foraging distances of species, although it is important to note that distances at which floral VOCs are actively used may be shorter. Small solitary bees such as *Hylaeus punctulatissimus J.Fabr.* have been shown to only forage on average 100m and larger bumblebees, such as *Bombus terrestris* L. has been shown to forage on average 267m (Zurbuchen et al. 2010). *Apis mellifera* has been shown to have larger foraging distances ranging from 1.5km to 6km depending on the environment in which the bee was foraging and the colony size (Abou-Shaara 2014). Season has also been shown to affect *A. mellifera* foraging distances with reductions in mean foraging distances from on average 1324m in spring to 435m in summer (Danner et al. 2016). Due to the large variation in stated foraging distances, a conservative estimate of 400m will be applied when analysing any effects of tropospheric ozone on the ability of pollinators to use floral VOCs to locate floral resources.

2.1.3 Rationale for electrophysiological experiments

Previous work has generally explored the behavioural effects of ozone upon VOC mediated interactions (Harvey et al. 2016; Farré-Armengol et al. 2016); however, it has proved challenging to isolate the effects of the individual mechanisms by which VOC mediated interactions are perturbed. Girling et al. (2013) managed to achieve this by using proboscis extension reflex (PER) experiments to identify the behavioural effects of one of these mechanisms (VOC ratio alteration), as a result of exposure of *B. napus* floral volatiles to diesel emission.

By using a behavioural approach to explore the effects of ozone in isolation, it may be argued that the data produced may be of more utility because it is likely to directly relate to previously made behavioural observations; however, there is a greater chance of the findings containing confounding

factors due to the insects neurological processing of the blend as well as the greater complexity of the experiments.

By using an electrophysiological approach, fewer confounding factors are present, experiments are generally quicker and simpler; however, it may be argued that the data produced may have less utility as it does not necessarily directly relate to the observed behavioural effects.

An electrophysiological approach was taken by this work due to the suitability of electrophysiological methods for relative comparisons as a result of the lower likelihood of confounding factors, and the quicker and easier experimental setup allowing for a greater number of mechanisms by which VOC mediated interactions are perturbed to be explored.

2.2 Chemistry theory

Some key chemistry concepts are now introduced in order to aid the reader in understanding this thesis. For further explanation please consult any general chemistry text (Atkins and De Paula 2014).

2.2.1 Rate of reaction

The rate of reaction between two molecules may be rationalised by using many complex principles including classical and quantum physics. A classical thermodynamic approach to rate of reaction shows that several factors affect the rate of reaction between two molecules such as temperature, pressure and concentration. To be able to compare two reactions independently of thermodynamic factors a rate constant (k) is used.

$$rate\ of\ reaction = k[A]$$

Equation 2.1 – General rate equation describing 1st order kinetics with respect to the concentration of reactant A, where k = rate constant (molecule^{-1} cm^3 s^{-1}), [A] = concentration (molecule cm^{-3}).

The kinetics of a reaction may be measured experimentally and allows for the rate of reaction to be linked to the concentration of reactants in a rate equation (Equation 2.1). A 0th order reaction means that the rate of reaction is not linked to the concentration of any of the reactants. A 1st order reaction means the rate of reaction is proportional to the concentration of a reactant and finally, a 2nd order reaction means the rate of reaction is proportional to the square of the concentration of a reactant.

By utilising the rate constant and rate equation the concentration of a reactant may be estimated at any time point and thus, this is used in this thesis to model how the concentration of a reactant changes over time and thus distance.

2.2.2 Reaction mechanisms

Much like rates of reaction, reaction mechanisms may be rationalised using both classical and quantum physics. Fundamentally, reaction mechanisms describe the theorised interaction between molecules to create products and allow for the rationalisation of both products produced, and when used with quantum physics, physical properties of the reaction such as the rate of reaction.

Of particular interest for this work is the reaction of gaseous atmospheric oxidants such as ozone, NO_3 and OH with VOCs. Both addition to a double bond and hydrogen abstraction mechanisms are known (Figure 2.2) and these mechanisms lead to differing products (Monks 2005); however, ozone exclusively follows the addition mechanism (Figure 2.3, Lin et al. (2016)). By applying general reaction mechanisms to reactants, the reaction products for a reaction may be hypothesised thus allowing for greater targeting of efforts to capture them.

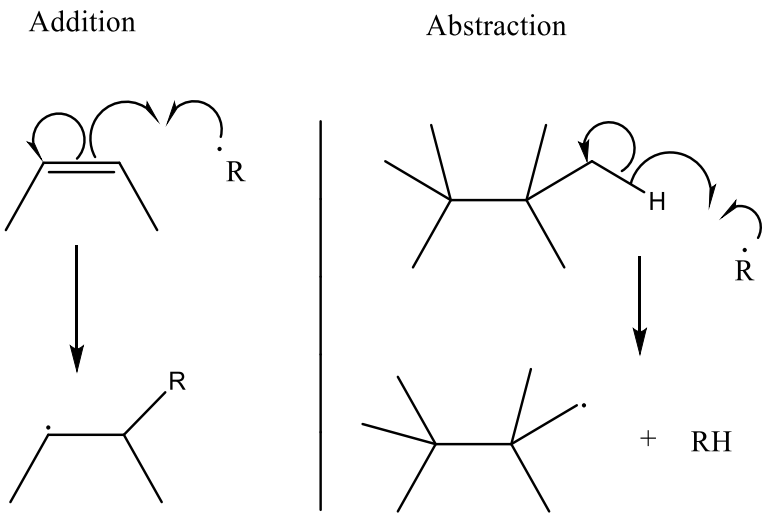

Figure 2.2 – General reaction mechanism for reactant addition (left) and Hydrogen abstraction (right)

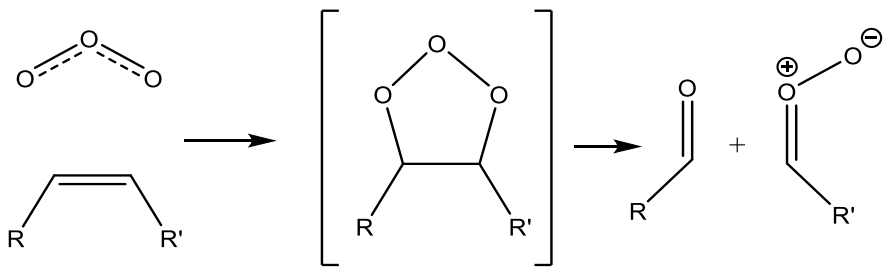

Figure 2.3 - General reaction mechanism for the addition of O_3 to a carbon-carbon double bond showing a Criegee intermediate denoted by [ ].

Literature provides evidence for further “secondary” reactions of primary reaction products, which explain the formation of secondary organic aerosol (SOA) constituent products. Auto-oxidation (Richters et al. (2016b); Figure 2.4) is seen when the radical based products formed in the initial

addition mechanism undergo rearrangement to produce a hydroxyl radical and subsequently reacts with oxygen. Auto-oxidation increases the polarity of the product; therefore reducing the vapour pressure and producing a product that has a tendency to condense and “seed” SOA particle formation (Holloway and Wayne 2010, p. 90).

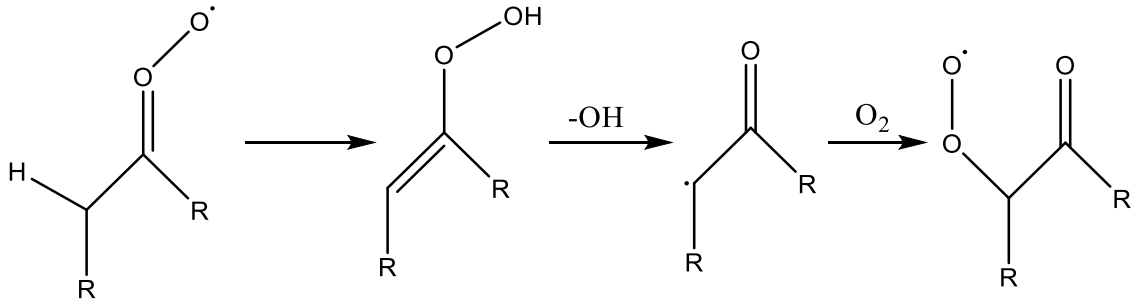

Figure 2.4 – General mechanism for auto-oxidation of ozonolysis products (Richters et al. 2016)

Hydroxyl radicals (•OH) are produced as a result of secondary reactions such as auto oxidation which may react further with both the initial reactant and any products formed from its ozonolysis. •OH radicals are also present in ambient air and are formed by a number of routes (see section 1.3.3). While these reactions are important in the atmosphere, it would be hard to attribute the influence of ozone or •OH radicals upon reaction products as well as SOA yield/size with •OH radicals present. As such, cyclohexane was used to scavenge •OH radicals during ozonolysis product identification and SOA size/yield experiments due to its fast rate of reaction with •OH and a lack of reaction with ozone.

2.3 Experimental consumables

2.3.1 Reagents

Table 2.3 – A list of chemicals used in this thesis including supplier, purity and lot number.

Chemical	Supplier	Purity	Lot #
hexane	Sigma Aldrich[a]	≥95%	STBH5346
cyclohexane	Acros organics[b]	HPLC grade	279590025
cyclohexanol	Acros organics[b]	99%	40519039
$CDCl_3$	Sigma Aldrich[a]	-	MKCC7283
Glacial acetic acid	Fisher[b]	-	0443263
Glyoxal 40% wt solution	Sigma Aldrich[a]	-	STBH3030
1-decene	Sigma Aldrich[a]	≥99%	30649
Linalool	Sigma Aldrich[a]	97%	L2602
nonanal	Merck chemicals[a]	≥95%	S73197
3-carene	Sigma Aldrich[a]	99%	441619
Z-3-hexenol	Sigma Aldrich[a]	98%	STBB7845
Z-3-hexenyl acetate	Sigma Aldrich[a]	99%	MKBQ0079V
1-undecene	Sigma Aldrich[a]	97%	MKCC0962
1-dodecene	Sigma Aldrich[a]	99%	MKQQ6114
cyclohexanone	British drug houses, Poole[a]	97%	-
Decanal	Sigma Aldrich[a]	>98%	MKB44382
Undecanal	Sigma Aldrich[a]	97%	MKB68537
Methyl glyoxal 40% wt solution	Sigma Aldrich[a]	-	STBH3031
acetaldehyde	Sigma Aldrich[a]	>99.5%	MKB87541

[a] Merck, Gillingham UK [b] Fisher scientific UK, Loughborough UK

2.3.2 Animals

For EAG assays, foraging free-flying western honeybee's (*A. mellifera)* were collected singularly in plastic cups from the University of Reading Harris Garden (51°26'11.0"N 0°56'28.7"W), which contains several managed hives. Specimens were captured while foraging on various species of flowering plants so as to increase the likelihood that the specimen was a worker. Specimens were identified as *A. mellifera* by visual inspection.

2.3.3 Static chamber

The static chambers used in these experiments were 80L capacity, constructed from fluorinated ethylene propylene (FEP) and fitted with a single 1/4" polytetrafluoroethylene (PTFE) connector (Adtech polymer engineering Ltd., Stroud UK). An FEP chamber was chosen due to its low reactivity and non-stick properties reducing wall loss of particles. Between experiments, the chamber was "cleaned" by filling the chamber with air to capacity and then evacuating the chamber three times. Testing showed that this was sufficient to reduce SOA mass below 1µg/cm^3.

2.4 Instrumentation

2.4.1 Gas handling apparatus (GHA)

The gas handling apparatus (GHA, Figure 2.5) is bespoke equipment that allows for the precise dilution, mixing and sampling of gas phase compounds. The GHA is made of borosilicate glass and breaks down into several smaller components which allow for easy dismantling for repair and transportation. Central to the GHA are a 1L sampling bulb and a 1L mixing bulb which are both fully isolatable from each other via young's® taps. The GHA has the facility to introduce VOC compounds via cold finger (see 2.4.2), ozone from a silica trap (see 2.4.3) and compressed synthetic air. Vacuum is provided by an Edwards® RV8 rotary vane vacuum pump.

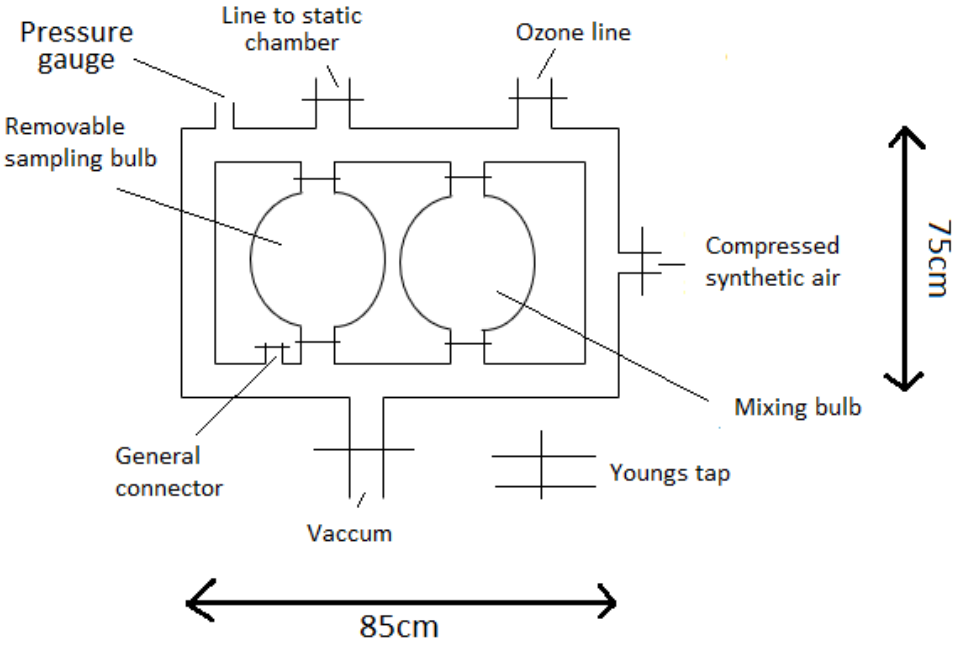

Figure 2.5 – Schematic showing the Gas handling apparatus (GHA) used in this work to dilute, mix and sample gas phase compounds. Both the mixing bulb and sampling bulb are of a 1L volume.

2.4.2 Cold finger

Glass “cold fingers” (Figure 2.6) are bespoke equipment that allows for the introduction of gas phase sample into the GHA. A liquid sample of the VOC of interest is placed in the bottom of the cold finger, an equilibrium then develops above the liquid giving gas phase VOC.

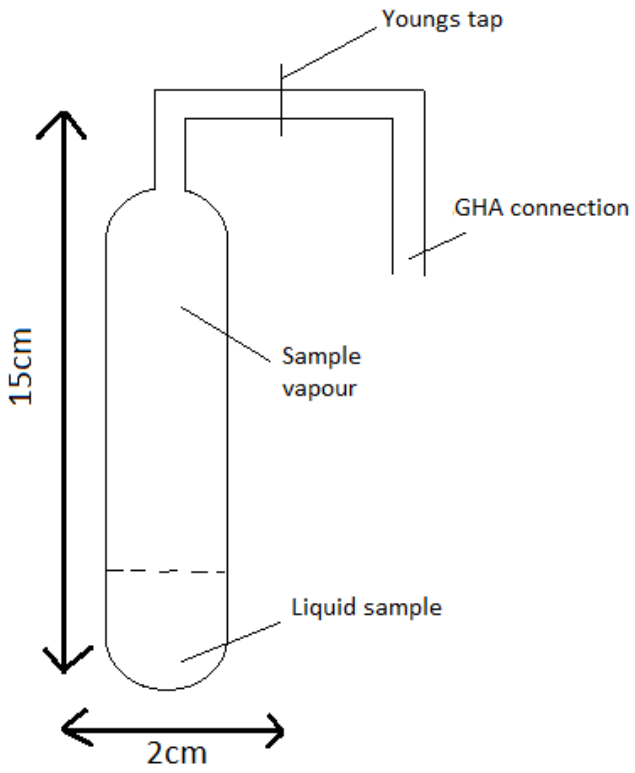

Figure 2.6 – Schematic of cold finger vessel used in this work.

2.4.3 O_3 generation

Ozone (O_3) was produced using a bespoke experimental setup which flowed compressed oxygen via a spark discharge ozone generator before to a cooled silica filled glass trap where ozone adsorbed to the silica (Figure 2.7). Waste gasses were then passed over a heated hopcalite® catalyst to degraded any residual ozone before being exhausted to the environment. The use of the ozone trap apparatus allowed for easy and rapid access to ozone over several days, thus reducing burden on experimental operation as opposed to spontaneous generation.

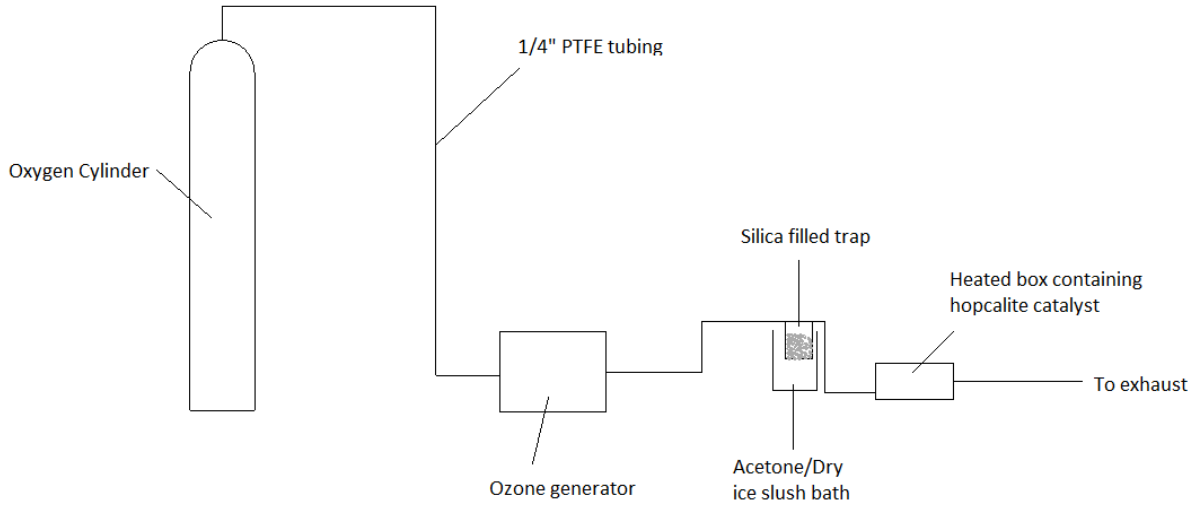

Figure 2.7 – Schematic of O_3 generation and trapping apparatus

2.4.4 Gas chromatography (GC)

Gas chromatography is a widely used mixture separation technique and was first invented by James and Martin (1952) to separate mixtures of fatty acids. A gas chromatograph or GC (Figure 2.8) at its most basic consists of a gas stream or "mobile phase" (usually Helium) which flows through a heated inlet port, into which a sample is injected, then into an analyte separation column contained in a temperature programmable oven before flowing into a detector.

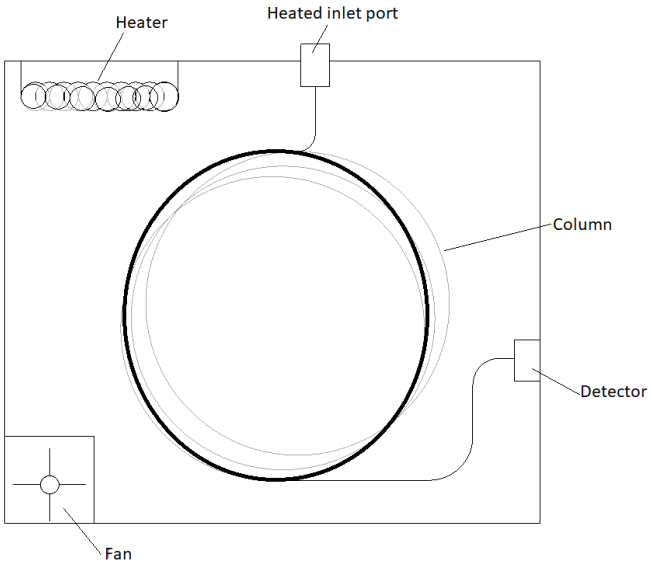

Figure 2.8 – A basic schematic of a gas chromatograph (GC)

The inlet port primarily serves two functions; To vaporise liquid samples into the gas phase and to control the amount of sample that is introduced to the column which is achieved by "Splitting" the gas flow. The column element of the GC serves to separate the analyte solution into its constituent components by utilising differences in the analytes binding affinities for the columns internal coating or "stationary phase". The most common type of columns in GC are capillary columns which are

characteristically of a small internal diameter (ca.0.25mm) and a long length (10-100m). The stationary phase consists of a crosslinked silicon oxide polymer, which often has one of several different chemical substituents attached to it. These chemical substituents alter the chemistry of the stationary phase and alter the binding affinity of molecules passing through the column and as such column choice can be optimised to ensure that it provides the greatest separation power.

The most common form of detector is a flame ionisation detector (FID) (Figure 2.9) which consists of a central flame in which the mobile phase output from the GC is burnt. Burning produces ions which are collected on a plate at the side of the FID chamber, the contact of the ions with the collection plate creates an electrical current which can be measured. An increase in the concentration of a sample increases the number of ions produced and thus, increases the current recorded.

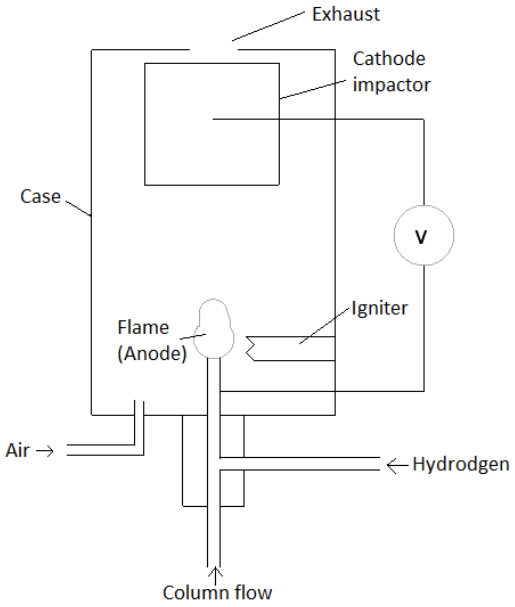

Figure 2.9 – A basic schematic of a flame ionisation detector (FID)

When separating a mixture consisting of several components it can be hard to achieve full separation. Carrier flow rate, Column length and stationary phase, oven temperature programme and split flow may all be adjusted and optimised to give the greatest separation in the shortest time possible (Charry-Parra et al. 2011). One measure of analyte separation efficiency is the retention factor (k) which is a measure of the relative amounts of time that an analyte resides in the mobile phase relative to the stationary phase. K factors should be constant over repeated runs; however, changes in k factor are often observed due to changes in carrier flow rate due to inlet port leaks which are caused by repeated perforation of the septa. This is a particular challenge when using SPME sampling which has a needle diameter that is larger than standard hypodermic needles. Peak splitting is characterised by two peaks that are close in retention time and have identical mass spectra. This may be as a result of several factors but may be observed where the amount of analyte

sampled is larger than the column can cope with given the parameters employed. This causes condensation of the analyte in two places in the column as opposed to one (Gilpin 2001).

In the case of this work, 50:50 split flow and an optimised temperature programme were utilised to ensure sharper and better separated peaks.

GC-FID is a desirable technique when working with known samples as well as when quantification of samples is required. When using unknown samples; however, standards are needed to be able to ascertain the identity of an unknown sample.

2.4.5 Gas Chromatography-Mass Spectrometry (GC-MS)

For samples where the identity of a sample is unknown, mass spectrometry (MS) is a useful choice of detector. Mass spectrometry uses the fundamental relationship between mass and energy $E=mc^2$ to be able to ascertain the molecular weight of analytes. There are several different designs of mass spectrometers that are suited to different types of analysis; however, this section focuses on the principles of operation of the electron ionisation (EI) quadrupole equipment that was used during this thesis.

Electron ionisation imparts a significant amount of energy upon molecules and thus, destabilises them which frequently causes “Fragmentation” of the ion to occur, which produces several smaller “Ion fragments” (Figure 2.10).

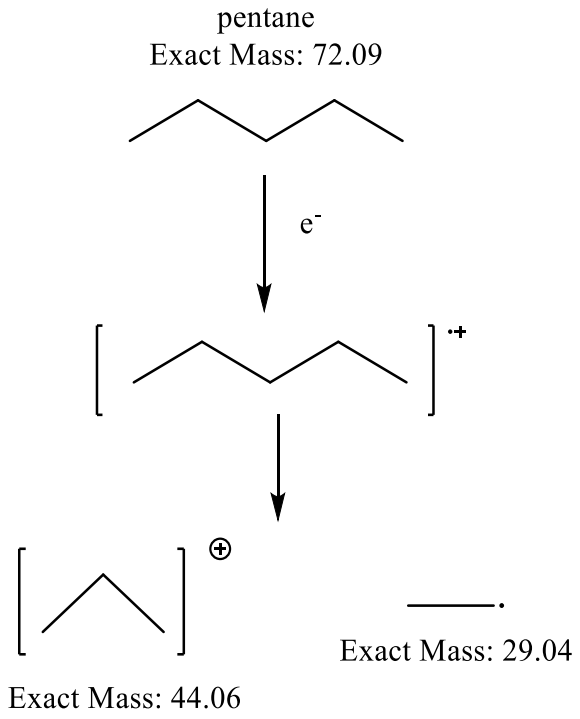

Figure 2.10 – A schematic of electron impact induced fragmentation of pentane.

These ion fragmentations occur in a structurally dependent manner which produces a mass fragmentation pattern that is unique to each molecule. In combination with standards, this fragmentation pattern is an effective method of determining the identity of an unknown sample.

An electron ionisation quadrupole mass spectrometer (Figure 2.11) consists of three main segments: ion production, ion segregation and ion detection.

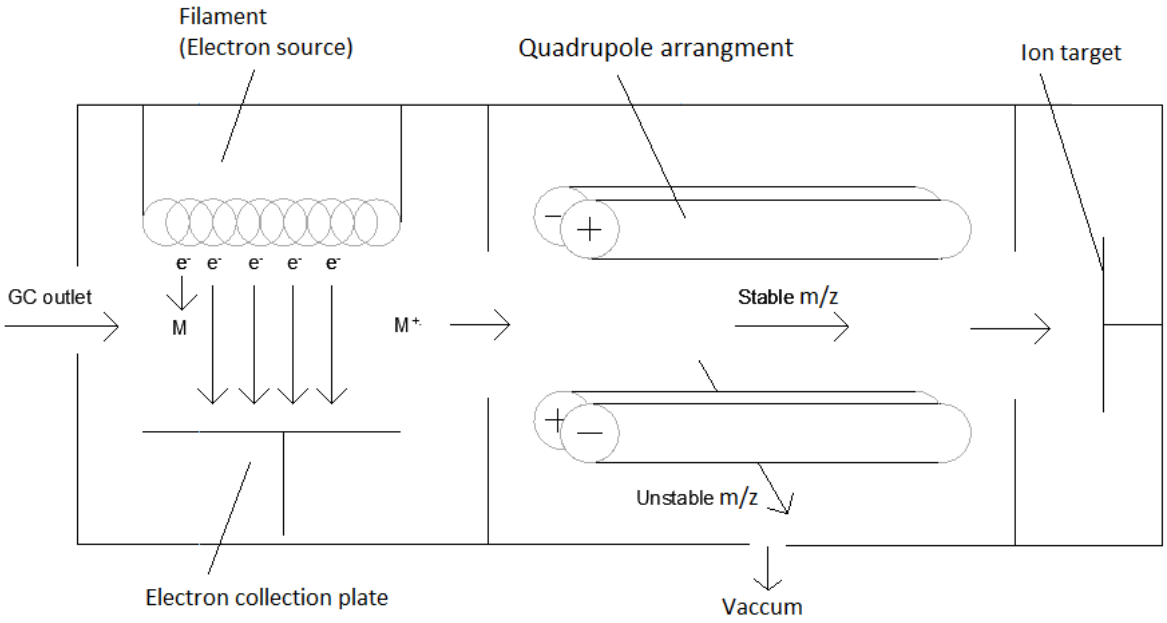

Figure 2.11 – A schematic of an electron ionisation quadrupole

In the ion production stage, the mobile phase outlet from the GC initially passes through an electron stream. On contact with the stream, a single electron from the outer electronic shell of a constituent atom contained within the neutral molecule is dislodged thus, creating a charged ion which may undergo fragmentation.

In the ion segregation stage, these ions are then directed towards a quadrupole arrangement which allows for ion segregation so only ions of a specific mass may pass to the detector. A Radiofrequency is applied to one pair of rods while a direct current is applied to the other pair of rods which creates an oscillating magnetic field. Mass is directly linked to energy by the equation $E=mc^2$ and thus, every molecule of mass X has an energy of Y. When ions of mass X and thus, energy Y, enter an oscillating magnetic field, only ions with the correct energy Y that corresponds to the selected magnetic field will have a stable trajectory and exit the quadrupole arrangement to the detector. Molecules that do not have the correct energy to resonate with the magnetic field have an unstable trajectory and are instead removed to waste. By rapidly altering the magnetic field of the quadrupole, a relevant mass range may be scanned to identify ion fragments of differing mass.

The final element of a mass spectrometer is an ion detector. The ion detector works by measuring the change in current produced by the neutralisation of the ions on impact to the detector plate. The

greater the number of ions impacting the detector plate, the greater the current produced and thus the intensity of a sample can be deduced. By varying the magnetic field in the quadrupole and combining it with intensity measurements from the detector a spectrum that shows the relative intensities of ions at each mass to charge (m/z) ratio may be collected.

2.4.6 Solid phase microextraction (SPME)

Solid-phase microextraction (SPME) is a common method used to sample gaseous volatiles that is popular as a result of its simple sample preparation, selectivity and sensitivity (Baltussen et al. 2002). SPME fibres are coated either with a polymeric absorptive film that directly absorbs analyte molecules (e.g., Polydimethylsiloxane, PDMS), or they are coated with a pure polymer with absorptive particles embedded within the polymer (e.g., Polydiemthyl siloxane-Divinyl Benzene, PDMS/DVB).

The fibre coating affects the ability of the fibre to absorb specific molecules, with particle coated fibres being better suited to trace analysis of small molecules and film-coated fibres being more suited to high concentration, high molecular weight analysis (Vas and Vékey 2004, Table 2.4).

Table 2.4 – SPME fibre types and recommended uses adapted from (Vas and Vékey 2004). (PDMS=Polydimethylsiloxane, PA=Polyacrylate, DVB=Divinylbenzene, CAR = Carboxen, PEG= Polyethylene glycol, MW= Molecular weight)

Fibre coating	Film thickness (µm)	Application
PDMS	100	Volatiles (MW 60-275)
PDMS	30	Non-polar semi volatiles (MW 80-500)
PDMS	7	Non-polar high MW compounds (MW 125-600)
PDMS/DVB	65	Volatiles, amine and nitroaromatic compounds (MW 50-300)
PA	85	Polar semi volatiles (MW 80-300)
CAR/PDMS	All	Gases and low molecular weight compounds (MW 30-225)
PEG	60	Alcohols and polar compounds (MW-40-275)
DVB/CAR/PDMS	50/30	Volatiles and Semi volatiles (MW 40-275)

2.4.7 Tenax® TA

Tenax® TA, like SPME, is a common choice for collecting headspace volatiles. Tenax® TA is a porous polymer resin based on 2,6-diphenyl oxide and is usually packed inside small glass tubes measuring ca.5cm to allow for sample collection. Gaseous samples are drawn through the tubes and thus, over the Tenax during collection (Figure 2.12) before undergoing thermal desorption using specialised apparatus to be introduced into the GC system.

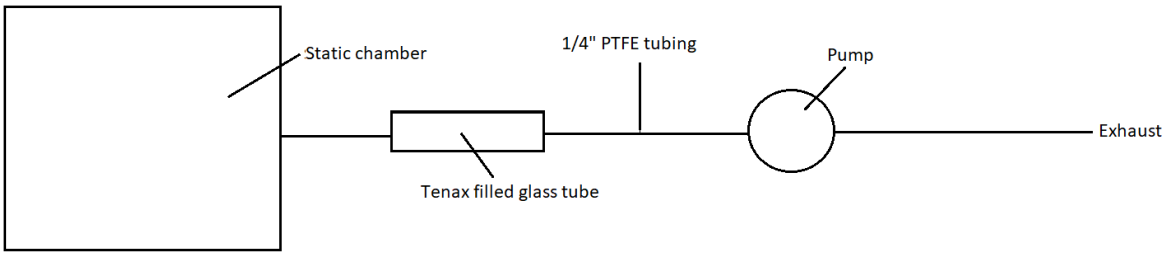

Figure 2.12 – Tenax collection apparatus

Tenax® TA shows low "bleed" and is often recommended for organic volatile and semi-volatile analysis as it provides a less cluttered spectrum and has been used previously for VOC trapping applications similar to the aims of this work (Calogirou et al. 1997; Li et al. 2016). A consideration when using Tenax® TA Is the need for an automated thermal desorption unit (ATD) to desorb the Tenax® TA filled tubes on to the GC column which adds another level of complexity and cost for Tenax analysis compared to SPME.

2.4.8 Electroantennography (EAG)

Insect antennae are complex structures that possess numerous chemical receptors called sensilla (Figure 2.13) which act to capture signalling chemicals and elicit physiological and potentially behavioural responses.

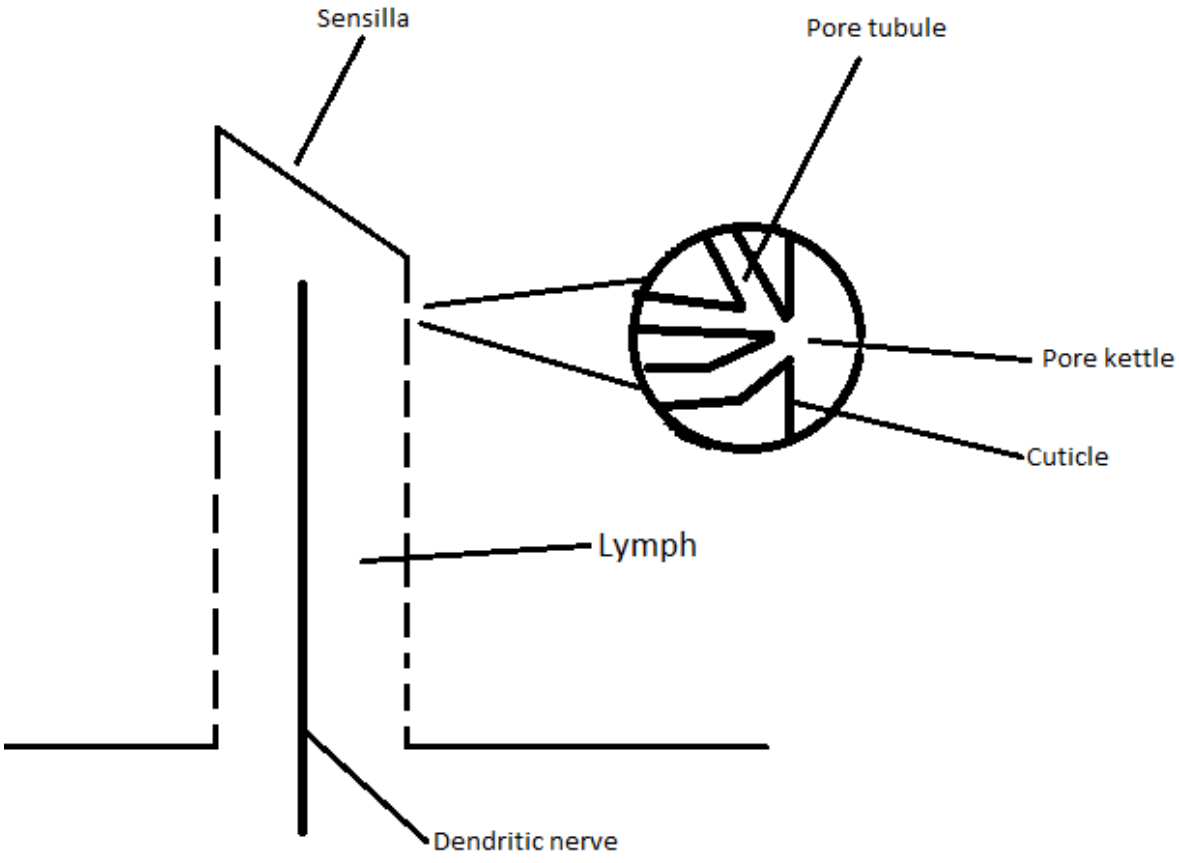

Figure 2.13 – A simplified schematic of an antennal sensilla based upon the work of Archer (2005)

Each sensillum consists of a porous cuticular layer which contains branch-like channels called pore tubules that a chemical must flow down. Inside these tubules, the stimulus (i.e. VOCs, of which most are hydrophobic) is combined with an odorant-binding protein (OBP) to create a hydrophilic complex which is able to pass through the cuticle layer of the pore tubule (Tegoni et al. 2004). The stimulus-OBP complex then moves across the lymph towards the negatively charged dendrite nerve binding site where the complex decomposes. The stimulus then binds to the dendrite which causes electrical stimulation which is sent on via the sensory neurons to the antennal lobe of the insect's brain.

Electroantennography (EAG) is widely used in insect ecology and measures the total response of all insect antennal sensilla combined to a stimulant. It was first used in 1957 to investigate how silk moth antennae respond to pheromones and since then has been widely used to determine antennal physiological responses (Schneider 1957).

A basic EAG setup is presented in figure 2.14. An antenna is excised and placed between two glass electrodes filled with a conductive solution of KCl thus, creating an electrical circuit. Clean air is blown at a continuous flow rate over the antenna with an interspersion of pulses of the analyte to be tested, the resulting current from the excitation of the antenna by the analyte is then amplified and recorded. Classification of a positive response is subjective; however, literature favours a response that is greater than the antennae's response to the solvent in which the stimulus is dissolved as a positive response (Vuts et al. 2010).

A limitation of the experimental design is the length of life of the antenna once excised from its body. Experiments may be performed with the antenna still attached to the body of the insect; however, this results in a more complex experimental preparation. In addition, direct comparisons of relative EAG responses of two VOCs cannot be made due to the fact that differing compounds will usually exhibit different vapour pressures (see section 1.4), therefore providing different doses of each VOC to the antennae.

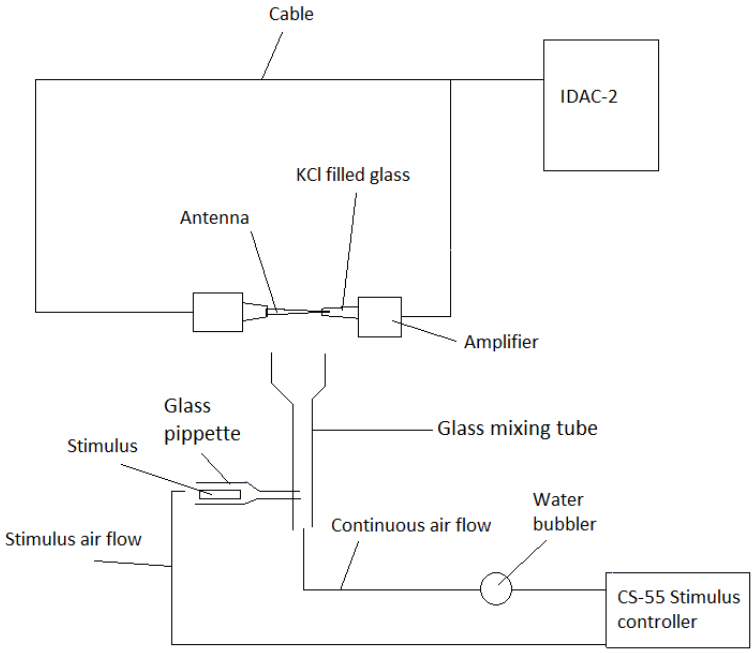

Figure 2.14 – A high level schematic of an electroantennogram apparatus

2.4.8.1 Use of EAG to find physiological detection limits

Electroantennography may be used as a quantitative technique when testing one VOC. By using a series of standard concentrations of VOCs and recording antennal responses at each dose the physiological detection limit of a VOC may be determined.

Work has shown that the exact physiological detection limits are unique to each VOC (Vuts et al. 2010). This is likely a result of differing chemical structures giving different chemical properties such as their ability to move into the gas phase (vapour pressure) and the reliance on interactions with generalist odorant-binding proteins (OBP) (Brito et al. 2016). In the presence of a more diverse floral background, as would be seen in many natural environments, moth detection limits have been found to be generally higher when compared to assays in a chemically pure environment (Party et al. 2013).

A drawback of the EAG technique is that it only provides information about a VOCs physiological and not behavioural effects and thus, outcomes from EAG experiments cannot be directly correlated with behavioural observations.

2.4.9 Scanning mobility particle sizer (SMPS)

Secondary organic aerosol (SOA) particles are often measured using a Scanning Mobility Particle Sizer (SMPS, Figure 2.15). The SMPS works much like the previously discussed quadrupole mass spectrometer which initially fractionates the incoming ions, or in this case SOA particles, and then counts the number of SOA particles in the fraction.

Particle mobility theory underpins SMPS operation. Electrical mobility (Equation 2.12) is a measure of the ability of a particle to move within an electrical field and can be expressed as a function of particle diameter.

$$Z_p = \frac{neC}{3\pi\mu D_p}$$

Z_p = electrical mobility n = number of charges of the particle e = elementary charge ($1.6x10^{-19}$C)
C = Cunningham slip correction which is temperature variable μ = gas viscosity
D_p = Particle diameter (cm)

Equation 2.2 – Formula for the electrical mobility of a particle

It can be seen from equation 2.2 that as particle diameter increases, the electrical mobility of the particle decreases. In an applied electric field, only molecules with the correct electrical mobility are able to successfully navigate the electrical field.

On entrance to the SMPS, the sampled aerosol first passes through a neutraliser and then a bipolar charger which charges each particle to a known amount. The aerosol flow then enters the differential mobility analyser (DMA) element of the machine. The DMA (Figure 2.16) features a long vertical column that has a strong electrical field applied to it. Only particles with the correct electrical mobility will have the correct trajectory to exit the classifier, creating a monodisperse flow of particles. Particles of all other electrical mobilities, and thus diameters, are recycled to begin the separation process again.

The monodisperse flow then moves to the condensation particle counter (CPC) element of the machine where particles are uniformly grown by condensing butanol onto them then particles are optically counted using a laser.

The DMA unit can be scanned to ascertain the total size and concentration profile of a sample with each scan usually taking ca.2 minutes 15 seconds followed by 45 seconds of idleness. Multiple scans can then be scheduled to gain data on how the sample profile changes over time.

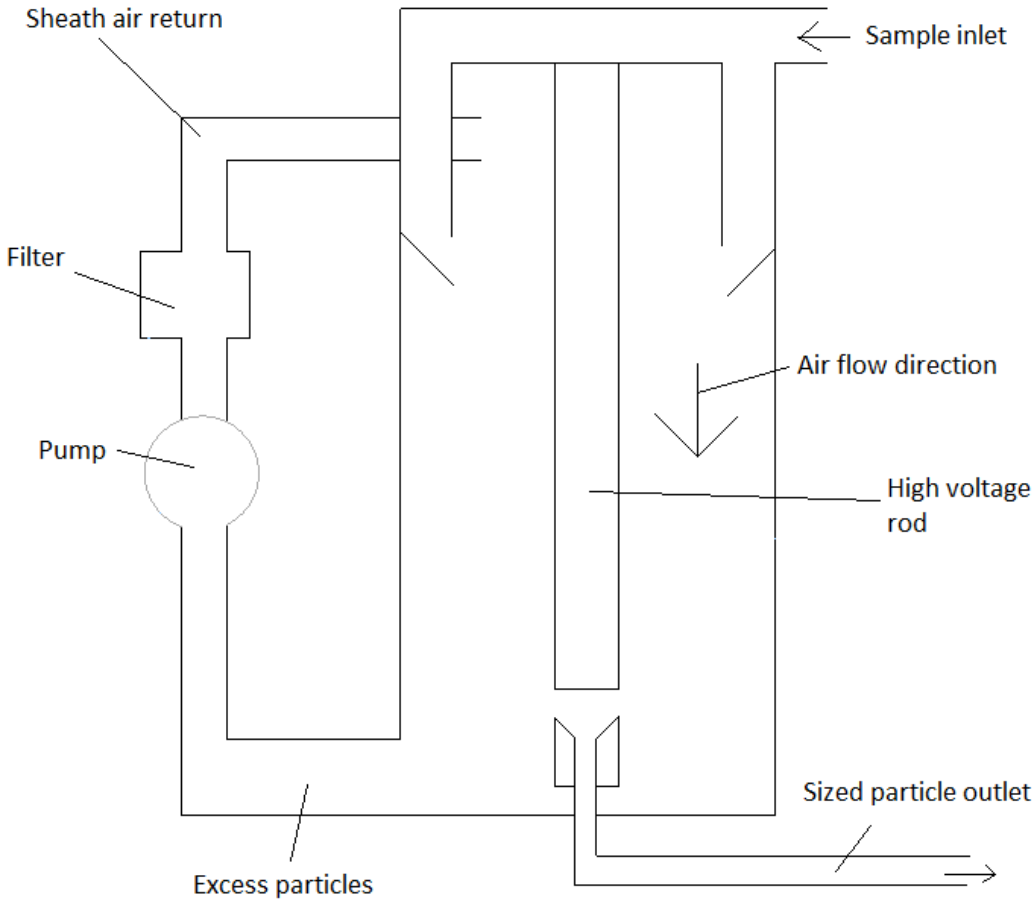

Figure 2.15 – High level schematic of the differential mobility analyser (DMA) component of a scanning mobility particle sizer (SMPS).

The orifice inlet flow of the SMPS requires periodic calibration to maintain accurate flows. The calibration apparatus (Figure 2.16) consists of an MKS (Swagelok, Solon USA) Type 179A All-Metal Mass-Flo® flow meter connected in series using PTFE tubing (Swagelok, Solon USA) and ultra torr connectors (Swagelok, Solon USA) with a static chamber full of air.

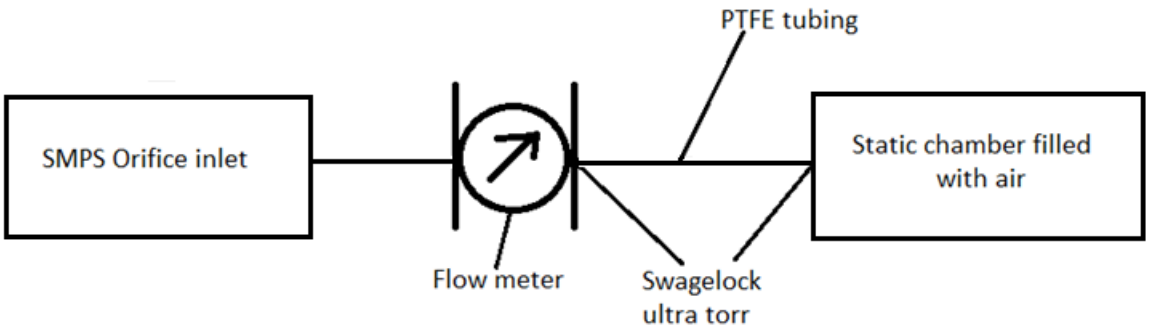

Figure 2.16 – Scanning mobility particle sizer (SMPS) orifice calibration apparatus diagram.

The flow meter was factory calibrated and this calibration was verified by displacing water from a container of known volume and measuring the time taken to complete the displacement. The orifice flow rate was measured using the flow meter at several differing flows and appropriate adjustments made to the SMPS calibration settings so as SMPS flow rate reading agreed with the flow meter reading.

2.5 Experimental methodology

Static reaction chambers were produced through a single core technique and used commonly during this thesis and as such the particulars of their production are detailed here. Analysis of the chamber constituents post reaction was undertaken using several different techniques so as to investigate the different constituents of the chamber. Particulars of these methods are described in section 2.5.

2.5.1 Cold finger preparation

Cold fingers were filled with 2.5ml of neat liquid VOC before being sealed and frozen in liquid nitrogen. The cold finger was then connected to the gas handling apparatus (GHA) and the pressure inside the cold finger reduced until it was stable. The cold finger was then isolated from the GHA and gently warmed to room temperature at which point gas would elute from the liquid sample. Once in a liquid state, the cold finger was re-frozen, and the process repeated until no gas eluted from the sample upon thawing.

2.5.2 O_3 generation

Ozone (O_3) was produced and stored prior to experiments taking place (Figure 2.7). O_3 was produced by using an O_3 generator (A2Z (Kentucky USA), 20GLAB, 25min, 0.5A, 0.2ml/min) which delivered an electrical discharge to an incoming O_2 flow (2 bar, Air Liquide UK, Birmingham UK). The resulting O_3/O_2 mixture then flowed over a silica filled glass "trap" (bespoke equipment) cooled to ca.-78^oC using an acetone/dry ice slush bath, with the O_3 adhering to the silica. The gas stream then flowed to a furnace (200^oC, bespoke equipment) which contained grains of Hopcalite™ catalyst which degraded any remaining O_3 back to O_2 thus, allowing the gas stream to be safely vented to the environment. O_3 was typically produced at the beginning of the week and gave 3 days of O_3 at acceptable concentration ranges (O_3 = 1-10% of total air mass). The O_3 trap connected to the gas handling apparatus via a Youngs tap built into the silica filled trap, a Cajon™ connector (Swagelok, Solon U.S.A) and a length of PTFE tubing (Swagelok, Solon U.S.A). A Tongdy® (Beijing, China) O_3 monitor was used to measure background O_3 concentrations in the lab environment.

2.5.3 Concentration calculations

Precise knowledge of the concentration of reactants is crucial when exploring chemical reactions both in the liquid and gas phase. Several calculations were undertaken to vary reactant conditions systematically and accurately in all experiments while accounting for the gaseous nature of the experiments, and thus their dependence on atmospheric conditions within the laboratory.

2.5.3.1 VOC concentration

Using equation 2.3 and equation 2.4 the concentration of VOCs in ppm were calculated using the initial VOC pressure, VOC air mixture pressure, atmospheric pressure, the volume of the mixing bulb and the volume of the static chamber.

$$P_{gas} = \frac{P_i \times P_{am}}{P_{atm}}$$

Equation 2.3 – Pressure to concentration equation where; P_{gas} = Partial pressure (Torr), P_i = initial pressure of VOC (Torr), P_{am} = Pressure of VOC air mixture (Torr), P_{atm} = Atmospheric pressure (Torr).

$$Concentration = \frac{P_{gas} \times V_b \times 10^6}{P_{atm} \times V_{rc}}$$

Equation 2.4 – Pressure to concentration equation where; P_{gas} = Partial pressure (Torr), V_b = Mixing bulb volume (L), P_{atm} = Atmospheric pressure (Torr), V_{rc} = Volume reaction chamber (L), concentration (ppm).

Further dilution of VOCs was often necessary, and this required the use of equation 2.5 to ascertain the concentration of the diluted VOC.

$$P_{gas} = \left({}^{P_{init}}/_{P_{atm}}\right) \times \left({}^{P_{red}}/_{P_{atm}}\right) \times P_{req}$$

Equation 2.5 – Gaseous dilution equation where; P_{init} = initial pressure of sample, P_{atm} = atmospheric pressure, P_{red} = reduced pressure that the sample is vacuumed to, P_{gas} = Partial pressure (Torr), P_{req} = Required pressure.

This methodology only works for pure VOCs, impure VOCs such as the O_2/O_3 mixture must undertake a different treatment for their concentration to be calculated.

2.5.3.2 Scavenger concentration

The amount of scavenger (cyclohexane was used in this work) that needed to be added to individual reactions was calculated. The aim was to ensure 95% of •OH radicals were removed from the reaction system and thus equation 2.6 was formulated.

$$\frac{k\ (OH, Scavanger) \times [Scavanger]}{k\ (OH, Alkene) \times [Alkene]} \geq \frac{95}{5}$$

Equation 2.6 – Scavenger concentration equation where k = rate constant (molecule^{-1} cm^3 s^{-1}) and [Alkene] = alkene concentration (molecule cm^{-3}).

Rearrangement gives equation 2.7.

$$[Scavanger] = 19\ \times \frac{k\ (OH, Alkene)}{k\ (OH, Scavanger)} \times [Alkene]$$

Equation 2.7 – re-arranged scavenger concentration equation where k = rate constant (molecule^{-1} cm^3 s^{-1}) and [Alkene] = alkene concentration (molecule cm^{-3}).

With accurate use of equation 2.6 and accurate knowledge of the parameters within the equation the influence of •OH on the ozonolysis reaction being studied can be reduced to insignificant amounts.

2.5.3.3 Ozone purity

Ozone was produced in an impure O_2/O_3 mixture and as such the concentration of the O_3 was determined using UV-Vis absorption. The basis of UV-Vis concentration determination is the beer lambert law (Equation 2.8)

$$abs = \ln(I_0/I) = \sigma\, c\, l$$

Equation 2.8 – beer lambert law equation where, Abs = Natural log absorbance, I_o = incident radiation intensity, I = Transmitted radiation intensity, σ = absorption cross section of O_3 (1.150×10^{-17} cm^2 $molecule^{-1}$ at 254nm), c=concentration (molecule cm^{-3}) and L=path length of the cell (10cm).

Conversion from concentration to pressure can be undertaken by using a re-arrangement of the ideal gas law equation (Equation 2.9)

$$c = \left(\frac{n}{V}\right) = \frac{p}{RT}$$

Equation 2.9 – Re-arranged ideal gas law where C = concentration ($molm^{-3}$) n = Number of moles of O_2/O_3 mixture in the cell V = Volume (m^3) p = Pressure (Pa) R = ideal gas constant T = Temperature (K)

At 298K and converting to units so P is in torr and C is in molecules cm^{-3} the equation 2.10 may be derived from equation 2.9.

$$c = 3.234 \times 10^{16} \times p$$

Equation 2.10 – Re-arranged ideal gas law using units of torr. C= Concentration (molecule cm^{-3}), p = pressure (Torr).

If fractional purity of O_3 in the cell = f, the partial pressure of O_3 in the cell is equivalent to f X p and by combining this with equation 2.8, equation 2.11 is formed.

$$f = \frac{2.303 \times abs_{10}}{\sigma\, c\, l}$$

Equation 2.11 – The description of how partial pressure f relates to the beer lambert law (Equation 2.7). Abs = Natural log absorbance, σ = absorption cross section of O_3 (1.150×10^{-17} cm^2 $molecule^{-1}$ at 254nm), c=concentration (molecule cm^{-3}) and L=path length of the cell (10cm).

By substituting the concentration in equation 2.11 for the re-arranged ideal gas law using units of torr in equation 2.10, equation 2.12 is finally produced.

$$f = \frac{0.619 \times abs_{10}}{p}$$

Equation 2.12 – Relationship of fractional purity to pressure and absorbance of ozone sample. Abs = Natural log absorbance, p = pressure (Torr).

By using $P_2 \div f$ in place of P_2 in combination with the dilution calculations highlighted in section 2.5.3.1, the required dilutions of the ozone may be deduced to achieve the desired ozone concentration.

2.5.4 Static chamber preparation

2.5.4.1 VOC introduction

Initially, a cold finger (see 2.4.2/2.5.1) containing the hydrocarbon of interest was attached to the GHA and the GHA was evacuated (Figure 2.18, 1). After isolating the vacuum, a small pressure of alkene vapour was introduced into the GHA (Ca. 0.4 torr for high volatility VOCs and 0.2 torr for low volatility VOCs, Figure 2.18 2). The alkene vapour was then isolated in the 1L bulb and the rest of the GHA evacuated (Figure 2.18, 3). The vacuum line was once again isolated and synthetic air was then introduced to the GHA, and subsequently, the 1L bulb, to bring the alkene vapour to atmospheric pressure (Figure 2.18,4). The 1L bulb was then isolated and the GHA evacuated to leave a 1L sample of alkene at atmospheric pressure (Figure 2.18, 5).

Dilution of the sample was achieved by releasing the 1L sample of alkene vapour into a pre-evacuated GHA (Figure 2.18,6). The pressure of the GHA and bulb was then reduced in tandem to the desired value which corresponded to the desired concentration of alkene vapour (see section 2.5.3) (Figure 2.18,7). Once the desired pressure, and thus concentration, was reached; the 1L bulb was isolated, the GHA was evacuated (Figure 2.18,8) and then synthetic air was introduced to return the 1L bulb to atmospheric pressure (Figure 2.18, 9). The 1L bulb was then subsequently isolated leaving the desired concentration of VOC vapour (Figure 2.18, 10). This was repeated as required to achieve the desired VOC concentration.

The alkene sample was then introduced into the static chamber by first isolating the two side arms of the GHA to ensure airflow solely via the 1L bulb. Synthetic air was then introduced to the GHA and taps opened in succession from the air inlet towards the static chamber interface (Figure 2.18, 11). A bung was then placed in the air bubbler and air flowed in at a rate of 8L/min for 2 minutes. This allowed the contents of the 1L bulb to be displaced 16x and therefore maximised the amount of alkene vapour transferred to the static chamber. At the end of the introduction, the rubber bung was removed from the bubbler, the static chamber interface closed, the air isolated, the two side arms opened and the GHA evacuated (Figure 2.18, 1).

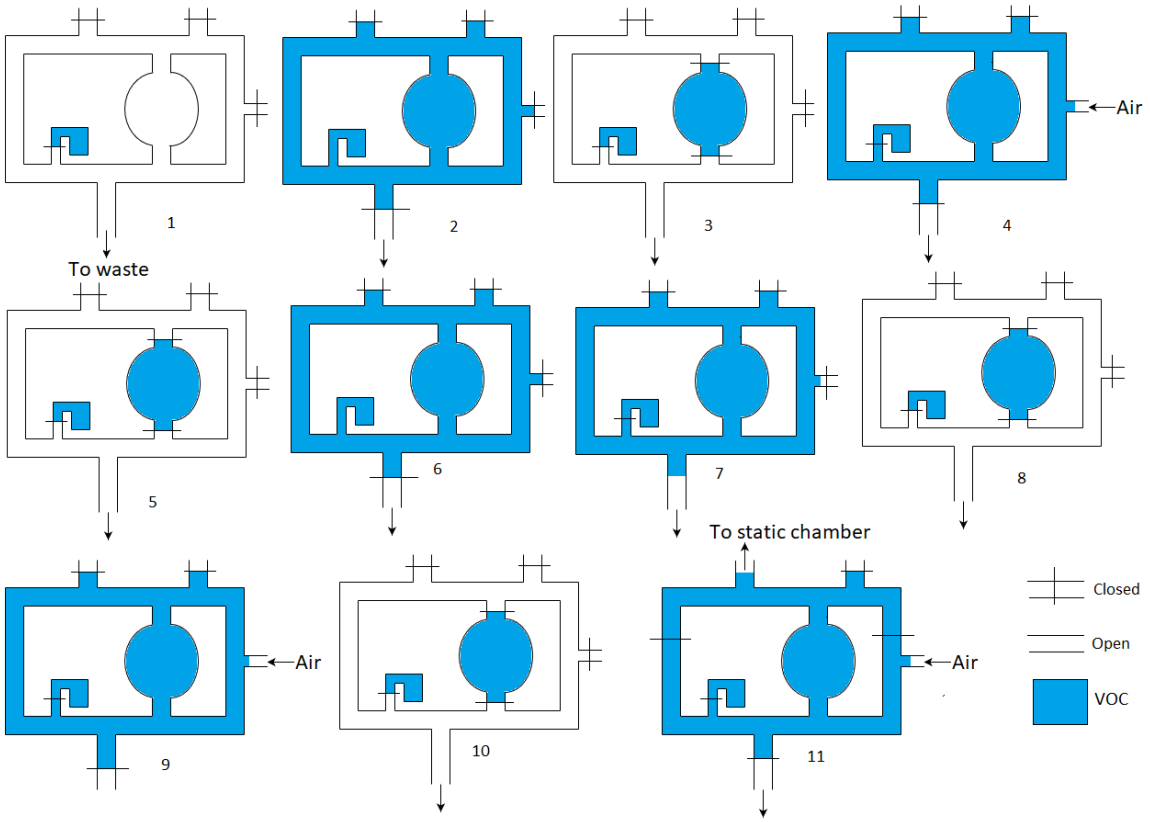

Figure 2.18 – Pictorial description of the process of using the gas handling apparatus for the introduction of a VOC sample ((1-5), its dilution (5-8) and its introduction to a static chamber (9).

Scavenger vapour was prepared in the same fashion as the alkene vapour with no dilution step (Figure 2.18, excluding 5-9). The air flowed at 8L/min for 1 minute. The reduction in flow time was accounted for due to the increased volatility of the scavenger used and therefore, a lower likely hood of scavenger deposition in the GHA.

2.5.4.2 Ozone introduction

Finally, O_3 was added to the static chamber. A gas cell was connected to the GHA and the GHA, the cell and the O_3 interface line between the O_3 trap and the GHA were evacuated (Figure 2.19, 1). The O_3 interface line was then isolated, and the trap connection valve opened to release the O_3/oxygen mix to fill the interface line. The GHA and cell were isolated from the vacuum and filled with a pressure of the O_3/oxygen mixture (Ca. 10-20 torr) (Figure 2.19, 2). Both the GHA and the cell were isolated respectively and the GHA was again evacuated (Figure 2.19, 3). The cell was then used in combination with UV-Vis spectroscopy to determine the purity of the O_3/oxygen mixture and subsequent dilutions (Figure 2.18,5-8) followed by an introduction to the static chamber (Figure 2.18,9) at a flow rate of 8L/min for 2 minutes took place accordingly.

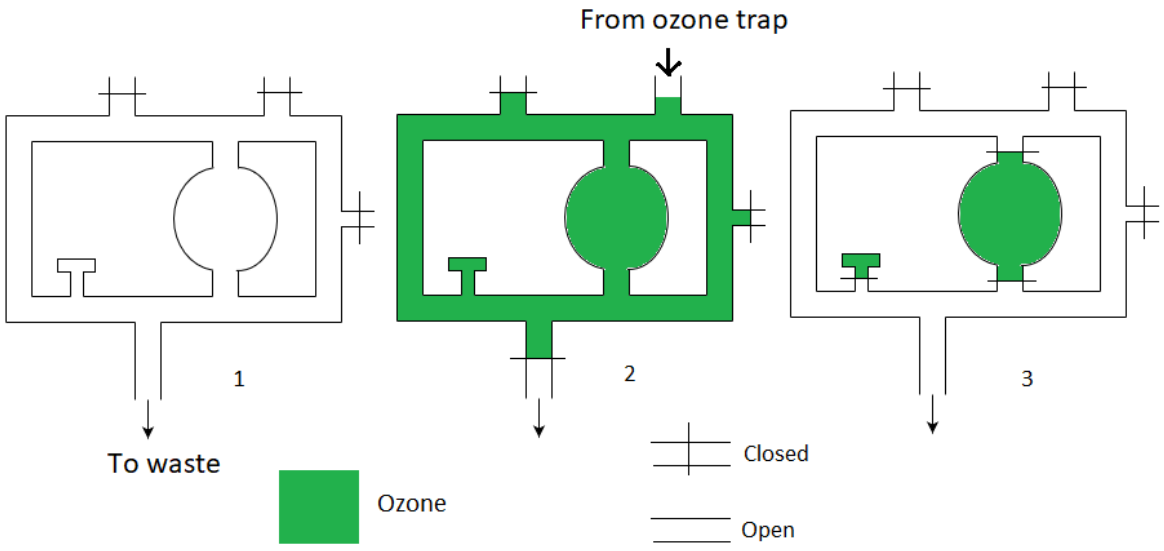

Figure 2.19 - Pictorial description of the process of using the gas handling apparatus for the introduction of an ozone sample.

For both SMPS and SPME-GC-MS experiments, a standard reaction time of 3 minutes 30 seconds took place from the moment the O_3 was introduced to the first SMPS scan or SPME sampling being initiated. A standard 40L static chamber volume was chosen for several reasons. Firstly, it maximises the number of sample bulb contents displacements that take place; therefore, maximising the amount of reactant transferred to the static chamber. Secondly, it was the minimum volume to achieve these displacements; therefore, allowing for the large reactant concentrations required to see a signal on the SMPS. And finally, to allow the maximum sampling time given the first two constraints.

2.5.5 Error estimations

When preparing static chambers two main error sources are apparent. The first being the uncertainty in the pressure gauge readings and the second being the synthetic air flow rate.

The pressure gauges give an uncertainty of 0.05 torr thus the maximum error possible when dispensing VOCs into the GHA during the study is ±17%. The synthetic air flow rate was calibrated using a water displacement technique where the time to displace a known volume of water from a vessel was recorded. This was undertaken once during the PhD. The calibration graph produced is displayed below (Figure 2.20). Wall loss of SOA particles is another area where uncertainty may be introduced into the values determined during this work; however, no corrections were made for wall loss.

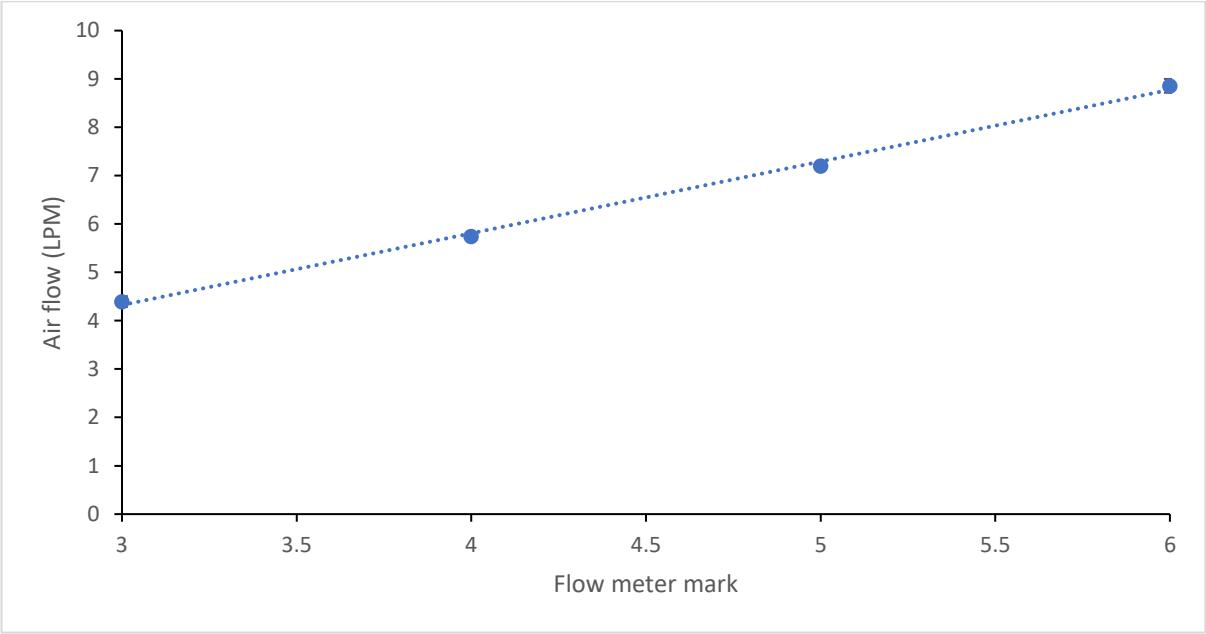

Figure 2.20 – Calibration graph for synthetic air flow into the GHA

2.5.6 Electroantennography (EAG)

Honeybees (*A.* mellifera), that had been collected in accordance with methods described in section 2.3.2, were chilled on ice until sedated before the bee's right antenna was excised. The final antennal segment was dissected, and the antenna placed between two KCl (0.1%) filled glass electrodes (Figure 2.14). The signal was then recorded using the IDAC 2 signal acquisition interface (Syntech, Germany) in combination with the EAGpro software (Syntech, Germany) (Spaethe et al. 2007).

Stimuli were prepared by applying 10µL of stimuli solution to a pre-cut filter paper (0.25cmx5cm, Grade 1, Whatman, Loughborough UK). The solution was allowed to evaporate for at least 10 seconds and then placed into a glass long-nosed Pasteur pipette. A CS-55 stimulus controller (Syntech, Germany) provided a continuous airflow which was charcoal filtered and subsequently moistened as a result of bubbling through tap water. The air was flowed at 560ml/min because this caused the least antennal noise as a result of poor electrical connection and was then blown through a glass mixing tube over the antennal preparation. The stimulus airflow was connected to the wide end of the pipette and the narrow end inserted into the hole in the mixing tube. A puff of stimuli (470ml/min, 0.2s) was applied to the antenna and the electrophysiological antennal response recorded. The flow rate of 470ml/min was chosen as this caused the lowest amount of antennal noise as a result of the airflow changes.

The response of each antenna to a blank control (air), negative control (hexane) and a positive control (linalool, 10^{-1}, Figure 2.21) was measured (Vuts et al. 2010). The responses to air, hexane and linalool were then compared to verify that the antenna only responded to the linalool stimuli and then experiments were initiated.

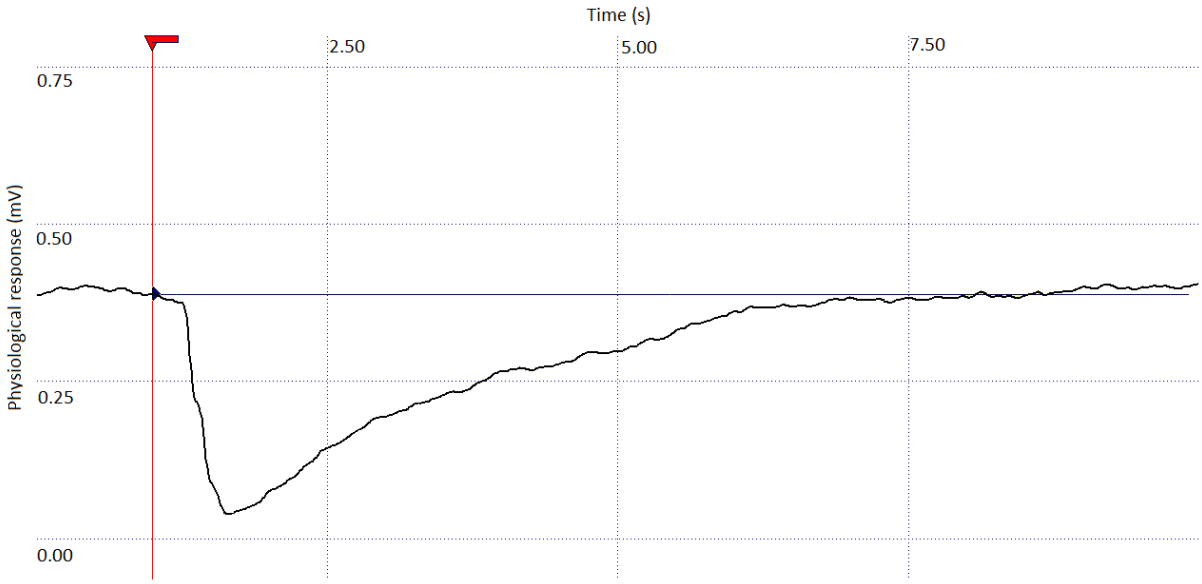

Figure 2.21 – An example physiological response of an *A. mellifera* antenna to linalool (10^{-1}) recorded using EAG, the red line marks stimulus delivery.

Stimuli were presented in a randomised order, and where appropriate from low to high concentration, to avoid carryover effects (Stelinski et al. 2003). At the end of the experiment, all three controls were presented again but in reverse order to verify the function of the antenna and to, where appropriate (see chapter) allow for normalisation of responses to account for the deterioration of the preparation (Vuts et al. 2010).

Chapter 3 - Exploring the effect of blend component degradation on the physiological ability of *A. mellifera* to detect selected VOC components from the blend of *B. napus*

3.1 Introduction

Blend ratio and intensity are key elements that effect how pollinating insects locate a flower (see chapter 1.4.3) and it has been shown that these elements may be perturbed as a result of blend degradation (see chapter 1.5).

The effect of changes in the ratios of VOCs within a blend, due to blend degradation, upon plant-pollinator chemical signalling has been investigated by several authors. McFrederick et al. (2008) initially modelled the effect of several realistic air pollution scenarios (comprised of mixtures of atmospheric oxidants such as O_3, NO_3 and OH) upon common VOCs. It was observed that VOC concentrations reduced over distance at differing rates thus, it was hypothesised that both the ratio and intensity of a blend under polluted air conditions are likely to be altered and the effectiveness of VOC mediated communication between a plant and a pollinator may be reduced.

The hypothesis set forward by McFrederick et al. (2008) has been tested experimentally, with several authors identifying qualitative changes in blend ratio upon mixing with atmospheric oxidants and subsequent behavioural effects. Girling et al. (2013) showed that, upon exposure to diesel exhaust emissions (primarily NO and NO_2), a synthetic blend of eight floral VOCs identified from oilseed rape (*Brassica napus* L.) showed complete loss of two VOCs and reductions to the concentration of the six remaining VOCs. Subsequent behavioural testing using Proboscis Extension Reflex (PER) experiments, where western honeybees (*Apis mellifera* L.) were trained to recognise an undegraded *B. napus* synthetic blend, found that a reduced PER response was seen when the bees were exposed to a *B. napus* synthetic blend that was missing the two diesel exhaust emission degraded VOC components . Farré-Armengol et al. (2016) also found alterations to VOC blend ratio upon exposure of the floral VOC blend produced by black mustard plants (*Brassica nigra* L.) to ozone at varying concentrations (80ppb, 120ppb) with the extent of the ratio perturbation increasing with time since ozone exposure. Subsequent behavioural testing using a buff-tailed bumblebee (*Bombus terrestris* L.) during flight arena behavioural experiments found that a behavioural preference for the undegraded blend.

Farré-Armengol et al. (2016) showed a clear behavioural effect of ozone exposure on blend preference; however, it is unclear if this change in behaviour was a result solely of blend ratio alteration or if other blend degradation factors, such as reaction product production, also contributed to the observed behavioural effects. The work of Girling et al. (2013) explored the effects of blend ratio alteration as a result of diesel exhaust exposure in isolation of other blend degradation factors; however, it only does so for one discrete situation where two VOCs are completely removed.

The aim of this chapter was to create a model that is capable of exploring the effect of blend ratio alteration, as a result of ozone exposure, on the electrophysiological response of *A. mellifera* both in isolation of other blend degradation factors and at varying degrees of ozone exposure. The objective was to use the model to characterise the effect of blend ratio alteration on ecologically relevant spatial scales such as the foraging distance of an insect. To achieve this, modelling was undertaken to represent an oilseed rape (*B. napus*) – western honeybee (*A. mellifera)* system and describe the rate of degradation of five selected VOCs under two reactant scenarios using a parsimonious model parameterised with reaction rate constants from the scientific literature. Subsequently, electroantennography (EAG) dose-response relationships for honeybee antennae were formulated for all five VOCs and the degradation modelling was then combined with the dose-response EAG data. This created a final model that was used to evaluate how a physiological response may change at different distances from a floral odour source under both VOC excess and ozone excess conditions in comparison to no ozone conditions. In parameterising the model, antennal response was measured as opposed to behavioural response during this work (see section 2.1.3 for further rationale).

3.2 Materials and methods

3.2.1 Establishment of a model system

As detailed in section 2.1.1, a *B. napus – A. mellifera* model system was selected due to both of the organism's prominence in British agriculture as well as the wealth of literature surrounding these species (Blight et al. 1997; Wright and Smith 2004; Kluser and Peduzzi 2007). Using a list of floral volatiles of *B. napus* created from literature (Evans and Allen-Williams 1992; Jakobsen et al. 1994; Blight et al. 1997), a model floral blend consisting of Z-3-hexenol, Z-3-hexenyl acetate, 1-undecene, 1-dodecene and 3-carene was selected as a result of each VOCs suitability to several criteria (reactivity with ozone, commercial availability, lack of crossover with the postdoc project running alongside this one, see section 2.1.1). An approximation was made of the distance that VOC blends may prove useful to our model organism, *A. mellifera*, of 400m. This is the mean foraging distance identified for *A. mellifera* in the literature. A wind speed of 1m s^{-1} was assumed for modelling calculations.

3.2.2 Construction of a VOC degradation model

The rate of reaction is linked to the concentration of reactants via a rate constant (k) as displayed in equation 1. k is constant for each compound regardless of reactant concentration but may be affected by other attributes such as temperature and pressure (see section 2.2.1).

$$\frac{dv}{dt} = k[A][B]$$

Equation 3.1 - *dv/dt* = change in concentration over time, k = rate constant (molecule^{-1} cm^3 s^{-1}), [A] = concentration (molecule cm^{-3}), [B] = concentration (molecule cm^{-3}).

Equation 3.1 was used in combination with the starting concentrations of reactants and rate constants to deduce the rates of reaction, as exemplified in equation 3.2 (reactants are often quantified in units of parts per million (ppm) and are converted to units of molecule cm^{-3} using the methodology described in Hobbs (2002)).

$$\frac{dv}{dt} = 4.5 \times 10^{-17} cm^3 molecule^{-1} s^{-1} \times 2.46 \times 10^{13} molecule\ cm^{-3} \times 9.84 \times 10^{13}\ molecule\ cm^{-3}$$

$$\frac{dv}{dt} = 1.186\text{x}10^{11}\ \text{molecule}\ cm^{-3} s^{-1}$$

Equation 3.2 – Derivation of rate of reaction for 3-carene, assuming 4 ppm of ozone (ca. 9.84 x10^{13} molecule cm^{-3}) and 1ppm of 3-Carene (ca. 2.46x10^{13} molecule cm^{-3}). Rate constant for 3-carene = 4.5x10^{-17} cm^{3}molecule^{-1}s^{-1}.

The rate of reaction (result of Equation 3.2) was then used in combination with the time since the start of the reaction to elucidate the number of molecules that had reacted at timepoint x. This is summarised in equation 3.3.

$$\frac{dv}{dt} = 1.186\text{x}10^{11}\ \text{molecule}\ cm^{-3} s^{-1} \times 100s$$

$$dv = 1.186\text{x}10^{13}\ \text{molecule}\ cm^{-3}$$

Equation 3.3 – Use of equation 3.2 in combination with reaction time to find the number of molecules that have reacted over 100s.

The number of molecules that had reacted at timepoint x (result of Equation 3.3) was then used in combination with the initial reactant concentrations to determine the percentage loss of compound. This Is summarised in equation 3.4.

$$\%\ of\ compound\ left = \frac{C_i - C_x}{C_i}\ X\ 100$$

$$\%\ of\ compound\ left = 100\ \times \frac{2.46\text{x}10^{13}\text{molecule}\ cm^{-3} - 1.186\text{x}10^{13}\ \text{molecule}\ cm^{-3}}{2.46\text{x}10^{13}\ \text{molecule}\ cm^{-3}}$$

$$\%\ of\ compound\ left = 52\%, \%\ loss\ of\ compound = 48\%$$

Equation 3.4 – general equation for the percentage of initial compound remaining at timepoint x, C_i = Initial concentration (molecule cm^{-3}), C_x = Concentration at time x (molecule cm^{-3}), Equation 4 substituted with values to assess the percentage of 3-carene (1ppm) remaining at after 100 seconds of reaction with 4ppm ozone.

By altering the reaction time and the VOC rate of reaction, the VOC concentration over time can be modelled for any VOC at any time point. Time may be related to distance by multiplying time since reaction initiation in seconds by wind speed in units of ms^{-1}.

For simplicity, the effects of dilution on VOC concentration, and thus antennal response, are assumed to be negligible in this model. Literature shows that molecular diffusion is likely to be negligible (Vogel 1994; Koehl 2006); however, turbulent motion has been shown to alter VOC concentrations (Mylne and Mason 1991). It is, therefore, noted that this model is parsimonious relative to real world conditions.

3.2.3 Comparison of constructed VOC degradation model with a literature model

An initial study was undertaken to compare the outcomes of the more parsimonious model described in this work (3.2.2) to a less conservative, large eddy simulation (LES) model that incorporates complex fluid dynamics (Fuentes et al. 2016). Using the model developed in this chapter (3.2.2) in combination with parameters detailed in Table 3.1, concentration values of both β-myrcene and β-caryophyllene as a result of their reaction with ozone over distance were determined. It was noted that Fuentes *et al.* (2016) used a complex emission source of a ca.200m simulated field of emitters whereas this work used a single point emission source thus, for direct comparison, both studies were assumed to have started from the final point of emission (Figure 3.1).

Table 3.1 – Reactant concentration parameters used in the comparison of the model developed in this work with that from an LES determination model. [a] (Atkinson et al. 1999)

	Ozone concentration (ppb)	OH concentration (0.02 pptv)	VOC concentration (ppt)	Rate of reaction ($cm^3 molecule^{-1} s^{-1}$) [a]	Wind speed ($m\ s^{-1}$)
Fuentes *et al.*	20	0.02	10	4.7×10^{-16}	0.5
Current work	20	0	10	4.7×10^{-16}	0.5

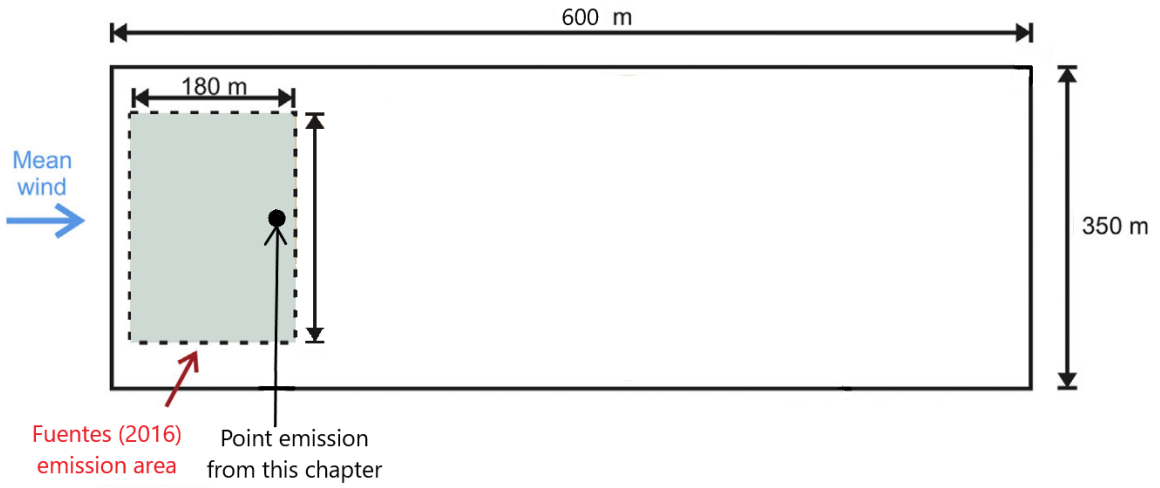

Figure 3.1 – Schematic adapted from (Fuentes et al. 2016) showing how both the LES model and the model developed in this chapter compare in consideration of emission point.

3.2.4 Literature VOC rate constant determinations

Experimental rate constant determinations for the reactions of ozone with the five VOCs used in these studies were collected from the literature (see appendix - AP1). Determinations with abnormalities, as described in their source papers, or that were not recorded at 298K±5K were discarded, thus removing the majority of clear outliers. The distribution of the values for each VOC exhibited little skew, therefore, the mean values of the rate constants were then calculated, and the resulting value used in further calculations.

3.2.5 Establishment of reactant concentration to be used in modelling under ozone excess and VOC excess conditions

The relationship of VOC concentration over distance under VOC excess and ozone excess conditions was explored (Z-3-hexenol was chosen for the comparison due to it having the fastest rate constant and thus, the greatest chance of identifying any differences in the data sets) to identify if trends observed while using ppm region modelling values represented trends seen while using ppb region modelling values. A 3x VOC excess and 4x ozone excess was chosen as these were used in the experimental work in this thesis due to being the maximum achievable concentrations given equipment constraints (see section 2.1.2). Initially, modelling was undertaken using Z-3-hexenol in the ppb region using values detailed in Table 3.2 to ascertain the relationship between ozone excess and VOC excess conditions at both low and high reactant concentrations. The reactant concentrations detailed in Table 3.2 were chosen because 20ppb has been used as a background ozone level in the literature (Fuentes et al. 2013) and is commonly seen in the environment (Fann et al. 2012) while 80 ppb has been identified to be the critical ozone concentration beyond which statistically significant changes in behaviour as a result of ozone exposure have been noted in various organisms during lab studies (Fuentes et al. 2013; Blande et al. 2015).

Table 3.2 – Reactant conditions used for modelling of VOC concentration over distance for Z-3-hexenol in the ppb region

	low concentration		high concentration	
	Ozone (ppb)	VOC (ppb)	Ozone (ppb)	VOC (ppb)
Ozone excess	20	5	80	20
VOC excess	20	80	80	240

Subsequent ppm region modelling was undertaken using Z-3-hexenol and the values detailed in Table 3.3 to once again ascertain the relationship between ozone excess and VOC excess conditions at both low and high reactant concentrations.

Table 3.3 – Reactant conditions used for modelling of VOC concentration over distance for Z-3-hexenol in the ppm region

	low concentration		high concentration	
	Ozone (ppm)	VOC (ppm)	Ozone (ppm)	VOC (ppm)
Ozone excess	1	0.25	4	1
VOC excess	1	3	4	12

The low concentration ppm region values for VOC excess (VOC=3ppm, ozone=1ppm) and ozone excess (VOC=0.25, ozone = 1ppm) were chosen to be used in further modelling as a result of displaying similar trends to ppb region data while being in the ppm region which was used in the rest of this thesis due to equipment sensitivity constraints.

3.2.6 Comparison of modelled VOC blend component concentration over distance using both ppm and ppb region reactant concentrations

The rate constants of the five study VOCs determined in section 3.2.4 were used in combination with the modelling methodology presented above (section 3.2.2) to produce models to estimate how VOC concentrations change over distance as a result of reaction with ozone in both the ppm and ppb regions, assuming constant wind conditions (Table 3.4). This allowed for any overestimation as a result of using ppm region values to be characterised.

Table 3.4 – Reactant conditions used for modelling of VOC concentration over distance for all five model VOCs to compare reductions in VOC concentration in the ppb and ppm region.

	ppm		ppb	
	Ozone	VOC	Ozone	VOC
Ozone excess	1	0.25	20	5
VOC excess	1	3	20	80

3.2.7 Parameterisation of literature VOC emission rates

For each of the five model VOCs, values for its percentage contribution to total VOC emission were derived from literature (Blight et al. 1997; McEwan and Macfarlane Smith 1998). No single paper listed percentage contributions for all five model VOCs. As a result, values for 1-dodecene and 1-undecene derived from Blight *et al.* (1997) were scaled so as to be comparable to values for other VOCs found by McEwan and Macfarlane (1998) (Table 3.5) and ultimately produce comparable emission values for all five compounds (Table 3.6). Scaling was undertaken by using the determinations for limonene in both Blight *et al.* (1997) and McEwan and Macfarlane (1998) as an intermediary to understand how values aligned between the two papers.

Table 3.5 – Experimentally determined percentage emissions of VOCs relative to the total determined emission for *B. napus* and determinations scaled to that of McEwan and Macfarlane 1998

	Mcewan and Macfarlane (1998) (%)	Blight *et al.* (1997) (%)	Blight *et al.* (1997) values Scaled to McEwan and Macfarlane 1998 (%)
limonene	19.93	1.95	19.93
1-undecene	-	8.67	16.38
1-dodecene	-	11.27	21.28

Subsequent values for all five VOCs were then converted to make them relative to the VOC with the largest percentage of emission (Z-3-hexenyl acetate) as shown in Table 3.6.

Table 3.6 – Floral VOC emissions of *B. napus* using scaled emission values from both Blight *et al.* 1997 and McEwan and McFarlane 1998. Values are then presented relative to Z-3-hexenyl acetate.

	Literature (%)	Relative to Z-3-hexenyl acetate (%)
3-carene	2.45	4.75
Z-3-hexenyl acetate	51.76	100
Z-3-hexenol	8.12	15.69
1-undecene	16.38	31.64
1-dodecene	21.28	77.66

The values for relative emission rates were subsequently applied to our VOC concentration over distance data. This was done by translating graphs so as the concentration at zero meters was equivalent to that found at the relative percentage concentration emitted of each VOC e.g., Z-3-hexenol was translated so zero meters was aligned to the concentration at 15.69% of VOC remaining.

3.2.8 Application of the model to the five-component model blend

The reactant scenario values chosen for this work (VOC excess, VOC=3ppm, ozone=1ppm, ozone excess, VOC=0.25, ozone = 1ppm) were used in conjunction with the aforementioned model to illustrate the composition of a VOC blend over distance upon reaction with ozone. The Model outputs were subsequently adjusted to account for VOC relative emission rates as described in section 3.2.7 to give equivalent starting reactant concentrations detailed in Table 3.7. Note that the two reactant scenarios produce equivalent rate constant data and thus, only the ozone excess scenario is presented.

Table 3.7 – Ozone excess reactant concentrations (ppm) formulated from application of relative emission rates (Table 3.6) to ozone excess reactant scenario compound concentrations (VOC=0.25, ozone = 1ppm).

	Ozone (ppm)	VOC (ppm)
3-carene	0.04	0.01
Z-3-hexenyl acetate	1.00	0.25
Z-3-hexenol	0.32	0.04
1-undecene	0.32	0.08
1-dodecene	0.76	0.19

3.2.9 Electroantennography

A dilution series was created by dissolving VOC standards in n-hexane to create the concentrations shown in Table 3.8. All VOCs were tested on the 10^{-5}-10^{-1} dilution scale; however, for 1-dodecene and 3-Carene this scale was expanded to range from 10^{-6}-10^{-0}, as a result of low antennal responses to verify that a real physiological response trend was being seen and the collected data was not noise.

Table 3.8 – Dilution series table for five model VOCs used in EAG experiments where Y= Dilution was prepared and N= Dilution was not prepared.

	10^{-6}	**10^{-5}**	**10^{-4}**	**10^{-3}**	**10^{-2}**	**10^{-1}**	**$10^{-0.5}$**	**10^{-0}**
Solution concentration	1µg/mL	10µg/mL	100µg/mL	1mg/mL	10mg/mL	100mg/mL	500mg/mL	1g
Mass presented	10ng	100ng	1µg	10µg	100µg	1mg	5mg	10mg
Z-3-hexenol [a]	N	Y	Y	Y	Y	Y	N	N
Z-3-hexenyl acetate [b]	N	Y	Y	Y	Y	Y	N	N
1-dodecene [c]	Y	Y	Y	Y	Y	Y	Y	Y
1-undecene [d]	N	Y	Y	Y	Y	Y	N	N
3-carene [e]	Y	Y	Y	Y	Y	Y	Y	Y

[a]Z-3-hexenol (sigma-Aldrich, 98%), [b]Z-3-hexenyl acetate (sigma-Aldrich, 99%), [c]1-dodecene (sigma-Aldrich, 99%), [d]1-undecene (sigma-Aldrich, 97%), [e]3-carene (sigma-Aldrich, 99%),

EAG assays were prepared and conducted as described in section 2.4.8 with stimuli presented from low to high concentration in a randomised stimuli order to avoid carryover effects (Stelinski et al.

2003). The normalisation of responses was undertaken post experiment to account for the deterioration of the preparation (Vuts et al. 2010).

3.2.10 Electrophysical response normalisation and addition of limits of saturation and detection

To account for antennal deterioration during the progress of an experiment, a positive control (linalool, 10^{-1}) was applied at the beginning and end of testing. The data was subsequently normalised by the EAGpro software (Syntech, Germany), in reference to the electrophysiological responses to the positive control, to account for any antennal deterioration.

Data below the activation threshold, defined as "The lowest dose at which the lower limit of the standard error of the mean response was greater than the upper limit of the standard error for the lowest dilution tested", and above the saturation point, defined as "The lowest dose at which the mean response was equal to or less than the previous dose", was subsequently disregarded according to the methodology presented in Germinara et al. (2009).

Logarithmic relationships were then fitted to the data sets using Microsoft Excel® and the equations of the relationships between antennal response and concentration were derived.

3.2.11 Model of changes in antennal response over distance under both no and 1ppm ozone

The three model fits describing; percentage concentration of VOC versus antennal response, percentage concentration of VOC versus distance from emission in the absence of ozone and percentage concentration of VOC versus distance from emission in the presence of 1ppm ozone were combined to produce two relationships describing; antennal response versus distance from emission in the absence of ozone and antennal response versus distance from emission in the presence of ozone for all five VOCs. Both models considered VOC relative emission rates by using equivalent reactant concentrations as described in section 3.2.7. It is presumed that for modelling with no ozone, a reaction would not take place and thus, VOC concentration and the resulting antennal response would stay constant (see 3.2.2).

The data for all five blend components are presented in unison so as the relative ratios of antennal response over distance may be compared.

3.3 Results

3.3.1 Comparison of constructed VOC degradation model with a literature model

For the reactions of β-myrcene and β-caryophyllene with ozone, the outputs of the model developed in this work and the LES experiments of Fuentes *et al.* were plotted and compared (Figure 3.2). The

values produced by the model used in this chapter show good agreement with the LES modelling values for β-myrcene while β-caryophyllene shows a lower level of agreement.

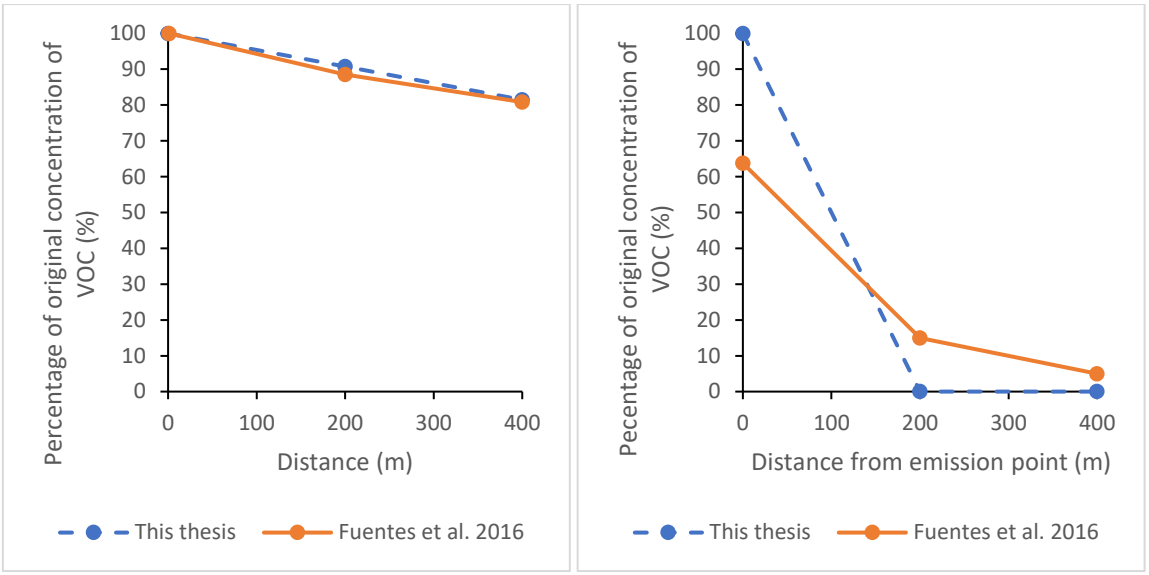

Figure 3.2 – Comparison of values from the model presented in this chapter and LES experiments from Fuentes *et al.* for β-myrcene (Left) and β-caryophyllene (Right). VOC=10ppt, ozone = 20ppb, Wind speed =0.5m s^{-1}

3.3.2 Rate constant determination from literature

Literature rate constant values for the five VOCs being studied that conform to the methodology set out in section 3.2.4 are presented in appendix section AP1. The mean rate constants used in the rest of this chapter are displayed in Table 3.9.

Table 3.9 – Summary of mean literature derived rate constants for the five VOCs used in this thesis. a=standard error of literature values, b= standard error from Ghalaieny et al. (2012).

Z-3-hexenol (cm^3 $molecule^{-1}s^{-1}$)	Z-3-hexenyl acetate (cm^3 $molecule^{-1}s^{-1}$)	3-carene (cm^3 $molecule^{-1}s^{-1}$)	1-dodecene (cm^3 $molecule^{-1}s^{-1}$)	1-undecene (cm^3 $molecule^{-1}s^{-1}$)
$6.0x10^{-17}\pm0.1^a$	$5.7x10^{-17}\pm0.2^a$	$4.5x10^{-17}\pm0.4^a$	$1.2x10^{-17}\pm0.2^a$	$1.0x10^{-17}\pm0.1^b$

3.3.3 Establishment of reactant concentration to be used in modelling under ozone excess and VOC excess conditions

Models exploring the degradation of VOCs over distance under both ozone excess and VOC excess conditions and at high and low reactant concentration were formulated both in the ppb (Figure 3.3) and ppm (Figure 3.4) regions.

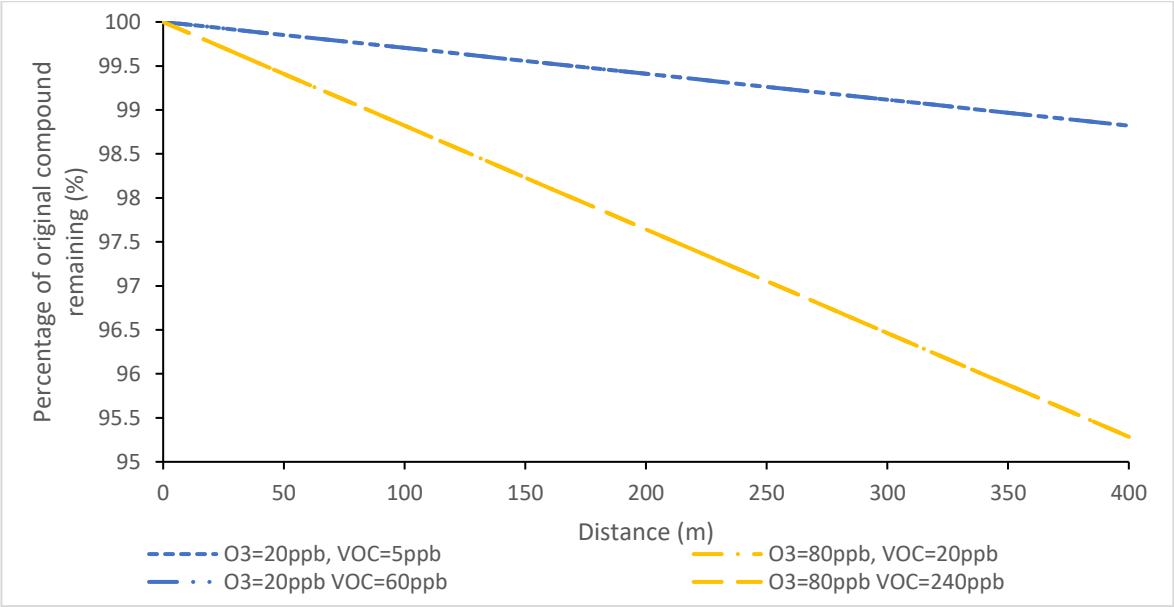

Figure 3.3 – Plot of the percentage of original VOC concentration versus distance in the ppb region for Z-3-hexenol under excess ozone conditions and VOC excess conditions at high (yellow) and low (blue) concentration and a constant wind speed (1m/s). Note, the low concentration data sets (O_3=20ppb, VOC=5ppb/ O_3=20ppb, VOC=60ppb) and high concentration data sets (O_3=80ppb, VOC=20ppb/ O_3=80ppb, VOC=240ppb) lie on top of each other.

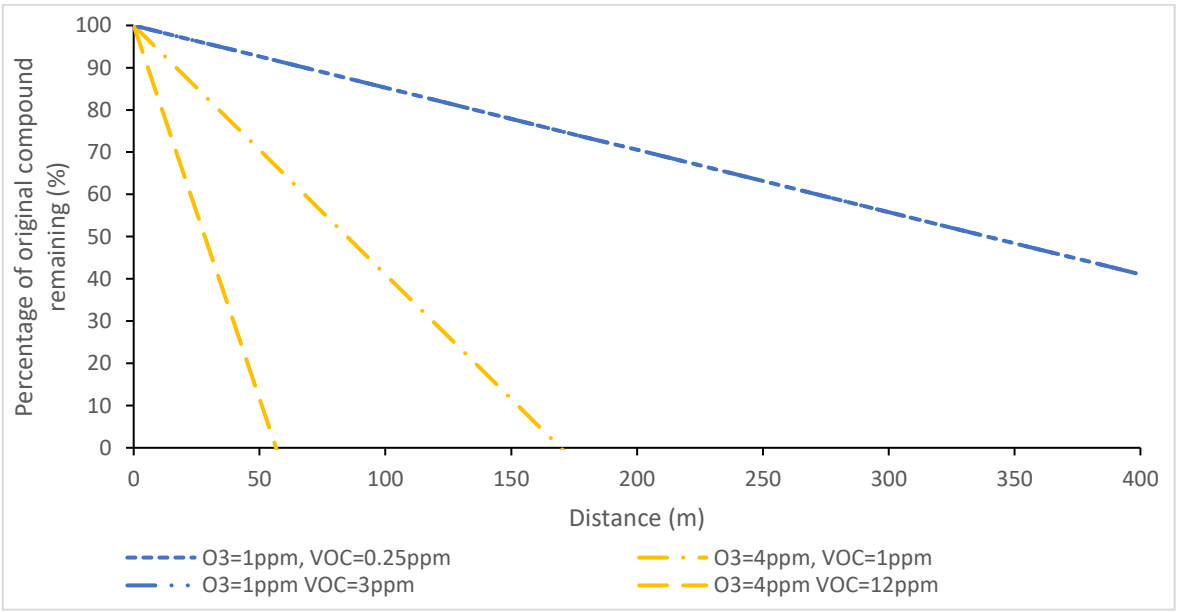

Figure 3.4 – Plot of the percentage of original VOC concentration versus distance in the ppm region for Z-3-hexenol under excess ozone conditions and VOC excess conditions at high (yellow) and low (blue) concentration and a constant wind speed (1m/s). Note, the low concentration data sets (O_3=1ppm, VOC=0.25ppm/ O_3=1ppm, VOC=3ppm) lie on top of each other.

For ppb region modelling (Figure 3.3) the ozone excess and VOC excess data sets were equal at both low (blue) and high reactant concentrations (yellow). The low concentration data set (blue) showed a

shallower gradient in comparison to the high concentration data set (yellow). The ppm region modelling (Figure 3.4) showed the ozone excess and VOC excess data sets were equal at low reactant concentration (blue) and increasingly divergent over distance at high reactant concentrations (yellow). Once again, the low concentration data set (blue) showed a shallower gradient in comparison to the high concentration data set (yellow). It was observed that low concentration ppm region values (O_3=1ppm, VOC=0.25ppm/ O_3=1ppm, VOC=3ppm) most closely replicated the trends seen in the ppb region and as such, these concentration values were selected for use in further experiments.

3.3.4 Comparison of modelled VOC blend component concentration over distance using both ppm and ppb region reactant concentrations

Modelling in both the ppb region (Figure 3.5) and the ppm region (Figure 3.6) demonstrated that 1-undecene showed the slowest rate of degradation while Z-3-hexenol showed the fastest rate of degradation. However, the change in concentration over distance was more rapid under the ppm modelling scenario for all VOCs.

For sake of continuity, reactant concentration values used in the experimental work of this thesis (Figure 3.7, O_3=1ppm, VOC=0.25ppm/ O_3=1ppm, VOC=3ppm) were used in further modelling and thus, the relationship between the percentage of original VOC concentration and distance for this modelling was derived from Figure 3.6 and is summarised in Table 3.10.

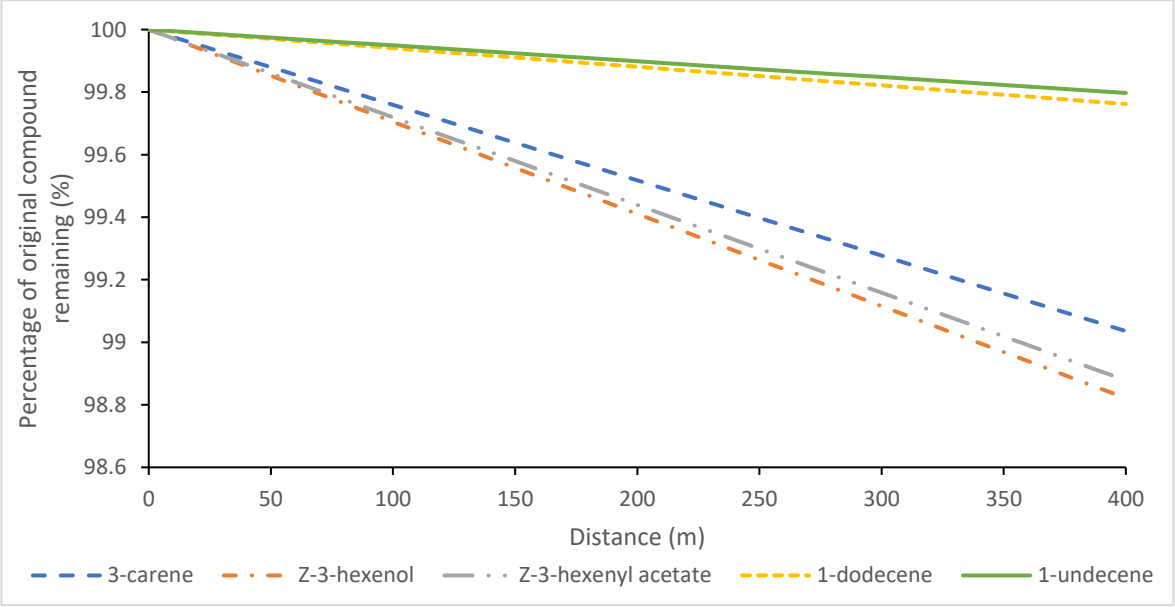

Figure 3.5 – Plot of the percentage of original VOC concentration versus distance for all 5 study VOCs (5ppb) under excess ozone conditions (20ppb) and a constant wind speed (1m/s). Due to the concentrations chosen this is equal to the modelling for distance for all 5 study VOCs (80ppb) under excess VOC conditions with ozone in a minority (20ppb) and constant wind speed (1m/s).

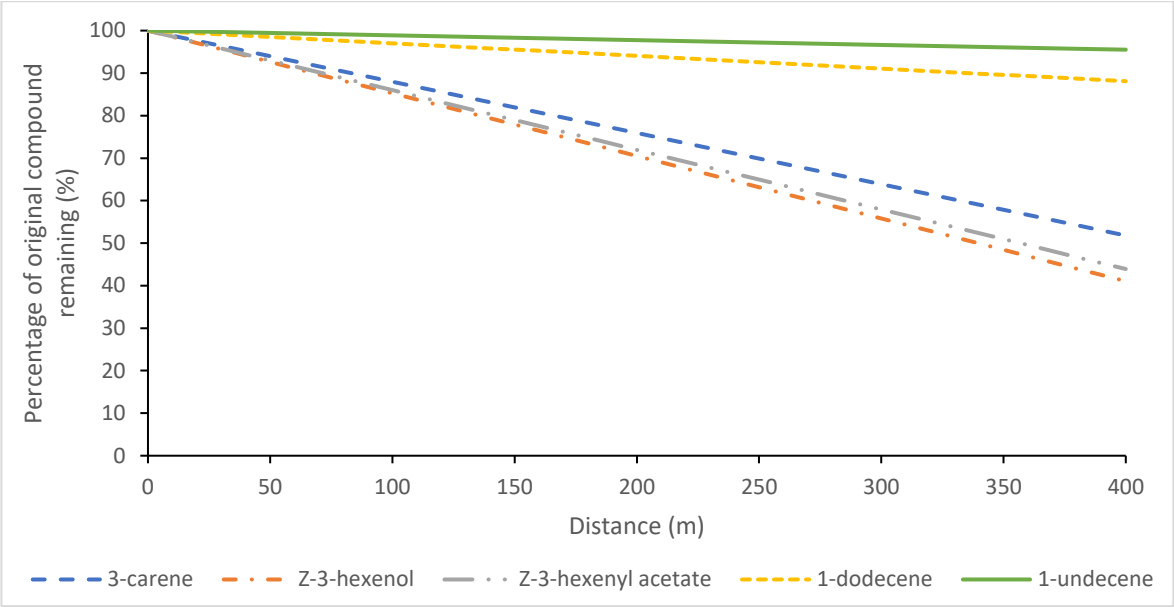

Figure 3.6 – Plot of the percentage of original VOC concentration versus distance for all 5 study VOCs (0.25ppm) under excess ozone conditions (1ppm) and a constant wind speed (1m/s). Due to the concentrations chosen this is equal to the modelling for distance for all 5 study VOCs (3ppm) under VOC excess conditions with ozone in a minority (1ppm) and constant wind speed (1m/s).

Table 3.10 –Equations relating percentage left of VOC to distance under both excess ozone conditions (VOC=0.25ppm, O_3 = 1ppm) and excess VOC conditions (VOC=3ppm, O_3 = 1ppm) which are equal at this set of reactant concentrations. Based upon data shown in Figure 3.7. [a]=standard error of literature values, [b]= standard error from Ghalaieny et al. (2012).

Compound	Rate constant ($cm^3molecule^{-1}s^{-1}$)	Line equation
3-carene	$4.5x10^{-17}$±0.4[a]	Y=-0.1206x+100
1-dodecene	$1.2x10^{-17}$±0.2[a]	Y=-0.0300x+100
1-undecene	$1.0x10^{-17}$±0.1[b]	Y=-0.0252x+100
Z-3-hexenol	$6.0x10^{-17}$ ±0.1[a]	Y=-0.1476x+100
Z-3-hexenyl acetate	$5.7x10^{-17}$±0.2[a]	Y=-0.1402x+100

3.3.5 Application of the model to the five-component model blend

Over a 400m scale, the ratio of blend components changed as the distance from emission increased, which is as a result of differences in the rates of reaction of individual blend components (Figure 3.7, left). It was also seen that the total concentration of the blend decreased over distance (Figure 3.7, right).

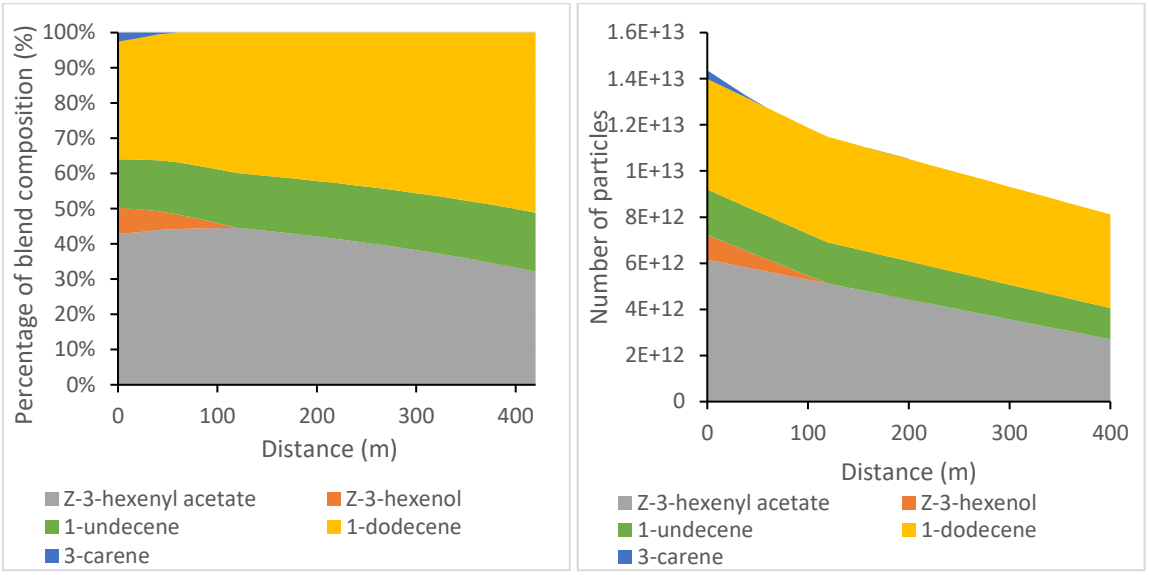

Figure 3.7 – 5 component, relative emission, VOC Blend (Z-3-hexenyl acetate = 0.25ppm, 1-dodecene = 0.19ppm, 1-undecene = 0.08ppm, Z-3-hexenol = 0.04ppm, 3-carene = 0.01ppm) composition over time upon ozone degradation under excess ozone (Z-3-hexenyl acetate = 1ppm, 1-dodecene = 0.76ppm, 1-undecene = 0.32ppm, Z-3-hexenol = 0.32ppm, 3-carene = 0.04ppm) conditions at a wind speed of 1m/s. normalised to 100% (left) and raw counts (right). Note that ozone excess data is equivalent to VOC excess data for the concentrations used in this work. Equivalent starting concentrations are listed as a result of methodology (see 3.2.7).

3.3.6 Electroantennography results

3.3.6.1 Mean Electroantennography dose-response graphs

All stimuli showed an increasing physiological response as stimuli concentration is increased. However, 3-Carene and 1-Dodecene reached a maximum at 10^{-1} and $10^{-0.5}$ respectively with the physiological response then decreasing as stimuli concentration was increased (Figure 3.8). This was hypothesised to be caused by saturation of the olfactory neuron (Deisig et al. 2006).

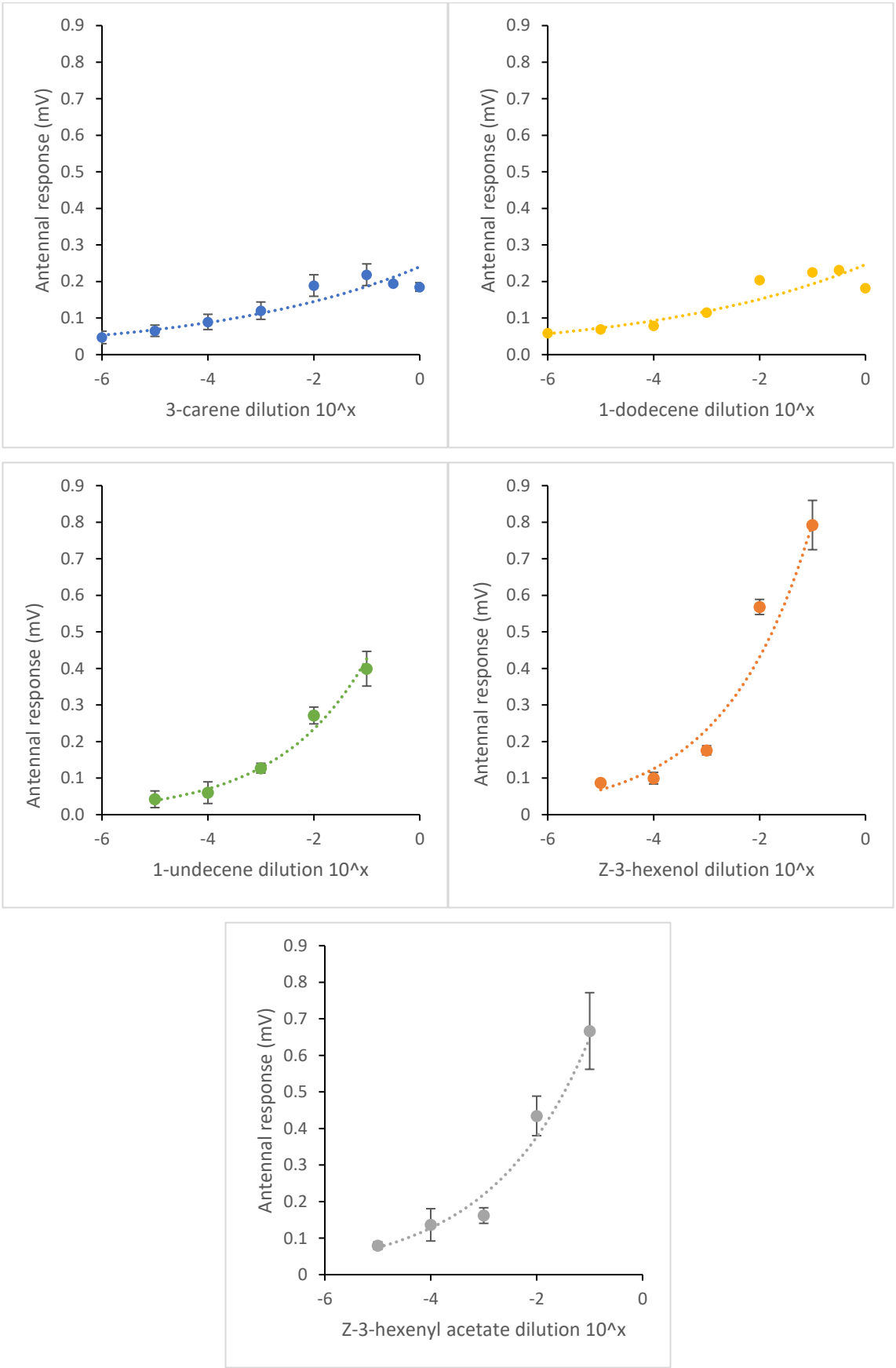

Figure 3.8 – Uncorrected EAG dilution response curves for *A. mellifera* for; 1-dodecene (n=12), 1-undecene (n=14), Z-3-hexenol (n=7), Z-3-hexenyl acetate (n=12) and 3-carene (n=10).

3.3.6.2 Mean EAG dose-response graphs considering limits of saturation and detection

The methodology described in section 3.2.10 was applied to the EAG dose-response graphs presented above (Figure 3.8) and the following physiological limits of detection and saturation were determined (Table 3.11). VOCs had differing rates of change in antennal response per unit change in concentration (Table 3.12/Figure 3.9) with Z-3-hexenol and Z-3-hexenyl acetate showing the greatest changes in antennal response per unit concentration change while 1-undecene and 1-dodecene showed the smallest changes in antennal response per unit concentration change. Differing levels of equation fit quality (R^2) were seen ranging from 0.91-0.99, thus introducing varying levels of error into calculations based upon these fits.

Table 3.11 – List of limits of detection and limits of saturation for dilution series of 5 model VOCs tested with *A. mellifera*, displaying dilution step and in parentheses the percentage concentration of the original VOC sample.

Compound	Limit of detection 10^x	Limit of saturation 10^x
3-carene	-4 (0.01%)	-1 (10%)
1-dodecene	-4 (0.01%)	-1 (10%)
1-undecene	-4 (0.01%)	-1 (10%)
Z-3-hexenol	-3 (0.1%)	-1 (10%)
Z-3-henxeyl acetate	-3 (0.1%)	-1 (10%)

The limits of detection and saturation (Table 3.11) were subsequently applied to the EAG response data (Figure 3.9) and the individual data sets combined to form Figure 3.10.

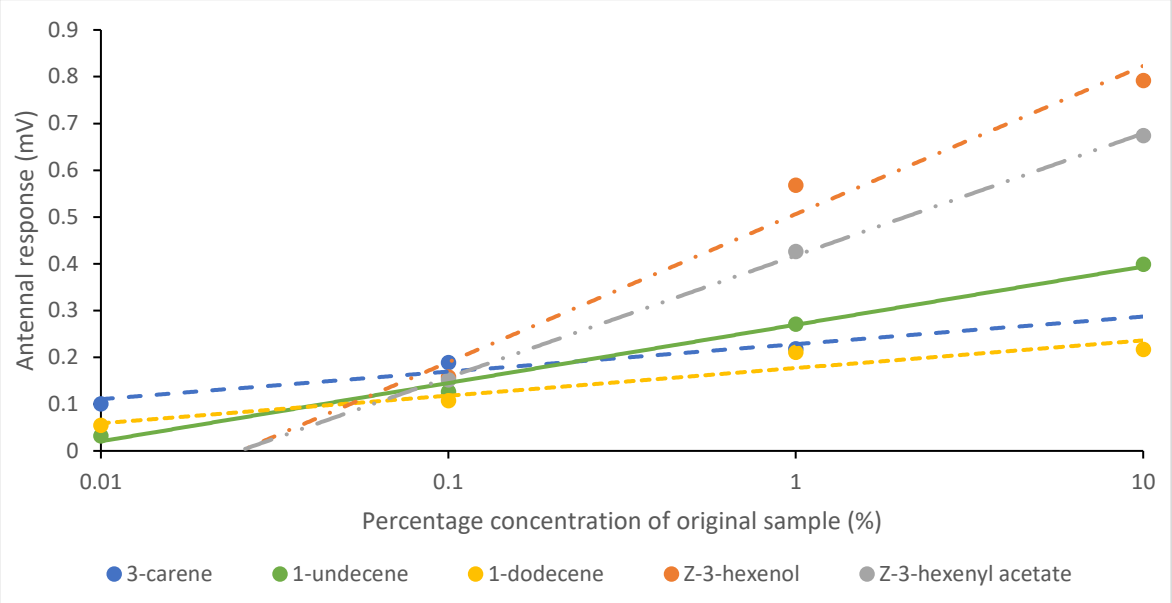

Figure 3.9 – Dilution response curves for the physiological responses of *A. mellifera* to all five model VOCs (see Figure 3.9) at concentrations bounded by the limits of detection and saturation (see Table 3.10) on a logarithmic scale. Logarithmic relationships are fitted to each data set. 1-dodecene (n=12), 1-undecene (n=14), Z-3-hexenol (n=7), Z-3-hexenyl acetate (n=12) and 3-carene (n=10).

Table 3.12 – Equations for the logarithmic relationships fitted to responses from the 5 model VOCs.

	3-carene	1-dodecene	1-undecene	Z-3-hexenol	Z-3-hexenyl acetate
Fitted equation	Y=0.0256+0.2283	Y=0.0256ln(x)+0.1771	Y=0.0541ln(x)+0.2697	Y=0.1376ln(x)+0.5062	Y=0.1133ln(x)+0.4178
R^2	0.9393	0.9136	0.9938	0.9722	0.9991

3.3.7 Visual representation of how antennal response varies over distance with and without ozone

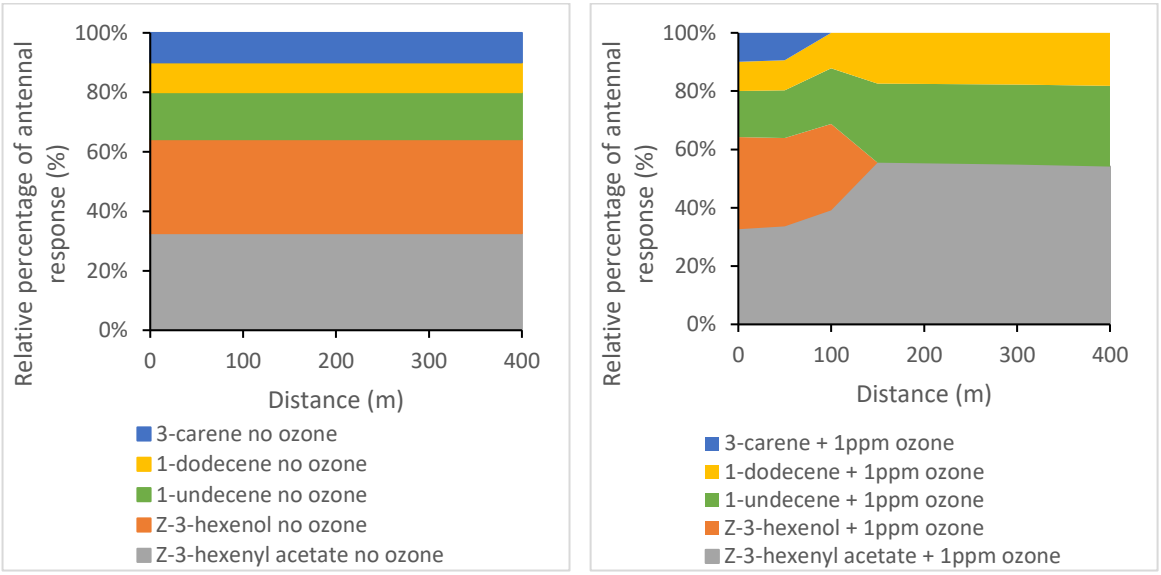

Figure 3.10 – Comparison of relative antennal response of *A. mellifera* to VOC stimuli (initial equivalent starting concentrations are; Z-3-hexenyl acetate = 0.25ppm, 1-dodecene = 0.19ppm, 1-undecene = 0.08ppm, Z-3-hexenol = 0.04ppm, 3-carene = 0.01ppm) over a 400m distance for no ozone (left) and a 4x ozone excess (right, initial equivalent starting concentrations are; Z-3-hexenyl acetate = 1ppm, 1-dodecene = 0.76ppm, 1-undecene = 0.32ppm, Z-3-hexenol = 0.32ppm, 3-carene = 0.04ppm) while considering relative emission rates.

Under no ozone conditions, antennal responses were constant while under 1ppm ozone, the relative proportions of antennal response per VOC varied over time with 3-carene and Z-3-hexenol showing no antennal response by 150m (Figure 3.10).

3.4 Discussion

A reasonable level of agreement was seen between the data produced by the model described in this work and the LES model used by Fuentes et al. (2016) (Figure 3.2). The deviation between the two models was seen more prominently for β-caryophyllene because it has a rate of reaction with ozone (1.09×10^{-14} $cm^3 molecule^{-1} s^{-1}$, Shu and Atkinson (1994)) which is 1000x faster than that of β-myrcene with ozone (1.25×10^{-17} $cm^3 molecule^{-1} s^{-1}$, Atkinson and Carter (1984)). β-myrcene data is most relevant due to its rate constant being more representative of the other VOCs studied in this work and it was seen that, while the deviation between the model data sets does occur for β-myrcene, the deviation was small up to 400m, the distance used in this comparison. The divergence of the two models is likely to be a result of the assumption of a constant rate of reaction but may also be due to a lack of consideration of side reactions and molecular diffusion. The effect of molecular diffusion at the distances studied are; however, thought to be minimal (Koehl 2006).

Modelling of the degradation of Z-3-hexenol in the ppm region (Figure 3.4) showed differences between ozone excess and VOC excess reactant concentrations for high reactant concentrations (yellow) but not for low reactant concentrations (blue). The lack of divergence between the two scenarios for low reactant concentrations (blue) is likely due to the parameters being mathematically equivalent. The same scenario would be expected to be displayed in the ppb region (Figure 3.3); however, both high and low reactant concentrations appear to show mathematical equivalence. This is a result of the low reactant concentrations used and when the graph is extrapolated, the high concentration data set diverges, replicating the trend seen in the ppm region. Modelling of all five VOCs in the ppb (Figure 3.5) and ppm (Figure 3.6) regions shows that the rate of degradation is greater in the ppm region due to the greater molecular concentrations and thus, a faster rate of reaction.

Modelling of the rate of degradation of a relative emission blend showed changes in both the total blend concentration as well as the relative ratio of its constituent VOCs over a 400m modelling distance (Figure 3.7). This result concurs with the results of modelling by McFrederick et al. (2008) and the experimental work of several authors (Girling et al. 2013; Farré-Armengol et al. 2016). Total blend concentration has been shown to be important for both successful olfactory discrimination and acceptability of the blend. Thus, the modelled reductions in total blend concentration may cause a reduction in discriminatory ability and or a lack of response to the blend (see section 1.4.3, Wright et al. 2002; Ditzen et al. 2003). Given that changes in VOC concentrations are likely to occur over the foraging distance of *A. mellifera* it is also important to understand how changes of this magnitude are likely to be perceived by the insect's antennae.

Modelling of relative antennal response over distance (Figure 3.10) showed constant relative antennal response over distance under no ozone conditions as no reaction, and thus no change in VOC concentration, took place and dilution was not accounted for in this model. However, under 1ppm ozone conditions, large changes in individual antennal responses were seen with both Z-3-hexenol and 3-carene eliciting no antennal response by 150m. The behavioural significance of this result cannot be drawn without behavioural testing; however, it may be inferred from experiments such as that undertaken by Girling et al. (2013), which showed that *A. mellifera* showed a decreased PER response to a trained synthetic floral blend with two components removed, that a transition to zero antennal response for two blend components, which may be seen as a proxy for removal of blend components, is likely to have a significant behavioural effect on our model pollinator.

However, due to overshadowing (see section 1.4.3, (Getz and Smith 1987)), if the compound(s) that transition to zero antennal response are not learnt to the same efficacy as other compounds in the VOC blend, their absence may not impede the efficacy of the blend to the same degree as if it was a VOC which was learnt to a high efficacy that was absent. Further to this, reductions in total blend

concentration and thus antennal response, as a result of ozone exposure may show a lesser impact because the level of overall concentration plasticity has been demonstrated to be species specific (see section 1.4.3). However, behavioural testing is needed to confirm if individual VOC removals are problematic (as a result of the compound of interest being overshadowed), as well as further studies/behavioural testing to characterise the extent of concentration perturbation that is acceptable for *A. mellifera*.

By comparing antennal response over distance (Figure 3.10) and VOC concentration over distance (Figure 3.7), it can be seen that changes in antennal response do not completely correlate with changes in VOC concentration. This may be observed by the high concentration of 1-dodecene (Figure 3.7) not corresponding in size to that of its antennal response (Figure 3.11). This is a result of the differing EAG dose-response relationships of each compound.

A comparison of the effects of reductions in blend component concentration on relative antennal response under both ozone excess and VOC excess conditions could not be drawn due to the reactant conditions chosen. It may, however, be inferred from earlier modelling (section 3.3.4, Figure 3.3) that there may be little difference at atmospherically relevant ppb concentrations at a 400m distance because even the high concentration reactant scenario showed negligible divergence in concentration between ozone excess and VOC excess scenarios.

It must be noted that the use of ppm region reactant concentration values during this modelling may over-estimate the reductions in VOC concentration over distance (Figure 3.5/3.6). This will mean that subsequent modelling of changes in antennal response may overestimate the extent of these changes and thus, changes to ratio may have less impact on bee electrophysiological detection than highlighted. It is also of note that, application of limits of detection and saturation to the EAG data (Figure 3.9) did not increase the parsimony of this modelling because it is unlikely that concentrations close to or above the limits of saturation are likely to be experienced in the real world. VOC emission rates for *B. napus* are in the range of 1-10ng floret^{-1} hour $^{-1}$ (Jakobsen et al. 1994) which is 10^6 lower than the 1mg presented at the lowest saturation limit (10^{-1}).

3.5 Conclusions

Overall Conclusions

This work produced a novel model that is able to, under differing environmental conditions and spatial resolutions, describe changes in antennal response as a result of reductions in VOC concentration as a result of ozone exposure, in isolation of other effects of ozone exposure of VOCs.

Modelling of changes in antennal response over distance for the model blend as a result of 1ppm ozone exposure with VOC relative emission rate considerations projected complete extinction of

antennal response for two compounds (3-carene, Z-3-hexenol) over a 400m distance. The modelling outcomes are seen as significant because the 100% reduction in antennal response is the result of a 100% reduction in VOC concentration and it has been shown experimentally that removal of blend components affects the ability of *A. mellifera* to recognise a floral blend during PER experiments (Girling et al. 2013). It is important to note, however, that to make this work comparable to the other chapters of this thesis, ppm region reactant concentrations were used. This means that the modelled changes in VOC concentration, and thus the modelled changes in antennal response, may be greater than that seen in the environment where ppb concentrations values are common.

It is envisaged that future work in relation to this modelling would attempt to increase its applicability to the real world as well as create the ability to predict the behavioural effect of changes in antennal response. Increased applicability to the real world would be achieved by using; ppb concentration values, a fluid dynamics VOC degradation model and more liberal EAG dose-response assumptions. To give the model the ability to predict the behavioural effect of changes in antennal response, experiments to test quantitative stepwise changes in both blend composition and antennal response are envisaged to ascertain any effects on behavioural response Another experiment of interest may be to compare electroantennography responses of individual VOCs within a blend to behavioural experiments which explore the redundancy of each VOC to blend attraction. This may then allow for the prediction, using simple electroantennography experiments, of whether the removal of individual VOC compounds from a blend as a result of ozone exposure may or may not hamper blend perception. A technically challenging experiment is also envisaged where changes in behaviour as a result of ozone-initiated changes in VOC concentration may be tested in isolation in a wind tunnel setting. Initially, a quantification method such as a PTR-MS or fast FID would be used to map how VOC concentrations of the blend evolve over distance in the wind tunnel under ozone degradation. Blends could then be prepared which replicate the level of blend degradation at varying distances with subsequent proboscis extension reflex measurements (PER) undertaken to determine what level of blend degradation is deemed acceptable.

Chapter 4 – Exploring the physiological response of *Apis mellifera* to degradation products from the reaction of selected *B. napus* floral VOCs with ozone

4.1 Introduction

Volatile organic compound (VOC) blends are complex in their ratio, consistency and intensity and are unique to the organism releasing the blend, thus allowing for resource discrimination by the blend receiver (Bruce et al. 2005; Bruce and Pickett 2011, see section 1.4). The effects of non-blend VOCs on blend efficacy is still unclear; however, it has been shown that the presence of non-blend VOCs may act to enhance, mask or have no effect on the attractiveness of the blend (see section 1.5.3, (Schröder and Hilker 2008; Wilson et al. 2015). The action of non-blend VOCs upon blend perception has been suggested to be related to the chemical similarity of the supplementary VOC(s) to those contained within the VOC blend (Riffell et al. 2014).

Non-blend VOCs may also be produced as a result of blend degradation (see chapter 1.5). Several authors have shown experimentally that VOC blends change upon mixing with ozone and have suggested, but not verified, the formation of new VOCs. Li et al. (2016) showed that upon exposure to ozone (50ppb, 100ppb), cabbage plant (*Brassica oleracea* L.) vegetative VOCs showed a statistically significant change in the ratio of the VOCs collected from their headspace with diamond back moth adults (*Plutella xylostella* L.) preferring undegraded cabbage plant VOCs during Y-tube olfactometer experiments. For plant-pollinator systems, Farré-Armengol et al. (2016) also found quantitative changes in floral blend ratio upon exposure of the floral blend of black mustard plants (*Brassica nigra* L.) to ozone at varying concentrations (80ppb, 120ppb) when sampling at various distances. In addition, Buff-tailed bumblebee (*Bombus terrestris* L.) showed a preference for the undegraded floral blend of black mustard plants during behavioural experiments in a flight arena.

While both experiments demonstrated changes in the ratio of the degraded blends as well as differences in the behaviour of a blend receiver to the degraded blend, neither experiment was able to verify the identity of blend oxidation products. Further to this, neither experiment managed to successfully ascertain if this change in behaviour was a result of either; the reduction in the concentration of the original blend and the resulting changes in blend ratio, or the production of new VOCs as a result of the ozonolysis of the original blend, or a combination of the two.

The lack of knowledge surrounding the effects of blend oxidation products on VOC communication has been highlighted by both Blande et al. (2015) and Jürgens and Bischoff (2016). It is plausible that VOC communication may be perturbed by blend oxidation products, due to their similarity to the parent blend component VOCs from which they are formed. For example, experimental work by Riffell et al. (2014) showed that VOCs that are structurally similar to the VOCs present in a blend can reduce the blend tracking ability of an organism. Behavioural effects of non-blend VOC oxidation

products have been shown experimentally by Mofikoya et al. (2020) who demonstrated a reduction in oviposition by *P. xylostella* on artificial *B. oleracea* leaves (glass microscope slides coated in epicuticular waxes) that had been coated in α-pinene oxidation products which indicated that oxidation products may be physiologically active.

Thus, this chapter aims to begin to fill this knowledge gap and explore the effect of blend degradation reaction products on a plant-pollinator interaction in isolation of the other effects of blend degradation such as changes in VOC ratios and SOA formation. The aim was to characterise blend degradation reaction products from a model blend and then conduct electroantennography (EAG) experiments with a model insect to ascertain if the resulting reaction products could be physiologically detected. An exploration of the effects of two extreme landscape scale situations (VOC excess, ozone excess, see section 2.1.2) upon the identity of reaction products was also undertaken.

An oilseed rape (*Brassica napus* L.) – honeybee (*Apis mellifera* L.) model system was chosen for this work with 1-undecene, 1-dodecene, Z-3-hexenol, Z-3-hexenyl acetate and 3-carene the VOCs of interest (see 2.1.1 for further rationale).

Initially, experiments to determine the nature of ozone induced oxidation products of the model VOCs were undertaken using an SPME-GC-MS (Solid phase microextraction-Gas chromatography-Mass spectrometry) methodology. Experiments using both individual VOCs as well as VOC mixtures were then undertaken to explore more closely any inter blend component interactions that may have occurred. For selected runs, a Tenax® collection system was used in addition to SPME, so as to capture the greatest breadth of reaction products (see 2.4.7 for a more in-depth rationale). Using EAG of a honeybee antenna, identified products were tested for electrophysiological activity at a single concentration. Reaction product standards were either acquired commercially or, where feasible, synthesised during this work.

4.2 Materials and methods

4.2.1 Liquid phase characterisation of unreacted blend VOCs using GC-MS

An aliquot of the reactant sample contained in the cold finger (1 drop from a long-nosed Pasteur pipette, see section 2.5.1 for cold finger preparation methodology) was dissolved in cyclohexane (5ml). The GC-MS run was prepared (using details from Table 4.1) and initiated with the sample injected (0.5µL) directly into the GC-MS inlet port (200°C). The resulting mass spectrum data was compared with the NIST 2011 database and retention times were also noted.

Table 4.1 – Trace GC-MS parameters used to analyse VOC oxidation product samples collected using SPME-GC-MS.

Column	DB-5 30m x 0.25mm x 0.25mm
Carrier gas	He, 100KPa, Constant pressure
Injector	Splitless, 200 °C
Oven Program	50°C held 1min 50°C - 250°C at 10°C/min 250°c held 2 min
Transfer line temperature	250°C
Quadrupole temperature	200°C
Ionisation type	EI mode (70eV)

4.2.2 SPME fibre selection

Due to the differing selectivity of SPME coatings (Table 2.4), it is important to select an appropriate SPME fibre in relation to the volatiles being captured (Augusto and Luiz Pires Valente 2002). From molecular predictions and literature evidence, a wide variety of oxidation products are expected from the reactions of ozone with the five model VOCs; however, a universal aldehyde functionality was expected with varying length of carbon chain.

Literature cites the use of PDMS/DVB, PDMS/CAR/DVB and 100 µm PDMS fibres for similar collections such as; static headspace extraction of grassland volatiles using 100 µm PDMS (Cornu et al. 2001), headspace extraction of *Allium cepa* L. flower volatiles using CAR/PDMS (Soto et al. 2015) and collection of floral volatiles from *Petunia hybrida* Hort. using 100 µm PDMS (Verdonk et al. 2003). However, PDMS/DVB and 100 µm PDMS fibres are not listed as being suitable for the potentially semi volatile as low molecular weight products produced as a result of the ozonolysis experiments undertaken in this work (chapter 2, Table 2.3). Thus, due to the wide variety of products and the need for potential semi-volatile trapping, a generalist fibre suited to both volatiles and semi volatiles was chosen in the form of the DVB/CAR/PDMS fibre (Merck, Gillingham UK). This choice of a generalist fibre, in combination with a static sampling methodology, means a potential reduction in sensitivity. To increase sensitivity, Tenax flow sampling was used for selected experiments to allow for potential isolation of products missed by SPME sampling.

4.2.3 Comparison of gas phase VOC sampling techniques

One ppm of pure Z-3-hexenyl acetate vapour was prepared using the gas handling apparatus (GHA) in a sampling bulb (1L), according to the method described in general methodology section 2.5.4. For SPME sampling, an SPME fibre (Merck, Gillingham UK) that had been previously desorbed in the GC

injection port (200°C, 5min, DVB/CAR/PDMS 50/30) was exposed to the gas phase sample (22±2°C, 30min). The GC-MS run was prepared (Table 4.1) and initiated, and the fibre inserted into the GC-MS inlet port (200°C, 3min). For Gas syringe sampling, the sample was allowed to stand in the sampling bulb for 5 minutes before a gaseous sample of 0.5ml was extracted. The GC-MS run was then prepared (using details from Table 4.1) and initiated with the sample injected directly into the GC-MS inlet port (200°C). For both samples peak area was subsequently determined using the Xcalibur® software and peak identity verified as a result of comparison with the NIST database and liquid characterisations (see 4.2.1).

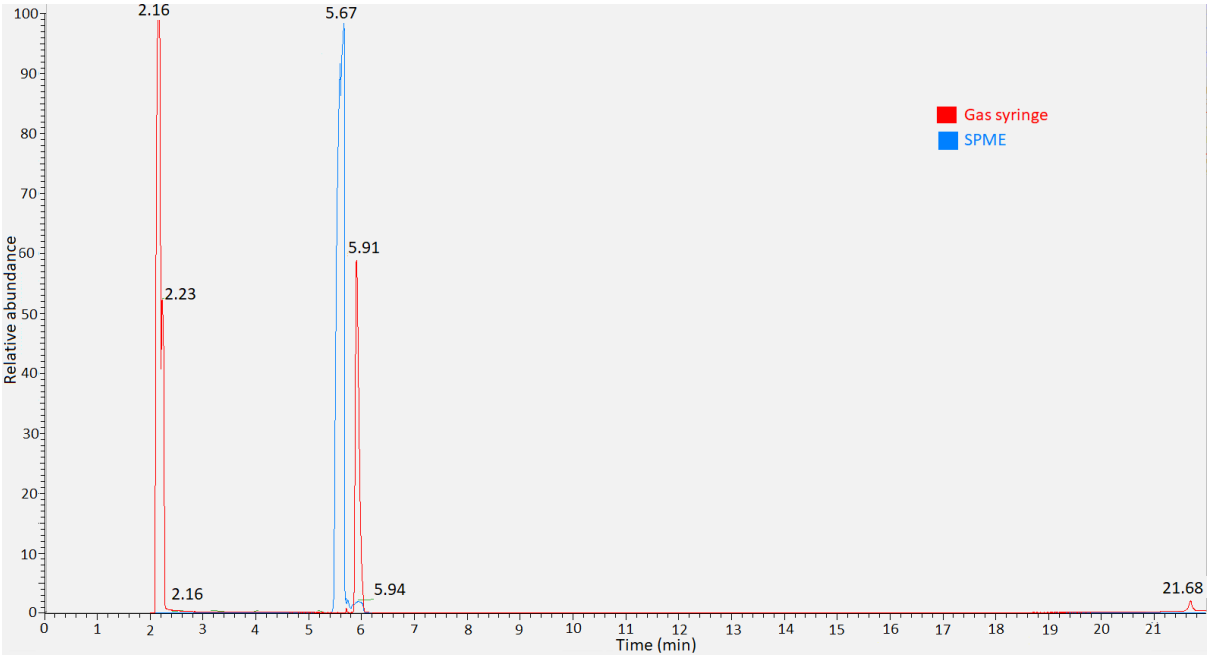

Figure 4.1 – GC-MS chromatograph trace of Z-3-hexenyl acetate (1ppm) sampled using SPME (blue, n=3) and gas syringe (red, n=3). Hexane (RT=Ca. 2.2 min), Z-3-hexenol (RT=5.67/5.94 (SPME), RT=5.91 (Gas syringe).

Table 4.2 – Peak height and area comparison for Z-3-hexenyl acetate at 1ppm sampled using both SPME and a gas syringe.

	SPME	Gas syringe
Peak height	$3.37e^{7}$	$1.94e^{6}$
Peak area	$7.16e^{7}$	$9.99e^{6}$

SPME sampling was chosen as the primary sampling method to be used in this chapter as it gave a greater peak height and area than gas syringe sampling (Table 4.2) and did not sample trace impurities (such as heavy fuel oil from the GHA, RT=21.68 min) unlike gas syringe sampling (Figure 4.1). A slight variation in retention time of Z-3-hexenyl acetate was seen which may be due to the

large amounts of Z-3-hexenyl acetate sampled using SPME causing peak splitting and or as a result of an alteration in K factor (see section 2.4.4).

4.2.4 Gas-phase characterisation of unreacted blend components by SPME-GC-MS

All five study VOCs had their retention times and mass spectra characterised using the SPME-GC-MS methods described in section 4.2.3. Cyclohexane was not used for these experiments.

4.2.5 Ozonolysis of individual blend components

4.2.5.1 Prediction of ozonolysis product

The general mechanism for ozonolysis (Figure 4.2) was used to predict primary reaction products by applying this general mechanism to the VOCs being studied.

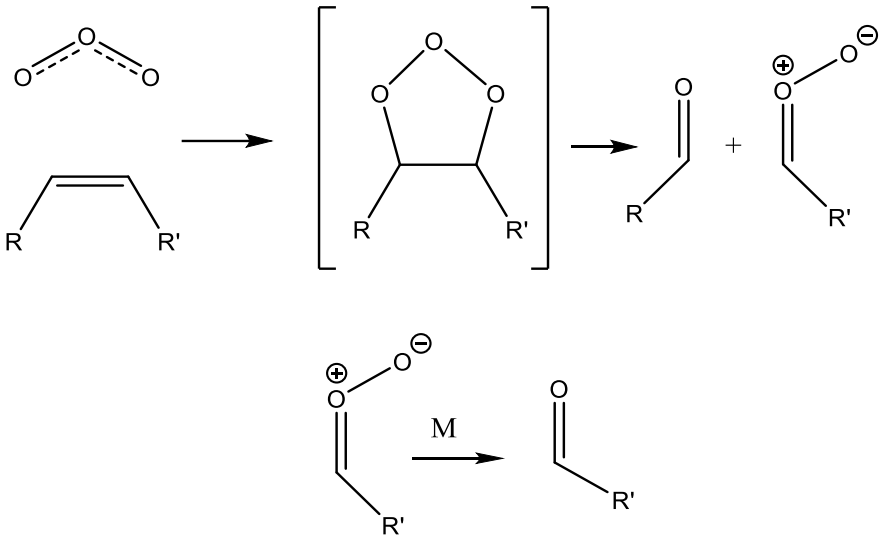

Figure 4.2 – Generic mechanism for the attack of ozone at a Carbon-Carbon double bond (C=C) followed by the stabilisation of the carbonyl oxide by a third body intermediate (M=N_2, O_2 etc.) adapted from Monks (2005).

Secondary reaction products may also form as a result of subsequent reactions of primary reaction products, however, they are often unique to each reaction with a myriad of potential formation mechanisms and as such, secondary reaction products were not predicted during this work.

4.2.5.2 Comparison of mass spectrum data to NIST spectral library

Reaction product determinations were made as a result of comparison of mass spectra with the NIST spectral database, matching with authentic standards as well as chemical intuition. NIST database comparisons are based on a similarity index which compares both the mass fragments present and their relative intensities, to library spectra. A score of 700—800 indicates a fair match, 800-900 a good match and >900 an excellent match with a hypothetical 1000 for a perfect match.

4.2.5.3 Acknowledgment of fluctuations in peak intensity and retention time

In this work, although peak intensities were observed to vary between VOC excess and ozone excess conditions, quantitative comparisons of peak intensities were not made. This was due to the low quantitative reproducibility of SPME (which was demonstrated during testing of a 1ppm Z-3-hexenol standard (see appendix AP3)). However, the qualitative reproducibility of peak presence was high with multiple concordant experiments (n≥3).

Fluctuations in compound retention time of up to 0.5min between runs were also noted which was likely a result of small alterations in the K factor (see section 2.4.4). For brevity, it will be assumed that there are no differences in compound identification as a result of changes in retention time <0.5min due to identical MS spectra being produced, unless otherwise stated.

4.2.5.4 Gas-phase reaction product characterisation using SPME-GC-MS

Static reaction chambers were produced using the GHA according to the methodology described in section 2.5.4 in combination with values presented in Table 4.3. Immediately after the sample was prepared in the static chamber, it was transferred into the GHA sampling bulb (1L, Atmospheric pressure) and an SPME fibre that had been previously desorbed (200°C, 5min, DVB/CAR/PDMS 50/30) was exposed to the reaction mixture (22±2°C, 30min). The GC-MS run (section 4.2.1, Table 4.1) was initiated and the fibre inserted into the GC-MS inlet port (200°C, 3min) and the resulting retention times noted and the mass spectrum data compared with the NIST 2011 database (NIST 2011).

Table 4.3 – VOC, ozone and scavenger mixing ratios used for the analysis of VOC oxidation products. All reaction conditions underwent SPME-GC-MS sampling while items marked with "*" underwent additional Tenax-GC-MS sampling.

VOC	ozone conc. (ppm)	VOC conc. (ppm)	cyclohexane (ppm)
3-carene	1	3	745
	1*	0.25*	64*
Z-3-hexenol	1	3	870
	1*	0.25*	74*
Z-3-hexenyl acetate	1	3	636
	1*	0.25*	55*
1-undecene	1	3	392
	1	0.25	33
1-dodecene	1	3	414
	1	0.25	36

4.2.5.5 Gas-phase characterisation by Tenax-GC-MS

Specific experimental conditions (Table 4.3, denoted with a *) underwent dual sampling using both SPME (Merck, Gillingham UK) and Tenax® TA (60-80 mesh, Merck, Gillingham UK) sampling techniques. Static chambers were produced using the GHA and sampled using SPME-GC-MS as above (see section 4.2.5.4) before the remaining contents of the static chamber were isolated from the gas handling apparatus and connected to the Tenax collection apparatus (Figure 4.3). 22.5L aliquots were collected onto desorbed Tenax filters (see section 2.4.7) using an electric pump (DYMAX 2, Charles Austen Pumps Ltd.). After collection, the filters were desorbed and qualified using an ATD-GC-MS system (see section 2.4.7 and see Table 4.4/4.5 for ATD and GC-MS parameters). Results were then compared against the NIST 2011 database (see section 4.2.5.2) as well as being compared with the corresponding SPME derived data.

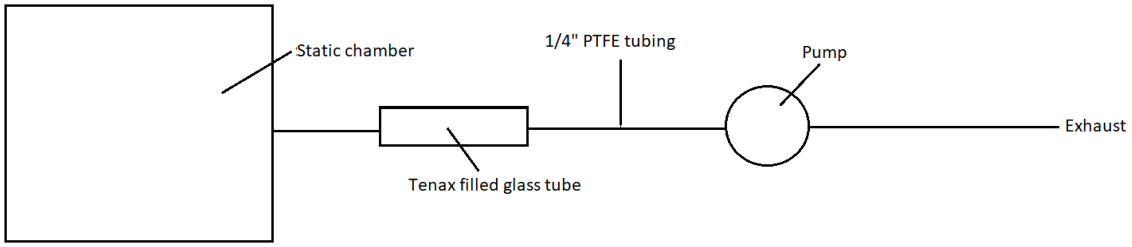

Figure 4.3 – A schematic of the Tenax sample collection apparatus (not to scale) that was used for Tenax-GC-MS experiments to analyse VOC oxidation products.

Table 4.4 – Perkin Elmer® turbomatrix® automated thermal desorption (ATD) unit parameters used to analyse VOC oxidation product samples collected using Tenax-GC-MS.

Tube temperature	320 °C
Tube Desorption time	5 minutes
Valve temperature	220 °C
Trap Low temperature	-30 °C
Trap High temperature	300 °C
Trap heating rate	40 °C/s
Trap temperature hold	10 minutes
Flow rate	100KPa
Transfer line temperature	255 °C
Desorption split flow	40ccm
outlet split flow	100ccm

Table 4.5 – Agilent® 7890A/5975C GC-MS parameters used to analyse VOC oxidation products samples collected using Tenax-GC-MS.

Column	**DB-5 30m x 0.25mm x 0.25mm**
Carrier gas	He, 100KPa, Constant Pressure
Injector	Split, 1:100, 250 °C
Oven Program	50°C held 1min 50°C - 91°C at 14°C/min 91°C - 95°C at 1°C/min 95°C - 120°C at 5°C/min 120°C - 250°C at 15°C/min 250°c held 2 min
Transfer line Temperature	350°C
Quadrupole temperature	150°C
Source temperature	230°C
Ionisation type	EI mode (70eV)

4.2.5.6 Characterisation of reaction product standards

Liquid samples of standards were prepared by dissolving neat compound (1 drop from a long nose Pasteur pipette) in cyclohexane (5ml) and injecting (0.5µL) into the trace GC-MS (see Table 4.1 for parameters) and the resulting retention time noted and the mass spectrum data compared with the NIST 2011 database (NIST 2011) as well as relevant SPME data to allow for ozonolysis product identification.

4.2.6 Ozonolysis of synthetic blends

4.2.6.1 Characterisation of synthetic blend

A blend of 5 components was produced in a cold finger (see section 2.5.1) according to Table 4.6. The blend was then characterised using SPME sampling (see section 4.2.5.4 for methodology), and the peak area of each component compared. It was seen that (Figure 4.4), although the initial liquid blend component ratios were equal, the ratio of gaseous components were not equal with a dominance of 3-Carene. This is likely due to the differing vapour pressures of the blend components. As a result, a refined formulation was produced according to Table 4.6 and treated as above and once again characterised using SPME sampling (see section 4.2.5.4 for methodology). The refined synthetic blend showed a far more equal ratio of components when peak areas were compared and thus, was used for further ozonolysis experiments.

Table 4.6 – Composition of initial and refined five VOC synthetic blend of which the refined synthetic blend was used to explore the effect of ozone exposure of VOCs as a blend as opposed to individual exposure.

VOC	Initial blend VOC volume (ml)	Refined blend VOC volume (ml)
3-carene	0.5	0.5
Z-3-hexenol	0.5	0.5
Z-3-hexenyl acetate	0.5	1.5
1-undecene	0.5	0.5
1-dodecene	0.5	0.5

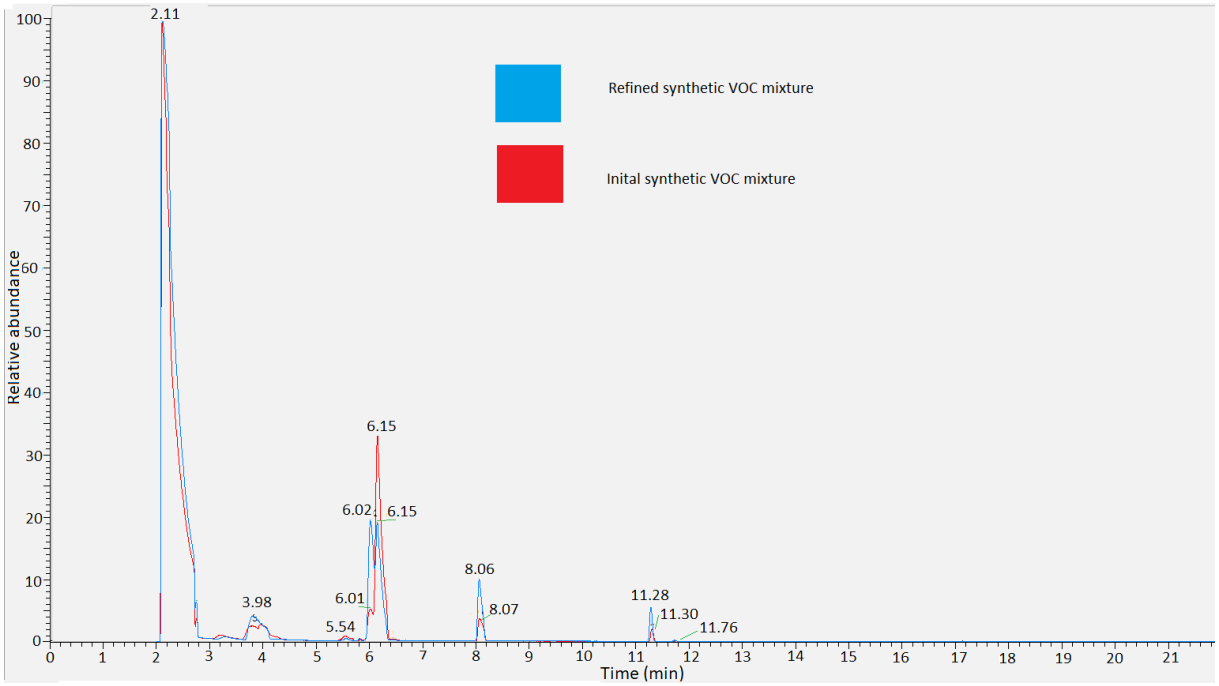

Figure 4.4 – Comparison of initial (n=3) and refined (n=5) five VOC synthetic blend, analysed using SPME-GC-MS. 2.11 = cyclohexane, 3.98 = Z-3-hexenol, 6.02 = Z-3-hexenyl acetate, 6.15 = 3-carene, 8.91 = 1-undecene, 11.28 = 1-dodecene.

4.2.6.2 Ozonolysis of synthetic blends by SPME-GC-MS

Ozonolysis of the refined synthetic blend and subsequent sampling using SPME-GC-MS was undertaken as described in section 4.2.5.4. Peaks were identified by comparing retention times and mass spectra to products identified in section 4.2.5.

4.2.7 Synthesis of non-commercially available literature identified reaction products for use in electroantennography testing

Literature synthesis pathways and commercially available feedstock for non-commercially available, literature identified, reaction products were generally lacking, thus limiting the number of non-

commercially available degradation products that could be synthesised. However, literature synthesis methodologies for 3-oxoproyl acetate (Hofstraat et al. 1988) and 2-oxoethyl acetate (Kim et al. 2000), which are both identified as Z-3-hexenyl acetate oxidation products by Grosjean and Grosjean (1999), were identified. Standard ^{13}C and ^{1}H NMR were undertaken in addition to GC-MS analysis (using the method identified in 4.2.4) to verify the nature of the synthesis products.

4.2.7.1 Synthesis of 3-oxopropyl acetate

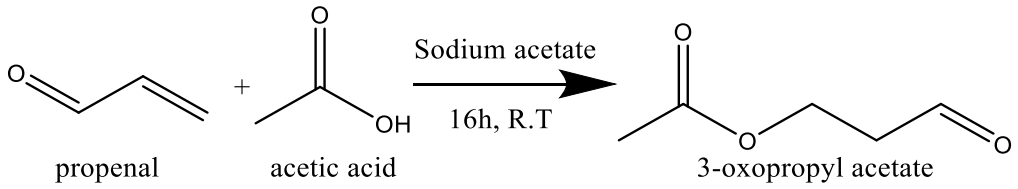

Figure 4.5 – Reaction scheme derived from (Hofstraat et al. 1988) for the synthesis of 3-oxopropyl acetate from propenal and acetic acid.

Acrolein (5.207g) and sodium acetate (0.873g) were dissolved in acetic acid (10.87g) and mixed overnight (298K). The product was concentrated and re-dissolved in diethyl ether (30ml). The mixture was then filtered, and the liquor further concentrated producing a yellow oil (680mg,6%); ^{1}H NMR δ (2.05, S) (2.08, S) (2.78, T) (4.4, Quin) (9.79, S) ^{13}C NMR δ (20.81) (42.68) (57.95) (170.90) (199.41).

4.2.7.2 Synthesis of 2-oxoethyl acetate

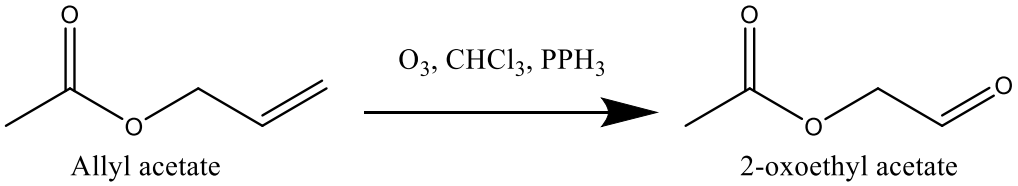

Figure 4.6 – Reaction scheme derived from (Kim et al. 2000) for the synthesis of 2-oxoethyl acetate from allyl acetate.

O_3 (2L/min, 0.5A) was bubbled through allyl acetate (5.181g) in $CHCl_3$ (35ml,220K) until the solution turned blue (ca.40min). PPh_3 (23.98g) in $CHCl_3$ (50ml) was added dropwise to the reaction and stirred overnight (298K). The solution was concentrated and re-dissolved in Et_2O (45ml). The solution was frozen (253K, 3 days) and the liquor collected and concentrated under vacuum to leave a yellow oil (53mg,1%); ^{1}H NMR δ (2.19, S) (4.67, S) (9.73, D) ^{13}C NMR δ (20.37) (68.69) (170.35) (195.72).

4.2.8 Electroantennography

4.2.8.1 Electroantennography physiological response experiments

Electroantennography (EAG) experiments were undertaken to determine responses to the identified ozonolysis products of the model floral blend.

Several reaction products were tested for antennal activity using EAG. Due to the unsuccessful synthesis of non-commercially available reaction products, only commercially available reaction products were tested, and no selection bias was made as to their ozonolysis formation yields.

Liquid reaction product standards were produced (Table 4.7) by dissolving 100µL of stimuli in 1mL of n-hexane (Sigma, >95%).

Table 4.7 – List of identified VOC degradation products and concentrations that were tested for physiological activity using EAG of *A. mellifera* antennae. [a] identified in this work, [b] identified by Lee et al. (2006), [c] identified by Aschmann et al. (1997) [d] identified by Grosjean and Grosjean (1999).

VOC	Dilution relative to neat VOC	Parent VOC
nonanal[a]	10^{-1}	1-undecene
decanal[a]	10^{-1}	1-dodecene/1-undecene
propanal[a, c, d]	10^{-1}	Z-3-hexenol
acetic acid[b, c]	10^{-1}	3-carene
undecanal[a]	10^{-1}	1-dodecene
acetaldehyde[d]	10^{-1}	Z-3-hexenyl acetate
glyoxal[d]	10^{-1}	Z-3-hexenyl acetate

EAG assays were prepared as described in section 2.4.8 with stimuli presented in a randomised order to avoid carryover effects (Stelinski et al. 2003). The normalisation of responses was undertaken post experiment to account for the deterioration of the preparation (Vuts et al. 2010).

4.2.8.2 Statistical analysis

For EAG experiments, statistical analysis was undertaken to explore data relationships. Paired Wilcoxon signed-rank tests were undertaken due to the two factor non-parametric nature of the data set.

4.3 Results

4.3.1 Products from the oxidation of individual blend components

GC traces for ozonolysis reactions of the five study VOCs are presented below; however, there are common themes to all traces with several peaks seen repeatedly in both SPME and Tenax traces. These peaks were the result of the thermal degradation of the polymer that forms the basis of the respective collection methods. These peaks were identified by their presence in all of the GC traces for each collection method at roughly the same retention time, showing high molecular weight mass spectra and producing silicone based NIST matches. Silated peaks will be presented where visible for completeness and omitted where not visible due to the relative peak height.

Further to this, cyclohexane (the reactions hydroxyl radical scavenger) and its reaction products were also captured by both sampling methodologies. SPME predominantly captured cyclohexane in its unreacted form while Tenax captured both cyclohexanone and cyclohexanol which are formed as the result of the reaction of OH radicals with cyclohexane. These peaks are mentioned because they usually dominate spectra.

4.3.1.1 1-dodecene

Undecanal and formaldehyde were predicted as oxidation products of 1-dodecene (Figure 4.7) and subsequent ozonolysis of 1-dodecene and collection with SPME showed a GC trace with several peaks (Figure 4.8)

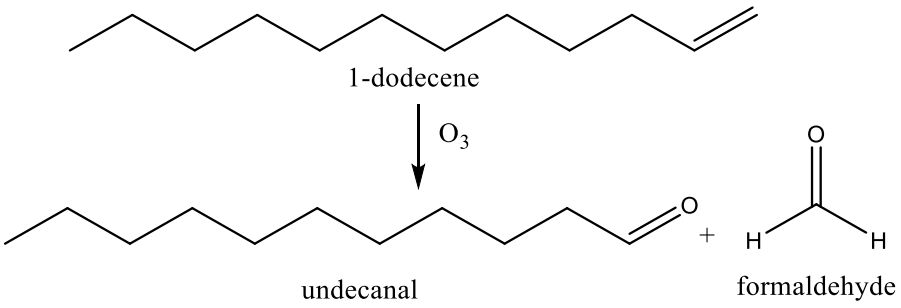

Figure 4.7 – Prediction that upon the reaction of ozone and 1-dodecene, undecanal and formaldehyde will be formed.

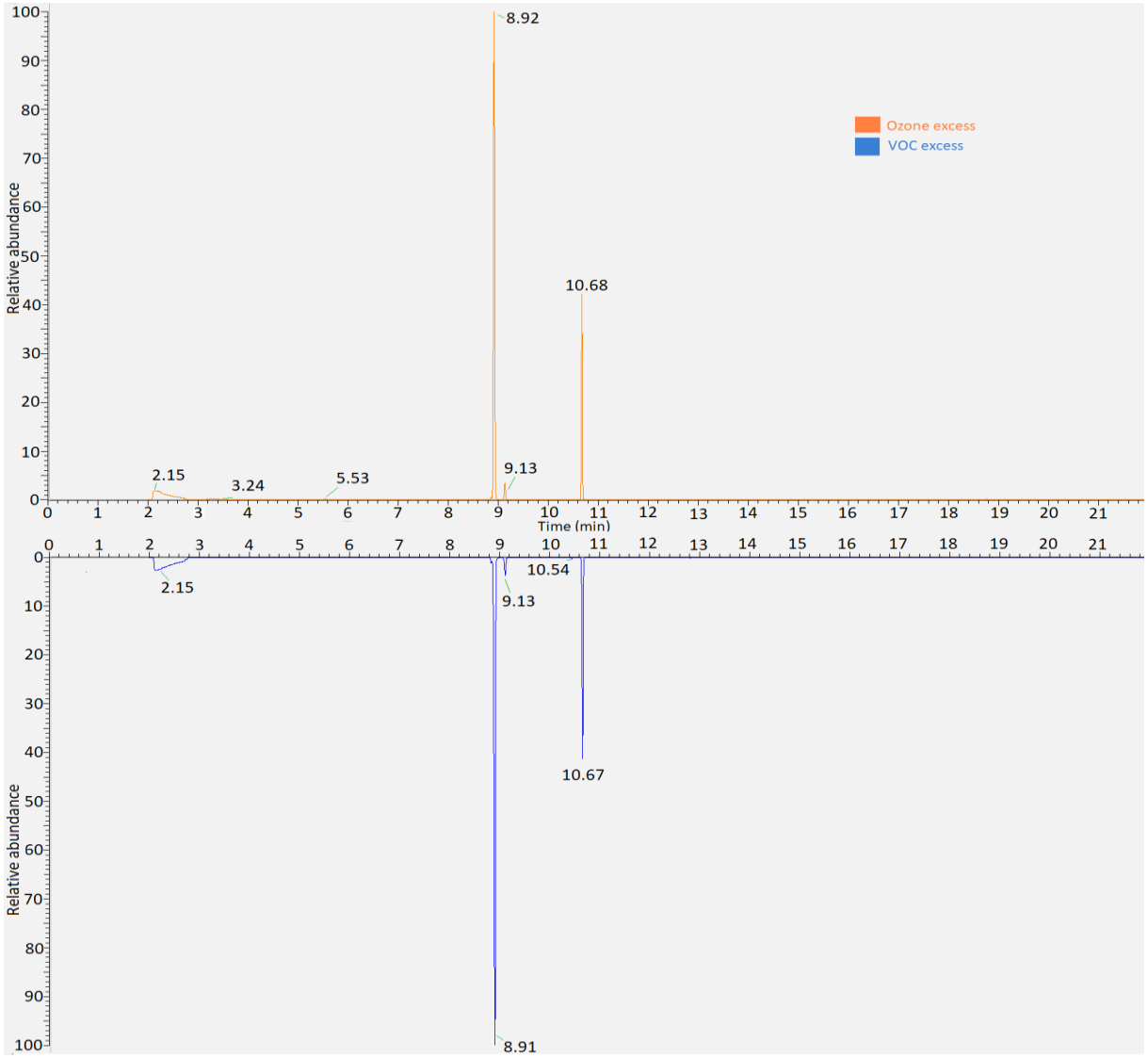

Figure 4.8 – Typical GC trace for the ozone excess (orange, n=3) reaction of ozone (1ppm) and 1-dodecene (0.25ppm) contrasted with the VOC excess reaction (blue, n=3) of ozone (1ppm) and 1-dodecene (3ppm) both sampled using SPME. 2.15 min = cyclohexane, 8.91 min = 1-dodecene, 9.13 min = decanal, 10.68 min = undecanal. Silated compound: RT = 3.24,5.53,10.54 min.

Table 4.9- Table of GC peaks and assignments from the ozonolysis of 1-dodecene and ozone under both ozone excess and VOC excess conditions captured using SPME.

Retention time (min)	Identification	Identification method	SI matching factor
2.15	cyclohexane	NIST	794
8.91	1-dodecene	NIST/Standard	923
9.13	decanal	NIST/standard	886
10.68	undecanal	NIST/standard	952

*Silated compound: RT = 3.24,5.53, 10.54 min.

From comparison of peaks (Figure 4.8) with the NIST mass spectrum database, a number of assignments were made (Table 4.9). For both the VOC and ozone excess reactions, peaks were seen with similar retention times (Figure 4.8). The previously predicted product of undecanal was detected and its retention time (RT=10.68min) was confirmed by using a standard for comparison (Figure 4.9). Notably, the predicted product formaldehyde (Figure 4.7) was not identifiable from the GC trace which is likely due to it being co-eluted at the same time as cyclohexane. Method optimisation was attempted to resolve the peaks but this was not successful. An unpredicted product of decanal (RT=9.13min) was, however, detected and its presence confirmed by the running of a decanal standard (Figure 4.10) which showed a similar retention time and fragmentation pattern. No noticeable differences in peak retention times between VOC and ozone excess situations were seen, which indicates no changes in reaction product formation. The SPME trace for unreacted 1-dodecene (Figure 4.11) showed two peaks, both of which returned NIST database searches as 1-dodecene.

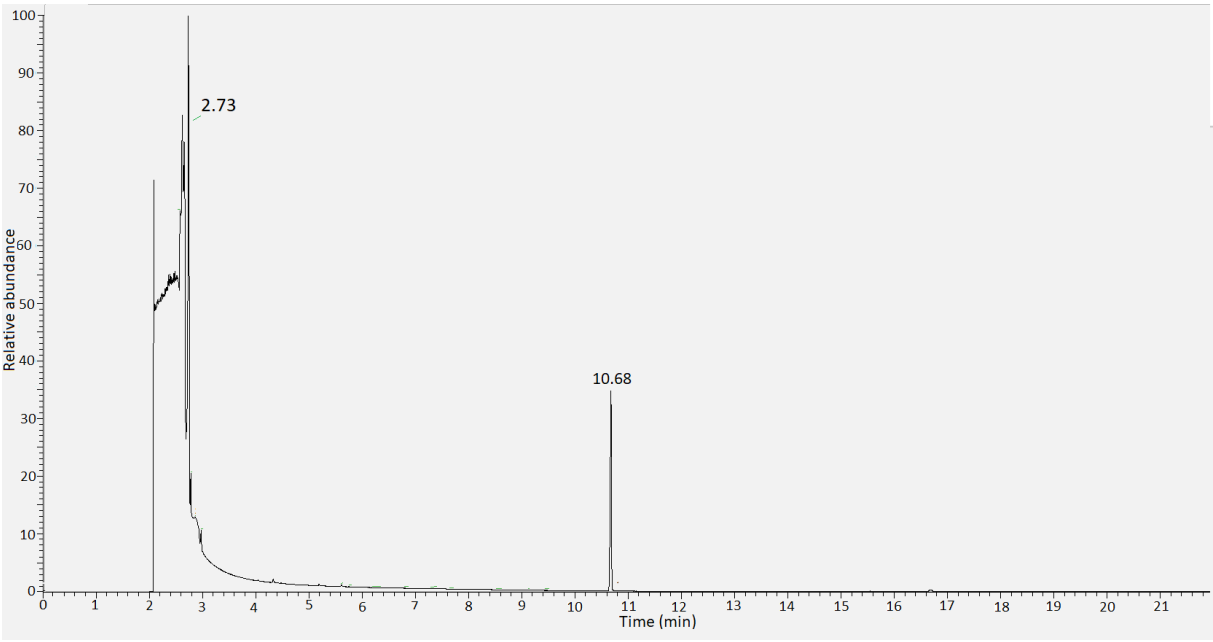

Figure 4.9 – GC trace for a liquid injection of undecanal in hexane recorded under the standard GC conditions (n=2). 2.73min = hexane, 10.68min = undecanal.

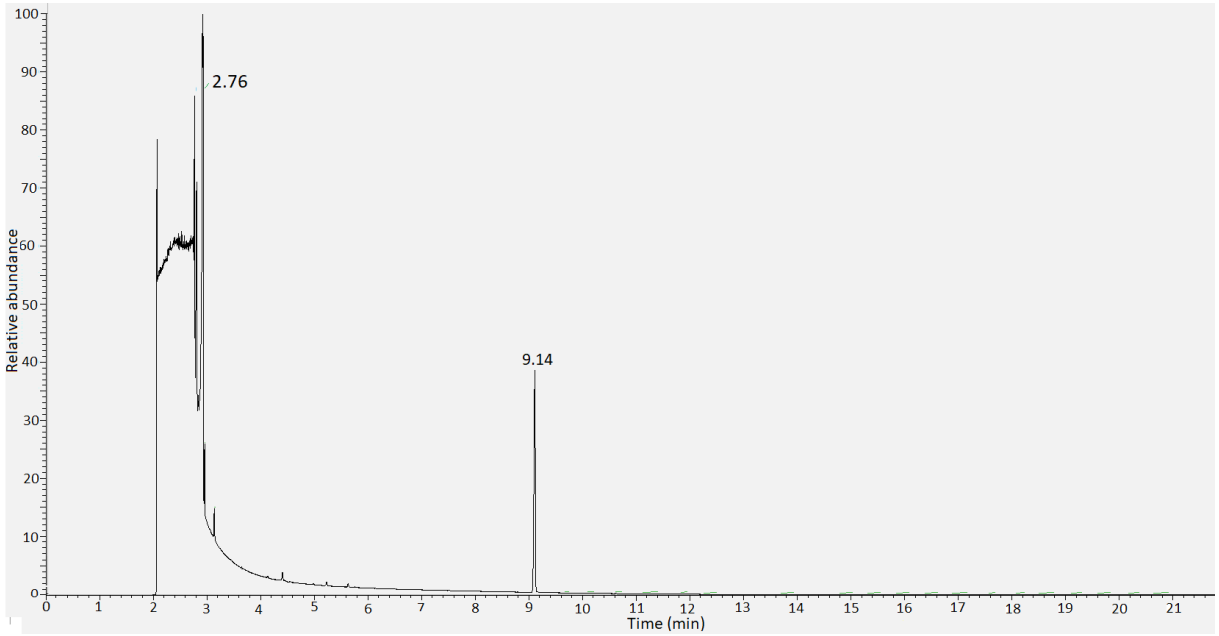

Figure 4.10 – GC trace for a liquid injection of decanal in hexane under the standard GC conditions (n=3). 2.76min = hexane, 9.14 min = decanal.

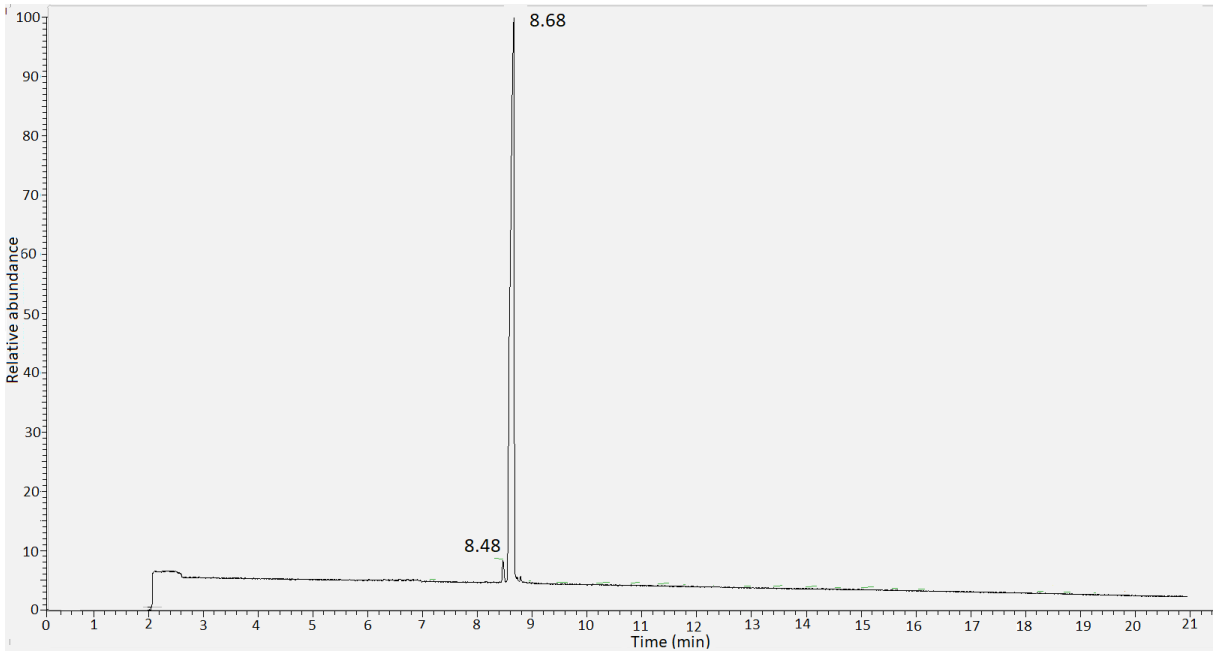

Figure 4.11 – GC trace for a SPME sampling of 1-dodecene under the standard GC conditions (n=3). 8.48min = 1-dodecene, 8.68 min = 1-dodecene.

4.3.1.2 1-undecene

Decanal and formaldehyde were predicted as oxidation products of 1-undecene (Figure 4.12) and subsequent ozonolysis of 1-undecene and collection with SPME showed a GC trace with several peaks (Figure 4.13).

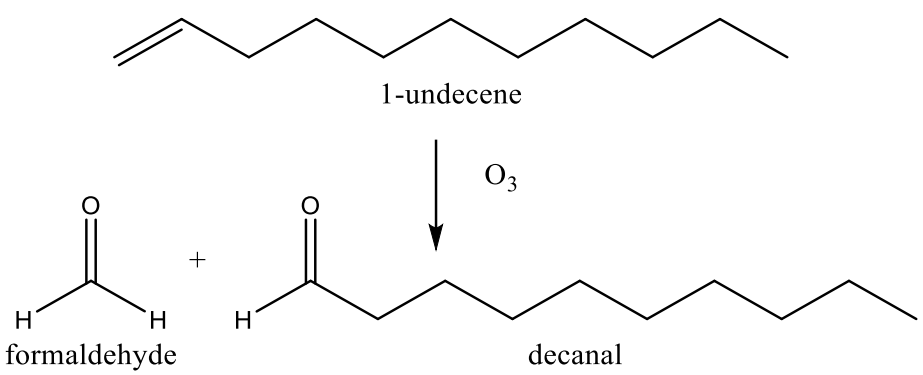

Figure 4.12 – Prediction that upon the reaction of ozone and 1-undecene, decanal and formaldehyde will be formed.

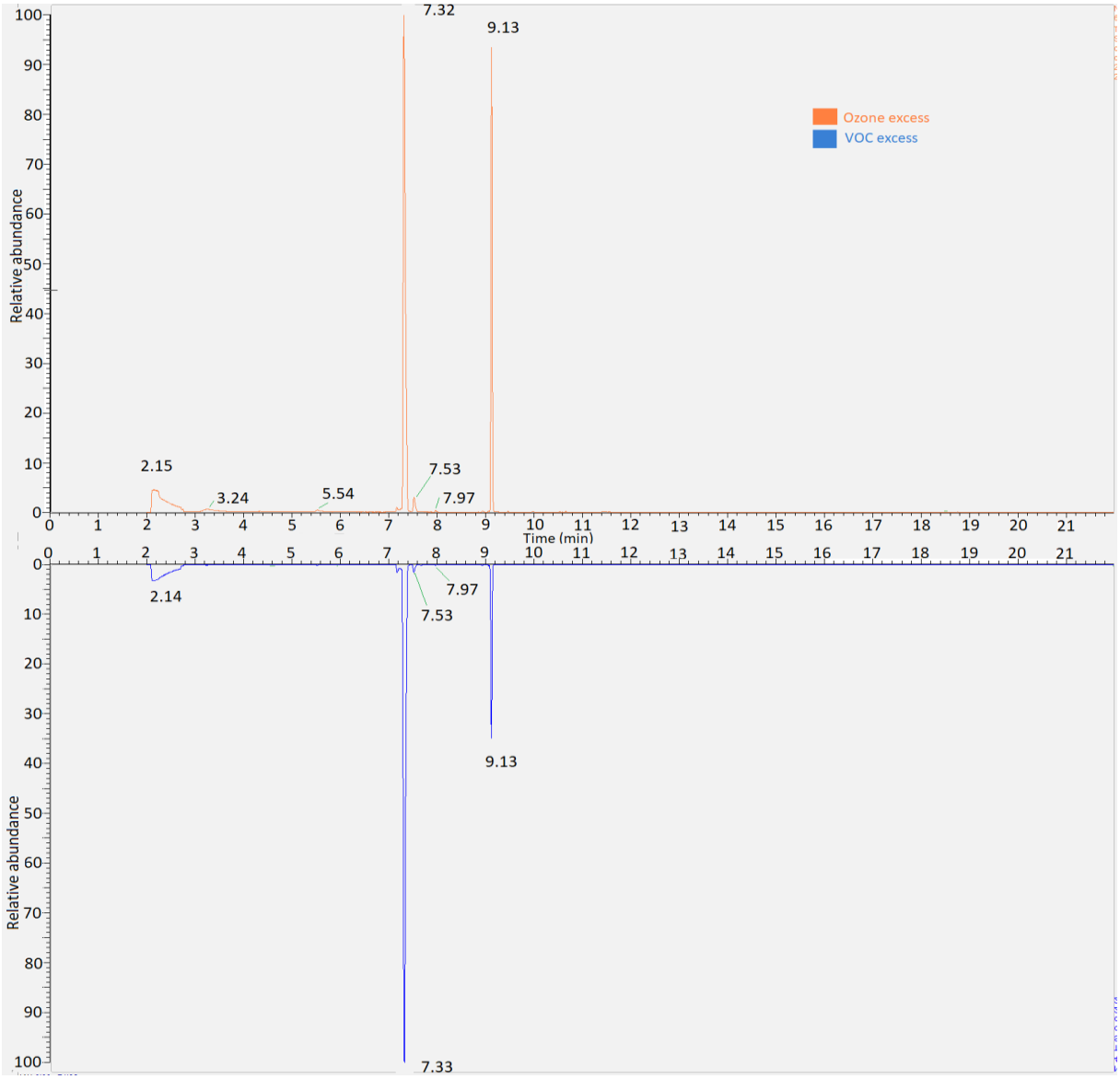

Figure 4.13 – Typical GC trace for the ozone excess (orange, n=4) reaction of ozone (1ppm) and 1-undecene (0.25ppm) contrasted with the VOC excess reaction (blue, n=3) of ozone (1ppm) and 1-undecene (3ppm) both sampled using SPME. 2.15 min = cyclohexane, 7.32 min = 1-undecene, 7.53 min = nonanal, 9.13 min = decanal. Silated compound: RT = 3.24,5.53,7.97 min.

Table 4.10- Table of GC peaks and assignments from the ozonolysis of 1-undecene and ozone under both ozone excess and VOC excess conditions captured using SPME.

Retention time (min)	Identification	Identification method	SI matching factor
2.15	cyclohexane	NIST	825
7.32	1-undecene	NIST/Standard	924
7.53	nonanal	NIST/Standard	744
9.13	decanal	NIST/Standard	905

*Silated compound: RT = 3.24,5.53,7.97 min

From comparison of peaks (Figure 4.13) with the NIST mass spectrum database, a number of assignments were made (Table 4.10). For both the VOC and ozone excess reactions, peaks were seen with similar retention times (Figure 4.13). The predicted product of decanal was detected and its retention time was confirmed by using an authentic standard for comparison (Figure 4.10). Notably, formaldehyde was not identifiable from the GC trace (see 4.3.1.1); however, an unpredicted product of nonanal was also detected and its presence confirmed by the running of a nonanal standard (Figure 4.14) which showed a similar retention time and fragmentation pattern. The decanal peak appeared to be larger under ozone excess conditions; however, quantitative comparisons could not be made due to the lack of quantitative reproducibility of SPME sampling (see appendix AP3). The SPME-GC-MS trace for unreacted 1-undecene (Figure 4.15) showed three peaks of which two had similar retention time, mass spectra and NIST search results and the third had a differing retention time but similar mass spectra and NIST search results.

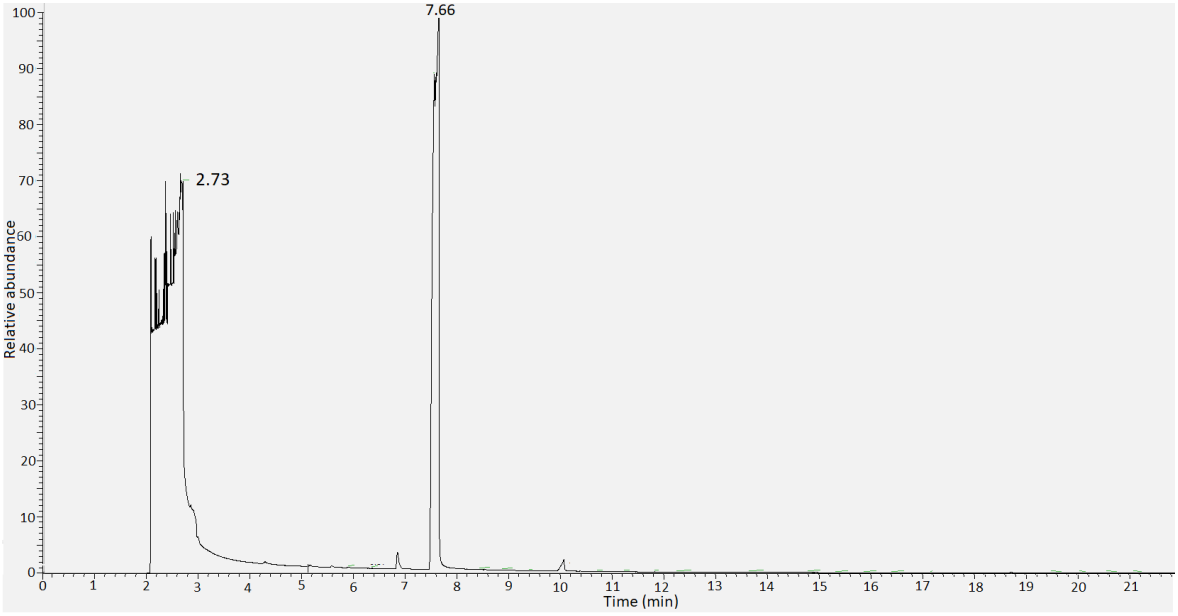

Figure 4.14 – GC trace for a liquid injection of nonanal in hexane under the standard GC conditions (n=2). 2.73min = hexane, 7.66 min = nonanal.

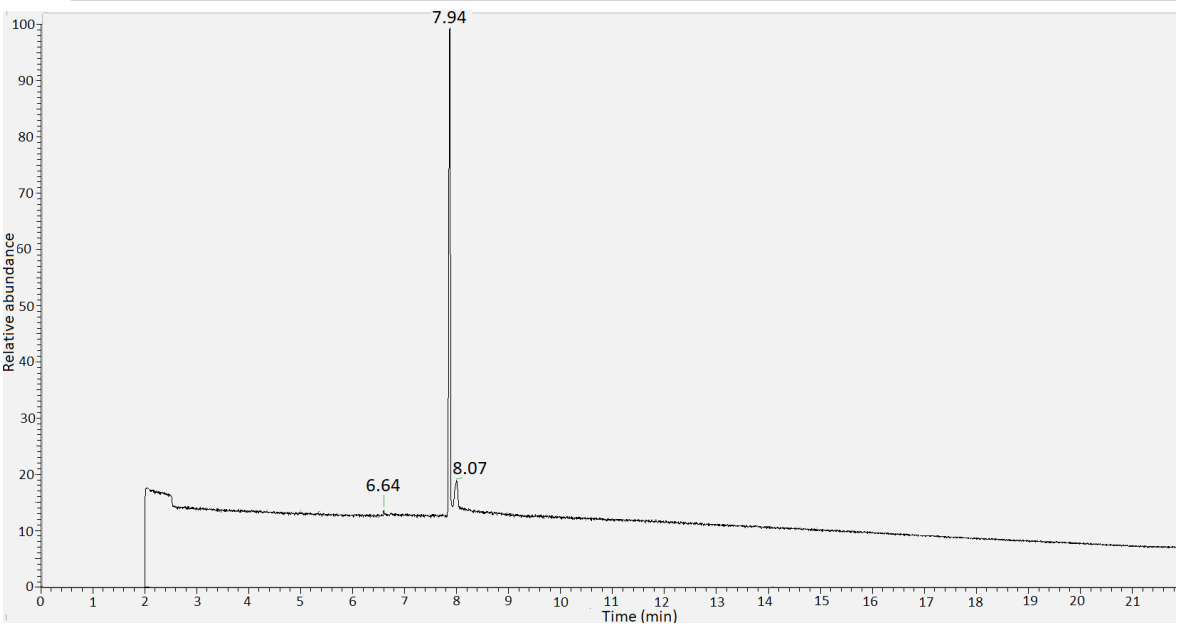

Figure 4.15 – GC trace for a SPME of 1-undecene under the standard GC conditions (n=2). 7.94/8.07 min = 1-undecene, 6.64min = 1-undecene (tentative, NIST).

4.3.1.3 3-carene

A single first-generation oxidation product of caronaldehyde was predicted from the ozonolysis of 3-carene (Figure 4.16). Subsequent ozonolysis of 3-carene and collection with SPME showed a GC trace with several peaks (Figure 4.18).

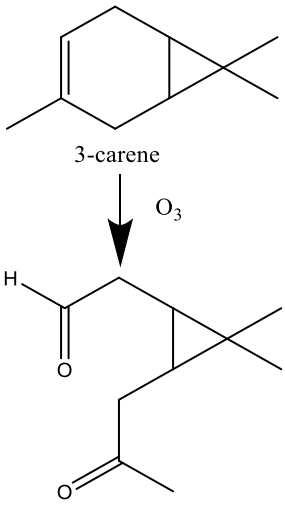

2-(2,2-dimethyl-3-(2-oxopropyl)cyclopropyl)acetaldehyde

Caronaldehyde

Figure 4.16 – Prediction that upon the reaction of ozone and 3-carene, caronaldehyde will be formed.

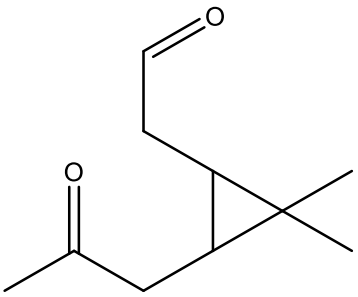

Caronaldehyde
Molecular Weight: 168.24

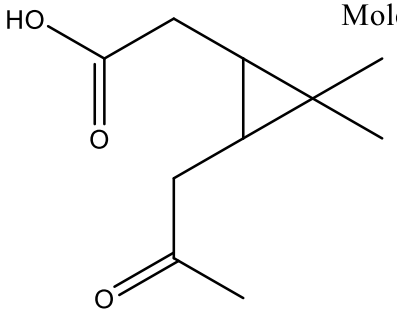

3-caronic acid
Molecular Weight: 184.24

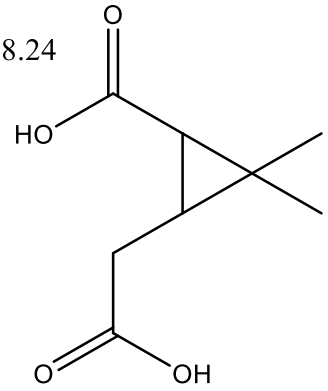

Nor-3-caric acid
Molecular Weight: 172.18

Figure 4.17 – Summary of literature identified compounds for the reaction of 3-carene with ozone based on the work of Yu et al. (1999), Ma et al. (2009). These works used derivatisation.

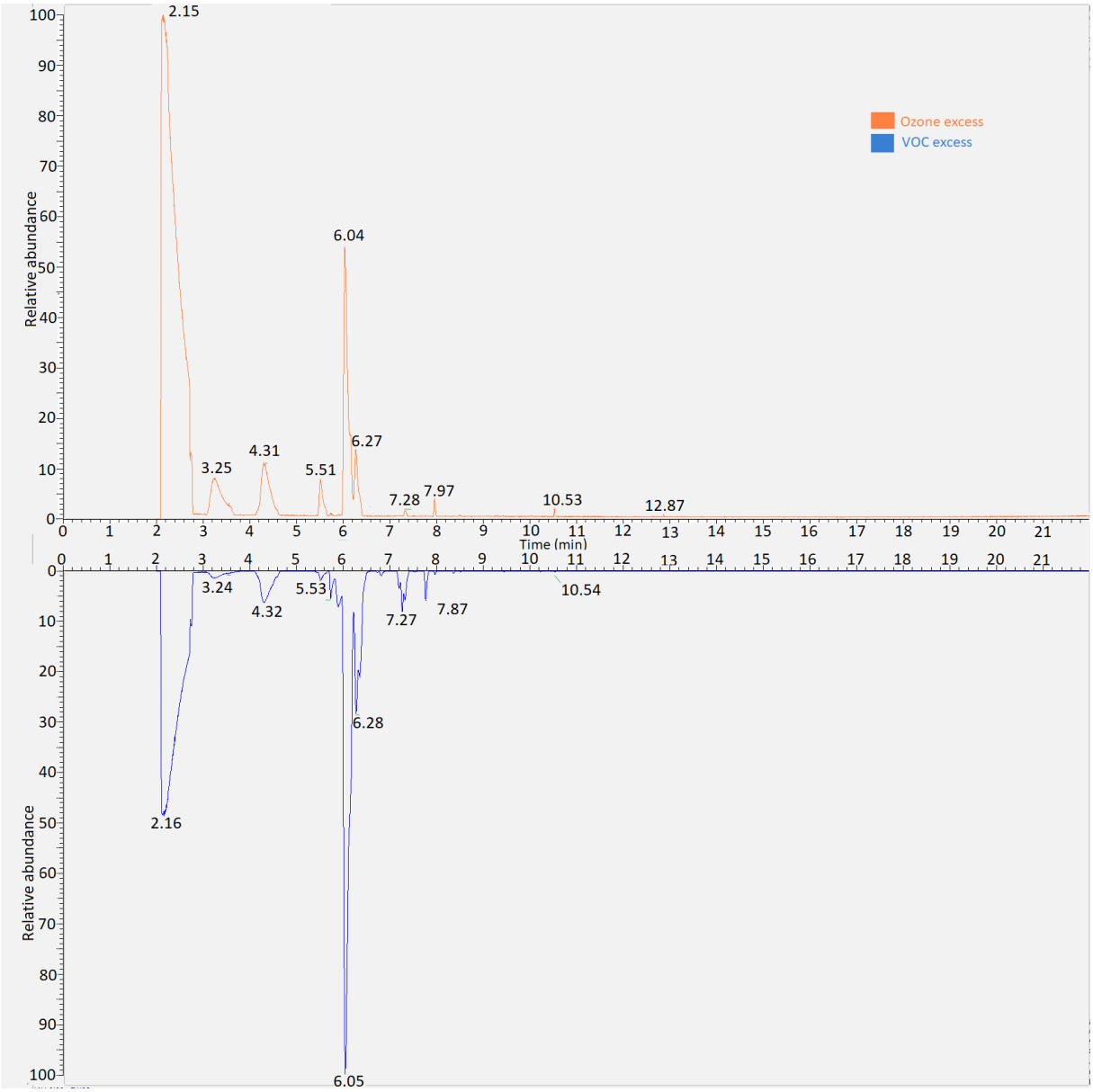

Figure 4.18 – Typical GC trace for the ozone excess (orange, n=4) reaction of ozone (1ppm) and 3-carene (0.25ppm) contrasted with the VOC excess reaction (blue, n=4) of ozone (1ppm) and 3-carene (3ppm) both sampled using SPME. 2.15min = cyclohexane, 4.31min = cyclohexanone, 6.05/6.28min = 3-carene. Silated compound: RT = 3.24,5.53,7.97,10.54,12.87 min.

Table 4.11 – Table of GC peaks and assignments from the ozonolysis of 3-carene and ozone under both ozone excess and VOC excess conditions captured using SPME.

Retention time (min)	Identification	Identification method	SI matching factor
2.15	cyclohexane	NIST	816
4.31	cyclohexanone	NIST/Standard	712
6.05	3-carene	NIST/Standard	824
6.04/6.28	Peak split 3-carene	NIST	769
7.28	m/z=136.02, 120.98, 116.99, 93.05, 79.05, 65.02	-	-

*Silated compound: RT = 3.24,5.53,7.97,10.54,12.87 min

From the SPME qualification of products under both ozone and VOC excess, several peaks were seen (Figure 4.18). On comparison with the NIST mass spectrum database, a number of peak assignments were made (Table 4.11); however, none of these could be positively identified as any of the predicted or previously identified reaction products (Figure 4.17, Yu et al. (1999), Ma et al. (2009)). It was seen that several of the visible peaks were silated compounds resulting from the breakdown of the SPME fibre coating. Further to this, it was seen that peak retention times under VOC excess and ozone excess conditions (Figure 4.18) were consistent; however, peak intensities were noticeably different. The peak at RT=6.28 min had a similar fragmentation pattern to that at RT=6.05 min and reduced in intensity concurrently with RT=6.05 min on moving from ozone excess to VOC excess and thus, RT=6.28 min is suggested to be peak split 3-carene (peak splitting is seen when a large concentration of a compound is present, as is shown in Figure 4.19). The peak at RT=7.28 min has a similar fragmentation pattern to that of 3-carene and is likely to react with ozone due to the decrease in concentration between VOC excess and ozone excess conditions. However, the exact identity of the peak is difficult to elucidate because several compounds have similar fragmentation patterns and there are no authentic standards for the literature reaction products available in the NIST database. As such, no assignment is made in this case. Tenax sampling produced several peaks (Figure 4.20) of which the identification was complex and no literature reaction products were identified (Table 4.12).

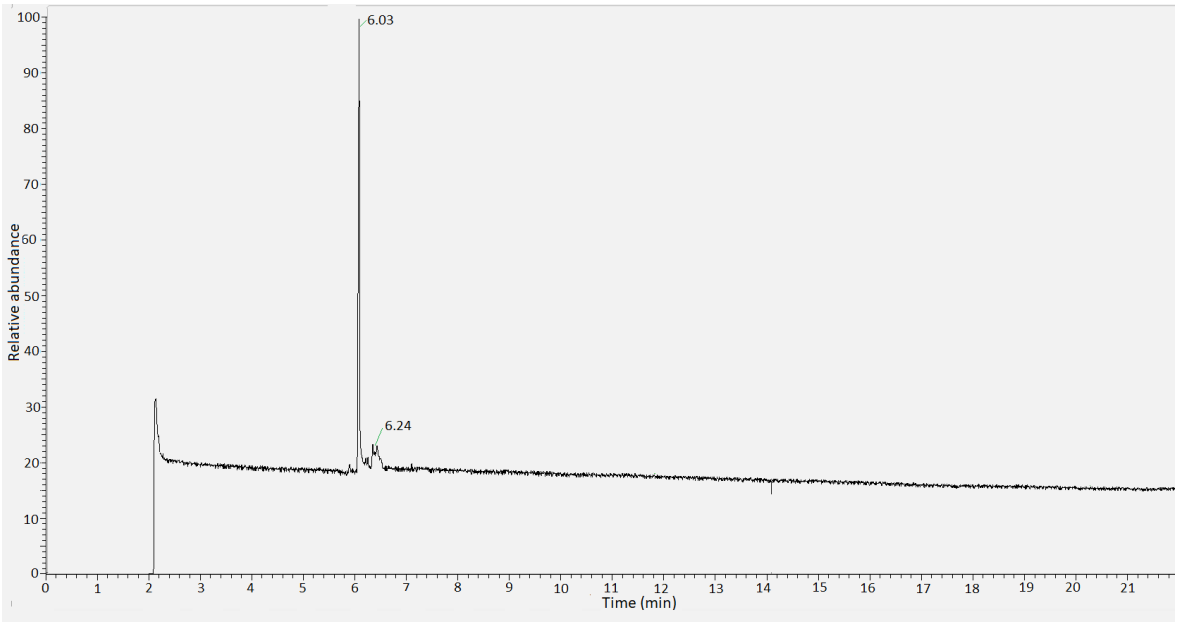

Figure 4.19 – Typical GC trace for 3-carene (1ppm, RT = 6.03/6.24min) sampled using SPME (n=3).

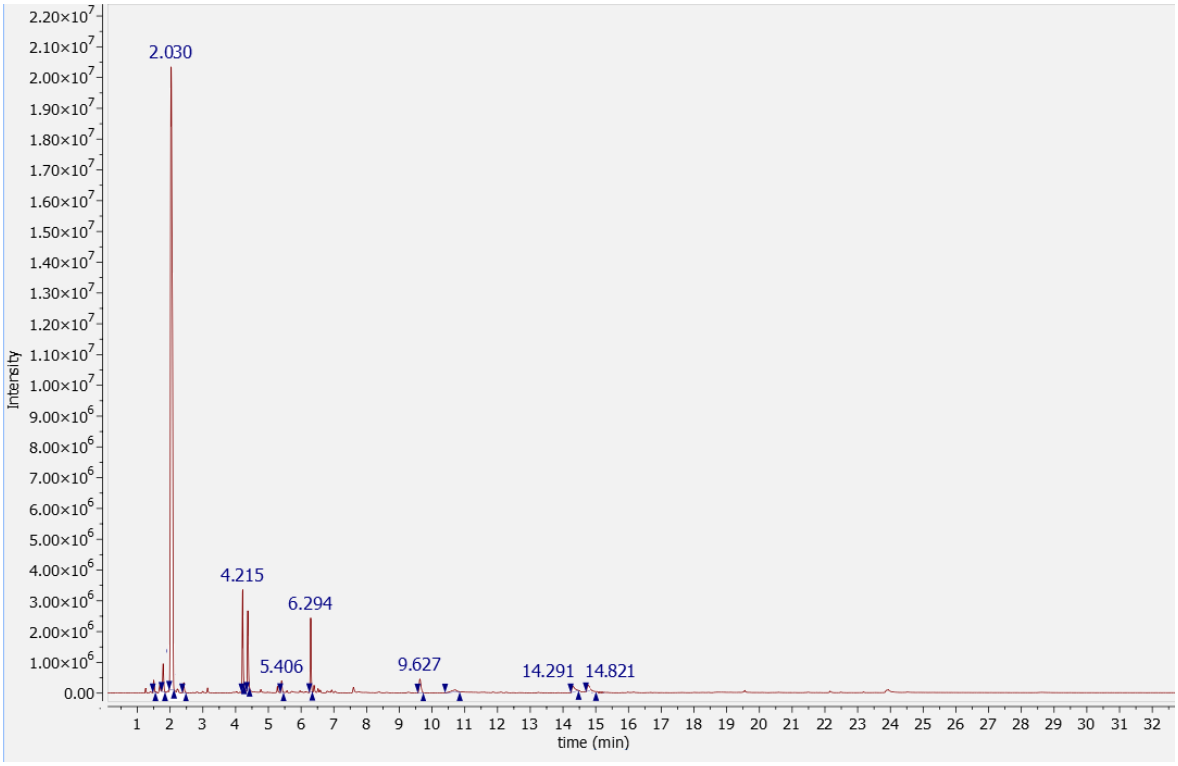

Figure 4.20 – Typical GC trace for the ozone excess reaction of ozone (4ppm) and 3-carene (1ppm) sampled using Tenax (n=2). 2.06min = cyclohexane, 4.22min = cyclohexanol, 4.37min = cyclohexanone, 5.41min = benzaldehyde, 6.29 = 3-carene, 10.71 = benzoic acid.

Table 4.12 – Identified peaks from the reaction of ozone and 3-carene sampled using Tenax

Retention time (min)	Identification	Identification method	Percentage NIST match
2.06	Cyclohexane	NIST	91
4.22	Cyclohexanol	NIST	94
4.37	Cyclohexanone	NIST	95
5.41	benzaldehyde	NIST	96
6.29	3-carene	NIST	97
9.63	m/z=43.1,55.1,67.1,81.1,95.1,109.1,119.1 ,137.1,138.1	-	-
10.71	benzoic acid	NIST	95
14.29	m/z=43.1,55.1,81.1,107.1,111.1,139.1, 140.1	-	-
14.82	m/z=43.1,55.1,71.1,81.1,95.1,96.1,109.0, 124.0,139.1,140.1,207.0	-	-

4.3.1.4 Z-3-hexenol

3-hydroxypropanal and propanal were predicted as oxidation products of Z-3-hexenol (Figure 4.21) and subsequent ozonolysis of Z-3-hexenol and collection with SPME showed a GC trace with several peaks (Figure 4.22).

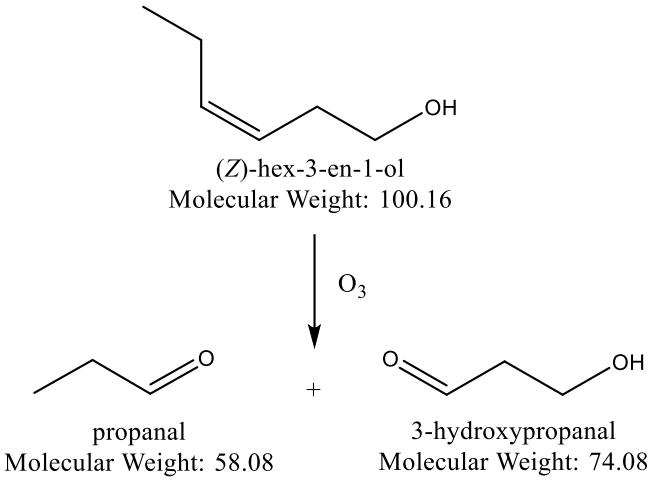

Figure 4.21 – Prediction that upon the reaction of ozone and Z-3-hexenol, propanal and 3-hydroxypropanal will be formed.

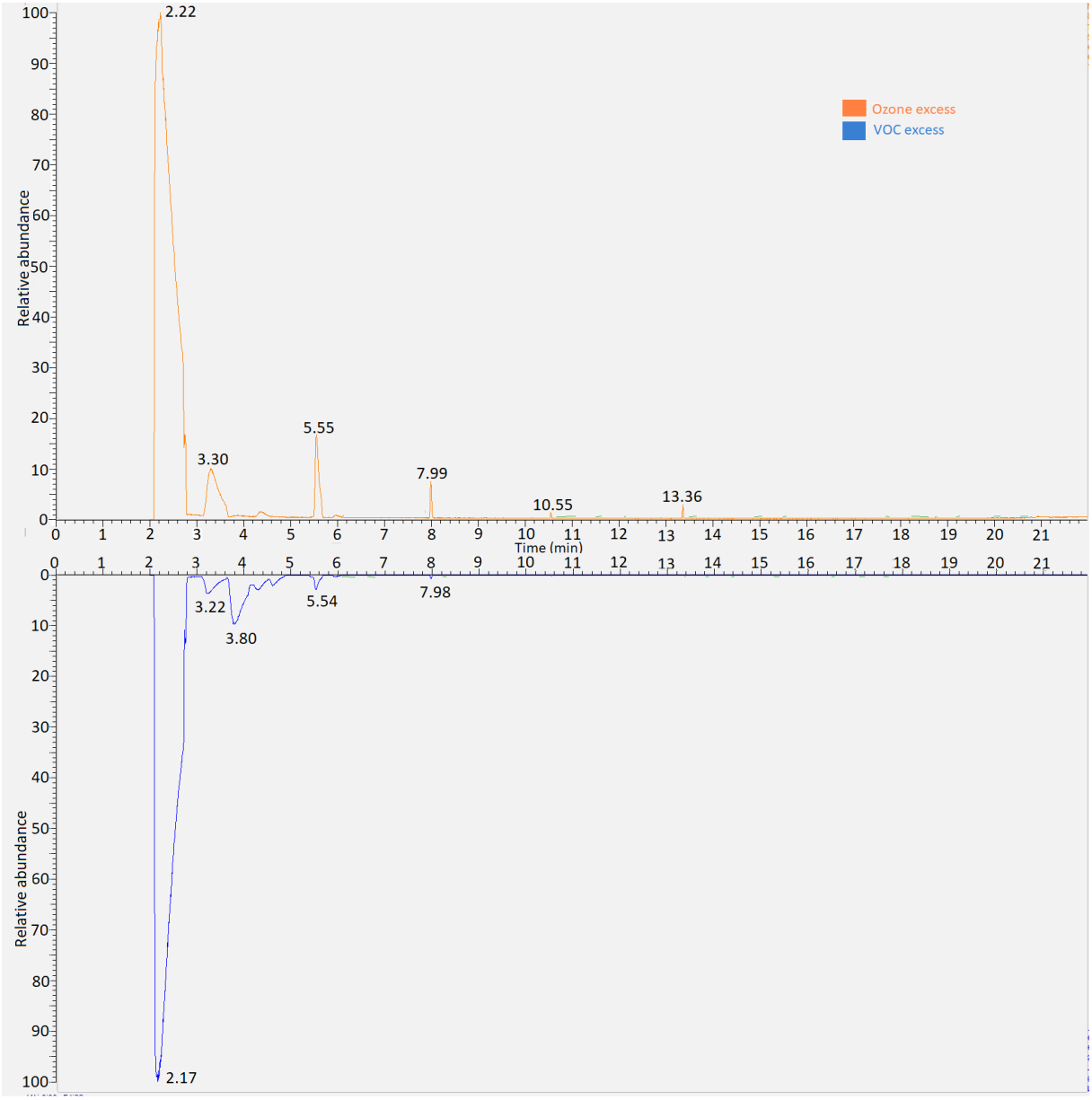

Figure 4.22 – Typical GC trace for the ozone excess (orange, n=5) reaction of ozone (1ppm) and Z-3-hexenol (0.25ppm) contrasted with the VOC excess reaction (blue, n=4) of ozone (1ppm) and Z-3-hexenol (3ppm) both sampled using SPME. 2.17min=cyclohexane, 3.80min=Z-3-hexenol, 4.26min = cyclohexanol. Silated compound: RT = 3.30,5.54,7.98,10.55 min.

Table 4.13 – Table of GC peaks and assignments from the ozonolysis of Z-3-hexenol and ozone under both ozone excess and VOC excess conditions captured using SPME.

Retention time (min)	Identification	Identification method	SI matching factor
2.17	cyclohexane	NIST	885
3.80	Z-3-hexenol	NIST/Standard	869
4.26	cyclohexanol	NIST/Standard	836
13.36	Isomaltol*	NIST	616*

Silated compound: RT = 3.30,5.54,7.98,10.55 min, *=tentative

From comparison of peaks (Figure 4.22) with the NIST mass spectrum database, a number of assignments were made (Table 4.13). Although several peaks were seen in both the VOC and ozone excess scenarios, most of these were artefacts as a result of either scavenger reactions or breakdown of the SPME fibre. Retention times between the two excess scenarios were consistent (Figure 4.22); however, noticeable differences in peak intensity were observed although quantitative comparisons could not be made (see appendix AP3). For the VOC excess scenario, Z-3-hexenol was seen at RT=3.80 min. The presence of cyclohexanol (RT=4.26 min) in addition to Z-3-hexenol was confirmed by the use of standards (Figure 4.23). The NIST database suggested that the peak at RT=13.36 min was likely to be Isomaltol; however, its formation could not be easily explained from primary reaction products and an authentic standard was not available to allow further identification. The lack of a peak at RT=13.36 min under VOC excess conditions indicates that it is likely a secondary ozonolysis product. Due to the lack of product identification using SPME sampling, Tenax sampling was subsequently tested (Figure 4.24).

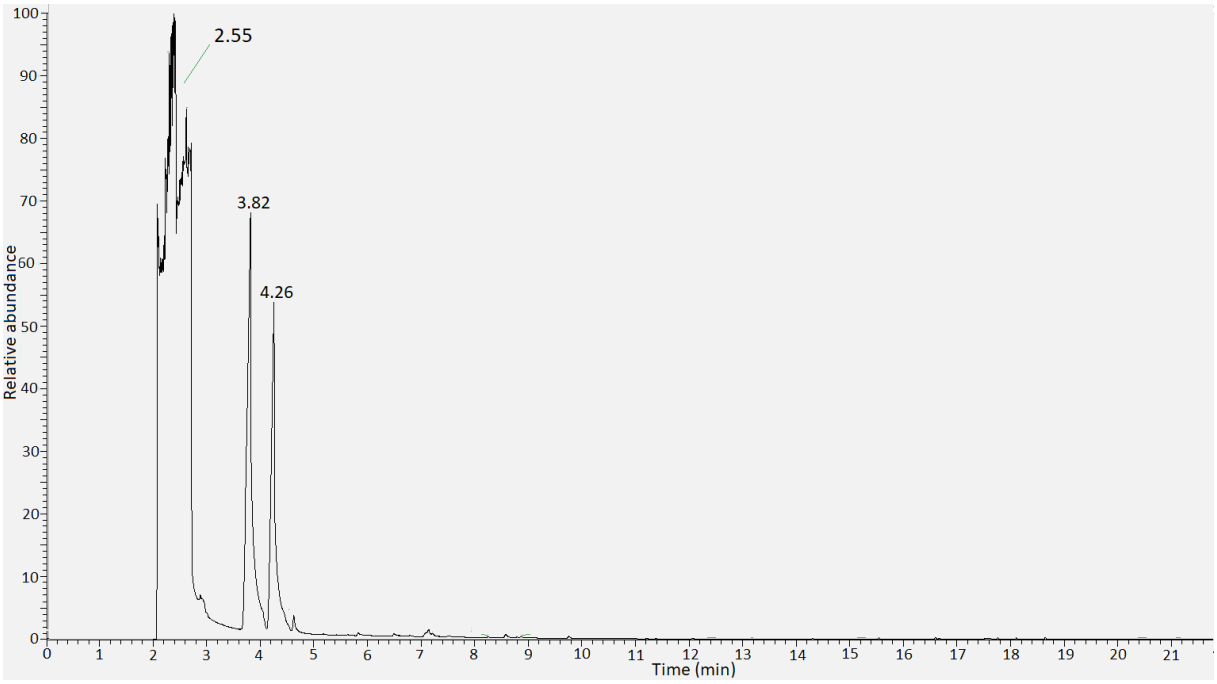

Figure 4.23 – GC trace for a liquid injection of Z-3-hexenol and cyclohexanol (1:1) in hexane recorded under the standard GC conditions (n=2). 2.55min= hexane,3.82min= Z-3-hexenol, 4.26min= cyclohexanol.

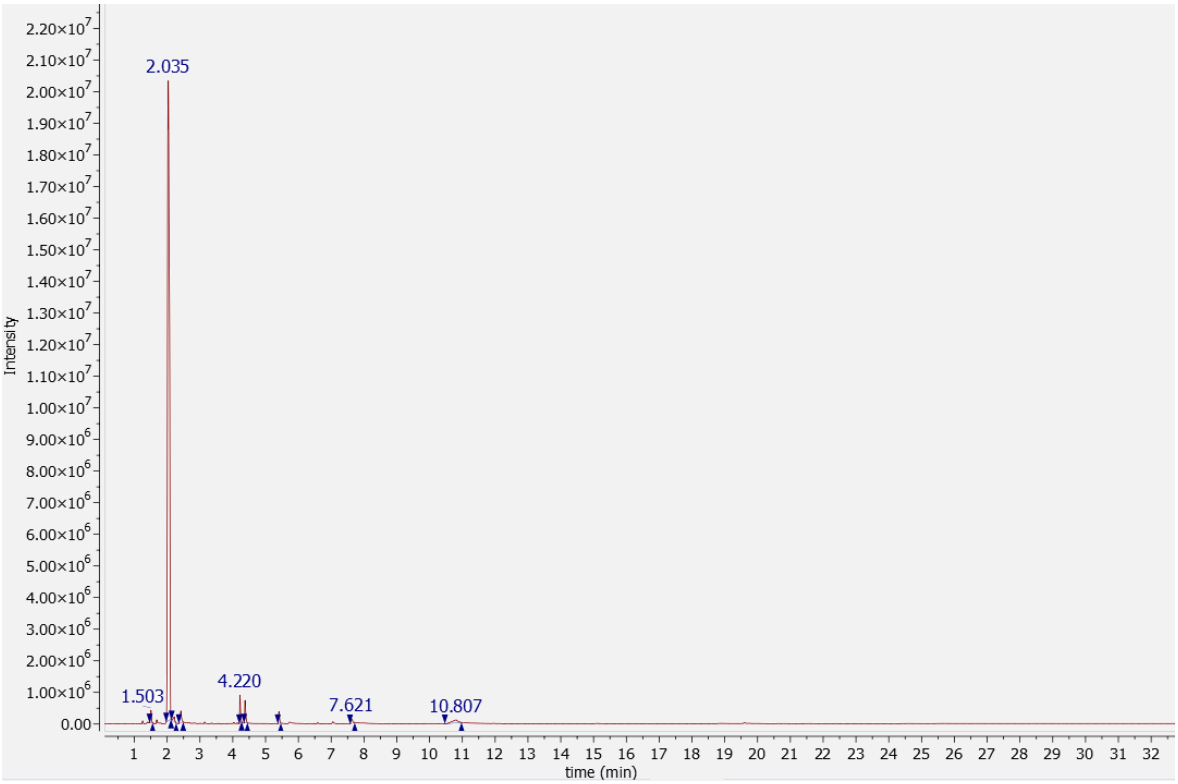

Figure 4.24 – Typical GC trace for the ozone excess reaction of ozone (4ppm) and Z-3-hexenol (1ppm) sampled using Tenax (n=2). 1.50min = propanal, 2.01min = cyclohexane, 2.42min = methylcyclohexane, 4.22min = cyclohexanol, 4.37min = cyclohexanone, 5.40min = benzaldehyde, 7.62min = acetophenone, 10.80min = benzoic acid.

Table 4.14 – Identified peaks from the reaction of ozone and Z-3-hexenol sampled using Tenax.

Retention time (min)	Identification	Identification method	Percentage NIST match
1.50	propanal	NIST	80
2.01	cyclohexane	NIST	91
2.42	methylcyclohexane	NIST	94
4.22	cyclohexanol	NIST	94
4.37	cyclohexanone	NIST	94
5.40	benzaldehyde	NIST	96
7.62	acetophenone	NIST	91
10.80	benzoic acid	NIST	95

From comparison with the NIST mass spectrum database, a number of assignments were made as a result of Tenax sampling (Table 4.14). Several peaks were attributable to breakdown products of Tenax; however, propanal was identified (RT=1.51 min, Figure 4.25, NIST=80). 3-hydroxypropanl (predicted in Figure 4.21) was not identified.

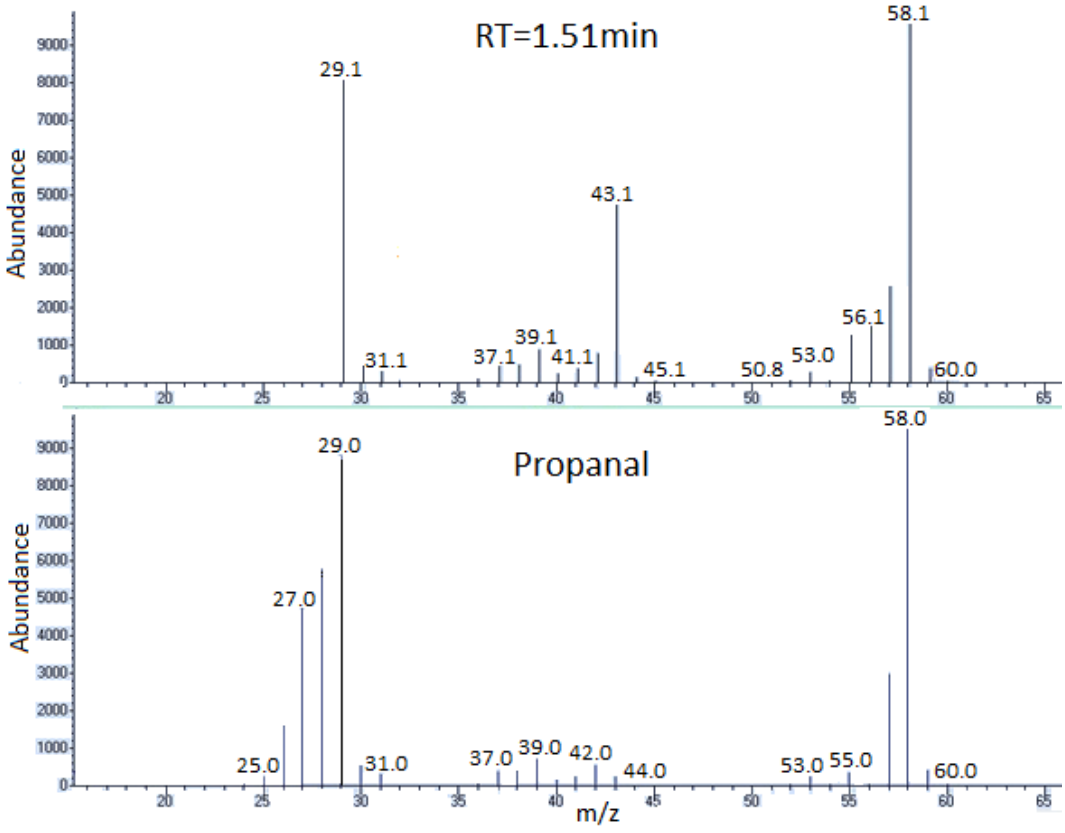

Figure 4.25 – Mass spectrum comparison of the Tenax sampled peak from the ozonolysis of Z-3-hexenol believed to be propanal (RT=1.51min) to the NIST database mass spectrum for propanal.

4.3.1.5 Z-3-hexenyl acetate

3-oxopropyl acetate and propanal were predicted as oxidation products of Z-3-hexenyl acetate (Figure 4.26). Subsequent ozonolysis of Z-3-hexenyl acetate and collection with SPME showed a GC trace with several peaks (Figure 4.27).

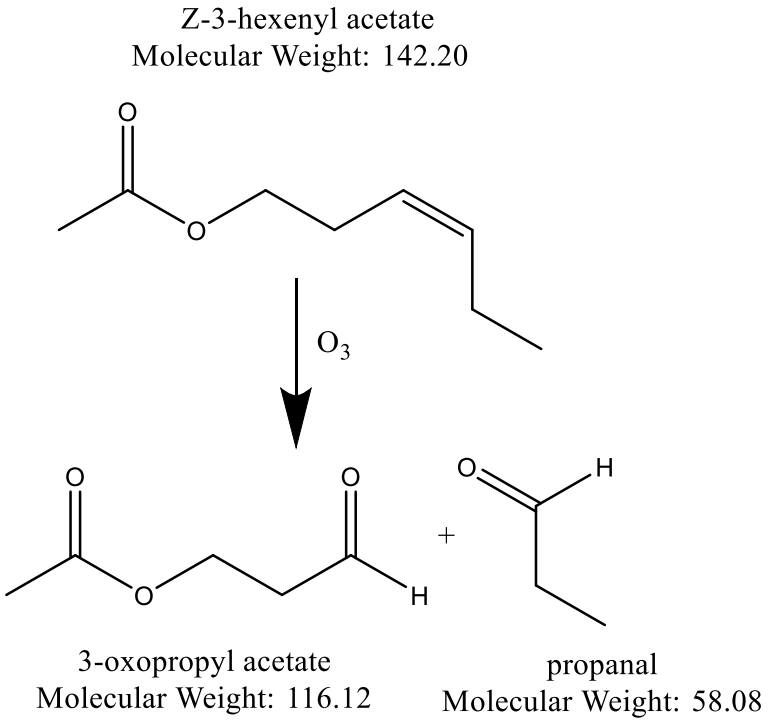

Figure 4.26 – Prediction that upon the reaction of ozone and Z-3-hexenyl acetate, 3-oxopropyl acetate and propanal will be formed.

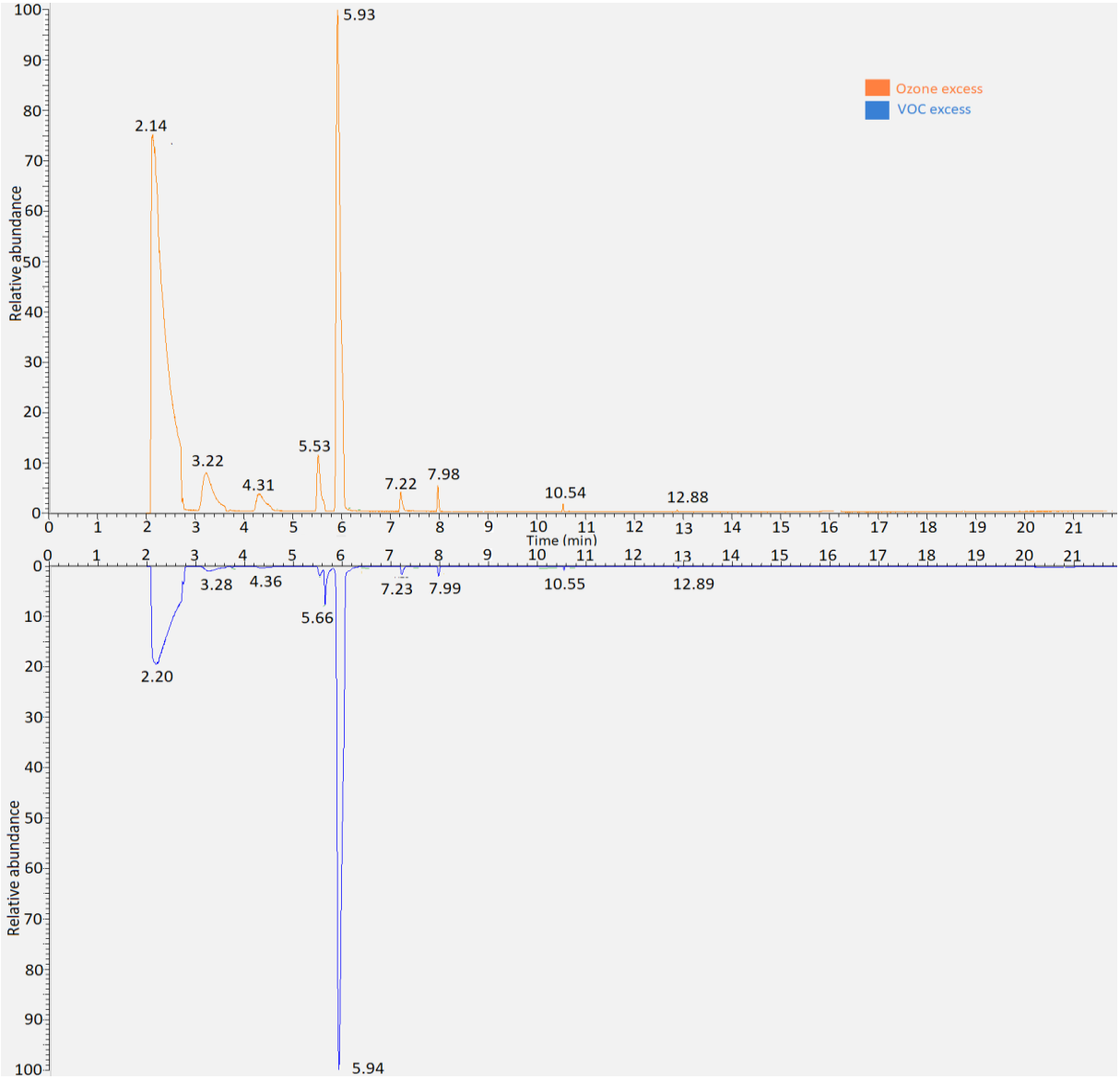

Figure 4.27 – Typical GC trace for the ozone excess (orange, n=3) reaction of ozone (1ppm) and Z-3-hexenyl acetate (0.25ppm) contrasted with the VOC excess reaction (blue, n=3) of ozone (1ppm) and Z-3-hexenyl acetate (3ppm) both sampled using SPME. 2.14min = cyclohexane, 4.31min = cyclohexanol, 5.93 = Z-3-hexenyl acetate. Silated compound: RT = 3.22,5.53,7.98,10.54,12.88 min.

Table 4.15 – Table of GC peaks and assignments from the ozonolysis of Z-3-hexenyl acetate and ozone under both ozone excess and VOC excess conditions sampled using SPME.

Retention time (min)	Identification	Identification method	SI matching factor
2.14	cyclohexane	NIST	816
4.31	cyclohexanol	NIST/Standard	743
5.93	Z-3-hexenyl Acetate	NIST/Standard	843
7.22	m/z=128,98,81,57,43	N/A	N/A

Silated compound: RT = 3.22,5.53,7.98,10.54,12.88 min.

Retention times between both VOC and ozone excess scenarios were generally consistent with small variations in peak intensity seen (Figure 4.27). From comparison with the NIST mass spectrum database, a number of assignments were made (Table 4.15). The peak at RT=7.22 could not be identified.

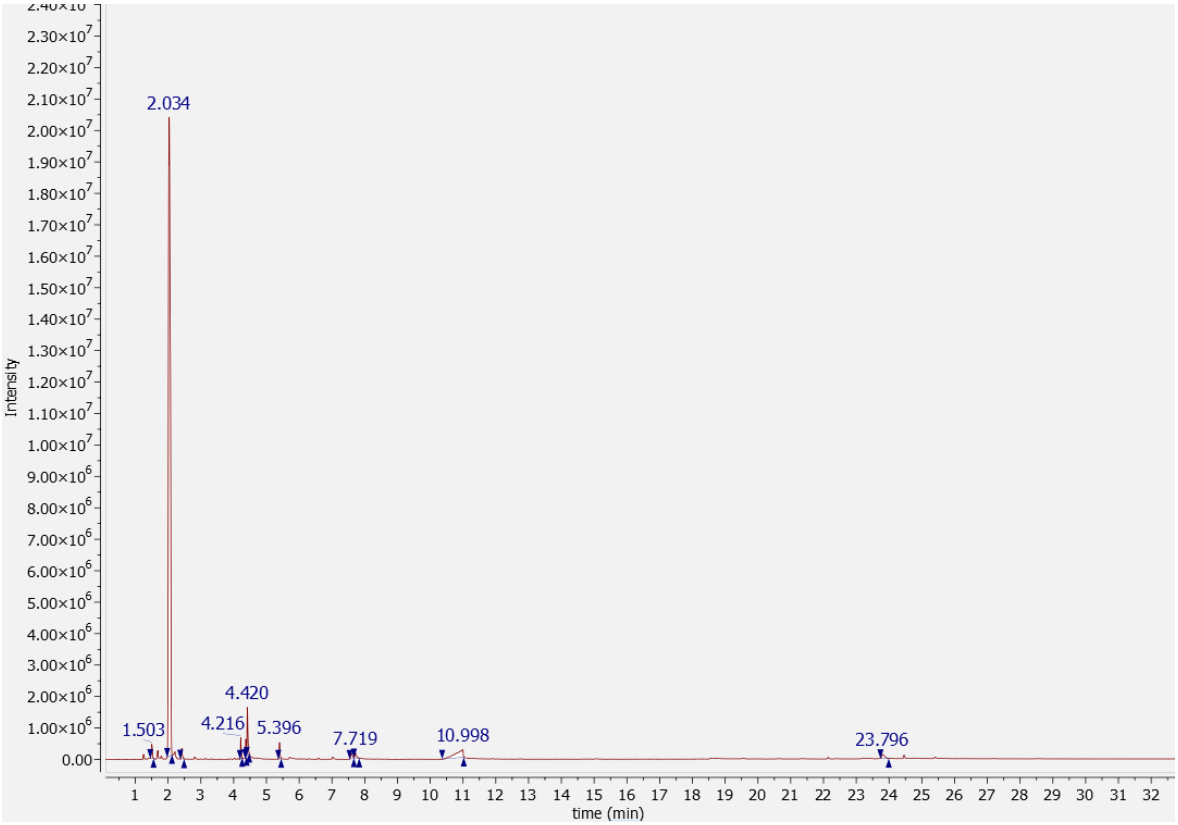

Figure 4.28 – Typical GC trace for the ozone excess reaction of ozone (4ppm) and Z-3-hexenyl acetate (1ppm) sampled using Tenax (n=2). 1.51min = propanal, 2.03min = cyclohexane, 2.82min = methylcyclohexane, 4.22min = cyclohexanol, 4.37min = cyclohexanone, 5.40min = benzaldehyde, 7.72min = acetaphenone, 10.99min =benzoic acid, 23.80min = heavy fuel oil.

Table 4.16 – Identified peaks from the reaction of ozone and Z-3-hexenyl acetate sampled using Tenax.

Retention time (min)	Identification	Identification method	Percentage NIST match
1.51	propanal	NIST	80
2.03	cyclohexane	NIST	91
2.82	methylcyclohexane	NIST	94
4.22	cyclohexanol	NIST	95
4.37	cyclohexanone	NIST	94
4.44	m/z=43.1,53.0,61.1,73.1,80.1,88.1,98.1,116.0,128.1	-	-
5.40	benzaldehyde	NIST	96
7.72	acetaphenone	NIST	91
10.99	benzoic acid	NIST	95
23.80	heavy fuel oil	NIST	95

From comparison with the NIST mass spectrum database, the following assignments were made as a result of Tenax sampling (Table 4.16). Several peaks (Figure 4.28) were attributable to breakdown products of Tenax; however, a key peak was elucidated. Propanal was identified (RT=1.51 min, Figure 4.25, NIST=80). The peak at RT=4.44min could not be identified.

4.3.2 Summary of identified reaction products

From the products identified in both this work and in literature (Table 4.17), comparisons are made to highlight novel determinations such as ozonolysis products from 1-dodecene and 1-undecene. The commercial availability and the ability to synthesise products identified in both this work and in literature is also assessed to allow determination of identified ozonolysis products that are suitable for electrophysiological response testing.

Table 4.17 – A summary of ozonolysis products for the five model VOCs from both literature products and this work. Green indicates availability for further experiments. [a] identified by Lee et al. (2006), [b] identified by Aschmann et al. (1997), [c] identified by Grosjean and Grosjean (1999), [d] as of June 2019.

Parent VOC	Reaction product	Identified in literature?	Identified in this work?	Commercially available? [d]	Literature synthesis route and feedstock available?
1-dodecene	undecanal	N	Y	Y	N/A
	acetone	N	N	Y	N/A
	decanal	N	Y	Y	N/A
1-undecene	decanal	N	Y	Y	N/A
	acetone	N	N	Y	N/A
	nonanal	N	Y	Y	N/A
3-carene	3-caronic acid	Y[a]	N	N	N
	3-caronaldehyde	Y[a]	N	N	N
	acetic acid	Y[a]	N	Y	N/A
Z-3-hexenol	propanal	Y[b]	Y	Y	N/A
	3-hydroxy propanal	Y[b]	N	N	N
Z-3-hexenyl acetate	Propanal	Y[c]	Y	Y	N/A
	3-oxoproyl acetate	Y[c]	N	N	Y
	2-oxoethyl acetate	Y[c]	N	N	Y
	acetaldehyde	Y[c]	N	Y	N/A
	methyl glyoxal	Y[c]	N	N	N
	acetone	Y[c]	N	Y	N/A
	glyoxal	Y[c]	N	Y	N/A

4.3.3 Synthetic blend ozonolysis

Due to the lack of qualitative differences in identified reaction products from ozone excess to VOC excess reactions, as demonstrated from the individual VOC ozonolysis experiments above, only the ozone excess reaction was studied moving forward. As described in the methodology section, initial SPME sampling experiments showed that the ratio described in Table 4.6 (section 4.2.6.1) produced a dominance of 3-carene and thus, refinement was undertaken until the blend described in Table 4.6 (section 4.2.6.1) was reached. This refined synthetic blend was then used in ozonolysis experiments. Comparison of ozonolysis products from the synthetic blend (Figure 4.29) with the retention times and mass spectra of products identified in section 4.3.1 of this work saw no new peaks produced.

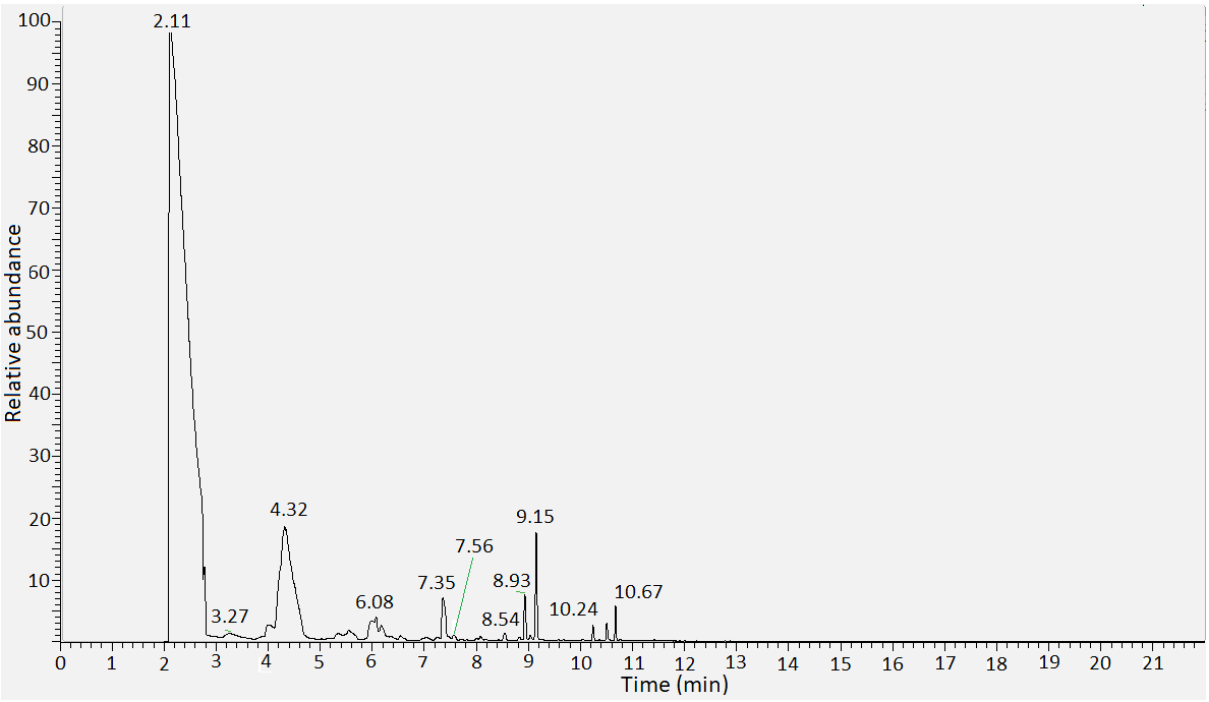

Figure 4.29- Reaction of refined blend mixture (1ppm) with ozone (4ppm) sampled using SPME-GC-MS. Peaks were identified by comparing retention times and mass spectra to products identified in section 4.3.2. RT=2.11min cyclohexane, RT=4.32min cyclohexanone, RT=6.08min Z-3-hexenyl acetate/3-carene, RT=7.35min 1-undecene, RT=7.56min nonanal, RT=8.54min 3-carene impurity, RT=8.93 1-dodecene, RT=9.15min decanal, RT=10.24min 3-carene impurity, RT=10.67 undecanal. Silated compounds, RT= 3.27,5.55,7.99,10.55 min

4.3.4 Results – compound synthesis

4.3.4.1 Synthesis of 3-oxopropyl acetate

The GC-MS spectrum for the liquid injection of 3-oxopropyl acetate in hexane showed several peaks, suggesting a number of impurities and 3-oxopropyl acetate was unable to be identified (Figure 4.30). Low product yields are attributed to loss during repeated concentration steps.

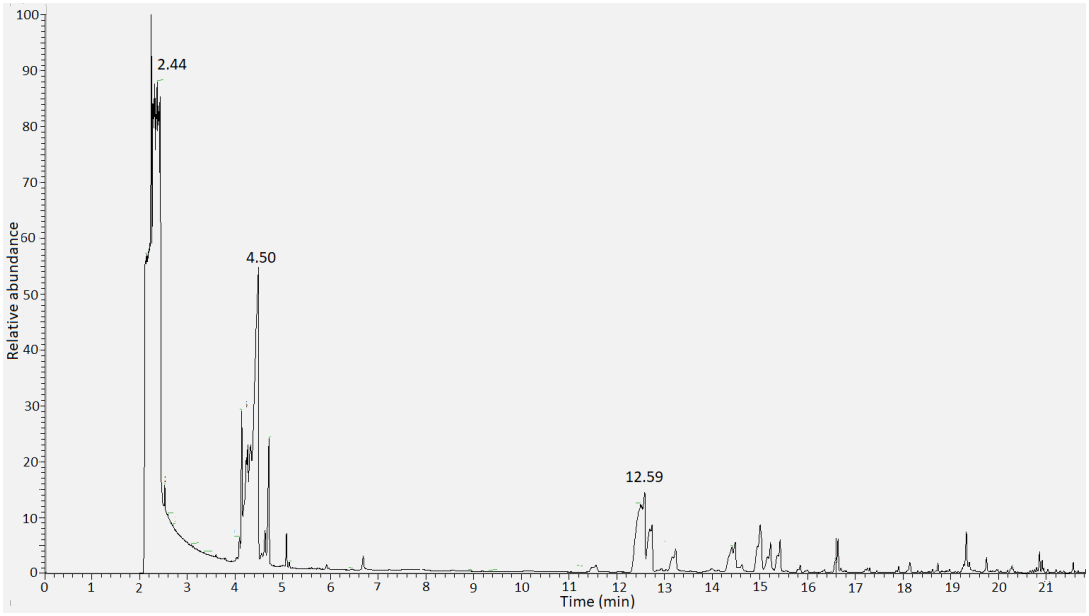

Figure 4.30 – GC-MS analysis of synthesised 3-oxopropyl acetate. (RT=2.44 min hexane, RT=4.50 min 3-oxopropyl acetate (tentative), RT=12.59min acrolein dimer).

The structure of 3-oxoproyl acetate predicts four hydrogen environments with five carbon environments (Figure 4.31). The ^{1}H NMR of 3-oxopropyl acetate showed the correct number of dominant hydrogen environments (Figure 4.32); however, the wrong multiplicities are initially apparent. This is rationalised by weak spin-spin coupling between the aldehyde proton and neighbouring protons, thus producing the observed aldehyde singlet (δ=9.80ppm) and triplet methyl group (δ=2.78ppm). On closer inspection of the singlet, a weak amount of splitting may be observed giving the expected triplet, thus adding clarity to this argument (Figure 4.32). Minor ^{1}H NMR peaks are also observed which indicates that a mixture was likely produced. The ^{13}C NMR experiment (Figure 4.33) showed five carbon environments which agrees with prediction; however, the signals were weak which indicates a dilute sample. While the NMR spectra for 3-oxopropyl acetate provided some indication that 3-oxopropyl acetate may have been formed as a result of this synthesis, the GC data indicates that an authentic standard was not formed. This means that one cannot conclusively attribute any peak as 3-oxopropyl acetate and thus, the sample was unsuitable for use in EAG experiments.

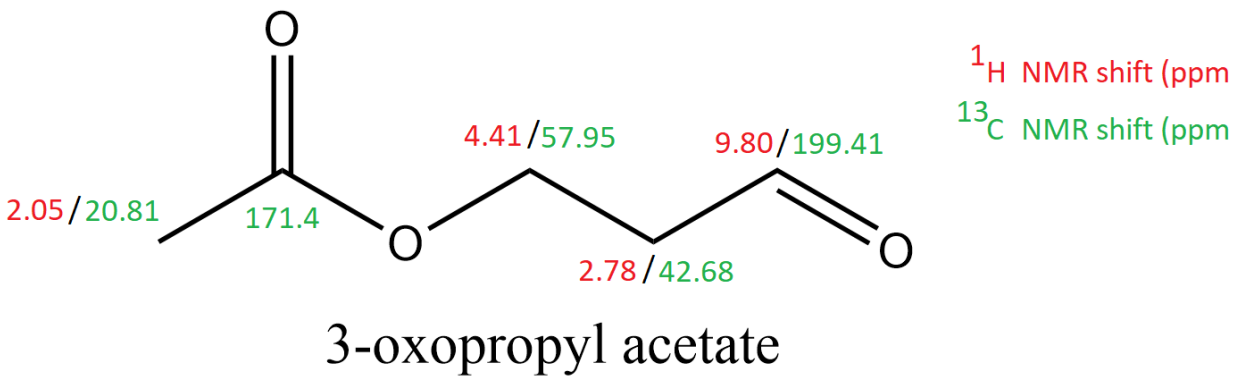

Figure 4.31 – Molecular structure of 3-oxopropyl acetate with experimental ^{1}H and ^{13}C NMR shifts.

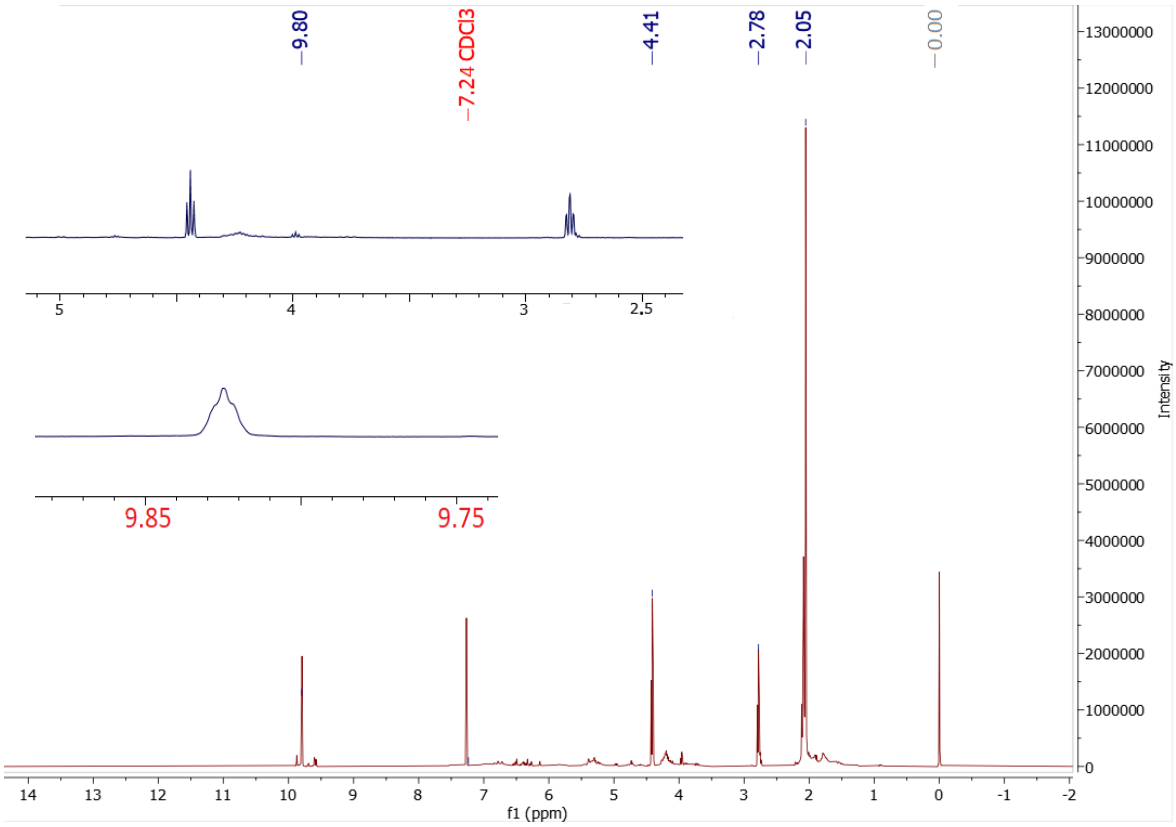

Figure 4.32- Final ^{1}H NMR of 3-oxopropyl acetate showing intensity and chemical shift of proton environments in the synthesised sample. Closeup on aldehydic singlet at 9.83ppm shows minor triplet splitting causes by weak spin-spin coupling. Four proton environments are expected and four major environments are seen (7.24ppm is the environment for the solvent $CDCl_3$ and 0.00 is for TMS). ^{1}H NMR δ (2.05, S) (2.78, Trip) (4.4, trip) (9.79, S).

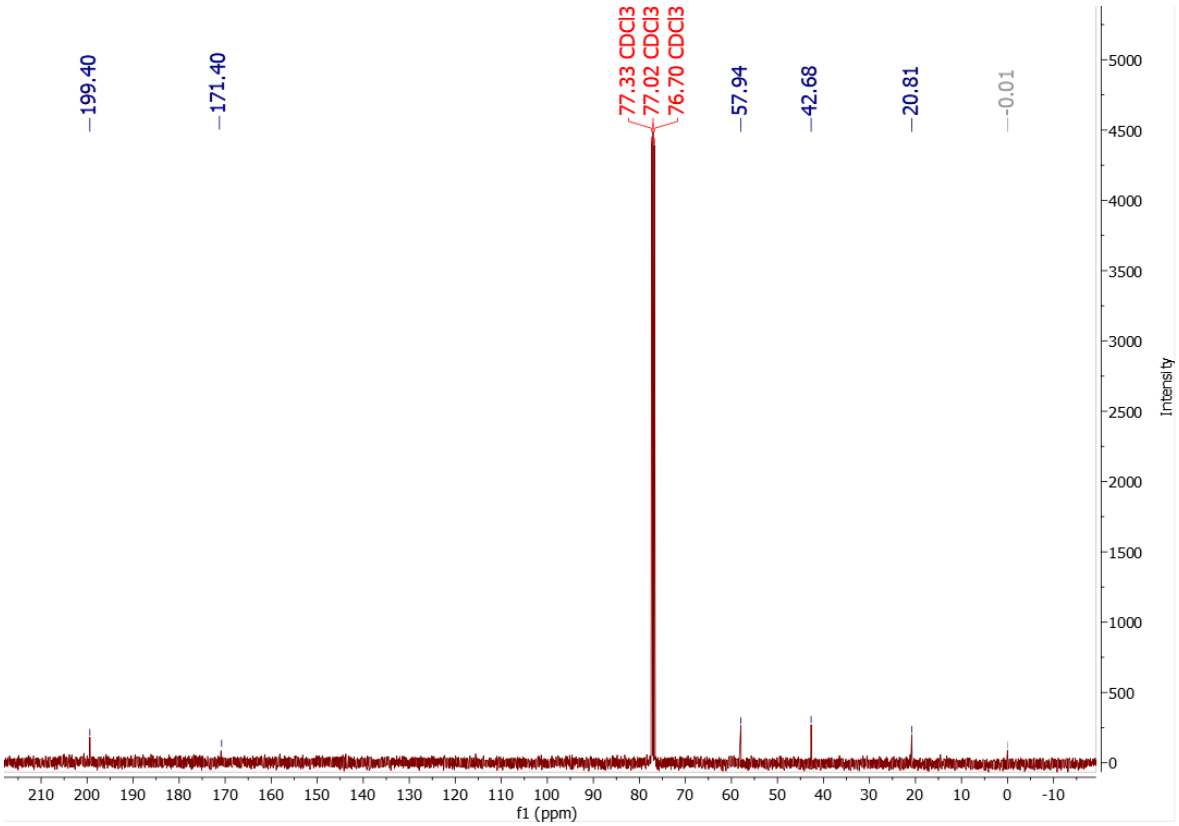

Figure 4.33- Final ^{13}C NMR of 3-oxopropyl acetate showing chemical shift of carbon environments in the synthesised sample. Four carbon environments are predicted from the structure of 3-oxopropyl acetate and are seen. ^{13}C NMR δ (20.81) (42.68) (57.95) (171.40) (199.41).

4.3.4.2 Synthesis of 2-oxoethyl acetate

The GC-MS spectrum for the liquid injection of 2-oxoethyl acetate in hexane showed several peaks, suggesting a number of impurities (Figure 4.34) and thus, 2-oxoethyl acetate could not be identified. Low product yields are attributed to loss during repeated concentration steps.

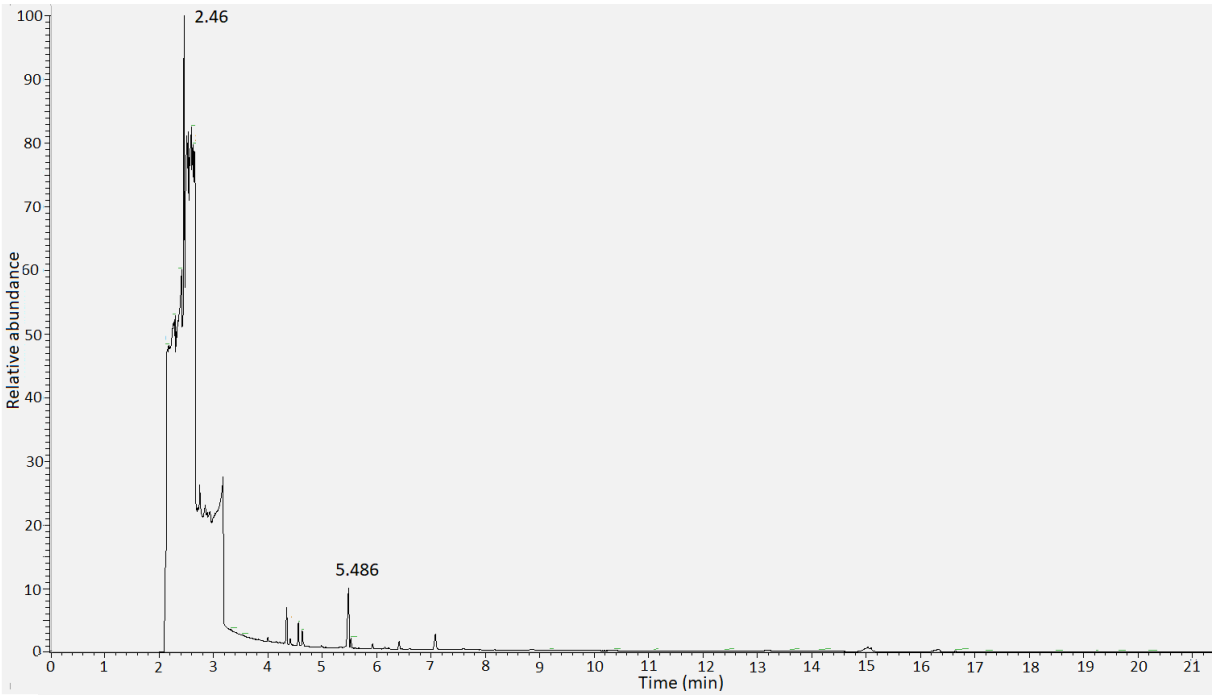

Figure 4.34 – GC-MS analysis of synthesised 2-oxoethyl acetate (RT=2.46 min hexane, RT=5.486 min 2-oxoethyl acetate (tentative).

The structure of 2-oxoethyl acetate predicts three hydrogen environments with four carbon environments (Figure 4.35). The ^{1}H NMR (Figure 4.36) for 2-oxoethyl acetate showed the correct number of dominant environments (when the presence of residual PPh_3=8.01ppm, $CDCl_3$=7.27ppm, H_2O=2.11ppm and TMS=0.00ppm are taken into account). However, the wrong multiplicities are initially apparent for the ^{1}H NMR. This is rationalised by weak spin-spin coupling between the aldehyde proton and neighbouring protons (see Figure 4.32 for similar effect), thus producing the observed aldehyde singlet (δ=9.62ppm) and singlet methyl group (δ=2.20ppm). Minor ^{1}H NMR peaks are also observed which indicates that a mixture was likely produced. The ^{13}C NMR experiment (Figure 4.36) showed five carbon environments which agrees with prediction; however, the signals were again weak which indicates a dilute sample. While the NMR spectra for 2-oxoethyl acetate provided some indication that 2-oxoethyl acetate may have been formed as a result of this synthesis, the GC data indicates that an authentic standard was not formed. This means that one cannot conclusively attribute any peak as 2-oxoethyl acetate and thus, the sample was unsuitable for use in EAG experiments.

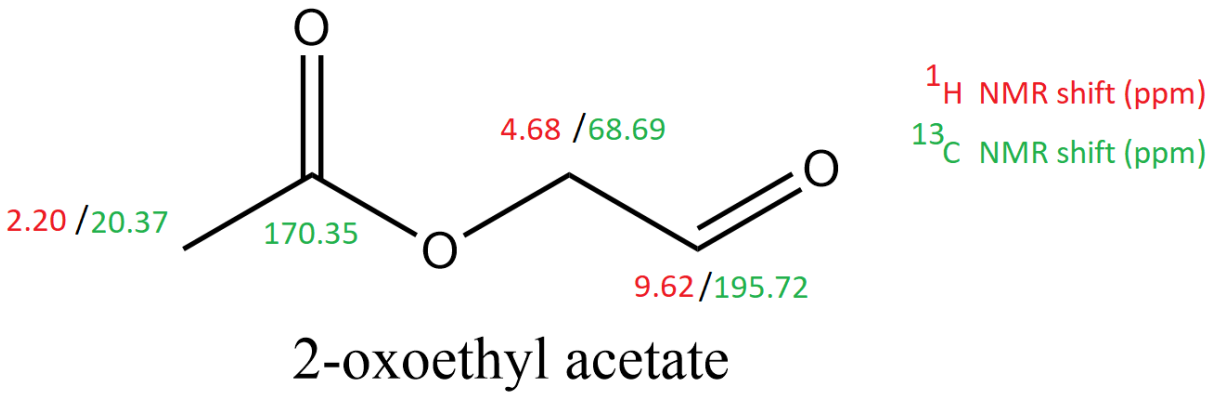

Figure 4.35 – Molecular structure of 2-oxoethyl acetate with experimental ^{1}H and ^{13}C NMR shifts.

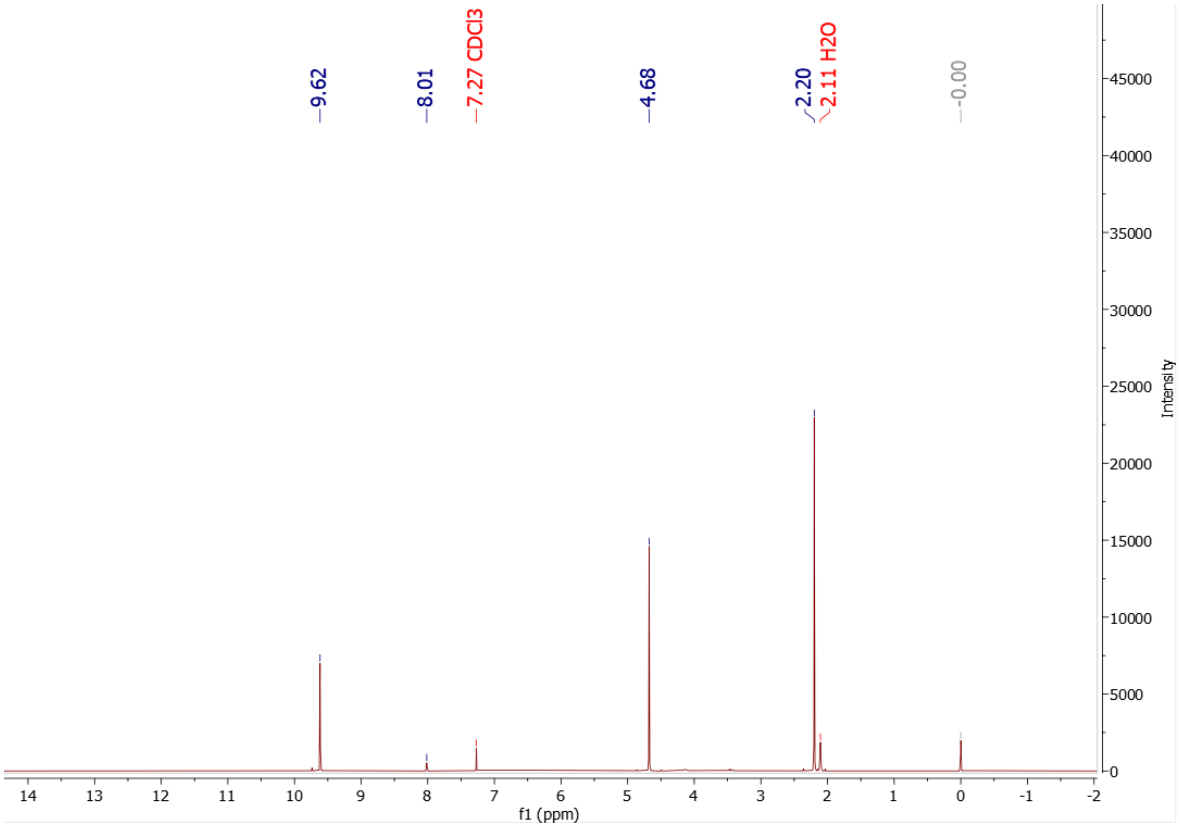

Figure 4.36 – Final ^{1}H NMR of 2-oxoethyl acetate showing intensity and chemical shift of proton environments in the synthesised sample. Three proton environments are expected, and three dominant environments are seen (7.24ppm is the environment for the solvent $CDCl_3$, 2.11ppm is for H_2O and 0.00ppm is for TMS). ^{1}H NMR δ (2.20, S) (4.68, S) (9.62, S).

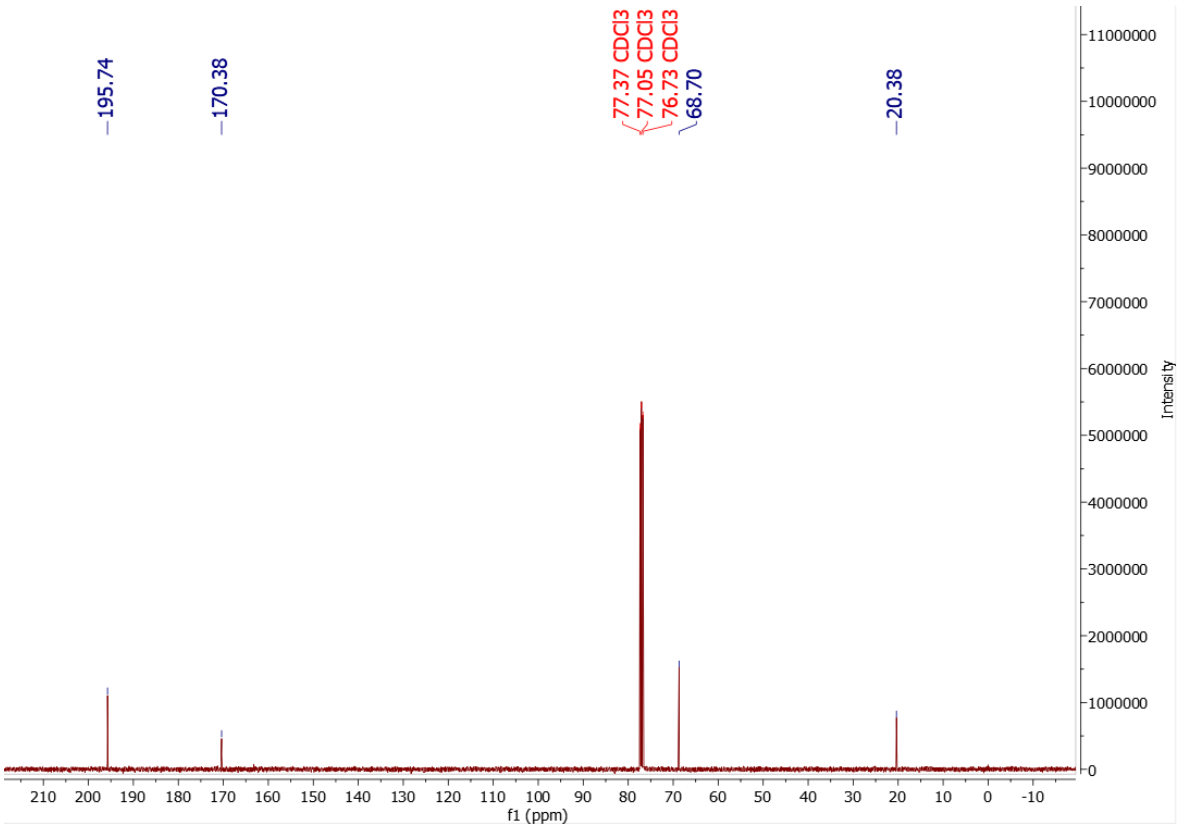

Figure 4.37- Final ^{13}C NMR of 2-oxoethyl acetate showing chemical shift of carbon environments in the synthesised sample. Four carbon environments are predicted from the structure of 2-oxoethyl acetate and are seen. ^{13}C NMR δ (20.37) (68.69) (170.35) (195.72).

4.3.5 Electroantennography results

Figure 4.38 shows that each stimuli produced an electrophysiological response that was greater than the control antennal response to hexane, except for glyoxal which showed a smaller antennal response than to hexane. All data sets showed statistical significance except for acetaldehyde which showed borderline significance (n=6, V=19.5, p=0.074) which is likely to be due to the non-parametric nature of the test being less powerful than its parametric equivalent. As a result of the syntheses of 3-oxopropyl acetate and 2-oxoethyl acetate not producing unambiguous authentic standards coupled EAG experiments could not be undertaken.

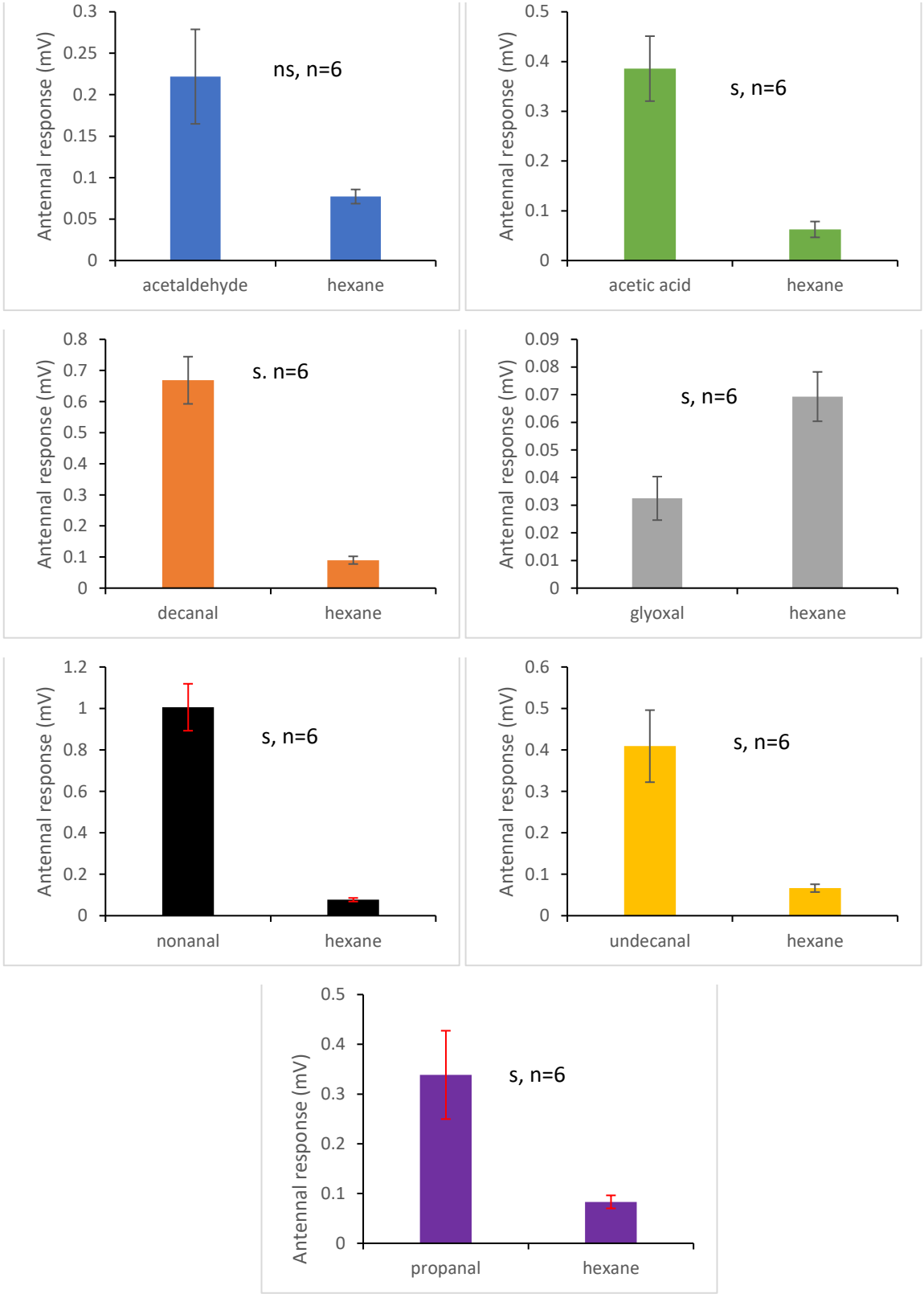

Figure 4.38 – Mean electrophysiological responses of *A. mellifera antennae* (± SE) to ozonolysis product stimuli (10^{-1}) in comparison to control stimuli (Hexane). S=statistically significant, ns= not statistically significant at the 95% confidence interval. Statistical significance is seen for acetic acid (v=21, p=0.031, n=6), decanal (v=21, p=0.031, n=6), glyoxal (v=0, p=0.031, n=6), nonanal (v=0, p=0.031, n=6), undecanal (v=0, p=0.031, n=6), acetaldehyde (V=19, p=0.093, n=6) and Propanal (v=0, p=0.031, n=6).

4.4 Discussion

4.4.1 Summary of identified reaction products

From Table 4.17 it may be seen that previously undiscovered reaction products were detected for certain VOCs while some compounds that had been previously identified in the literature could not be identified. 1-dodecene and 1-undecene have no literature regarding ozonolysis products and thus, the conformation of predicted primary reaction products (undecanal and decanal) is novel as well as the discovery of secondary reaction products (decanal and nonanal). A possible formation mechanism for the observed secondary reaction products, based upon the proposed scheme of (Rissanen et al. 2015), is proposed in Figure 4.39. A hydrogen shift is proposed to create a new double bond which may then be further attacked by ozone. There is also the possibility of contamination of 1-undecene in the 1-dodecene sample and 1-decene in the 1-undecene sample being the source of the newly identified products. Close examination of SPME-GC-MS spectra for unreacted 1-dodecene (Figure 4.11) showed one major peak (RT=8.68min) and one minor peak (RT=8.48min), both of which returned NIST matches as 1-dodecene indicating peak splitting. For unreacted 1-undecene, SPME-GC-MS spectra (Figure 4.15) showed three peaks of varying sizes. The two major peaks (RT=7.94min/8.07min) are close in retention time and both returned NIST matches as 1-undecene indicating peak splitting. The smaller peak (RT=6.64min) also returned NIST matches as 1-undecene, however, it is possible from the peak separation that the peaks may be of differing identities and thus, may be a trace of 1-decene contamination in the 1-undecene sample.

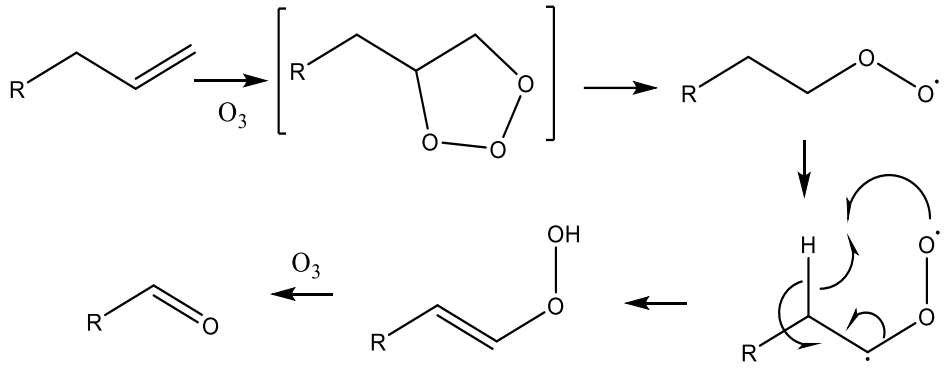

Figure 4.39- Application of a general mechanism suggested by Rissanen et al. (2015) to rationalise the formation of decanal and nonanal from ozonolysis of 1-dodecene or 1-undecene respectively.

For 3-carene, Z-3-hexenol and Z-3-hexenyl acetate, most literature identified reaction products could not be detected using SPME in this work which is likely due to a combination of factors. The presence of large amounts of scavenger may have obscured low molecular weight reaction products, such as propanal and formaldehyde (despite efforts to resolve any potential peaks), while first generation product yields were generally seen to be low in previous work (Aschmann et al. 1997; Grosjean and Grosjean 1997).

Tenax sampling allowed for the identification of low molecular weight products such as propanal, which was able to be resolved from cyclohexane due to the differing absorptive properties of Tenax relative to SPME. However, high molecular weight reaction products such as those produced from the ozonolysis of 3-carene remained elusive which may be as a result of their incorporation into SOA (Lee et al. 2006b).

For all VOCs, no qualitative differences were observed between the reaction products formed under ozone excess conditions relative to VOC excess conditions. It would be expected that ozone excess conditions may allow secondary reaction products to form due to the presence of ozone beyond the quantity needed to form primary products (Lee et al. 2006a). It is unclear what caused this observation but it may be as a result of several factors. Secondary reaction products are more highly oxidised and thus may have either been incorporated into SOA which is unable to be captured by SPME or may have been too highly oxidised to adhere to the fibre used in this work (previous work used direct injection proton transfer reaction mass spectrometry (PTR-MS) (Lee et al. 2006a) and DNPH collection media with GC-MS (Grosjean and Grosjean 1999) both of which may have been more suited to the collection of highly oxidised molecules). It is also possible that formation yields of secondary reaction products may have been lower due to the stability of primary reaction products (Grosjean and Grosjean 1999) and or substantial yields of secondary reaction products may not have formed during the timescale used in these experiments.

Most identified ozonolysis products were commercially available; however, where they were not commercially available only the synthesis of 3-oxoproyl acetate and 2-oxoethyl acetate could be attempted as they both had literature synthesis routes and commercially available feedstock.

4.4.2 Blends

Upon exposure of the blend to ozone (Figure 4.29), all of the major peaks observed were accounted for by the individual ozonolysis experiments of the blend components which suggests that little to no interactions occurred between blend components during ozonolysis. This suggests that evidence collected during ozonolysis of individual blend components is applicable to the overall blend, thus making the prediction of oxidation products from any single VOC blend predictable which allows for simple characterisation of how a blend may be affected by reaction product formation.

4.4.3 Electroantennography (EAG) experiments

EAG analysis of physiological response to ozonolysis products (Figure 4.38) generally showed a statistically significant difference in response to compounds relative to the hexane control, thus inferring that ozonolysis products elicited electrophysiological responses and thus, have the potential to affect plant-pollinator signalling. The electrophysiological responses indicate that behavioural

responses could follow, which such effects being previously observed where non-blend VOC degradation products acted as behavioural repellents (Mofikoya et al. 2020).

These responses also support the theory that reaction products could be used in lieu of emitted VOC's, either with external stimuli to aid blend learning (utilising plasticity), or without (generalisation), to locate flowers (Blande et al. 2015; Cook et al. 2020). Plasticity may be more likely in practice as the ability to generalise between odours is not necessarily linear (Guerrieri et al. 2005) and thus, may work better in some cases and worse in others (see section 1.4.3).

Of the tested reaction products, only glyoxal showed a statistically significant decrease in antennal response relative to hexane, which is hypothesised to be as a result of glyoxal functioning as a receptor antagonist. A receptor antagonist works by blocking the receptor, thus blocking the response to the hexane in which the glyoxal is diluted and producing a lower antennal response (Battista 2015). This effect has been noted previously by Koczor et al. (2012) who showed that Lucerne bug (*Adelphocoris lineolatus* Goeze) showed a lower EAG response to (E)-cinnamic-alcohol than hexane. The borderline statistical significance for Acetaldehyde is likely an artefact of having to use a less powerful nonparametric statistical test. Although acetone was commercially available, it proved challenging to test due to its very high vapour pressure and thus, the response to acetone was not measured.

Unfortunately, efforts to synthesise authentic 3-oxopropyl acetate and 2-oxoethyl acetate standards proved unsuccessful and thus, their electrophysiological responses could not be measured using EAG.

4.5 Conclusion

This work aimed to both identify VOC degradation products and assess their ability to provoke an antennal physiological response in *A. mellifera*. Several VOC degradation products were identified during this work and of these, several provoked an antennal physiological response in *A. mellifera*.

Initial experiments to characterise the reaction products of the model floral blend components were challenging due to the volatile nature of the ozonolysis reaction products produced, the lack of mechanistic information regarding secondary reactions and the niche nature of the reaction products meaning they were not present in the NIST database. However, this work has managed to identify novel products from the ozonolysis of 1-dodecene and 1-undecene as well as identify literature stated reaction products for Z-3-hexenol and Z-3-hexenyl acetate. It was observed that VOC blend component oxidation products elicited an antennal response in *A. mellifera*. This provides a precedent that will allow for later exploration of the hypotheses that ozonolysis products may be able to be used in lieu of undegraded blend components (as a result of generalisation without prior learning or as a result of plasticity with learning see 1.4.3/1.5.4) to aid navigation or alternatively ozonolysis products may potentially perturb the functioning of chemical blends (see section 1.4/4.1);

however, exploration of both theories requires further behavioural research studies. These findings complement the work of Mofikoya et al. (2020) by showing that ozonolysis products can be electrophysiologically active, and thus may have been the root cause of the observed behavioural changes. It also indicates that observed behavioural changes as a result of ozone degradation of a blend (Li et al. 2016; Farré-Armengol et al. 2016) could be, at least in part, as a result of degradation products.

The outcomes of this work necessitate future work to not only explore whether blend VOC degradation products provoke antennal responses in other plant-pollinator systems but also to begin the task of ascertaining the behavioural effects of these degradation products not only upon the plant-pollinator system from which they are formed but also upon neighbouring VOC communication systems within the environment. Little to no qualitative differences in the products produced by VOC ozonolysis were seen between VOC excess and ozone excess conditions indicating secondary gas phase reaction products may not be prominent; however, it may also be of utility to undertake quantitative comparisons (which were not undertaken here due to instrument limitations) because even slight alterations in product formation yields may have profound effects on behaviour.

Chapter 5 – Exploring how SOA, and associated reaction mixture constituents, affect the electrophysiological response of A. mellifera antennae to selected floral VOC stimuli

5.1 Introduction

Insects use specialised sense organs known as an olfactory (Figure 5.1) system to interact with VOC cues from their environment (See sections 1.4 and 2.4.8). Insect olfactory systems are complex and adapted to be able to sense finite quantities of VOCs from great distances and as such have many specialised features. The antennal cuticle is coated with apolar long-chain hydrocarbons (Steinbrecht 1997) which channel gas-phase polar VOC molecules that land on the cuticle towards the cuticular pores. Within the pores, olfactory binding proteins solubilise VOCs to allow them to diffuse from the gas-phase, pass through the antennal lymph and finally attach to the dendritic nerve, creating an electrical impulse which is transported to the brain (Rützler and Zwiebel 2005). If any single element of this process is disrupted it has the potential to hinder the insect's ability to participate in VOC communication.

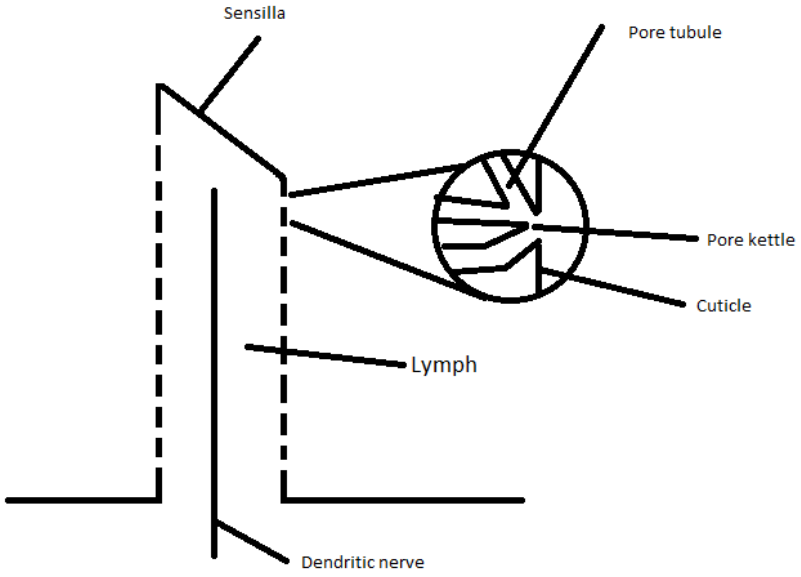

Figure 5.1 – A simplified schematic of an antennal sensilla based upon the work of Archer (2005).

As explained in detail in chapter 1.5, gas-phase VOCs in the troposphere that are used as cues by insects may react with common tropospheric oxidants such as ozone (O_3), nitrogen trioxide (NO_3) and hydroxyl radicals (OH), both reducing the concentration of the original VOC molecules as well as forming gas phase reaction products (Monks 2005). It has been shown that some of these gaseous reaction products may coagulate to form larger secondary organic aerosol (SOA) particles (Chen and Hopke 2009, see section 1.5.1).

SOA particles have been shown to affect the environment at a global scale by altering the earth's radiative forcing and thus, altering the earth's climate (Hoyle et al. 2009; Carslaw et al. 2010) which

in turn may cause several changes within the environment such as; altered VOC emissions (Yuan et al. 2009) asynchrony between organisms in the environment (Richman et al. 2020) and reductions in plant fitness (Goulson et al. 2015). However, there is still much uncertainty regarding the direct effects of SOA on terrestrial organisms. SOA has been suggested to play a role in pheromone transportation within the environment (Jami et al. 2020); however, it has also been suggested by Holopainen et al. (2017) that SOA may negatively affect organisms, for example by decreasing plant fitness as a result of reductions in photosynthesis due to SOA coating of leaves. A negative feedback loop is proposed by Holopainen and Blande (2013) where SOA formation alters the earth's climate which would thus, alter VOC emission rates of plants and potentially increase the formation of SOA particles. One part of this feedback loop has been demonstrated experimentally by Yli-Pirilä et al. (2016) who used an autumnal moth (*Epirrita autumnata* Borkhausen) – downy birch (*Betula pubescens* Ehrh.) system to show that feeding by *E. autumnata* caused changes in the VOC emissions of the birch trees which contributed to a 150 fold increase in the formation of SOA particles.

An interesting focal point in the broader discussion of the effect of SOA particles on terrestrial organisms is the direct interaction of SOA particles with an insect's olfactory system. To date little is known regarding this interaction, yet SOA is likely to be relatively abundant in the troposphere with SOA particles accounting for between 1-54% of the total product yield from the ozonolysis of six of the most common floral blend VOCs found in nature (Knudsen et al. 2006; Lee et al. 2006a).

There are a number of ways that SOA particles may be hypothesised to interact with an insect's olfactory system. SOA particles may enter, and thus disrupt, the internal functioning of the pore kettle; may block the entrance to the pore kettle or may affect the functioning of the antennal cuticle, thus reducing the ability of gas-phase molecules to be directed to the pore kettle. SOA particles have been shown to have a size range of ca.1-100nm (Shrivastava et al. 2017) and the size of a pore kettle has been shown to range between 20nm and 60nm in diameter (Whitehead and Larsen 1976; Steinbrecht 1997; Anderson et al. 2000) and thus, it is thought plausible that some kind of interaction between SOA and pore kettles may take place.

Previous work by Dötterl et al. (2016) has investigated the effect of ozone exposure upon an insect's olfactory system by examining the ability of a honeybee (*Apis mellifera* L.) to physiologically detect selected VOCs (Z-3-hexenyl acetate, linalool, 2-phenylethanol) during ozone fumigation. A reduction in the antennal response to stimuli undergoing ozone fumigation was seen; however, the extent of the reduction in response seemed to be VOC specific with only Z-3-hexenyl acetate showing a statistically significant difference in electrophysiological response. Leonard et al. (2019) showed, using behavioural bioassays, that prior exposure to diesel exhaust reduces the ability of *A. mellifera* to learn undegraded floral odours. Vanderplanck et al. (2021) also demonstrated both reductions in EAG responses and behavioural responses of bumblebee (*Bombus terrestris* L.) to benzaldehyde

when insects had been previously exposed to ozone. These studies indicate the potential for long term effects of exposure to tropospheric oxidants, however, it remains unclear as to whether previous exposure to tropospheric oxidants directly effects the physiological functioning of the antennae, the CNS or both.

The effect of SOA on antennal functioning and thus, its effect on the efficacy of VOC based communication, has however yet to be explored in isolation of other ozone degradation factors. Farré-Armengol et al. (2016) used a black mustard (*Brassica nigra* L.) – bumble bee (*B. terrestris*) system to demonstrate a reduced attraction to the ozone degraded floral blend relative to an undegraded floral blend during a flight chamber dual choice assay. While this work demonstrated an effect of ozone on VOC mediated communication, the efficacy of the various effects of ozone degradation on VOC mediated communication (such as VOC blend ratio alteration, formation of reaction products and formation of SOA particles) have not been demonstrated in isolation of each other.

In this chapter, using laboratory-based studies, I aimed to initially explore the prevalence of SOA, as well as particle size, at distances that *A. mellifera* may be thought to utilise floral VOCs (400m), and thus, the potential for impact on VOC communication, under two landscape scenarios (VOC excess/ozone excess, see section 2.1.2). I also investigated whether SOA was able to perturb the antennal response of *A. mellifera* elicited by two model stimuli (nonanal, Z-3-hexenol) either during or after exposure to SOA.

An oilseed rape (*Brassica napus* L.) – honeybee (*A. mellifera*) model system was chosen for this work with 1-undecene, 1-dodecene, Z-3-hexenol, Z-3-hexenyl acetate and 3-carene the VOCs of interest (see 2.1.1 for further rationalisation).

To achieve the aims of the study, I first investigated the yields, particle sizes and rate of production of SOA from each of the model VOCs. This was conducted by taking scanning mobility particle sizer (SMPS) measurements of static chambers (see section 2.4.10) containing one of the five volatiles and ozone under both ozone excess and VOC excess conditions. Then, using similar methods to those established by Dötterl et al. (2016), I investigated the effect of SOA particles (generated from 3-carene which was selected due to its low antennal response and high SOA yield), on a honeybee antennae's electrophysiological response to both high and low doses of two VOCs, to which *A. mellifera* is known to exhibit a strong electrophysiological response, nonanal, Z-3-hexenol. Because SOA cannot be generated in isolation of its constituent parts it was necessary to also investigate the effects of the VOC and ozone precursors in isolation on the electrophysiological response of *A. mellifera*.

5.2 Materials and methods

5.2.1 Establishment of reactant concentrations

Both ozone excess (1ppm ozone, 0.25ppm VOC) and VOC excess (1ppm ozone, 3ppm VOC) scenarios were tested for all five VOCs, with a 400m foraging distance used (assuming 1m/s windspeed) when assessing likely impacts of SOA upon the model pollinator *A. mellifera*. Further rationale is presented in the general methodology (section 2.1).

5.2.2 SOA particle yield and particle size determination

All SOA particle yield and size data were collected using a scanning mobility particle sizer (SMPS, see section 2.4.10) (TSI®, Minnesota, USA) which consisted of a model 3080 differential mobility analyser (DMA) and a model 3775 condensation particle counter (CPC) unit, using the settings detailed in Table 5.1.

Static chambers were constructed for all VOCs using the methodology detailed in section 2.5.4 in combination with the conditions detailed in Table 5.2. The parameters without an asterisk were used for all VOCs while the conditions marked with an asterisk were used for 3-carene only when undertaking experiments to explore the effect of concentration on SOA yield.

For all experiments, on completion of static chamber filling, a 90-second pause was taken before sampling commenced to allow for transport of the static chamber from the gas handling apparatus to the SMPS. For each VOC, under each reaction conditions, at least five replicates were performed, which was deemed sufficient to account for the variation observed in the data. Ozone was held constant as opposed to VOC because in nature ozone is less liable to fluctuations in concentration than VOCs emitted by plants, which will vary significantly depending on the proximity to a plant that the recording is made.

Table 5.1 – TSI® SMPS Parameters used during experiments to characterise SOA particle yield and size.

Sheath flow rate	3.00L/Min
sample flow rate	0.27L/Min
Scan range	14.3-673.2nm
Impactor Type	0.0457cm
td(s),tf(s),D50(nm)	3.03,7.6,653
Scan up (s), retrace (s), idle (S)	120, 15, 45
Overall Scan length (Min)	3
DMA polarity	Negative
Particle density (g/cc)	1.2
Multiple charge correction	Yes
Diffusion correction	Yes
Gas density (g/cc)	0.0012
Reference gas properties	Defaults for air

Table 5.2 – Static chamber reaction conditions used to create samples for SMPS analysis of SOA particle size and yield from reaction of the five model VOCs (3-carene, Z-3-hexenol, Z-3-Hexenyl acetate, 1-undecene, 1-dodecene) with ozone. *= 3-carene only.

[VOC] ppm	[O_3] ppm	Scavenger	O_3: VOC ratio
3	1	cyclohexane	1:3
0.25	1	cyclohexane	4:1
1*	0.33*	cyclohexane*	1:3*

5.2.3 Analysis methodologies

5.2.3.1 SOA yield calculation

SOA yield calculations used equation 5.1 to relate the total produced SOA particle mass to the total starting mass of VOC. Contrary to standard convention, yield values were not corrected to account for differing reactant ratios, as is commonly seen for VOC excess conditions, so as to allow comparison of yields under the two extreme landscape scenarios proposed in this work.

$$\gamma = \frac{M_x}{M_0} \times 100$$

Equation 5.1 – SOA yield equation where: γ = SOA yield (%), z= M_x = total mass SOA concentration at time "X" (µg/m^3), M_0 = total mass concentration of initial VOC (µg/m^3).

5.2.3.2 SOA yield data analysis

Initial screening of each set of data was undertaken to check for a continuous set of both SOA yield and SOA size data points over time that showed a curve shape. Any data sets that were derived from experiments where technical problems occurred, such as disturbance of the static chamber or rapid temperature changes, and thus contained missing data or showed a clear divergence from the expected continuous curve shape, were discarded. Subsequently, the mean for both SOA yield and SOA size data at each time point was calculated to produce average data sets. From the mean data sets, key metrics namely, maximum yield, time to maximum yield, particle size at maximum yield, yield at a 400m equivalent time point (given a windspeed of 1m/s) and particle size at 400m equivalent time point were calculated. The SOA particle size at maximum SOA yield was chosen as opposed to the maximum SOA particle size because this is likely to be the most abundant particle size produced by the reaction and thus, the size most likely to be encountered by an antenna.

Unprocessed data sets, as well as mean data sets, for SOA yield and SOA particle size plotted over time may be viewed in the appendix (AP12/13).

5.2.4 Electroantennogram – VOC/O_3/SOA treatment methodology

5.2.4.1 Modified electroantennogram preparation

Electroantennogram (EAG) assays were conducted, which included exposures to two stimuli (nonanal and Z-3-hexenol) following the procedures described in section 2.5.6. These two VOC stimuli were chosen because both have been shown to elicit a strong antennal response in *A. mellifera* (see section 4.3.5). Both were diluted individually in n-hexane to produce solutions of 10mg/mL and 0.1mg/mL which, because 10µL of solution was applied to the filter paper, produced presentations of 100µg and 1µg respectively. These concentrations were chosen because they elicited good levels of antennal response in previous experiments (see 4.3.5) and match concentrations previously used in literature (Luo et al. 2013).

5.2.4.2 Treatment preparation methodology

Treatments were created in a specialist 4.5L "sausage shaped" glass cylinder with a Young's tap sealing each end (Figure 5.2). Four treatments were tested during the experiment, air, ozone, VOC and SOA. The treatments were initially prepared in a static chamber according to the general methods presented in section 2.5.2 in combination with the parameters for their formulation that are listed in Table 5.3, before being transferred to the glass cylinder. Only ozone excess conditions

were used to produce the treatments used during EAG-SOA experiments. This was as a result of the consideration that, in the real world, by the time SOA yields have generally peaked (in excess of 7.5 minutes) such a distance will have been covered by the reactants that the concentration of VOC is likely to have been diluted such that ozone excess conditions are predominant.

The process of SOA formation from an ozonolysis reaction is not complete and thus a static chamber, post-reaction, may contain air, unreacted ozone, unreacted VOC and SOA. To be able to ascertain the effect, if any, of SOA treatment upon the olfactory system of the antennae, the effects of air, unreacted ozone, and unreacted VOC were quantified. This allowed for subsequent subtraction of the effects of individual components from the effects of all components, including SOA. 3-carene was chosen as the VOC for these treatments because it provided the highest SOA yield in earlier experiments (see section 5.3.1.1) and also resulted in one of the lowest electrophysiological responses (see section 3.3.6).

Table 5.3 – Parameters used to make treatments used in EAG-treatment experiments

Treatment	Ozone (ppm)	VOC (ppm)
Air	-	-
VOC (3-carene)	0	0.25
	0	1
Ozone	1	0
	4	0
SOA	1	0.25
	4	1

Figure 5.2 – Photo of the 4.5L “Sausage shape” glass treatment vessel.

5.2.4.3 Exploring the effect of removing a water bubbler on antennal response

It was hypothesised that water vapour from the EAG water bubbler (which are routinely included in such studies to ensure antennae do not desiccate) had the potential to interfere with the treatments to be applied to the antenna and thus, the preference was to remove the bubbler while treatments were applied. An experiment was undertaken to verify if removing the bubbler had any effect on the antennal response.

Initially, the response of each antenna to a blank control (air), negative control (hexane) and a positive control (linalool, 10^{-1}) was measured. The responses to air, hexane and linalool were then compared to verify the antenna only responded to the linalool stimuli and then experiments were initiated (Vuts et al. 2010). Stimuli exposures of both nonanal and Z-3-hexenol were undertaken as detailed in section 5.2.4.1 and upon completion of these exposures, the water bubbler was either left in place or isolated from the continuous air flow system and the treatment containing vessel (containing air) connected to the continuous air supply. The assay was allowed to equilibrate for 3 minutes before the second round of stimuli exposure began, thus completing the experiment.

5.2.4.4 Exploring the effect of treatments on antennal response

For treatment tests, initial antennal response verification and initial stimuli exposures were undertaken (Figure 5.3A) as detailed in section 5.2.4.3. On completion of initial stimuli exposures, the water bubbler was isolated and the treatment containing vessel connected to the continuous air supply (Figure 5.3B). The treatment being tested was allowed to equilibrate for 3 minutes before the second round of stimuli exposure began. On completion of the stimuli exposure, the treatment bulb was removed, and the water bubbler reinserted into the continuous airflow system (Figure 5.3A). The antenna was allowed to equilibrate in clean air for 4 minutes before the final round of stimulus exposure took place.

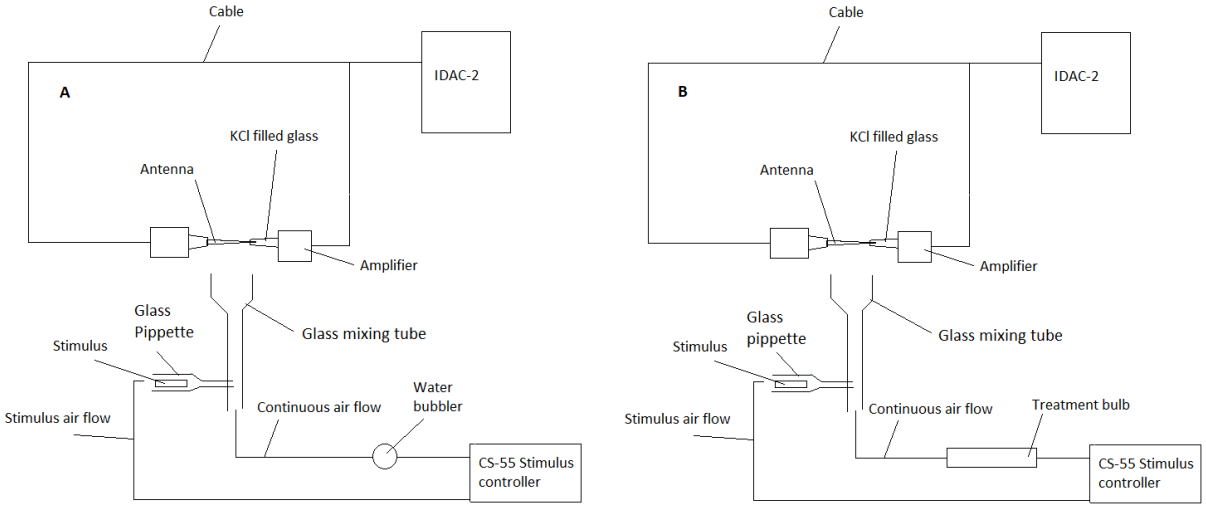

Figure 5.3 – Schematic of equipment setup for EAG-treatment experiments. The schematic on the left (A) represents the setup before/after treatments are applied. The schematic on the right (B) shows the setup during treatment.

5.2.4.5 EAG-treatment data processing

For EAG-treatment data, data was processed as described in (Dötterl et al. 2016). In summary, responses to a stimulus during treatment and post-treatment were taken as a percentage of the response to the stimulus before the treatment began. Means were then taken across replicates and statistical comparison was undertaken (see section 5.2.5).

5.2.5 Statistical testing methodologies

The "R" statistical package (Version 3.6.1) was used with various libraries (dplyr, ggplot2, PMCMR) to conduct statistical analysis. Statistical significance was measured at the 95% confidence interval for all tests. The data was initially analysed using histogram analysis to investigate the normality of the data sets.

For both SOA yield and SOA size comparisons, Mann-Whitney tests, or unpaired two-sample t-tests were selected for two-way comparisons based on data normality.

For normally distributed EAG-treatment data, t-tests were undertaken. A linear mixed effect model (LMER) approach for multi-way testing of EAG data was conducted. LMER was selected as it removes the need for post-hoc testing so as to reduce the occurrence of type 1 errors.

For comparison of the effect of high and low VOC treatment upon physiological responses, Mann Whitney U tests were conducted due to the non-parametric nature of the data.

5.3 Results

5.3.1 SOA particle size and yield results

5.3.1.1 Maximum SOA percentage yield and SOA percentage yield at 400m

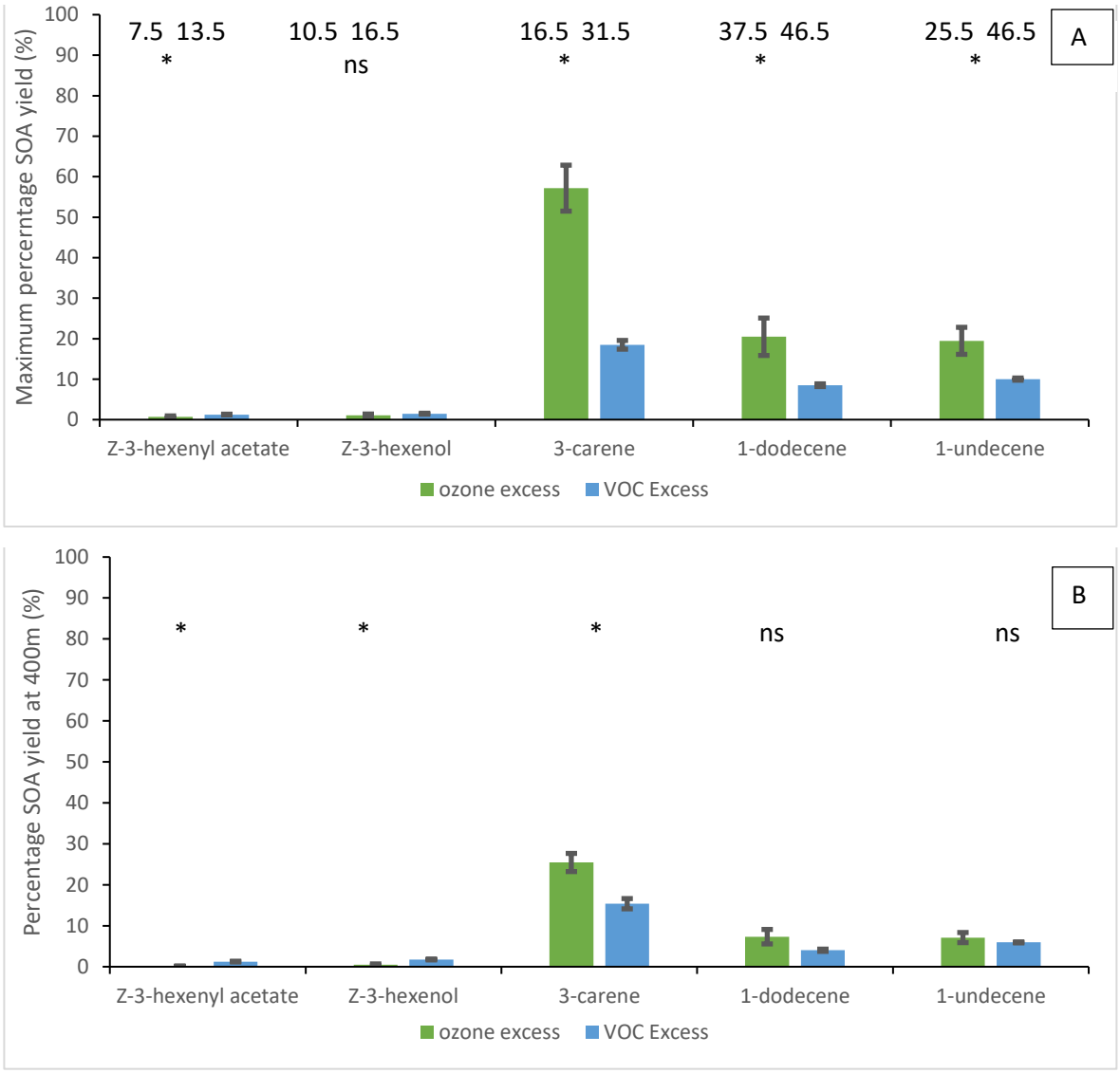

Figure 5.4 – Maximum SOA yield (A) and SOA yield at 400m equivalent timepoint (B) for the five study VOCs under both ozone excess (1ppm O_3,0.25ppm VOC) and VOC excess (1ppm O_3,3ppm VOC). Time to maximum yield (minutes) is displayed above the bars for ozone excess conditions (Left hand number) and VOC excess conditions (right hand number). *=statistically significant, ns= not statistically significant at the 95% confidence interval. For maximum SOA yield (A), there were statistically significant differences between ozone excess and VOC excess conditions for 3-carene (W = 0, N = 15, p = <0.001), Z-3-hexenyl acetate (W = 46, N = 15, p = 0.04), 1-dodecene (W = 3, N = 14, p = 0.004) and 1-undecene (W = 5, N = 13, p = 0.03) but no statistically significant difference for Z-3-hexenol. For SOA yield at 400m (B), there was a statistically significant difference in SOA yield between treatments for 3-carene (W=5, n=15,p=0.011), Z-3-hexenol (W=16,n=10,p=0.029) and Z-3-hexenyl acetate (W=54,n=15 0.002). All data are mean ± SE.

Table 5.4 – Rate constants for the reaction with ozone and vapour pressures ± standard error for the five model VOCs studied. [a]= This work [b]= Ghalaieny et al. (2012) [c] = Predicted by using ACD/Labs percepta platform

	Z-3-hexenyl acetate	Z-3-hexenol	3-carene	1-dodecene	1-undecene
Rate constant with ozone ($cm^3molecule^{-1}s^{-1}$)	5.7±0.2 $x10^{-17}$ [a]	6.0±0.1 $x10^{-17}$ [a]	4.5±0.4 $x10^{-17}$ [a]	1.2±0.2 $x10^{-17}$ [a]	1.0±0.1 $x10^{-17}$ [b]
Predicted vapour pressure (torr)[c]	1.2±0.3	1.0±0.6	1.9±0.1	0.2±0.2	0.7±0.2

For time to maximum SOA yield, a general trend is seen that those VOCs that showed faster times to reach maximum yield were those with faster rate constants (Figure 5.4/ Table 5.4). In addition, time to maximum yield was generally faster under ozone excess conditions, except for 1-dodecene.

Z-3-hexenyl acetate produced the lowest SOA yield while 3-carene produced the highest yield of SOA at both maximum yield and at a 400m equivalent timepoint. For Z-3-hexenol and Z-3-hexenyl acetate, higher SOA yields are seen under VOC excess conditions whereas higher yields are seen under ozone excess conditions for 3-carene, 1-undecene and 1-dodecene. A similar pattern was seen for projected SOA yield at 400m.

5.3.1.2 SOA increased concentration

Z-3-hexenol and Z-3-hexenyl acetate showed very low maximum yields and large levels of error under ozone excess conditions (Figure 5.4). On inspection of the raw particle concentration data, it was seen that the count was below the stated particle detection limit of $5x10^4$ counts (TSI 2007). If the assumption that percentage SOA yield is independent of concentration were true, experiments using elevated concentrations of reactants could be undertaken to try to increase the number of particles produced above that of the detection limit and thus, make a more accurate determination of SOA yield. To test if the assumption that percentage SOA yield is independent of concentration, experiments with 3-carene were undertaken. The results indicated that there is a statistically significant (W=3, N=14, p=0.0303) change in SOA yield (Figure 5.5) and thus, this assumption is false. It was therefore not possible to make a more accurate determination of the yields of Z-3-hexenol and Z-3-hexenyl acetate simply by increasing their concentrations. It is of note that these studies differed from the other SOA experiments in this chapter because the VOC was introduced to the static chamber first, whereas in all other experiment ozone had been introduced first. However, further

studies confirmed that changing the order of the introduction of the reactant did not have a statistically significant effect on the outcome of the experiment (see appendix AP6).

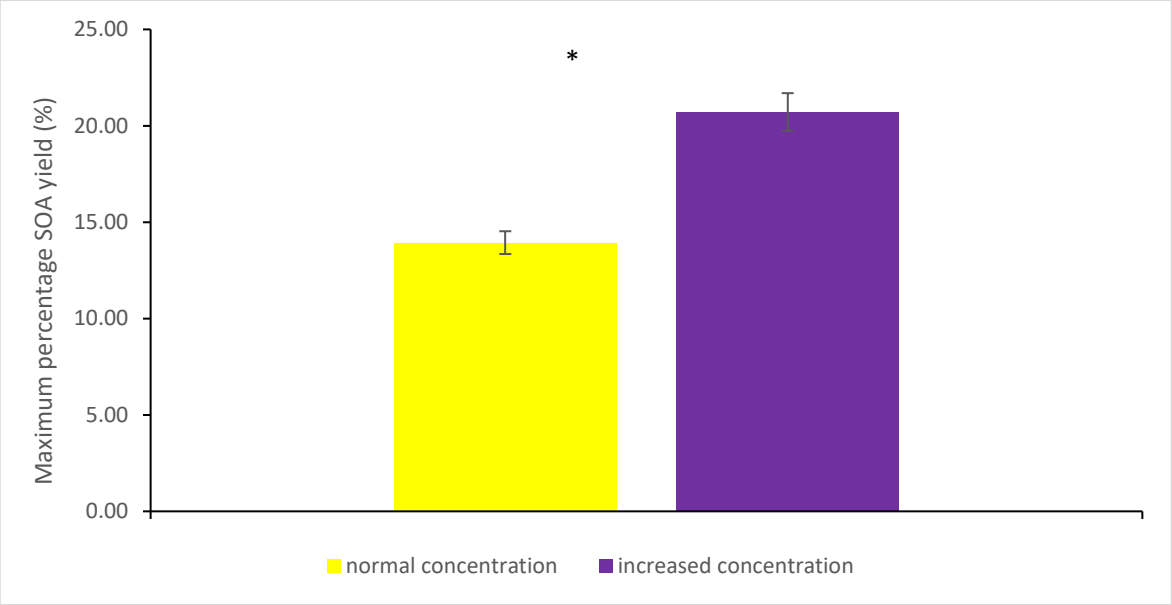

Figure 5.5 – Maximum SOA yield for 3-carene under high (VOC=3ppm, O_3=1ppm) and low (VOC=1ppm, O_3=0.33ppm) concentration VOC excess conditions. *=statistically significant, ns= not statistically significant at the 95% confidence interval. There was a statistically significant difference between treatments for 3-carene (W=3, n=14, p=0.030). All data are mean ± SE.

5.3.1.3 Comparison of SOA yields with literature

Table 5.5 shows that, due to significant differences in many of the parameters, there are no directly comparable SOA determinations in the literature for any of the 5 VOCs tested in this work.

Table 5.5 – Comparison of SOA yields from this work to literature values. NA = Data not available. Range = temperature range.

VOC	Author	Temperature ± Range (K)	VOC:O_3	Chamber size (L)	[VOC]:[O_3]	Mass yield (%) ± SE	Scavenger	Seed	Relative humidity (%)
Z-3-hexenol	This work	295±1	1:4	40	0.25ppm:1ppm	1.08±0.31	cyclohexane	No	≈0
	This work	295±1	3:1	40	3ppm:1ppm	1.46±0.13	cyclohexane	No	≈0
	(Chen et al. 2016)	298±1	1:1	1000	2.4ppm:2.2ppm	18.4±1.3	Carbon monoxide	No	≈0
	(Harvey et al. 2014)	297±1	1:1	775	1ppm:1ppm	3.3±3.1	None	No	≈0
	(Hamilton et al. 2009)	298±1	1:1	200,000	1.58ppm:1.6ppm	9.6±NA	None	No	6
Z-3-hexenyl acetate	This work	295±0.5	1:4	40	0.25ppm:1ppm	0.66±0.27	cyclohexane	No	≈0
	This work	296±1	3:1	40	3ppm:1ppm	1.25±0.10	cyclohexane	No	≈0
	(Harvey et al. 2014)	297±1	1:1	775	1.5ppm:1.5ppm	1.2±1.1	None	No	≈0
	(Hamilton et al. 2009)	298±1	1:1	200,000	1.6ppm:1.4ppm	8.5±NA	None	No	6
3-carene	This work	295±3.5	1:4	40	0.25ppm:1ppm	57.16±5.68	cyclohexane	No	≈0
	This work	295±2.5	3:1	40	3ppm:1ppm	18.48±1.08	cyclohexane	No	≈0
	(Lee et al. 2006a)	293±1	1:3	28,000	170ppb:510ppb	54±2	cyclohexane	Yes	<10%
	(Yu et al. 1999)	306±1	1:4	60,000	89.9ppb:360ppb	13±NA	2-butanol	Yes	≈5%
	(Griffin et al. 1999)	306±1	1:4	50,000	400ppb:1.5ppm	8-13±NA	2-butanol	Yes	≈5%
	(Hoffmann et al. 1997)	290±1	1:2.5	20,000	96.4ppb:249ppb	76±NA	none	Yes	≈10%
1-undecene	This work	295±1.5	1:4	40	0.25ppm:1ppm	19.46±3.33	cyclohexane	No	≈0
	This work	295±1.5	3:1	40	3ppm:1ppm	10.01±0.27	cyclohexane	No	≈0
1-dodecene	This work	295±0.5	1:4	40	0.25ppm:1ppm	20.47±4.62	cyclohexane	No	≈0
	This work	295±0.5	3:1	40	3ppm:1ppm	8.51±0.33	cyclohexane	No	≈0

5.3.1.4 SOA particle size at both maximum SOA yield and 400m

SOA particle sizes at maximum SOA yield and at a 400m equivalent time point for the five study VOCs, were recorded under both ozone excess and VOC excess conditions (Figure 5.6).

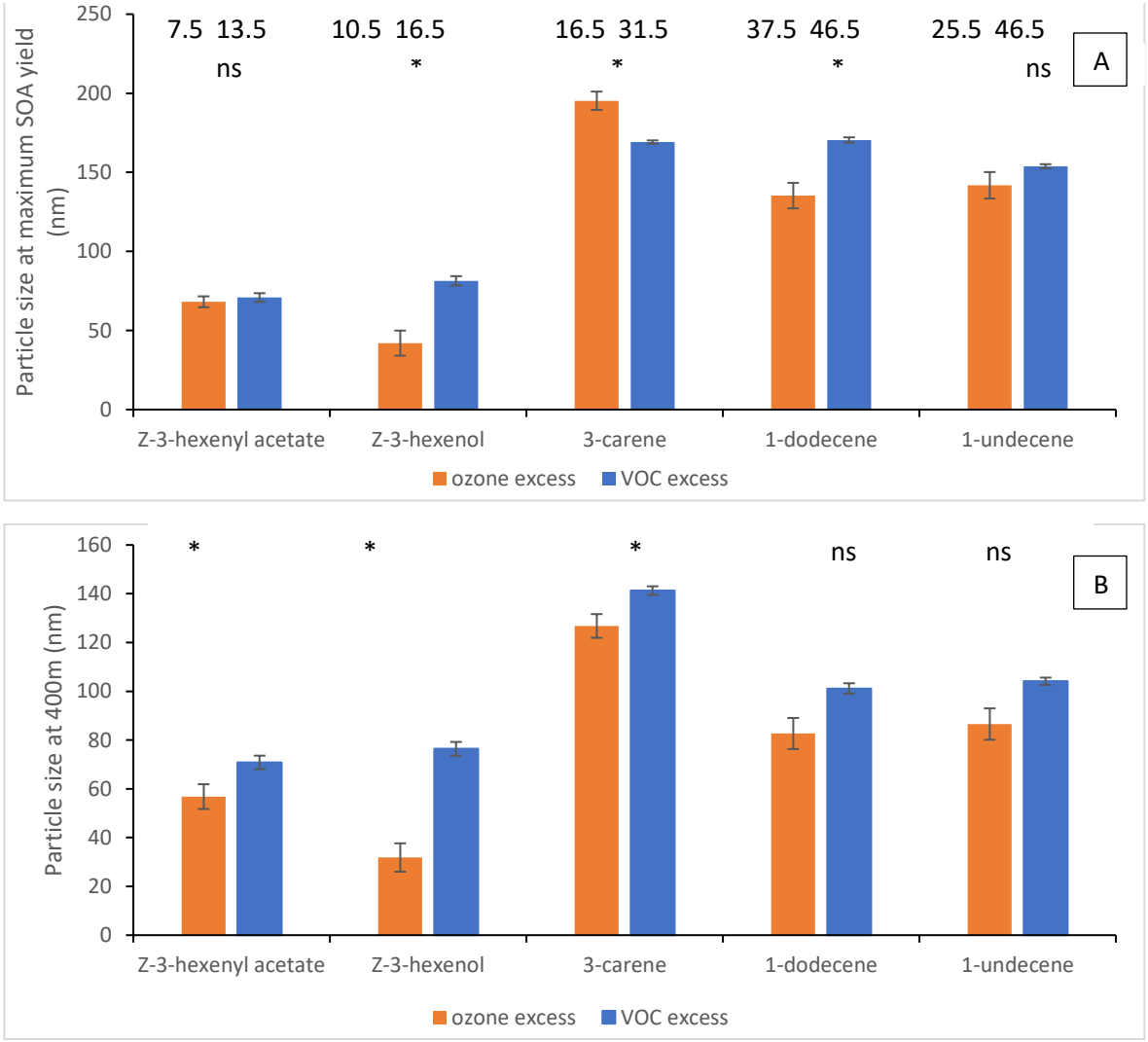

Figure 5.6 – SOA particle size at maximum yield (A) and at a 400m equivalent timepoint (B) for the five study VOCs under both ozone excess (1ppm O_3,0.25ppm VOC) and VOC excess (1ppm O_3,3ppm VOC). Time to maximum yield (minutes) is displayed above the bars for ozone excess conditions (Left-hand number) and VOC excess conditions (right-hand number). *=statistically significant, ns= not statistically significant at the 95% confidence interval. For SOA particle size at maximum yield (A), there was a statistically significant difference between the ozone excess and VOC excess treatments for Z-3-hexenol (W=16, n=8, P=0.029), 3-carene (W=0, n=15, P=<0.001) and 1-dodecene (W=42, n=13, P=0.001). A statistically significant difference was not seen for Z-3-hexenyl acetate and 1-undecene. For SOA particle size at 400m (B), a statistically significant difference in SOA particle size at 400m between treatments was seen for 3-carene (W=48,n=15,p=0.025), Z-3-hexenol (W=16,n=8,p=0.029) and Z-3-hexenyl acetate (W=45,n=15,p=0.035). All data are mean ± SE.

At maximum SOA yield mean particle sizes ranged between 42nm and 195nm with the size being dependant on the VOC from which the SOA was formed (Figure 5.6). An ozone excess generally seemed to produce smaller particles at maximum yield for all VOCs, except for 3-carene. At a projected distance of 400m from a VOC point source, mean particle sizes ranged between 31nm and 141nm with the size being dependant on the VOC from which the SOA was formed (Figure 5.6) and an ozone excess generally seeming to produce smaller particles for all VOCs.

5.3.2 EAG-treatment results

5.3.2.1 methodological verification

No statistically significant differences in antennal response to stimuli were observed as a result of removal of the water bubbler (Figure 5.7).

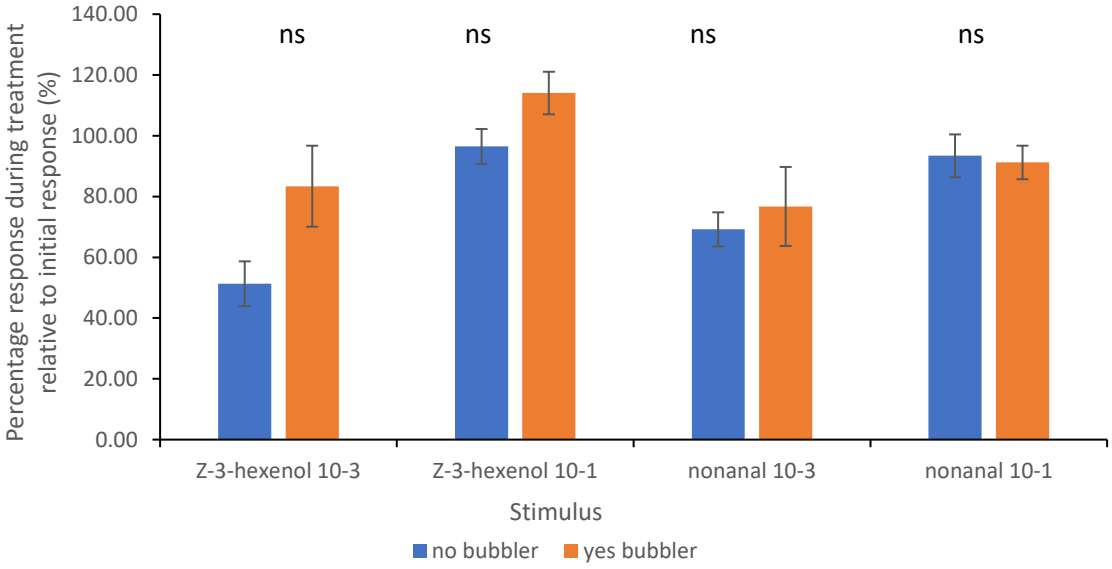

Figure 5.7 – Uncorrected averages of honeybee responses to stimuli during an air control treatment with (n=3) and without (n=7) a water bubbler. S=significant, ns=not significant. n=6 for all stimuli.

There were no statistically significant changes in insect antennal electrophysiological response to nonanal 10^{-3} (W=13, n=6, p=0.295), nonanal 10^{-1} (W=24, n=6, p=0.731) Z-3-hexenol 10^{-1} (W=9, n=6, p = 0.101) and Z-3-hexenol 10^{-3} (W=9, n=6, p = 0.101) as a result of removing the water bubbler from the treatment system.

5.3.2.2 Changes to antennal response during treatment

Figure 5.8/ table 5.6 demonstrates that none of the low or high concentration treatments caused a statistically significant change in antennal response during treatment for any of the stimuli tested. This indicates that none of the treatments affected antennal response.

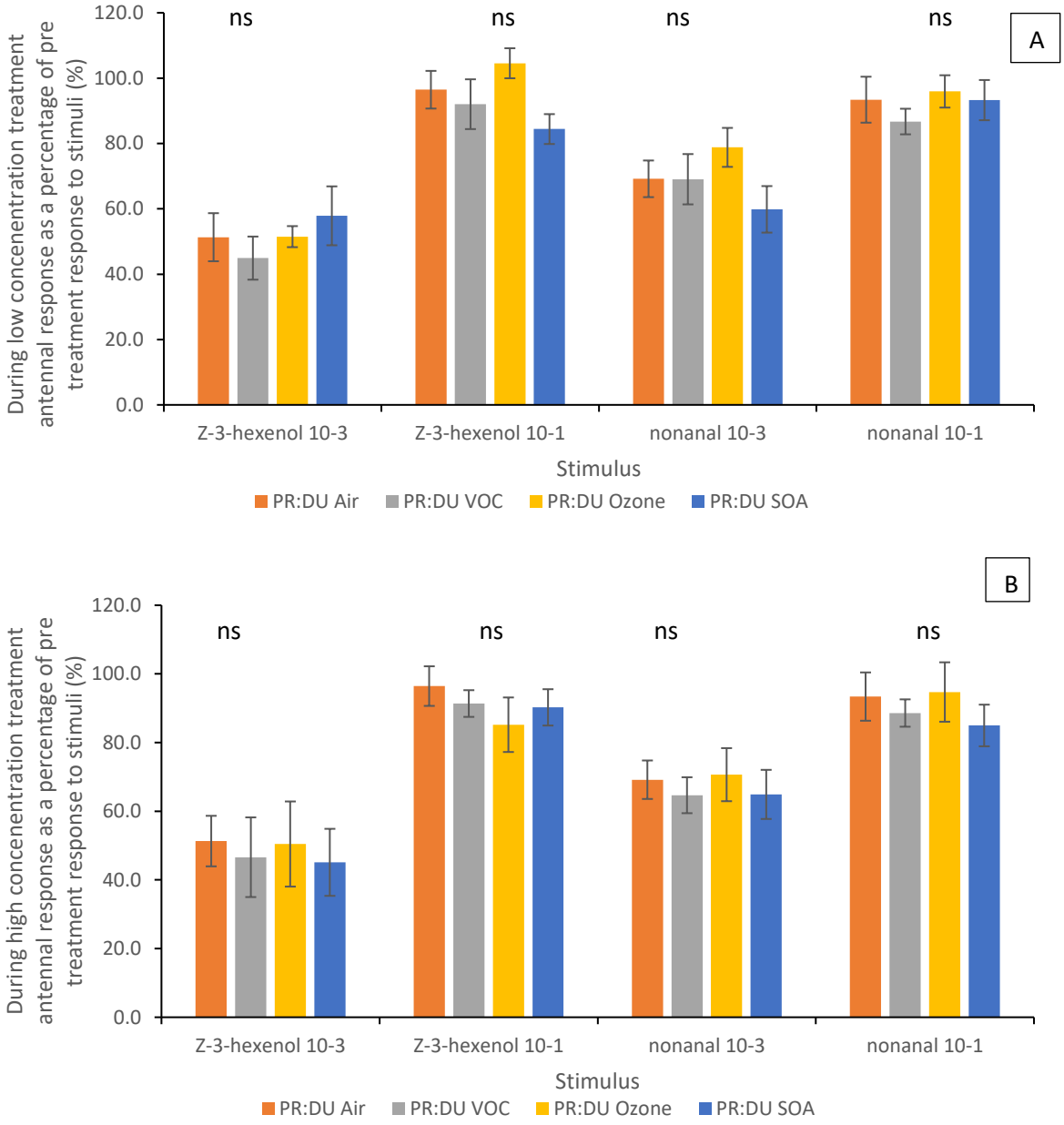

Figure 5.8 – Percentage response of *A. mellifera* antennae to either Z-3-hexenol or nonanal during low concentration (A) or high concentration (B) treatments with either air, VOC, ozone or SOA, relative to initial response. Data is displayed as average percentage changes in response. PR:DU=pre-treatment relative to during treatment. *=statistically significant, ns= not statistically significant at the 95% confidence interval. All data are mean ± SE.

Table 5.6 – Summary of statistical information, produced using LMER modelling, describing differences in antennal response of *A. mellifera* during exposure to low concentration treatments (VOC, ozone, SOA) relative to treatment with air. T= T statistic, p=significance value, n=number of data points.

Treatment	Concentration	Z-3-hexenol 10^{-3}	Z-3-hexenol 10^{-1}	nonanal 10^{-3}	nonanal 10^{-1}
VOC	L	t= -0.628, p = 0.536, n = 7	T=-0.540, p=0.594, n=7	T=0.962, p=0.345, n=7	T= -0.099, p=0.922, n=7
	H	T=-0.307, p=0.761, n=7	T=-0.597, p=0.568, n=7	T=-0.474, p=0.640, n=7	T=-0.487, p=0.631, n=7
Ozone	L	T= 0.017, p=0.986, n=7	T=0.987, p=0.333, n=7	T=1.256, p=0.221, n=7	T=0.085, p=0.933, n=7
	H	T=-0.058, p=0.954, n=8	T=-1.325, p=0.197, n=8	T=0.159, p=0.875, n=8	T=0.140, p=0.890, n=8
SOA	L	T=0.633, p=0.513, n=8	T=-1.516, p=0.142, n=8	T=-0.382, p=0.706, n=8	T=0.303, p=0.765, n=8
	H	T=-0.404, p=0.690, n=7	T=-0.707, p=0.486, n=7	T=-0.448, p=0.658, n=7	T=-0.855, p=0.401, n=7

5.3.2.3 Changes to antennal response post-treatment

For hexenol 10^{-3}, the low concentration VOC treatment showed a significant post-treatment effect while high concentration VOC treatment showed a borderline significant post-treatment effect on the responses to the stimuli. The antennal response to nonanal 10^{-3} showed a borderline significant difference for both high concentration ozone and VOC treatments (Figure 5.9/Table 5.7). No other stimuli appeared to indicate a significant post-treatment effect on antennal response as a result of the treatments.

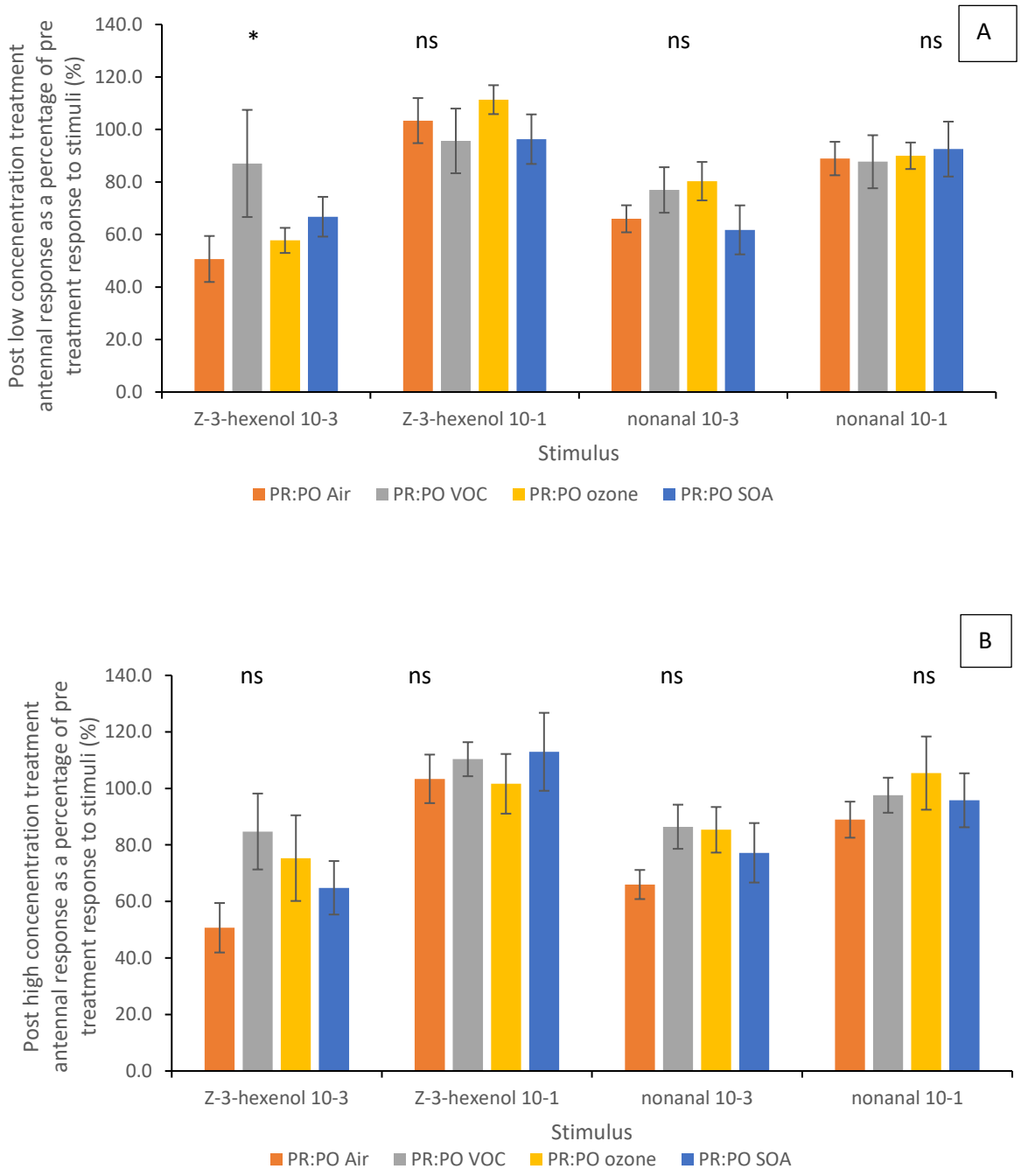

Figure 5.9 – Percentage response of *A. mellifera* antennae to either Z-3-hexenol or nonanal post low concentration (A) or high concentration (B) treatment with either air, VOC, ozone or SOA, relative to initial response. Data is displayed as average percentage changes in response. PR:PO=pre-treatment relative to post-treatment. *=statistically significant, ns= not statistically significant at the 95% confidence interval. All data are mean ± SE.

Table 5.7 – Summary of statistical information, produced using LMER modelling, describing differences in antennal response of *A. mellifera* post-exposure to low concentration treatments (VOC, ozone, SOA) relative to treatment with air. T= T statistic, p=significance value, n=number of data points.

Treatment	Concentration	Z-3-hexenol 10^{-3}	Z-3-hexenol 10^{-1}	nonanal 10^{-3}	nonanal 10^{-1}
VOC	L	T=2.157, p=0.041, n=7	T=-0.577, p=0.569, n=7	T=0.962, p=0.345, n=7	t=-0.099, p=0.922, n=7
	H	T=1.924, p=0.066, n=7	T=0.474, p=0.640, n=7	T=1.748, p=0.092, n=7	T=0.629, p=0.535, n=7
Ozone	L	T=0.419, p=0.679, n=7	T=0.595, p=0.557, n=7	T=1.256, p=0.221, n=7	T=0.085, p=0.933, n=7
	H	T=1.437, p=0.163, n=8	T=-0.123, p=0.903, n=8	T=1.710, p=0.098, n=8	T=1.237, p=0.227, n=8
SOA	L	T=0.985, p=0.334, n=8	T=-0.544, p=0.591, n=8	T=-0.382, p=0.706, n=8	T=0.303, p=0.765, n=8
	H	T=0.799, p=0.431, n=7	T=0.652, p=0.520, n=7	T=0.960, p=0.346, n=7	T=0.449, p=0.622, n=7

5.4 Discussion

5.4.1 SOA percentage yield

At a model windspeed of 1m/s, a 400m distance equates to roughly 6min 40 seconds of reaction time. Observed times to maximum yield for the five model VOCs (Figure 5.4a) were in the range of 7.5-46.5 minutes (reflecting a trend where VOCs with faster ozonolysis rate constants produced higher SOA yields) thus, it was hypothesised that SOA particle concentrations at 400m are likely to be generally lower than at maximum yield. This hypothesis is supported by SOA yield determinations which showed that maximum SOA yields varied between 1%-57% while at 400m, SOA yields varied between 0.5%-25.5% (Figure 5.4b, for direct comparison including statistical significance for each VOC, see appendix – AP15). This observation suggests that any effects of SOA on a bee's physiological ability to recognise a blend found at maximum yield (used in EAG-SOA experiments in this work) may be lower on the 400m equivalent foraging scale.

The broad range of SOA yields observed are a result of differing molecular structures giving a different propensity to form the low volatility particles needed to form SOA (Figure 5.4). This suggests that the constituent VOCs of a blend emission will dictate the susceptibility of a blend to

form SOA, thus meaning the susceptibility of VOC based plant-pollinator interactions to be perturbed by SOA will not be uniform. Prediction of the SOA formation potential of a blend may even be possible because it was observed that at both maximum yield and the 400m equivalent timepoint, VOCs with similar molecular structures showed similar SOA yields, which has previously been demonstrated by Lee et al. (2006). However, VOCs were tested in isolation during this work so further work is needed to explore the interactions between multiple VOCs in a blend. In addition, data showing SOA yield over time is not routinely published so comparisons of the highlighted trends to the literature cannot be made.

The higher levels of SOA that were generally formed under ozone excess conditions at both maximum yield (Figure 5.4a) and at the 400m equivalent time point (Figure 5.4b) are indicative that, interactions taking place in ozone excess environments may be more susceptible to any effects of SOA relative to VOC excess environments at maximum yield. However, the differences in yield between the two conditions were lower at the 400m equivalent timepoint (assumed maximum VOC communication distance) and may be even lower at distances below 400m where interactions are likely to occur. This shows that differences in SOA formation, and thus any effect on VOC signalling between ozone excess and VOC excess scenarios, may be smaller in a real-world context. The lack of a statistically significant difference in SOA yield between VOC excess and ozone excess conditions observed at the 400m equivalent timepoint for 1-dodecene and 1-undecene (Figure 5.4b) is likely to be due to the VOCs slow rate of reaction. Either 1:1 stoichiometry or ozone excess conditions are generally published in literature thus, no comparisons of the relative effects of an ozone vs VOC excess to literature can be made.

Comparisons of SOA yield to literature (Table 5.5) could not easily be made because factors such as; use of seed particles, presence of OH scavenger, experiment temperature and humidity have been shown to alter SOA yield and no previous determination used similar reaction conditions (Jonsson et al. 2008; Von Hessberg et al. 2009; Lambe et al. 2015).

5.4.2 SOA particle size

At the 400m modelling distance, SOA particle diameters were observed to be in the range of 31-141nm with smaller SOA diameters generally predicted under ozone excess conditions, although only Z-3-hexenyl acetate, Z-3-hexenol and 3-carene showed a statistically significant difference between the two conditions (Figure 5.6b). The diameter of an antennal pore kettle is estimated to be 20nm-60nm (Whitehead and Larsen 1976; Steinbrecht 1997; Anderson et al. 2000) and thus, it is conceivable that at the 400m modelling distance, SOA particles are too large to enter the pore kettle which could mean the SOA may not affect antennal functioning. The 400m modelling distance is the assumed maximum distance at which VOC signalling may be of utility to foraging *A. mellifera* (see

section 2.1.2) and thus, interactions that occur on a smaller spatial scale may encounter SOA particles with a smaller diameter that may be able to enter the pore kettle. As it can be inferred from Figure 5.6b that different parents VOCs produce SOA particles of varying sizes and thus, it is conceivable that SOA particles formed from VOCs not used in this work (particularly under ozone excess conditions) may be of an appropriate diameter to enter the pore kettle. It may also be hypothesised that SOA particles with diameters larger than the pore kettle diameter may still disrupt antennal functioning directly due to adherence to the antennal cuticle or blocking of the pore kettle or indirectly as a result of adsorbing VOCs before they are able to contact the antennae (Jami et al. 2020). Further research is needed to test these hypotheses.

SOA particle diameters at maximum SOA yield represent the most common size of SOA particles that may have been formed by the degradation of conspecific blends that are orthogonal to the interaction of interest (background SOA). SOA particle diameters were generally larger at maximum yield (42-195nm, Figure 5.6a) than at the 400m modelling distance (31-141nm, Figure 5.6b, for statistical comparisons per VOC please see appendix – AP15) thus, it is unlikely that background SOA will interact directly with a pore kettle but may as previously considered cause hindrance to antennal functioning by interacting with the antennal cuticle.

The lack of a clear trend as to which excess scenario produced the largest SOA particle at maximum yield is an artefact of comparing size at maximum yield because the time to maximum yield is non-uniform. Literature determinations for the size of SOA particles for our five VOCs were not readily available, thus the accuracy of our determinations is unknown. The SOA particle diameter determinations for Z-3-hexenyl acetate and Z-3-hexenol are treated with caution for the reasons outlined in the yield determination section.

5.4.3 EAG treatment

No single treatment of SOA, ozone, VOC, or air caused a statistically significant change in the ability of an antenna to respond to the stimuli used in this experiment during treatment exposure, when using either low or high concentration treatments (Figure 5.8 and Table 5.6). This is hypothesised to be as a result of either a stimuli specific effect or an SOA specific effect. A stimuli specific effect was observed by Dötterl et al. (2016), using similar conditions to this thesis (*A. mellifera*, O_3=1ppm), during experiments to test the effect of ozone fumigation on antennal response. Only one (Z-3-hexenyl acetate) of three VOCs tested (2-phenylethanol, linalool, Z-3-hexenyl acetate) produced a statistically significant change in antennal response. An SOA specific effect may have been seen because, during this work, the composition of SOA particles has been shown to affect SOA particle size and yield which may affect antennal functioning. A practical element that may also explain the differing result of ozone exposure between this work and that of Dötterl *et al.* (2016) may be the use

of a pre-filled glass treatment tube in this work (meaning treatment concentration decreased during exposure) as opposed to the continuous flow from an ozone generator used by Dötterl *et al.* (2016).

No statistically significant post-exposure effect of SOA was observed for any of the stimuli or treatment concentrations (Figure 5.9 / Table 5.7). However, for VOC exposure, a statistically significant post-exposure effect on antennal response to Z-3-hexenol 10^{-3} ($p=0.041$, 95% C.I) was seen for low concentration exposure while high concentration exposure resulted in borderline statistically significant effect ($p=0.066$, 95% C.I). It is postulated that the observed effect may be as a result of exposure to 3-carene priming the antenna (Zhang and Igwe 2018) to have an increased response to further stimuli. This would explain the VOC specific nature of this trend, and its presentation in low concentration stimuli, which would normally elicit a weaker antennal response. An attempt to mitigate the effect of antennal priming post-experiment was undertaken by exposing the antennae to air and not testing for 2 minutes post-treatment.

5.5 Conclusion

It was observed that, for the model system tested, SOA is unlikely to have an impact on the ability of a honeybee to detect a floral blend. EAG experiments showed that SOA did not have a statistically significant effect on antennal response during or after exposure to SOA at either high or low concentration. This lack of effect is hypothesised to either be a stimuli specific effect or may be due to an SOA specific effects such as the SOA particles tested (derived from 3-carene) having a larger diameter (ca.140nm, this work) than the literature determined antennal pore kettle diameter (ca.20-60nm, Whitehead and Larsen 1976; Steinbrecht 1997; Anderson et al. 2000). The real-world effect of SOA is also hypothesised to be potentially lower than what would be seen during experimental work, which utilised SOA at maximum yield. SOA yield was generally lower at the shorter 400m equivalent timepoint with greater SOA yields seen under ozone excess conditions. 400m is also the assumed maximum distance at which VOC signalling may be of utility and thus, interactions may take place on a smaller spatial scale which are likely to encounter even lower SOA yields, further reducing the chance of any potential effects of SOA exposure.

While the effect of SOA in isolation did not seem to have a statistically significant effect on this model system, it may be a contributing factor in reductions in antennal response when combined with other factors such as the masking effect of gaseous reaction products and alterations to ratio and reduction of blends and thus, future work should be undertaken. Further work should investigate the effects of SOA on antennae using SOA derived from other VOC sources, different stimuli, and different pollinator species. Future work could also attempt to repeat these experiments using more complex experimental apparatus such as an SMPS-EAG apparatus which would allow for real-time control over and quantification of SOA particles. Investigation of the interaction between

SOA particles of differing compositions and the antennal cuticle will also be of utility to allow for qualitative conclusions to be made as to the potential mechanisms by which SOA may impact olfactory functioning.

Chapter 6 - General conclusions

6.1 Key findings

The ubiquity of VOC communication within the environment has been extensively demonstrated in the scientific literature, with interactions between organisms such as; plant-plant (Schuman and Baldwin 2016), plant-herbivore (War et al. 2011) and plant-pollinator (Schiestl 2015b). Furthermore, pollinators have been experiencing declines worldwide (Potts et al. 2010) which is detrimental for both world food supply and the world economy because 78% of all food crop species are thought to require insect pollination (Ollerton et al. 2011), while pollination services are thought to contribute $127-$152 billion to the global economy every year (Bauer and Sue Wing 2016). Anthropogenic increases in tropospheric oxidants (such as ozone) have also been demonstrated (Jaffe and Ray 2007; Department for rural affairs 2018) with significant research to date concerning the effects of these increases on climatic cycles (Monks et al. 2015) and human health (Kampa and Castanas 2008). Research has also explored the effects of increased ozone on organisms and their communication such as between plants and pollinators (Figure 6.1A, Wilkinson et al. 2012; Dötterl et al. 2016; Saunier and Blande 2019). Therefore, it may be hypothesised that disruption of plant-pollinator communication as a result of increased levels of tropospheric oxidants (Farré-Armengol et al. 2016), may be hampering bee pollination and thus, contributing to bee losses (Jürgens and Bischoff 2017).

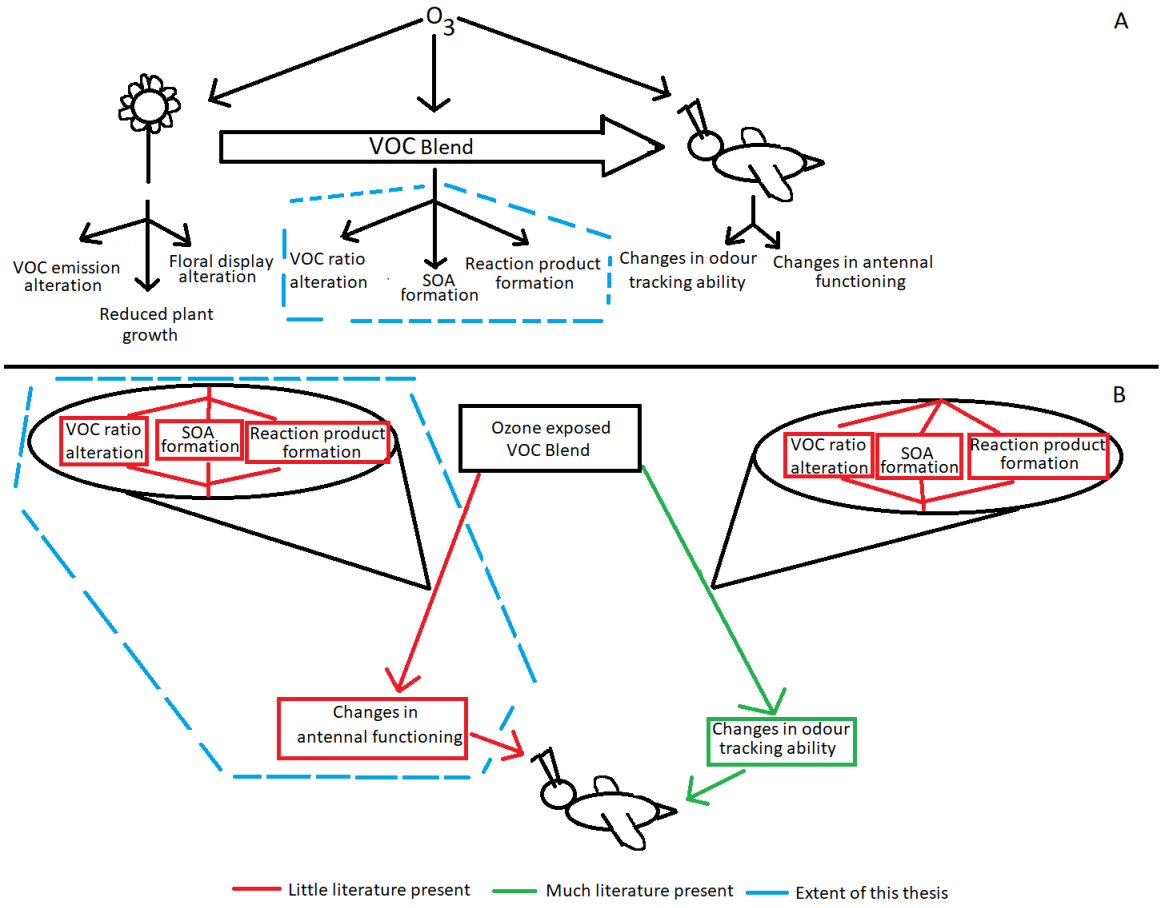

Figure 6.1 – (A) The effects of ozone exposure on different facets of plant-pollinator interactions (B) The effects of ozone exposed VOC communication on a pollinator.

The disruption of VOC blend-based plant-pollinator communication by ozone poses an interesting area for further research. Previous research (Figure 6.1B) has identified the effect of ozone exposure of a blend on pollinator behaviour (Farré-Armengol et al. 2016); however, the individual blend degradation mechanisms that may contribute to this behavioural change (VOC blend ratio alteration, SOA formation, Reaction product formation) have not yet been investigated in isolation of each other and therefore, this formed the basis of this thesis.

To explore the likely contribution of these mechanisms in isolation, this thesis used a honeybee (*Apis mellifera* L.)-oilseed rape (*Brassica napus* L.) model system in combination with two scenarios that characterised extreme situations which may be hypothetically found in nature. The first situation (ozone excess) was based on a high wind, low cumulative VOC emission model, which may be considered to be akin to reactant concentration seen with a single rape plant occurring in a field of wheat, where the floral VOC concentration may fall well below the background excess of ozone. A second situation (VOC excess) was developed based on a low wind, high cumulative VOC emission

model which may be considered to be akin to reactant concentrations seen at the centre of a large field of flowers.

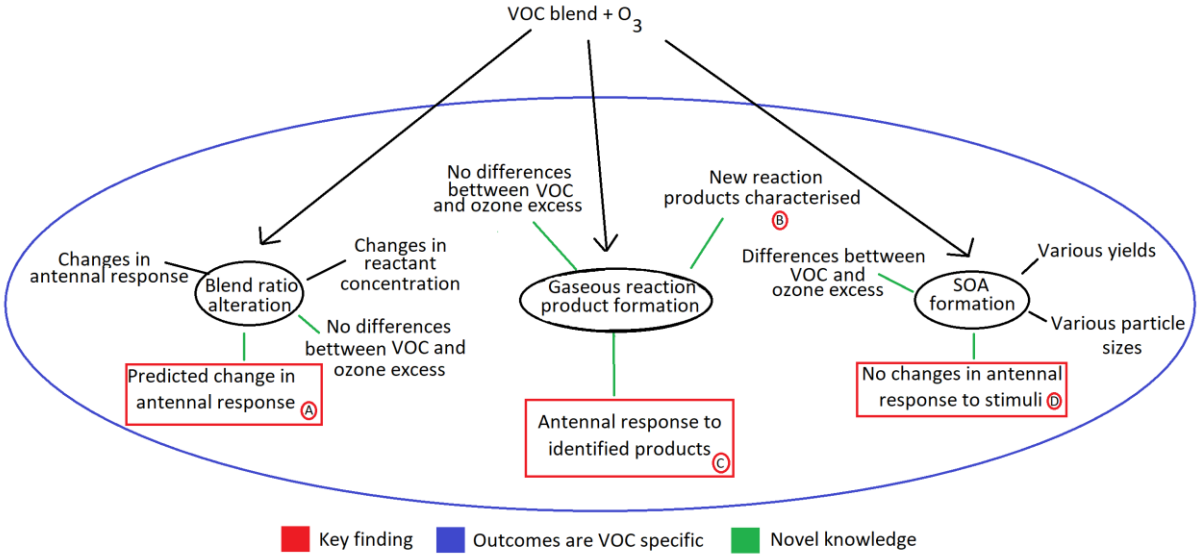

Figure 6.2 – Schematic showing outcomes from each chapter of this thesis including highlighting of key findings and the production of novel knowledge.

The first experimental chapter aimed to create a model to characterise the effect of reductions in blend VOC concentrations upon the physiological ability of *A. mellifera* to detect VOCs under differing modelling constraints (e.g., distance from emission). It was found that at a foraging distance of 400m, two of the model VOCs showed a 100% reduction in antennal response, while the other three VOCs showed only minimal reductions (Figure 6.2, A). When viewed in context with the study by Girling et al. (2013), which showed that blend component removal reduces VOC blend recognition by *A. mellifera*, it may be hypothesised that the observed changes in antennal physiological response could cause a change in behavioural response and thus, might be a driver of the reductions in the effectiveness of VOC communication. Modelling also indicated that in the ppm region, larger changes in blend ratio may be observed under ozone excess conditions (although not demonstrated here due to the mathematical equivalence of the concentrations used). However, this result is tempered by the observations that reductions in antennal response, and differences between ozone and VOC excess, may be less significant when reactant concentrations on the more environmentally relevant ppb scale are used. In addition, it is also possible that the components being degraded could be overshadowed during learning (see section 1.4), which could result in the effects of their depletion being less significant.

The second experimental chapter aimed to investigate whether the gaseous reaction products from the degradation of the model VOCs were physiologically active. Novel reaction products were

identified from 1-dodecene and 1-undecene (Figure 6.2, B) and electrophysiological experiments showed that VOC degradation products elicited a statistically significant antennal response in comparison to the hexane control (Figure 6.2, C). This observation builds upon literature evidence that has shown that the addition of VOCs to intact blends can result in changes in insect behavioural responses to those blends (Mozuraitis et al. 2002; Schröder and Hilker 2008; Riffell et al. 2014; Wilson et al. 2015; Lawson et al. 2017). The exact behavioural effects of individual oxidation products on *A. mellifera* are likely to be different with potential further differences in their behavioural effect if they are encountered in isolation or in unison with other VOCs (Riffell et al. 2009). The outcomes of this chapter also provide support for the hypothesis of Mofikoya et al. (2020) that VOC blend degradation products may be a driver of the reductions in the effectiveness of VOC communication. These results also provide an electrophysiological rationale for the work of Cook et al. (2020) who found that tobacco hawkmoth (*Manduca sexta*) was able to, in the absence of a nectar reward, adapt to an ozone degraded sweet tobacco (*Nicotiana alata*) floral blend (see 1.5.4 for further information).

The third experimental chapter aimed to explore the prevalence of SOA particle formation from model blend VOC components on the foraging scale as well as the effect of SOA particles on electrophysiological response of *A. mellifera* to VOC stimuli. It was found that SOA particles did not cause a statistically significant change in the antennal physiological responses to gaseous VOC stimuli during or after SOA exposure at either a high or low SOA concentration (Figure 6.2, D). This result suggests that exposure to SOA particles does not affect VOC communication. However, It may be hypothesised that the lack of effect of SOA exposure could be due to either a stimuli specific or SOA specific effect, which would concur with the stimuli specific effect of ozone observed by Dötterl et al. (2016) during similar experiments. Due to the subtractive method employed to investigate the effects of SOA on antennal physiological response, the effects of VOC and ozone exposure were also tested. It was seen that only the VOC treatment showed a statistically significant effect on long-term response to low concentration stimuli, potentially indicating that VOC exposure primed a subsequent response.

6.2 Broader implications

The results of this work demonstrate that (using the ppm modelling parameters) the presence of ozone in the environment alters VOC blend ratios, produces oxidation products and results in the formation of SOA. This is in contrast to theoretical “no ozone” conditions (using the assumptions dictated in section 3.2.2), where VOC concentrations would stay constant over distance post

emission with no SOA or oxidation products formed. Therefore, these ozone initiated changes to VOC blends are thus likely to reduce the efficiency of foraging activities by *A. mellifera*.

Three potential mechanistic causes for a reduction in foraging efficiency were considered in this thesis. After considering caveats such as the use of ppm region modelling values as opposed to ppb modelling values, the findings of this work suggest that the formation of gaseous reaction products is the key candidate for the mechanism by which VOC blend interactions may be perturbed. This is due to the mechanisms clear effect on electrophysiology, which not only concurs with literature observations of the behavioural effects of non-blend VOC oxidation products (Mofikoya et al. 2020) but also allows for the potential for both positive and or negative effects on bee behaviour. It may also be hypothesised that the effects of individual oxidation products may be different depending on if they are experienced in isolation or in chorus with a VOC blend. VOC blend oxidation products thus have the potential to alter the efficiency of bee foraging which in turn will effect individual bee survival and ultimately colony success.

On the basis of the results from this thesis, it is difficult to draw solid conclusions regarding whether there are likely to be any differences in the effects of the various degradation mechanisms on honeybee flower location in landscapes where ozone excesses dominate versus landscapes where VOC excess may dominate. In the atmospherically relevant ppb region, there is likely to be little difference in blend ratio alteration between VOC and ozone excess situations and although SOA seems to show different properties between the two excess situations, due to its apparently inert nature, with respect to its impact on VOC odour detection by honeybee, this is likely to have little impact on foraging efficiency. There were also no qualitative differences in degradation product formation between the VOC and ozone excess scenarios, further highlighting the potential lack of effect of landscape scale situation on foraging efficiency. There may, however, be quantitative changes in product yields that could not be measured in this work that may be of significance. It is also of note that the model situations used in this work are two extreme cases and thus, the findings discovered at these extreme cases may not be as drastic under real-world conditions. However, the impacts of VOC communication disruption demonstrated in this thesis are likely to increase throughout all environments as a result of the predicted future increases in tropospheric ozone (Jaffe and Ray 2007; Jiang et al. 2008).

The outcomes of this work are likely to have applicability beyond plant-pollinator interactions due to the ubiquity of VOC mediated communication in the environment such as explaining behavioural observations made with other organisms such as herbivores, for which there is evidence of a reduced

attraction to ozone exposed vegetative blends (Li et al. 2016). Complex hypotheses may also begin to be synthesised by combining the results of this thesis with previous studies, for example that increases in SOA yield found as a result of herbivore feeding by Yli-Pirilä et al. (2016) may have little effects on the physiological response of *A. mellifera* to floral VOCs. The results of this thesis may also be translatable to upon pheromone based communication, particularly because 1-dodecene and 1-undecene have similar chemical structures to some pheromones (Birch and Haynes 1982; Pichersky et al. 2006; De Bruyne and Baker 2008). However, no behavioural experiments concerning the effects of ozone on pheromone communication are present in the literature and only modelling studies have taken place (Boullis et al. 2016; Shi and Liu 2016).

6.3 Future work

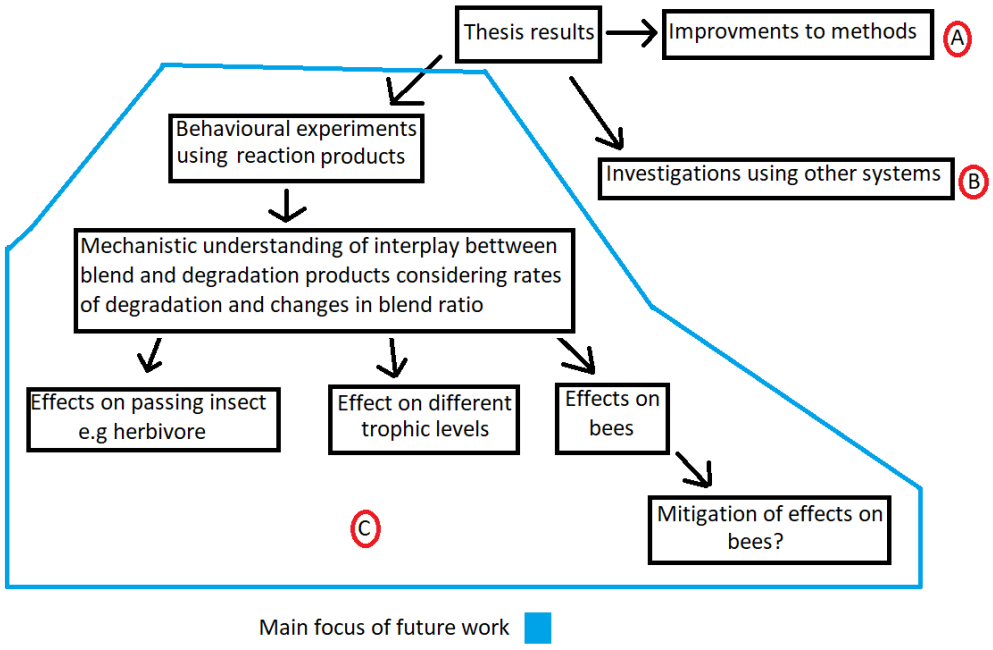

Figure 6.3 - Schematic detailing potential future work as a result of the work conducted in this thesis.

There are a number of pathways by which the results of this thesis could be supplemented. For example, there are a number of additional experiments that could be conducted with refinement of the current methods, (Figure 6.3, A) such as; i) investigations that make use of a more complex reaction degradation model than the one currently used in chapter three, which more accurately predicts changes in VOC, concentration, ii) the use of gas chromatography-electroantennography (GC-EAG, Moorhouse et al. 1969) in chapter four to ensure the complete vaporisation and thus exposure of reaction products, and iii) the use of a modified SMPS to more accurately control the size and concentration of SOA produced for EAG-SOA experiments in chapter five. In addition, repetition of this work using differing plant-pollinator systems would also be of utility to see if the observed effects are generalised or system specific (Figure 6.3, B).

On a broader scale, from examination of the literature in combination with the findings of this work, it may be seen that future work should focus on the behavioural effects of oxidation products. There are many key research questions (Figure 6.3, C) that stem from the findings of this PhD thesis that should be prioritised in future research, including:

- What are the behavioural effects of blend oxidation products in isolation of other ozonolysis mechanisms?
- What are the behavioural effects of blend oxidation products when presented in unison with an undegraded blend?
- What are the behavioural effects of blend oxidation products when presented in unison with a successively more degraded blend?
- What are the behavioural effects of blend oxidation products on blend utilisation by higher trophic level organisms such as parasitoids?
- What are the behavioural effects of degradation products on heterospecific blends such as between a plant and a herbivore?
- As a result of local variations in tropospheric oxidant concentration, are bee's either able to learn or show enough plasticity to deal with varying degrees of blend perturbation?
- Are floral interactions more or less likely to be perturbed by ozone exposure than other interactions such as mating or is plasticity uniform across an insect's various odour mediated interactions?

By answering these questions, the scientific community will have a far deeper understanding of the effect of blend product formation on VOC communication. It is hoped that with this knowledge, appropriate actions may be formulated and undertaken to mitigate any effects of VOC communication disruption on honeybees. One potential mitigation route could be to identify which VOC mediated interactions may be disproportionately affected as a result of ozone degradation. If future work can quantify the level of perturbation of each facet of the VOC blend that is tolerable by a receiving organism (e.g., the extent of blend ratio alteration, SOA concentrations, blend VOC concentrations), then quantitative comparisons of the most at-risk VOC mediated interactions may be undertaken. As a result of these comparisons, in lieu of reductions in tropospheric oxidant pollution, steps could be taken to partially mitigate VOC communication degradation such as growing crop cultivars that are less susceptible to perturbation by VOC blend degradation, thus facilitating the proper functioning of plant-pollinator interactions. This could potentially alleviate one of the potential stressors that may be causing the observed decline in honeybee colonies and thus support pollination services and a healthier ecosystem (see section 1.2). This would bring benefits for humans

by not only ensuring the longevity of pollinators, which in turn relates to a healthier environment but doing so in such a way that food production and livelihoods are not compromised.

It seems to also be of utility to explore the potential effects of ozone on differing ecological systems such as plant-herbivore, herbivore-parasitoid and insect-insect pheromone communication. Due to the lack of previous research, an initial experiment to test the effects of ozone on pheromone communication could be conducted, based upon the flight chamber experiments used by (Farré-Armengol et al. 2016), where the preference of a male for two artificial calling females (one emitting undegraded pheromone and the other emitting ozone degraded pheromone) is assessed. Subsequently, if a change in behavioural preferences is observed towards an ozone degraded pheromone blend, experiments resembling those in this thesis may then be undertaken to understand the chemical mechanisms that are driving the observed changes in behavioural preferences. It is key to understand the effects, if any, of ozone on pheromonal communication because pheromones are ubiquitous within the natural world (see section 1.4.1) and are responsible directly or indirectly for the reproductive success of many organisms. Pheromone communication is also chemically distinct from floral VOC based communication (see Table 1.2/section 1.4) and thus, study of the mechanisms that may cause changes in behavioural preferences towards an ozone degraded pheromone blend, when considered in comparison to VOC based communication, will provide further knowledge on the importance of the different ozonolysis chemical facets to the observed behavioural effects across different systems.

The future work proposed above is likely to be complex but has the potential to be transformative in catalysing the synthesis of attempts to mitigate the impacts of increases in tropospheric oxidants and thus, ensure the longevity of VOC mediated interactions. This work will form one small but significant piece of a greater effort to reduce the effects of humans on the natural world.

7 References

Abou-Shaara HF (2014) The foraging behaviour of honey bees, *Apis mellifera*: A review. Vet Med (Praha) 59:1–10. https://doi.org/10.17221/7240-VETMED

Acton WJF, Schallhart S, Langford B, et al (2016) Canopy-scale flux measurements and bottom-up emission estimates of volatile organic compounds from a mixed oak and hornbeam forest in northern Italy. Atmos Chem Phys 16:7149–7170. https://doi.org/10.5194/acp-16-7149-2016

Aizen MA, Harder LD (2009) The Global Stock of Domesticated Honey Bees Is Growing Slower Than Agricultural Demand for Pollination. Curr Biol 19:915–918. https://doi.org/10.1016/j.cub.2009.03.071

Akritidis D, Pozzer A, Zanis P (2019) On the impact of future climate change on tropopause folds and tropospheric ozone. Atmos Chem Phys 19:14387–14401. https://doi.org/10.5194/acp-19-14387-2019

Alaux C, Ducloz F, Crauser D, Le Conte Y (2010) Diet effects on honeybee immunocompetence. Biol Lett 6:562–565. https://doi.org/10.1098/rsbl.2009.0986

Allsopp MH, de Lange WJ, Veldtman R (2008) Valuing Insect Pollination Services with Cost of Replacement. PLoS One 3:e3128. https://doi.org/10.1371/journal.pone.0003128

Anderson P, Hallberg E, Subchev M (2000) Morphology of antennal sensilla auricillica and their detection of plant volatiles in the Herald moth, *Scoliopteryx libatrix* L. (Lepidoptera: Noctuidae). Arthropod Struct Dev 29:33–41. https://doi.org/10.1016/S1467-8039(00)00011-6

Andryszak NA, Payne TL, Dickens JC, et al (1990) Antennal Olfactory Responsiveness of the Texas Leaf Cutting Ant (Hymenoptera: Formicidae) to Trail Pheromone and its Two Alarm Substances. J Entomol Sci 25:593–600. https://doi.org/10.18474/0749-8004-25.4.593

Aneja VP, Schlesinger WH, Erisman JW (2008) Farming pollution. Nat Geosci 1:409–411. https://doi.org/10.1038/ngeo236

Archer M (2005) The Insects: An Outline of Entomology (3rd Edition)

Arndt U (1995) Air pollutants and pheromones — A problem? Chemosphere 30:1023–1031. https://doi.org/10.1016/0045-6535(95)00013-X

Aschmann SM, Shu Y, Arey J, Atkinson R (1997) Products of the gas-phase reactions of cis-3-hexen-1-ol with OH radicals and O3. Atmos Environ 31:3551–3560. https://doi.org/10.1016/S1352-2310(97)00205-7

Atema J (1996) Eddy Chemotaxis and Odor Landscapes: Exploration of Nature With Animal Sensors. Biol Bull 191:129–138. https://doi.org/10.2307/1543074

Atkins PW, De Paula J (2014) Atkins' Physical chemistry

Atkinson, sherri a. Mason SM, Arey J (2009) Rate Constants for the Gas-Phase Reactions of NO3 Radicals and O3 with C6-C14 1-Alkenes and 2-Methyl-1-alkenes at 296. J Phys Chem A 113:5649–5656. https://doi.org/10.1016/0960-1686(90)90144-C

Atkinson R, Arey J, Aschmann SM, et al (1995) Rate constants for the gas-phase reactions of cis-3-Hexen-1-ol, cis-3-Hexenylacetate, trans-2-Hexenal, and Linalool with OH and NO3 radicals and O3 at 296 ± 2 K, and OH radical formation yields from the O3 reactions. Int J Chem Kinet 27:941–955

Atkinson R, Baulch DL, Cox RA, et al (1999) Evaluated kinetic and photochemical data for atmospheric chemistry, organic species: Supplement VII. J Phys Chem Ref Data 28:191–393

Atkinson R, Carter WPL (1984) Kinetics and Mechanisms of the Gas-Phase Reactions of Ozone with Organic Compounds under Atmospheric Conditions. Chem Rev 84:437–470. https://doi.org/10.1021/cr00063a002

Atkinson R, Darnall KR, Lloyd AC, et al (2007) Kinetics and Mechanisms of the Reactions of the Hydroxyl Radical with Organic Compounds in the Gas Phase. 11:375–488. https://doi.org/10.1002/9780470133415.ch5

Atkinson R, Hasegawa D, Aschmann SM (1990) Rate constants for the gas-phase reactions of O3 with a series of monoterpenes and related compounds at 296K. Int J Chem Kinet 22:871–887

Augusto F, Luiz Pires Valente A (2002) Applications of solid-phase microextraction to chemical analysis of live biological samples. TrAC - Trends Anal Chem 21:428–438. https://doi.org/10.1016/S0165-9936(02)00602-7

Aylor DE, Wang Y, Miller DR (1993) Intermittent wind close to the ground within a grass canopy. Boundary-Layer Meteorol 66:427–448. https://doi.org/10.1007/BF00712732

Baltussen E, Cramers CA, Sandra PJF (2002) Sorptive sample preparation - A review. Anal Bioanal Chem 373:3–22. https://doi.org/10.1007/s00216-002-1266-2

Battista E (2015) Pharmacology. Elsevier, Edinburgh

Baude M, Kunin WE, Boatman ND, et al (2016) Historical nectar assessment reveals the fall and rise of floral resources in Britain. Nature 530:85–88. https://doi.org/10.1038/nature16532

Bauer DM, Sue Wing I (2016) The macroeconomic cost of catastrophic pollinator declines. Ecol Econ 126:1–13. https://doi.org/10.1016/j.ecolecon.2016.01.011

Bell ML, Zanobetti A, Dominici F (2014) Who is more affected by ozone pollution? A systematic review and meta-analysis. Am J Epidemiol 180:15–28. https://doi.org/10.1093/aje/kwu115

Bertrand C, Comte G, Piola F (2006) Solid-phase microextraction of volatile compounds from flowers of two Brunfelsia species. Biochem Syst Ecol 34:371–375. https://doi.org/10.1016/j.bse.2005.12.005

Bey I, Aumont B, Toupance G (1997) The nighttime production of OH radicals in the continental troposphere. Geophys Res Lett 24:1067–1070. https://doi.org/10.1029/97GL00889

Beyaert I, Hilker M (2014) Plant odour plumes as mediators of plant-insect interactions. Biol Rev 89:68–81. https://doi.org/10.1111/brv.12043

Bindi M, Hacour A, Vandermeiren K, et al (2002) Chlorophyll concentration of potatoes grown under elevated carbon dioxide and/or ozone concentrations. Eur J Agron 17:319–335. https://doi.org/10.1016/S1161-0301(02)00069-2

Birch MC, Haynes KF (1982) Insect pheromones. Edward Arnold, London

Black VJ, Stewart CA, Roberts JA, Black CR (2007) Ozone affects gas exchange, growth and reproductive development in *Brassica campestris* (Wisconsin Fast Plants). New Phytol 176:150–163. https://doi.org/10.1111/j.1469-8137.2007.02163.x

Blanco-Ward D, Ribeiro A, Paoletti E, Miranda AI (2021) Assessment of tropospheric ozone phytotoxic effects on the grapevine (*Vitis vinifera* L.): A review. Atmos Environ 244:117924. https://doi.org/10.1016/j.atmosenv.2020.117924

Blande JD, Holopainen JK, Li T (2010) Air pollution impedes plant-to-plant communication by volatiles. Ecol Lett 13:1172–1181. https://doi.org/10.1111/j.1461-0248.2010.01510.x

Blande JD, Holopainen JK, Niinemets Ü (2015) Plant volatiles in a polluted atmosphere : stress

response and signal degradation. plant cell envrionment 37:1892–1904. https://doi.org/10.1111/pce.12352.Plant

Blight MM, Métayer M Le, Delègue M-HP, et al (1997) Identification of Floral Volatiles Involved in Recognition of Oilseed Rape Flowers, *Brassica napus* by Honeybees, *Apis mellifera*. J Chem Ecol 23:1715–1727. https://doi.org/10.1023/B:JOEC.0000006446.21160.c1

Bommarco R, Marini L, Vaissière BE (2012) Insect pollination enhances seed yield, quality, and market value in oilseed rape. Oecologia 169:1025–1032. https://doi.org/10.1007/s00442-012-2271-6

Borges M, Jepson PC, Howse PE (1987) Long-range mate location and close-range courtship behaviour of the Green Stink Bug, *Nezara viridula* and its mediation by sex pheromones. Entomol Exp Appl 44:205–212. https://doi.org/10.1111/j.1570-7458.1987.tb00546.x

Böröczky K, Park KC, Minard RD, et al (2008) Differences in cuticular lipid composition of the antennae of *Helicoverpa zea*, *Heliothis virescens*, and *Manduca sexta*. J Insect Physiol 54:1385–1391. https://doi.org/10.1016/j.jinsphys.2008.07.010

Boullis A, Detrain C, Francis F, Verheggen FJ (2016) Will climate change affect insect pheromonal communication? Curr Opin Insect Sci 17:87–91. https://doi.org/10.1016/j.cois.2016.08.006

Brettell LE, Martin SJ (2017) Oldest Varroa tolerant honey bee population provides insight into the origins of the global decline of honey bees. Sci Rep 7:1–7. https://doi.org/10.1038/srep45953

Brito NF, Moreira MF, Melo ACA (2016) A look inside odorant-binding proteins in insect chemoreception. J Insect Physiol 95:51–65. https://doi.org/10.1016/j.jinsphys.2016.09.008

Brosset A, Saunier A, Kivimäenpää M, Blande JD (2020a) Does ozone exposure affect herbivore-induced plant volatile emissions differently in wild and cultivated plants? Environ Sci Pollut Res 27:30448–30459. https://doi.org/10.1007/s11356-020-09320-z

Brosset A, Saunier A, Mofikoya AO, et al (2020b) The Effects of Ozone on Herbivore-Induced Volatile Emissions of Cultivated and Wild *Brassica Rapa*. Atmosphere (Basel) 11:1213. https://doi.org/10.3390/atmos11111213

Bruce TJA, Pickett JA (2011) Perception of plant volatile blends by herbivorous insects - Finding the right mix. Phytochemistry 72:1605–1611. https://doi.org/10.1016/j.phytochem.2011.04.011

Bruce TJA, Wadhams LJ, Woodcock CM (2005) Insect host location: A volatile situation. Trends Plant Sci 10:269–274. https://doi.org/10.1016/j.tplants.2005.04.003

Burger H, Dötterl S, Ayasse M (2010) Host-plant finding and recognition by visual and olfactory floral cues in an oligolectic bee. Funct Ecol 24:1234–1240. https://doi.org/10.1111/j.1365-2435.2010.01744.x

Calogirou A, Kotzias D, Kettrup A (1997) Product analysis of the gas-phase reaction of ??-caryophyllene with ozone. Atmos Environ 31:283–285. https://doi.org/10.1016/1352-2310(96)00190-2

Cardé RT, Cardé AM, Girling RD (2012) Observations on the flight paths of the day-flying moth Virbia lamae during periods of mate location: Do males have a strategy for contacting the pheromone plume? J Anim Ecol 81:268–276. https://doi.org/10.1111/j.1365-2656.2011.01887.x

Cardé RT, Willis MA (2008) Navigational strategies used by insects to find distant, wind-borne sources of odor. J Chem Ecol 34:854–866. https://doi.org/10.1007/s10886-008-9484-5

Carey AF, Wang G, Su CY, et al (2010) Odorant reception in the malaria mosquito *Anopheles gambiae*. Nature 464:66–71. https://doi.org/10.1038/nature08834

Carreck N, Williams I (1998) The economic value of bees in the UK. Bee World 79:115–123. https://doi.org/10.1080/0005772X.1998.11099393

Carreck NL, Ball B V., Martin SJ (2010) Honey bee colony collapse and changes in viral prevalence associated with varroa destructor. J Apic Res 49:93–94. https://doi.org/10.3896/IBRA.1.49.1.13

Carslaw KS, Boucher O, Spracklen D V., et al (2010) A review of natural aerosol interactions and feedbacks within the Earth system. Atmos Chem Phys 10:1701–1737. https://doi.org/10.5194/acp-10-1701-2010

Carvalheiro LG, Kunin WE, Keil P, et al (2013) Species richness declines and biotic homogenisation have slowed down for NW-European pollinators and plants. Ecol Lett 16:870–878. https://doi.org/10.1111/ele.12121

Charry-Parra G, DeJesus-Echevarria M, Perez FJ (2011) Beer Volatile Analysis: Optimization of HS/SPME Coupled to GC/MS/FID. J Food Sci 76:205–211. https://doi.org/10.1111/j.1750-3841.2010.01979.x

Chen H, Ren Y, Cazaunau M, et al (2015) Rate coefficients for the reaction of ozone with 2- and 3-carene. Chem Phys Lett 621:71–77. https://doi.org/10.1016/j.cplett.2014.12.056

Chen X, Hopke PK (2009) A chamber study of secondary organic aerosol formation by linalool ozonolysis. Atmos Environ 43:3935–3940. https://doi.org/10.1016/j.atmosenv.2009.04.033

Chen Y, Wang J, Zhao S, et al (2016) An experimental kinetic study and products research of the reactions of O3 with a series of unsaturated alcohols. Atmos Environ 145:455–467. https://doi.org/10.1016/j.atmosenv.2016.09.057

Cook B, Haverkamp A, Hansson BS, et al (2020) Pollination in the Anthropocene: a Moth Can Learn Ozone-Altered Floral Blends. J Chem Ecol. https://doi.org/10.1007/s10886-020-01211-4

Cornu A, Carnat AP, Martin B, et al (2001) Solid-phase microextraction of volatile components from natural grassland plants. J Agric Food Chem 49:203–209. https://doi.org/10.1021/jf0008341

Danner N, Molitor AM, Schiele S, et al (2016) Season and landscape composition affect pollen foraging distances and habitat use of Honey bees. Ecol Appl 26:1920–1929. https://doi.org/10.1890/15-1840.1

De Bruyne M, Baker TC (2008) Odor detection in insects: Volatile codes. J Chem Ecol 34:882–897. https://doi.org/10.1007/s10886-008-9485-4

De Moraes CM, Lewis WJ, Pare PW, et al (1998) Herbivore-infested plants selectively attract parasitoids. Nature 393:570–573. https://doi.org/10.1038/31219

De Moraes CM, Mescher MC, Tumlinson JH (2001) Caterpillar-induced nocturnal plant volatiles repel conspecific females. Nature 410:577–579. https://doi.org/10.1038/35069058

Deisig N, Giurfa M, Lachnit H, Sandoz JC (2006) Neural representation of olfactory mixtures in the honeybee antennal lobe. Eur J Neurosci 24:1161–1174. https://doi.org/10.1111/j.1460-9568.2006.04959.x

Department for rural affairs (2018) Air pollution in the UK

Di Prisco G, Cavaliere V, Annoscia D, et al (2013) Neonicotinoid clothianidin adversely affects insect immunity and promotes replication of a viral pathogen in honey bees. Proc Natl Acad Sci U S A 110:18466–18471. https://doi.org/10.1073/pnas.1314923110

Dicke M, Sabelis MW (1988) Infochemical Terminology: Based on Cost-Benefit Analysis Rather than Origin of Compounds? Funct Ecol 2:131. https://doi.org/10.2307/2389687

Dickerson RR, Stedman DH, Delany AC (1982) Direct measurements of ozone and nitrogen dioxide photolysis rates in the troposphere. J Geophys Res 87:4933–4946. https://doi.org/10.1029/JC087iC07p04933

Dillon TJ, Crowley JN (2018) Reactive quenching of electronically excited NO2* and NO3* by H2O as potential sources of atmospheric HOx radicals. Atmos Chem Phys 18:14005–14015. https://doi.org/10.5194/acp-18-14005-2018

Ditzen M, Evers JF, Galizia CG (2003) Odor similarity does not influence the time needed for odor processing. Chem Senses 28:781–789. https://doi.org/10.1093/chemse/bjg070

Dolezal AG, Toth AL (2018) Feedbacks between nutrition and disease in honey bee health. Curr Opin Insect Sci 26:114–119. https://doi.org/10.1016/j.cois.2018.02.006

Dötterl S, Vater M, Rupp T, Held A (2016) Ozone Differentially Affects Perception of Plant Volatiles in Western Honey Bees. J Chem Ecol 42:486–489. https://doi.org/10.1007/s10886-016-0717-8

Dudareva N, Pichersky E, Gershenzon J (2004) Biochemistry of Plant Volatiles. Plant Physiol 135:1893–1902. https://doi.org/10.1104/pp.104.049981

Duque L, Poelman EH, Steffan-Dewenter I (2019) Plant-mediated effects of ozone on herbivores depend on exposure duration and temperature. Sci Rep 9:1–11. https://doi.org/10.1038/s41598-019-56234-z

Duque L, Poelman EH, Steffan-Dewenter I (2021) Effects of ozone stress on flowering phenology, plant-pollinator interactions and plant reproductive success. Environ Pollut 272:115953. https://doi.org/10.1016/j.envpol.2020.115953

Edgecomb RS, Harth CE, Schneiderman AM (1994) Regulation of feeding behavior in adult *Drosophila melanogaster* varies with feeding regime and nutritional state. J Exp Biol 197:215–235. https://doi.org/10.1242/jeb.197.1.215

Eilers EJ, Kremen C, Smith Greenleaf S, et al (2011) Contribution of Pollinator-Mediated Crops to Nutrients in the Human Food Supply. PLoS One 6:e21363. https://doi.org/10.1371/journal.pone.0021363

Evans KA, Allen-Williams LJ (1992) Electroantennogram responses of the cabbage seed weevil, *Ceutorhynchus assimilis*, to oilseed rape, *Brassica napus ssp.Oleifera* , volatiles. J Chem Ecol 18:1641–1659. https://doi.org/10.1007/BF00993236

Fann N, Lamson AD, Anenberg SC, et al (2012) Estimating the National Public Health Burden Associated with Exposure to Ambient PM 2.5 and Ozone. Risk Anal 32:81–95. https://doi.org/10.1111/j.1539-6924.2011.01630.x

Farré-Armengol G, Peñuelas J, Li T, et al (2016) Ozone degrades floral scent and reduces pollinator attraction to flowers. New Phytol 209:152–160. https://doi.org/10.1111/nph.13620

Fischer S, Samietz J, Wäckers F, Dorn S (2001) Interaction of vibrational and visual cues in parasitoid host location. J Comp Physiol - A Sensory, Neural, Behav Physiol 187:785–791. https://doi.org/10.1007/s00359-001-0249-7

Fuentes JD, Chamecki M, Roulston T, et al (2016) Air pollutants degrade floral scents and increase insect foraging times. Atmos Environ 141:361–374. https://doi.org/10.1016/j.atmosenv.2016.07.002

Fuentes JD, Roulston TH, Zenker J (2013) Ozone impedes the ability of a herbivore to find its host. Environ Res Lett 8:14048. https://doi.org/10.1088/1748-9326/8/1/014048

Gadenne C, Barrozo RB, Anton S (2016) Plasticity in Insect Olfaction: To Smell or Not to Smell? Annu

Rev Entomol 61:317–333. https://doi.org/10.1146/annurev-ento-010715-023523

Gallai N, Salles JM, Settele J, Vaissière BE (2009) Economic valuation of the vulnerability of world agriculture confronted with pollinator decline. Ecol Econ 68:810–821. https://doi.org/10.1016/j.ecolecon.2008.06.014

Gao R, Zhu L, Zhang Q, Wang W (2014) Atmospheric oxidation mechanism and kinetic studies for OH and NO3 radical-initiated reaction of methyl methacrylate. Int J Mol Sci 15:5032–5044. https://doi.org/10.3390/ijms15035032

Garratt MPD, Coston DJ, Truslove CL, et al (2014) The identity of crop pollinators helps target conservation for improved ecosystem services. Biol Conserv 169:128–135. https://doi.org/10.1016/j.biocon.2013.11.001

Gentner DR, Ormeño E, Fares S, et al (2014) Emissions of terpenoids, benzenoids, and other biogenic gas-phase organic compounds from agricultural crops and their potential implications for air quality. Atmos Chem Phys 14:5393–5413. https://doi.org/10.5194/acp-14-5393-2014

Germinara GS, De Cristofaro A, Rotundo G (2009) Antennal olfactory responses to individual cereal volatiles in *Theocolax elegans* (Westwood) (Hymenoptera: Pteromalidae). J Stored Prod Res 45:195–200. https://doi.org/10.1016/j.jspr.2009.02.002

Getz WM, Smith KB (1987) Olfactory sensitivity and discrimination of mixtures in the honeybee *Apis mellifera*. J Comp Physiol A 160:239–245. https://doi.org/10.1007/BF00609729

Ghalaieny M, Bacak A, McGillen M, et al (2012) Determination of gas-phase ozonolysis rate coefficients of a number of sesquiterpenes at elevated temperatures using the relative rate method. Phys Chem Chem Phys 14:6596–6602. https://doi.org/10.1039/c2cp23988d

Gibilisco RG, Bejan I, Barnes I, et al (2015) FTIR gas kinetic study of the reactions of ozone with a series of hexenols at atmospheric pressure and 298 K. Chem Phys Lett 618:114–118. https://doi.org/10.1016/j.cplett.2014.11.003

Gifford R, Kormos C, McIntyre A (2011) Behavioral dimensions of climate change: Drivers, responses, barriers, and interventions. Wiley Interdiscip Rev Clim Chang 2:801–827. https://doi.org/10.1002/wcc.143

Gilpin RK (2001) Liquid Chromatography Problem Solving and Troubleshooting. J Chromatogr Sci 39:497–498. https://doi.org/10.1093/chromsci/39.11.497

Gimeno BS, Bermejo V, Sanz J, et al (2004) Growth response to ozone of annual species from Mediterranean pastures. Environ Pollut 132:297–306. https://doi.org/10.1016/j.envpol.2004.04.022

Girling RD, Lusebrink I, Farthing E, et al (2013) Diesel exhaust rapidly degrades floral odours used by honeybees. Sci Rep 3:2779. https://doi.org/10.1038/srep02779

Goulson D, Nicholls E, Botias C, Rotheray EL (2015) Bee declines driven by combined stress from parasites, pesticides, and lack of flowers. Science (80-) 347:1255957–1255957. https://doi.org/10.1126/science.1255957

Griffin RJ, Cocker DR, Flagan RC, Seinfeld JH (1999) Organic aerosol formation from the oxidation of biogenic hydrocarbons. J Geophys Res Atmos 104:3555–3567. https://doi.org/10.1029/1998JD100049

Grimsrud EP, Westberg HH, Rasmussen RA (1975) Atmospheric reactivity of monoterpene hydrocarbons, NOx, photooxidation and ozonolysis. Int J Chem Kinet;(United States) 7:

Grosjean E, Grosjean D (1999) The reaction of unsaturated aliphatic oxygenates with ozone. J Atmos

Chem 32:205–232. https://doi.org/10.1023/A:1006122000643

Grosjean E, Grosjean D (1997) The gas phase reaction of unsaturated oxygenates with ozone: Carbonyl products and comparison with the alkene-ozone reaction. J Atmos Chem 27:271–289

Grosjean E, Grosjean D (1998) Rate constants for the gas-phase reaction of ozone with unsaturated oxygenates. Int J Chem Kinet 30:21–29. https://doi.org/10.1002/(SICI)1097-4601(1998)30:1<21::AID-KIN3>3.0.CO;2-W

Guenther A, Nicholas C, Fall R, et al (1995) A global model of natural volatile organic compound emissions. J Geophys Res 100:8873–8892

Guerrieri F, Schubert M, Sandoz JC, Giurfa M (2005) Perceptual and neural olfactory similarity in honeybees. PLoS Biol 3:0718–0732. https://doi.org/10.1371/journal.pbio.0030060

Hamilton JF, Lewis AC, Carey TJ, et al (2009) Reactive oxidation products promote secondary organic aerosol formation from green leaf volatiles. Atmos Chem Phys 9:3815–3823. https://doi.org/10.5194/acp-9-3815-2009

Hanna C, Foote D, Kremen C (2013) Invasive species management restores a plant-pollinator mutualism in Hawaii. J Appl Ecol 50:147–155. https://doi.org/10.1111/1365-2664.12027

Harvey RM, Bateman AP, Jain S, et al (2016) Optical Properties of Secondary Organic Aerosol from cis-3-Hexenol and cis-3-Hexenyl Acetate: Effect of Chemical Composition, Humidity, and Phase. Environ Sci Technol 50:4997–5006. https://doi.org/10.1021/acs.est.6b00625

Harvey RM, Zahardis J, Petrucci GA (2014) Establishing the contribution of lawn mowing to atmospheric aerosol levels in American suburbs. Atmos Chem Phys 14:797–812. https://doi.org/10.5194/acp-14-797-2014

Hegland SJ, Nielsen A, Lázaro A, et al (2009) How does climate warming affect plant-pollinator interactions? Ecol Lett 12:184–195. https://doi.org/10.1111/j.1461-0248.2008.01269.x

Himanen SJ, Nerg AM, Nissinen A, et al (2009) Effects of elevated carbon dioxide and ozone on volatile terpenoid emissions and multitrophic communication of transgenic insecticidal oilseed rape (Brassica napus). New Phytol 181:174–186. https://doi.org/10.1111/j.1469-8137.2008.02646.x

Hobbs P (2002) Basic physical chemistry for the atmospheric sciences, 2nd edn. Cambridge university press, cambridge

Hobbs P V. (2000) Introduction to Atmospheric Chemistry. Cambridge University Press

Hoffmann T, Odum JR, Bowman F, et al (1997) Formation of organic aerosols from the oxidation of biogenic hydrocarbons. J Atmos Chem 26:189–222. https://doi.org/10.1023/A:1005734301837

Hofstraat RG, Lange J, Scheeren HW, Nivard RJF (1988) Chemistry of ketene acetals. Part 9. A simple 'one-pot' synthesis of 4-hydroxy-δ-lactones and 5,6-dihydro-2-pyrones from 1,1-dimethoxypropene and β-oxy aldehydes. J Chem Soc, Perkin Trans 1 2315–2322. https://doi.org/10.1039/P19880002315

Holloway AM, Wayne RP (2010) Atmospheric Chemistry. Royal Society of Chemistry, Cambridge

Holopainen JK, Blande JD (2013) Where do herbivore-induced plant volatiles go? Front Plant Sci 4:185. https://doi.org/10.3389/fpls.2013.00185

Holopainen JK, Gershenzon J (2010) Multiple stress factors and the emission of plant VOCs. Trends Plant Sci 15:176–184. https://doi.org/10.1016/j.tplants.2010.01.006

Holopainen JK, Kivimäenpää M, Nizkorodov SA (2017) Plant-derived Secondary Organic Material in

the Air and Ecosystems. Trends Plant Sci 22:744–753. https://doi.org/10.1016/j.tplants.2017.07.004

Hoyle CR, Myhre G, Berntsen TK, Isaksen ISA (2009) Anthropogenic influence on SOA and the resulting radiative forcing. Atmos Chem Phys 9:2715–2728. https://doi.org/10.5194/acp-9-2715-2009

Ichiki RT, Kainoh Y, Kugimiya S, et al (2008) Attraction to herbivore-induced plant volatiles by the host-foraging parasitoid fly *Exorista japonica*. J Chem Ecol 34:614–621. https://doi.org/10.1007/s10886-008-9459-6

Iriti M, Faoro F (2008) Oxidative stress, the paradigm of ozone toxicity in plants and animals. Water Air Soil Pollut 187:285–301. https://doi.org/10.1007/s11270-007-9517-7

Jackson BD, Morgan ED (1993) Insect chemical communication: Pheromones and exocrine glands of ants. Chemoecology 4:125–144. https://doi.org/10.1007/BF01256548

Jaffe D, Ray J (2007) Increase in surface ozone at rural sites in the western US. Atmos Environ 41:5452–5463. https://doi.org/10.1016/j.atmosenv.2007.02.034

Jakobsen HB, Friis P, Nielsen JK, Olsen CE (1994) Emission of volatiles from flowers and leaves of *Brassica napus* in situ. Phytochemistry 37:695–699. https://doi.org/10.1016/S0031-9422(00)90341-8

James AT, Martin AJP (1952) Gas-liquid partition chromatography: the separation and micro-estimation of volatile fatty acids from formic acid to dodecanoic acid. Biochem J 50:679–690. https://doi.org/10.1042/bj0500679

Jami L, Zemb T, Casas J, Dufrêche JF (2020) How Adsorption of Pheromones on Aerosols Controls Their Transport. ACS Cent Sci 6:1628–1638. https://doi.org/10.1021/acscentsci.0c00892

Jepsen MR, Kuemmerle T, Müller D, et al (2015) Transitions in European land-management regimes between 1800 and 2010. Land use policy 49:53–64. https://doi.org/10.1016/j.landusepol.2015.07.003

Jiang X, Wiedinmyer C, Chen F, et al (2008) Predicted impacts of climate and land use change on surface ozone in the Houston, Texas, area. J Geophys Res Atmos 113:1–16. https://doi.org/10.1029/2008JD009820

Jonsson ÅM, Hallquist M, Ljungström E (2008) Influence of OH scavenger on the water effect on secondary organic aerosol formation from ozonolysis of limonene, Δ3-carene, and α-pinene. Environ Sci Technol 42:5938–5944. https://doi.org/10.1021/es702508y

Jürgens A, Bischoff M (2017) Changing odour landscapes: the effect of anthropogenic volatile pollutants on plant–pollinator olfactory communication. Funct Ecol 31:56–64. https://doi.org/10.1111/1365-2435.12774

Jürgens A, Glück U, Aas G, Dötterl S (2014) Diel fragrance pattern correlates with olfactory preferences of diurnal and nocturnal flower visitors in *Salix caprea* (Salicaceae). Bot J Linn Soc 175:624–640. https://doi.org/10.1111/boj.12183

Kampa M, Castanas E (2008) Human health effect of air polution-Enviro Polution. Environ Pollut 151:362–367. https://doi.org/10.1016/j.envpol.2007.06.012

Kelly FJ (2003) Oxidative stress: Its role in air pollution and adverse health effects. Occup Environ Med 60:612–616. https://doi.org/10.1136/oem.60.8.612

Kerr JT, Pindar A, Galpern P, et al (2015) Climate change impacts on bumblebees converge across continents. Science (80-) 349:177–180. https://doi.org/10.1126/science.aaa7031

Kessler A, Baldwin IT (2001) Defensive function of herbivore-induced plant volatile emissions in nature. Science (80-) 291:2141–2144. https://doi.org/10.1126/science.291.5511.2141

Kessler A, Halitschke R, Poveda K (2011) Herbivory-mediated pollinator limitation: Negative impacts of induced volatiles on plant-pollinator interactions. Ecology 92:1769–1780. https://doi.org/10.1890/10-1945.1

Kessler S, Tiedeken EJ, Simcock KL, et al (2015) Bees prefer foods containing neonicotinoid pesticides. Nature 521:74–76. https://doi.org/10.1038/nature14414

Kim OK, Murakami A, Nakamura Y, et al (2000) Inhibition by (-)-Persenone A-related Compounds of Nitric Oxide and Superoxide Generation from Inflammatory Leukocytes. Biosci Biotechnol Biochem 64:2500–2503. https://doi.org/10.1271/bbb.64.2500

Kluser S, Peduzzi P (2007) Global pollinator decline: a literature review. United Nations Enviroment programme

Knudsen JT, Eriksson R, Gershenzon J, Ståhl B (2006) Diversity and distribution of floral scent. Bot Rev 72:1–120. https://doi.org/10.1663/0006-8101(2006)72[1:dadofs]2.0.co;2

Koczor S, Vuts J, Tóth M (2012) Attraction of *Lygus rugulipennis* and *Adelphocoris lineolatus* to synthetic floral odour compounds in field experiments in Hungary. J Pest Sci (2004) 85:239–245. https://doi.org/10.1007/s10340-012-0422-5

Koehl M (2006) The Fluid Mechanics of Arthropod Sniffing in Turbulent Odor Plumes. Chem Senses 31:93–105. https://doi.org/10.1093/chemse/bjj009

Kohler F, Verhulst J, Van Klink R, Kleijn D (2008) At what spatial scale do high-quality habitats enhance the diversity of forbs and pollinators in intensively farmed landscapes? J Appl Ecol 45:753–762. https://doi.org/10.1111/j.1365-2664.2007.01394.x

Lambe AT, Chhabra PS, Onasch TB, et al (2015) Effect of oxidant concentration, exposure time, and seed particles on secondary organic aerosol chemical composition and yield. Atmos Chem Phys 15:3063–3075. https://doi.org/10.5194/acp-15-3063-2015

Laothawornkitkul J, Taylor JE, Paul ND, Hewitt CN (2009) Biogenic volatile organic compounds in the Earth system: Tansley review. New Phytol 183:27–51. https://doi.org/10.1111/j.1469-8137.2009.02859.x

Lathière J, Hauglustaine DA, Friend AD, et al (2006) Impact of climate variability and land use changes on global biogenic volatile organic compound emissions. Atmos Chem Phys 6:2129–2146. https://doi.org/10.5194/acp-6-2129-2006

Lawson DA, Whitney HM, Rands SA (2017) Colour as a backup for scent in the presence of olfactory noise: testing the efficacy backup hypothesis using bumblebees (*Bombus terrestris*). R Soc Open Sci 4:170996. https://doi.org/10.1098/rsos.170996

Lee A, Goldstein AH, Kroll JH, et al (2006a) Gas-phase products and secondary aerosol yields from the ozonolysis of ten different terpenes. J Geophys Res Atmos 111:1–18. https://doi.org/10.1029/2005JD006437

Lee A, Goldstein AH, Kroll JH, et al (2006b) Gas-phase products and secondary aerosol yields from the photooxidation of 16 different terpenes. J Geophys Res Atmos 111:1–26. https://doi.org/10.1029/2006JD007050

Leonard AS, Masek P (2014) Multisensory integration of colors and scents: Insights from bees and flowers. J Comp Physiol A Neuroethol Sensory, Neural, Behav Physiol 200:463–474. https://doi.org/10.1007/s00359-014-0904-4

Leonard RJ, Pettit TJ, Irga P, et al (2019) Acute exposure to urban air pollution impairs olfactory learning and memory in honeybees. Ecotoxicology 28:1056–1062. https://doi.org/10.1007/s10646-019-02081-7

Li C, Gu X, Wu Z, et al (2021) Assessing the effects of elevated ozone on physiology, growth, yield and quality of soybean in the past 40 years: A meta-analysis. Ecotoxicol Environ Saf 208:111644. https://doi.org/10.1016/j.ecoenv.2020.111644

Li T, Blande JD, Holopainen JK (2016) Atmospheric transformation of plant volatiles disrupts host plant finding. Sci Rep 6:33851. https://doi.org/10.1038/srep33851

Lin X, Ma Q, Yang C, et al (2016) Kinetics and mechanisms of gas phase reactions of hexenols with ozone. RSC Adv 6:83573–83580. https://doi.org/10.1039/C6RA17107A

Loarie SR, Duffy PB, Hamilton H, et al (2009) The velocity of climate change. Nature 462:1052–1055. https://doi.org/10.1038/nature08649

Loreto F, Velikova V (2001) Isoprene Produced by Leaves Protects the Photosynthetic Apparatus against Ozone Damage, Quenches Ozone Products, and Reduces Lipid Peroxidation of Cellular Membranes. Plant Physiol 127:1781–1787. https://doi.org/10.1104/pp.010497

Lu X, Zhang L, Shen L (2019) Meteorology and Climate Influences on Tropospheric Ozone: a Review of Natural Sources, Chemistry, and Transport Patterns. Curr Pollut Reports 5:238–260. https://doi.org/10.1007/s40726-019-00118-3

Lukas K, Dötterl S, Ayasse M, Burger H (2020) Olfactory and Visual Floral Signals of *Hedera helix* and *Heracleum sphondylium* Involved in Host Finding by Nectar-Foraging Social Wasps. Front Ecol Evol 8:1–14. https://doi.org/10.3389/fevo.2020.571454

Luo C, Huang ZY, Li K, et al (2013) EAG Responses of *Apis cerana* to Floral Compounds of a Biodiesel Plant, *Jatropha curcas* (Euphorbiaceae). J Econ Entomol 106:1653–1658. https://doi.org/10.1603/EC12458

Lusebrink I, Girling RD, Farthing E, et al (2015) The Effects of Diesel Exhaust Pollution on Floral Volatiles and the Consequences for Honey Bee Olfaction. J Chem Ecol 41:904–912. https://doi.org/10.1007/s10886-015-0624-4

Ma Y, Porter RA, Chappell D, et al (2009) Mechanisms for the formation of organic acids in the gas-phase ozonolysis of 3-carene. Phys Chem Chem Phys 11:4184–4197. https://doi.org/10.1039/b818750a

Martínez-Ghersa MA, Menéndez AI, Gundel PE, et al (2017) Legacy of historic ozone exposure on plant community and food web structure. PLoS One 12:1–14. https://doi.org/10.1371/journal.pone.0182796

Mas F, Horner RM, Brierley S, et al (2020) Selection of key floral scent compounds from fruit and vegetable crops by honey bees depends on sensory capacity and experience. J Insect Physiol 121:104002. https://doi.org/10.1016/j.jinsphys.2019.104002

McEwan M, Macfarlane Smith WH (1998) Identification of volatile organic compounds emitted in the field by oilseed rape (*Brassica napus ssp. oleifera*) over the growing season. Clin Exp Allergy 28:332–338. https://doi.org/10.1046/j.1365-2222.1998.00234.x

McFrederick QS, Fuentes JD, Roulston T, et al (2009) Effects of air pollution on biogenic volatiles and ecological interactions. Oecologia 160:411–420. https://doi.org/10.1007/s00442-009-1318-9

McFrederick QS, Kathilankal JC, Fuentes JD (2008) Air pollution modifies floral scent trails. Atmos Environ 42:2336–2348. https://doi.org/10.1016/j.atmosenv.2007.12.033

Millar RJ, Fuglestvedt JS, Friedlingstein P, et al (2017) Emission budgets and pathways consistent with limiting warming to 1.5°C. Nat Geosci 10:741–747. https://doi.org/10.1038/ngeo3031

Miyazaki K, Eskes H, Sudo K, et al (2017) Decadal changes in global surface NOx emissions from multi-constituent satellite data assimilation. Atmos Chem Phys 17:807–837. https://doi.org/10.5194/acp-17-807-2017

Mofikoya AO, Yli-Pirilä P, Kivimäenpää M, et al (2020) Deposition of α-pinene oxidation products on plant surfaces affects plant VOC emission and herbivore feeding and oviposition. Environ Pollut 263:114437. https://doi.org/10.1016/j.envpol.2020.114437

Monks PS (2005) Gas-phase radical chemistry in the troposphere. Chem Soc Rev 34:376–395. https://doi.org/10.1039/b307982c

Monks PS, Archibald AT, Colette A, et al (2015) Tropospheric ozone and its precursors from the urban to the global scale from air quality to short-lived climate forcer. Atmos Chem Phys 15:8889–8973. https://doi.org/10.5194/acp-15-8889-2015

Moorhouse JE, Yeadon R, Beevor PS, Nesbitt BF (1969) Method for use in studies of insect chemical communication. Nature 223:1174–1175. https://doi.org/10.1038/2231174a0

Mozuraitis R, Stranden M, M R, Mustaparta H (2002) (-)-Germacrene D Increases Attraction and Oviposition by the Tobacco Budworm Moth *Heliothis virescens*. Chem Senses 27:505–509. https://doi.org/10.1093/chemse/27.6.505

Murlis J, Jones CD (1981) Fine-scale structure of odour plumes in relation to insect orientation to distant pheromone and other attractant sources. Physiol Entomol 6:71–86. https://doi.org/10.1111/j.1365-3032.1981.tb00262.x

Mutyambai DM, Bruce TJA, Van Den Berg J, et al (2016) An indirect defence trait mediated through egg-induced maize volatiles from neighbouring plants. PLoS One 11:1–15. https://doi.org/10.1371/journal.pone.0158744

Mylne KR, Mason PJ (1991) Concentration fluctuation measurements in a dispersing plume at a range of up to 1000 m. Q J R Meteorol Soc 117:177–206. https://doi.org/10.1002/qj.49711749709

Nahlik AM, Kentula ME, Fennessy MS, Landers DH (2012) Where is the consensus? A proposed foundation for moving ecosystem service concepts into practice. Ecol Econ 77:27–35. https://doi.org/10.1016/j.ecolecon.2012.01.001

Najar-Rodriguez AJ, Galizia CG, Stierle J, Dorn S (2010) Behavioral and neurophysiological responses of an insect to changing ratios of constituents in host plant-derived volatile mixtures. J Exp Biol 213:3388–3397. https://doi.org/10.1242/jeb.046284

NCBI Pub chem. https://pubchem.ncbi.nlm.nih.gov. Accessed 1 Sep 2020

Nieto A, Roberts SPM, Kemp J, et al (2014) European red list of bees. European union, Luxembourg

Nikonov AA, Leal WS (2002) Peripheral coding of sex pheromone and a behavioral antagonist in the Japanese beetle, *Popillia japonica*. J Chem Ecol 28:1075–1089. https://doi.org/10.1023/A:1015274104626

NIST (2011) NIST/NIH/EPA Mass Spectral Library

Nottingham SF, Hardie J, Dawson GW, et al (1991) Behavioral and electrophysiological responses of Aphids to host and nonhost plant volatiles. J Chem Ecol 17:1231–1242. https://doi.org/10.1007/BF01402946

Okada T, Jayasinghe JEARM, Nansamba M, et al (2018) Unfertilized ovary pushes wheat flower open for cross-pollination. J Exp Bot 69:399–412. https://doi.org/10.1093/jxb/erx410

Ollerton J, Winfree R, Tarrant S (2011) How many flowering plants are pollinated by animals? Oikos 120:321–326. https://doi.org/10.1111/j.1600-0706.2010.18644.x

Olsson A, Jonsson J oke, Thelin B, Liljefors T (1983) Determination of the vapor pressures of moth sex pheromone components by a gas chromatographic method. J Chem Ecol 9:375–385. https://doi.org/10.1007/BF00988456

Ostle NJ, Levy PE, Evans CD, Smith P (2009) UK land use and soil carbon sequestration. Land use policy 26:274–283. https://doi.org/10.1016/j.landusepol.2009.08.006

Pajunoja A, Malila J, Hao L, et al (2014) Estimating the Viscosity Range of SOA Particles Based on Their Coalescence Time. Aerosol Sci Technol 48:i–iv. https://doi.org/10.1080/02786826.2013.870325

Party V, Hanot C, Büsser DS, et al (2013) Changes in Odor Background Affect the Locomotory Response to Pheromone in Moths. PLoS One 8:e52897. https://doi.org/10.1371/journal.pone.0052897

Peeters L, Totland Ø (1999) Wind to insect pollination ratios and floral traits in five alpine Salix species. Can J Bot 77:556–563. https://doi.org/10.1139/cjb-77-4-556

Piccot SD, Watson JJ, Jones JW (1992) A global inventory of volatile organic compound emissions from anthropogenic sources. J Geophys Res 97:9897–9912. https://doi.org/10.1029/92JD00682

Pichersky E, Noel JP, Dudareva N (2006) Biosynthesis of plant volatiles: Nature's diversity and ingenuity. Science (80-) 311:808–811. https://doi.org/10.1126/science.1118510

Pinto DM, Blande JD, Nykänen R, et al (2007) Ozone degrades common herbivore-induced plant volatiles: Does this affect herbivore prey location by predators and parasitoids? J Chem Ecol 33:683–694. https://doi.org/10.1007/s10886-007-9255-8

Pinto DM, Blande JD, Souza SR, et al (2010) Plant volatile organic compounds (vocs) in ozone (o 3) polluted atmospheres: The ecological effects. J Chem Ecol 36:22–34. https://doi.org/10.1007/s10886-009-9732-3

Pio CA, Silva PA, Cerqueira MA, Nunes T V. (2005) Diurnal and seasonal emissions of volatile organic compounds from cork oak (*Quercus suber*) trees. Atmos Environ 39:1817–1827. https://doi.org/10.1016/j.atmosenv.2004.11.018

Plepys D, Ibarra F, Lo C (2002) Volatiles from flowers of *Platanthera bifolia* (Orchidaceae) attractive to the silver Y moth , *Autographa gamma* (Lepidoptera : Noctuidae). Oikos 99:69–74. https://doi.org/10.1034/j.1600-0706.2002.990107.x

Potts SG, Biesmeijer JC, Kremen C, et al (2010) Global pollinator declines: Trends, impacts and drivers. Trends Ecol Evol 25:345–353. https://doi.org/10.1016/j.tree.2010.01.007

Poulain L, Wu Z, Petters MD, et al (2010) Towards closing the gap between hygroscopic growth and CCN activation for secondary organic aerosols-Part 3: Influence of the chemical composition on the hygroscopic properties and volatile fractions of aerosols. Atmos Chem Phys 10:3775–3785. https://doi.org/10.5194/acp-10-3775-2010

Primack RB, Inouye DW (1993) Factors affecting pollinator visitation rates: A biogeographic comparison. Curr Sci 65:257–262. https://doi.org/10.2307/24095126

Proffit M, Bessière JM, Schatz B, Hossaert-McKey M (2018) Can fine-scale post-pollination variation of fig volatile compounds explain some steps of the temporal succession of fig wasps associated with *Ficus racemosa*? Acta Oecologica 90:81–90. https://doi.org/10.1016/j.actao.2017.08.009

Raguso RA (2008) Wake Up and Smell the Roses: The Ecology and Evolution of Floral Scent. Annu Rev

Ecol Evol Syst 39:549–569. https://doi.org/10.1146/annurev.ecolsys.38.091206.095601

Raguso RA, Light DM (1998) Electroantennogram responses of male *Sphinx perelegans* hawkmoths to floral and "green-leaf volatiles." Entomol Exp Appl 86:287–293. https://doi.org/10.1023/A:1003151107426

Raguso RA, Willis MA (2002) Synergy between visual and olfactory cues in nectar feeding by naïve hawkmoths, *Manduca sexta*. Anim Behav 64:685–695. https://doi.org/10.1006/anbe.2002.4010

Reynolds AM, Reynolds DR, Smith AD, et al (2007) Appetitive flight patterns of male *Agrotis segetum* moths over landscape scales. J Theor Biol 245:141–149. https://doi.org/10.1016/j.jtbi.2006.10.007

Richman SK, Levine JM, Stefan L, Johnson CA (2020) Asynchronous range shifts drive alpine plant–pollinator interactions and reduce plant fitness. Glob Chang Biol 26:3052–3064. https://doi.org/10.1111/gcb.15041

Richters S, Herrmann H, Berndt T (2016) Different pathways of the formation of highly oxidized multifunctional organic compounds (HOMs) from the gas-phase ozonolysis of ??-caryophyllene. Atmos Chem Phys 16:9831–9845. https://doi.org/10.5194/acp-16-9831-2016

Riffell JA, Lei H, Hildebrand JG (2009) Neural correlates of behavior in the moth *Manduca sexta* in response to complex odors. Proc Natl Acad Sci U S A 106:19219–19226. https://doi.org/10.1073/pnas.0910592106

Riffell JA, Shlizerman E, Sanders E, et al (2014) Flower discrimination by pollinators in a dynamic chemical environment. Science (80-) 344:1515–1518. https://doi.org/10.1126/science.1251041

Rissanen MP, Kurtén T, Sipilä M, et al (2015) Effects of chemical complexity on the autoxidation mechanisms of endocyclic alkene ozonolysis products: From methylcyclohexenes toward understanding α-pinene. J Phys Chem A 119:4633–4650. https://doi.org/10.1021/jp510966g

Robinson AL, Donahue NM, Shrivastava MK, et al (2007) Rethinking organic aerosols: Semivolatile emissions and photochemical aging. Science (80-) 315:1259–1262. https://doi.org/10.1126/science.1133061

RSC chemspider chemspider. http://www.chemspider.com/Chemical-Structure.4444881.html. Accessed 21 Jul 2020

Ruther J, Meiners T, Steidle JLM (2002) Rich in phenomena-lacking in terms. A classification of kairomones. Chemoecology 12:161–167. https://doi.org/10.1007/PL00012664

Rützler M, Zwiebel LJ (2005) Molecular biology of insect olfaction:recent progress and conceptual models. J Comp Physiol A Neuroethol Sensory, Neural, Behav Physiol 191:777–790. https://doi.org/10.1007/s00359-005-0044-y

Ružička Z (1997) Recognition of oviposition-deterring allomones by aphidophagous predators (Neuroptera: Chrysopidae, Coleoptera: Coccinellidae). Eur J Entomol 94:431–434

Sarukhán J, Whyte A, Hassan R, et al (2005) Millenium ecosystem assessment: ecosystems and human well-being. Island Press, Washington DC.

Saunier A, Blande JD (2019) The effect of elevated ozone on floral chemistry of *Brassicaceae* species. Environ Pollut 255:113257. https://doi.org/10.1016/j.envpol.2019.113257

Saveer AM, Kromann SH, Birgersson G, et al (2012) Floral to green: Mating switches moth olfactory coding and preference. Proc R Soc B Biol Sci 279:2314–2322. https://doi.org/10.1098/rspb.2011.2710

Sbarbati A, Osculati F (2006) Allelochemical communication in vertebrates: Kairomones, allomones

and synomones. Cells Tissues Organs 183:206–219. https://doi.org/10.1159/000096511

Schiestl FP (2015a) Ecology and evolution of floral volatile- mediated information transfer in plants. New Phytol 206:571–577. https://doi.org/10.1111/nph.13243

Schiestl FP (2015b) Ecology and evolution of floral volatile-mediated information transfer in plants. New Phytol 206:571–577. https://doi.org/10.1111/nph.13243

Schlyter F, Birgersson G, Byers JA, et al (1987) Field response of spruce bark beetle, *Ips typographus*, to aggregation pheromone candidates. J Chem Ecol 13:701–716. https://doi.org/10.1007/BF01020153

Schneider D (1957) Electrophysiological investigation on the antennal receptors of the silk moth during chemical and mechanical stimulation. Experientia 13:89–91. https://doi.org/10.1007/BF02160110

Schröder R, Hilker M (2008) The Relevance of Background Odor in Resource Location by Insects: A Behavioral Approach. Bioscience 58:308–316. https://doi.org/10.1641/b580406

Schroeder DC, Martin SJ (2012) Deformed wing virus: The main suspect in unexplained honeybee deaths worldwide. Virulence 3:. https://doi.org/10.4161/viru.22219

Schuman MC, Baldwin IT (2016) The Layers of Plant Responses to Insect Herbivores. Annu Rev Entomol 61:373–394. https://doi.org/10.1146/annurev-ento-010715-023851

Schweiger O, Biesmeijer JC, Bommarco R, et al (2010) Multiple stressors on biotic interactions: How climate change and alien species interact to affect pollination. Biol Rev 85:777–795. https://doi.org/10.1111/j.1469-185X.2010.00125.x

Shepard R (1987) Toward a universal law of generalization for psychological science. Science (80-) 237:1317–1323. https://doi.org/10.1126/science.3629243

Shi R, Liu F (2016) Quantum chemical study on the stability of honeybee queen pheromone against atmospheric factors. J Mol Model 22:1–13. https://doi.org/10.1007/s00894-016-2993-1

Shrivastava M, Cappa CD, Fan J, et al (2017) Recent advances in understanding secondary organic aerosol: Implications for global climate forcing. Rev Geophys 55:509–559. https://doi.org/10.1002/2016RG000540

Shu Y, Atkinson R (1994) Rate constants for the gas-phase reactions of O3 with a series of Terpenes and OH radical formation from the O3 reactions with Sesquiterpenes at 296 ± 2 K. Int J Chem Kinet 26:1193–1205

Silva RA, West JJ, Lamarque JF, et al (2017) Future global mortality from changes in air pollution attributable to climate change. Nat Clim Chang 7:647–651. https://doi.org/10.1038/nclimate3354

Sitch S, Cox PM, Collins WJ, Huntingford C (2007) Indirect radiative forcing of climate change through ozone effects on the land-carbon sink. Nature 448:791–794. https://doi.org/10.1038/nature06059

Slessor KN, Winston ML, Le Conte Y (2005) Pheromone communication in the honeybee (*Apis mellifera* L.). J Chem Ecol 31:2731–2745. https://doi.org/10.1007/s10886-005-7623-9

Smith BH (1998) Analysis of interaction in binary odorant mixtures. Physiol Behav 65:397–407. https://doi.org/10.1016/S0031-9384(98)00142-5

Song YY, Zeng R Sen, Xu JF, et al (2010) Interplant Communication of Tomato Plants through Underground Common Mycorrhizal Networks. PLoS One 5:e13324. https://doi.org/10.1371/journal.pone.0013324

Soto VC, Maldonado IB, Jofré VP, et al (2015) Direct analysis of nectar and floral volatile organic compounds in hybrid onions by HS-SPME/GC-MS: Relationship with pollination and seed production. Microchem J 122:110–118. https://doi.org/10.1016/j.microc.2015.04.017

Spaethe J, Brockmann A, Halbig C, Tautz J (2007) Size determines antennal sensitivity and behavioral threshold to odors in bumblebee workers. Naturwissenschaften 94:733–739. https://doi.org/10.1007/s00114-007-0251-1

Steffan-Dewenter I, Westphal C (2008) The interplay of pollinator diversity, pollination services and landscape change. J Appl Ecol 45:737–741. https://doi.org/10.1111/j.1365-2664.2008.01483.x

Steinbrecht RA (1997) Pore structure in insect olfactory sensilla: a review of data and concepts.pdf. Int J Insect Morphol Embryol 26:229–245

Stelinski LL, Miller JR, Ressa NE, Gut LJ (2003) Increased EAG responses of tortricid moths after prolonged exposure to plant volatiles: Evidence for octopamine-mediated sensitization. J Insect Physiol 49:845–856. https://doi.org/10.1016/S0022-1910(03)00136-7

Stevens B, Feingold G (2009) Untangling aerosol effects on clouds and precipitation in a buffered system. Nature 461:607–613. https://doi.org/10.1038/nature08281

Stone D, Whalley LK, Heard DE (2012) Tropospheric OH and HO2 radicals: Field measurements and model comparisons. Chem Soc Rev 41:6348–6404. https://doi.org/10.1039/c2cs35140d

Tasin M, Bäckman AC, Coracini M, et al (2007) Synergism and redundancy in a plant volatile blend attracting grapevine moth females. Phytochemistry 68:203–209. https://doi.org/10.1016/j.phytochem.2006.10.015

Tasoglou A, Pandis SN (2015) Formation and chemical aging of secondary organic aerosol during the β-caryophyllene oxidation. Atmos Chem Phys 15:6035–6046. https://doi.org/10.5194/acp-15-6035-2015

Tegoni M, Campanacci V, Cambillau C (2004) Structural aspects of sexual attraction and chemical communication in insects. Trends Biochem Sci 29:257–264. https://doi.org/10.1016/j.tibs.2004.03.003

Terry LI, Roemer RB, Walter GH, Booth D (2014) Thrips' responses to thermogenic associated signals in a cycad pollination system: the interplay of temperature, light, humidity and cone volatiles. Funct Ecol 28:857–867. https://doi.org/10.1111/1365-2435.12239

Thiery D, Visser JH (1987) Misleading the Colorado potato beetle with an odor blend. J Chem Ecol 13:1139–1146. https://doi.org/10.1007/BF01020544

Thomas CD, Franco AMA, Hill JK (2006) Range retractions and extinction in the face of climate warming. Trends Ecol Evol 21:415–416. https://doi.org/10.1016/j.tree.2006.05.012

Tóth M, Szőcs G, Majoros B, et al (1983) Experiments with a two-component sex attractant of the silver Y moth (Autographa gamma L.), and some evidence for the presence of both components in natural female sex pheromone. J Chem Ecol 9:1317–1325. https://doi.org/10.1007/BF00994800

Tscharntke T, Brandl R (2004) Plant-Insect interactions in fragmented landscapes. Annu Rev Entomol 49:405–430. https://doi.org/10.1146/annurev.ento.49.061802.123339

TSI (2007) Model 3775 condensation particle counter manual, D. TSI, Shoreview

Tumlinson JH, Moser JC, Silverstein RM, et al (1972) A volatile trail pheromone of the leaf-cutting ant, *Atta texana*. J Insect Physiol 18:809–814. https://doi.org/10.1016/0022-1910(72)90018-2

United nations (1997) Glossary of environment statistics, studies in methods. United Nations, New

york

Vanbergen AJ, Espíndola A, Aizen MA (2018) Risks to pollinators and pollination from invasive alien species. Nat Ecol Evol 2:16–25. https://doi.org/10.1038/s41559-017-0412-3

Vanbergen AJ, Garratt MP, Vanbergen AJ, et al (2013) Threats to an ecosystem service: Pressures on pollinators. Front Ecol Environ 11:251–259. https://doi.org/10.1890/120126

Vanderplanck M, Lapeyre B, Brondani M, et al (2021) Ozone pollution alters olfaction and behavior of pollinators. Antioxidants 10:1–16. https://doi.org/10.3390/antiox10050636

Vas G, Vékey K (2004) Solid-phase microextraction: A powerful sample preparation tool prior to mass spectrometric analysis. J Mass Spectrom 39:233–254. https://doi.org/10.1002/jms.606

Verdonk JC, De Vos CHR, Verhoeven HA, et al (2003) Regulation of floral scent production in petunia revealed by targeted metabolomics. Phytochemistry 62:997–1008. https://doi.org/10.1016/S0031-9422(02)00707-0

Vicens N, Bosch J (2000) Weather-Dependent Pollinator Activity in an Apple Orchard, with Special Reference to *Osmia cornuta* and *Apis mellifera* (Hymenoptera: Megachilidae and Apidae). Environ Entomol 29:413–420. https://doi.org/10.1603/0046-225x-29.3.413

Vogel S (1994) Life in moving fluids : the physical biology of flow. Princeton University Press, Princeton, N.J.

Von Hessberg C, Von Hessberg P, Pöschl U, et al (2009) Temperature and humidity dependence of secondary organic aerosol yield from the ozonolysis of β-pinene. Atmos Chem Phys 9:3583–3599. https://doi.org/10.5194/acp-9-3583-2009

Vuorinen T, Nerg AM, Holopainen JK (2004) Ozone exposure triggers the emission of herbivore-induced plant volatiles, but does not disturb tritrophic signalling. Environ Pollut 131:305–311. https://doi.org/10.1016/j.envpol.2004.02.027

Vuts J, Szarukán I, Subchev M, et al (2010) Improving the floral attractant to lure *Epicometis hirta Poda* (Coleoptera: Scarabaeidae, Cetoniinae). J Pest Sci (2004) 83:15–20. https://doi.org/10.1007/s10340-009-0263-z

Vuts J, Woodcock CM, Sumner ME, et al (2016) Responses of the two-spotted oak buprestid, *Agrilus biguttatus* (Coleoptera: Buprestidae), to host tree volatiles. Pest Manag Sci 72:845–851. https://doi.org/10.1002/ps.4208

War AR, Sharma HC, Paulraj MG, et al (2011) Herbivore induced plant volatiles: their role in plant defense for pest management. Plant Signal Behav 6:1973–1978. https://doi.org/10.4161/psb.6.12.18053

Webster B, Bruce T, Pickett J, Hardie J (2010) Volatiles functioning as host cues in a blend become nonhost cues when presented alone to the black bean aphid. Anim Behav 79:451–457. https://doi.org/10.1016/j.anbehav.2009.11.028

Whitehead AT, Larsen JR (1976) Ultrastructure of the contact chemoreceptors of *Apis mellifera* L. (Hymenoptera : Apidae). Int J Insect Morphol Embryol 5:301–315. https://doi.org/10.1016/0020-7322(76)90030-1

Whitehorn PR, O'Connor S, Wackers FL, Goulson D (2012) Neonicotinoid pesticide reduces bumble bee colony growth and queen production. Science (80-) 336:351–352. https://doi.org/10.1126/science.1215025

Wilkinson S, Mills G, Illidge R, Davies WJ (2012) How is ozone pollution reducing our food supply? J Exp Bot 63:527–536. https://doi.org/10.1093/jxb/err317

Williamson SM, Willis SJ, Wright GA (2014) Exposure to neonicotinoids influences the motor function of adult worker honeybees. Ecotoxicology 23:1409–1418. https://doi.org/10.1007/s10646-014-1283-x

Willmer P (2011) Pollination and Floral Ecology. Princeton University Press, Princeton

Wilson EE, Holway DA (2010) Multiple mechanisms underlie displacement of solitary Hawaiian Hymenoptera by an invasive social wasp. Ecology 91:3294–3302. https://doi.org/10.1890/09-1187.1

Wilson JK, Kessler A, Woods HA (2015) Noisy Communication via Airborne Infochemicals. Bioscience 65:667–677. https://doi.org/10.1093/biosci/biv062

Witherspoon PA, Saraf DN (1965) Diffusion of methane, ethane, propane, and n-butane in water from 25 to 43°. J Phys Chem 69:3752–3755. https://doi.org/10.1021/j100895a017

Witter M, Berndt T, Böge O, et al (2002) Gas-phase ozonolysis: Rate coefficients for a series of terpenes and rate coefficients and OH yields for 2-methyl-2-butene and 2, 3-dimethyl-2-butene. Int J Chem Kinet 34:394–403. https://doi.org/10.1002/kin.10063

Wolkovich EM, Cook BI, Allen JM, et al (2012) Warming experiments underpredict plant phenological responses to climate change. Nature 485:494–497. https://doi.org/10.1038/nature11014

Wright GA, Lutmerding A, Dudareva N, Smith BH (2005) Intensity and the ratios of compounds in the scent of snapdragon flowers affect scent discrimination by honeybees (*Apis mellifera*). J Comp Physiol A Neuroethol Sensory, Neural, Behav Physiol 191:105–114. https://doi.org/10.1007/s00359-004-0576-6

Wright GA, Schiestl FP (2009) The evolution of floral scent: The influence of olfactory learning by insect pollinators on the honest signalling of floral rewards. Funct Ecol 23:841–851. https://doi.org/10.1111/j.1365-2435.2009.01627.x

Wright GA, Skinner BD, Smith BH (2002) Ability of honeybee, *Apis mellifera*, to detect and discriminate odors of varieties of canola (*Brassica rapa* and *brassica napus*) and snapdragon flowers (*Antirrhinum majus*). J Chem Ecol 28:721–740. https://doi.org/10.1023/A:1015232608858

Wright GA, Smith BH (2004) Different thresholds for detection and discrimination of odors in the honey bee (*Apis mellifera*). Chem Senses 29:127–135. https://doi.org/10.1093/chemse/bjh016

Xing YF, Xu YH, Shi MH, Lian YX (2016) The impact of PM2.5 on the human respiratory system. J Thorac Dis 8:E69–E74. https://doi.org/10.3978/j.issn.2072-1439.2016.01.19

Yli-Pirilä P, Copolovici L, Kännaste A, et al (2016) Herbivory by an Outbreaking Moth Increases Emissions of Biogenic Volatiles and Leads to Enhanced Secondary Organic Aerosol Formation Capacity. Environ Sci Technol 50:11501–11510. https://doi.org/10.1021/acs.est.6b02800

Yu J, Cocker III D, Griffin RJ, Flagan RC (1999) Gas-Phase ozone oxidation of monoterpenes: Gaseous and Particulate Products. J Atmos Chem 34:207–258. https://doi.org/10.1023/A:1006254930583

Yuan JS, Himanen SJ, Holopainen JK, et al (2009) Smelling global climate change: mitigation of function for plant volatile organic compounds. Trends Ecol Evol 24:323–331. https://doi.org/10.1016/j.tree.2009.01.012

Zakir A, Sadek MM, Bengtsson M, et al (2013) Herbivore-induced plant volatiles provide associational resistance against an ovipositing herbivore. J Ecol 101:410–417. https://doi.org/10.1111/1365-2745.12041

Zanen PO, Sabelis MW, Buonaccorsi JP, Carde RT (1994) Search strategies of fruit flies in steady and shifting winds in the absence of food odours. Physiol Entomol 19:335–341. https://doi.org/10.1111/j.1365-3032.1994.tb01060.x

Zhang Q, Lin X, Gai Y, et al (2018) Kinetic and mechanistic study on gas phase reactions of ozone with a series of: Cis-3-hexenyl esters. RSC Adv 8:4230–4238. https://doi.org/10.1039/c7ra13369c

Zhang Y, Igwe OJ (2018) Lipopolysaccharide (LPS)-mediated priming of toll-like receptor 4 enhances oxidant-induced prostaglandin E2 biosynthesis in primary murine macrophages. Int Immunopharmacol 54:226–237. https://doi.org/10.1016/j.intimp.2017.11.017

Zurbuchen A, Landert L, Klaiber J, et al (2010) Maximum foraging ranges in solitary bees: only few individuals have the capability to cover long foraging distances. Biol Conserv 143:669–676. https://doi.org/10.1016/j.biocon.2009.12.003

AP – Appendix

AP1 – Literature rate constant determinations

Table AP1 – List of literature derived rate constants for the five VOCs studied in this thesis. *=Removed due to being an outlier and technical difficulties observed in source paper.

compound	Rate constant ($cm^3 molecule^{-1} s^{-1}$) ± SE	Temp (K)	Reference compound	Reference
Z-3-hexenyl acetate	$5.4\pm1.4\times10^{-17}$	296±2	cyclohexane	(Atkinson et al. 1995)
	$5.8\pm0.7\times10^{-17}$	298±2	Absolute determination	(Zhang et al. 2018)
Z-3-hexenol	$5.9\pm0.9\times10^{-17}$	291±1	1-pentene	(Grosjean and Grosjean 1998)
	$6.0\pm0.6\times10^{-17}$	298±3	Isoprene	(Gibilisco et al. 2015)
	$6.2\pm0.3\times10^{-17}$	298±3	1,4-cyclohexadiene	(Gibilisco et al. 2015)
	$6.0\pm0.7\times10^{-17}$	298±1	1-chloro-3-methyl-2-butene	(Chen et al. 2016)
	$6.1\pm0.4\times10^{-17}$	298±1	Isoprene	(Chen et al. 2016)
	$5.8\pm0.7\times10^{-17}$	298±1	Absolute	(Chen et al. 2016)
	$6.4\pm1.7\times10^{-17}$	296±2	Absolute	(Atkinson et al. 1995)
	$5.5\pm0.7\times10^{-17}$	298*	Absolute	(Lin et al. 2016)
	$5.2\pm0.6\times10^{-17}$	296±2	Absolute	(Atkinson et al. 1990)
3-carene	$4.9\pm0.8\times10^{-17}$	293±2	Absolute	(Chen et al. 2015)
	$3.5\pm0.2\times10^{-17}$	295±1	Absolute	(Chen et al. 2015)
	$3.7\pm0.2\times10^{-17}$	296±3	Absolute	(Chen et al. 2015)
	$4.1\pm0.4\times10^{-17}$	296±2	α-pinene	(Atkinson et al. 1990)
	$5.6\pm1.0\times10^{-17}$	295±0.5	2-methylbut-2-ene	(Witter et al. 2002)
	$3.8\pm0.3\times10^{-17}$	296±2	cyclohexene	(Chen et al. 2015)
	$12\pm0.61\times10^{-17}$*	295±1*	Unknown due paywall*	(Grimsrud et al. 1975)*
1-dodecene	$1.4\pm0.1\times10^{-17}$	296±2	1-octene	(Atkinson, sherri a. Mason and Arey 2009)
	$1.0\pm0.1\times10^{-17}$	298±2	1-decene	(Ghalaieny et al. 2012)
1-undecene	$1.0\pm0.1\times10^{-17}$	298±2	1-decene	(Ghalaieny et al. 2012)

AP2 – Raw EAG responses of *Apis mellifera* antennae

Z-3-hexenol

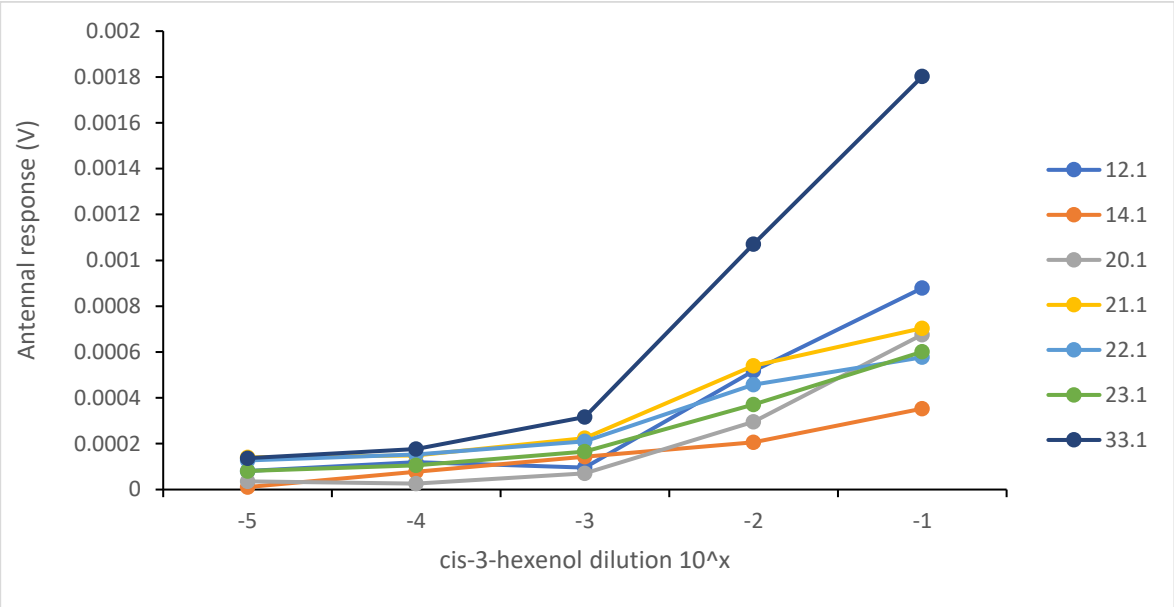

Figure AP1- Raw EAG responses of various *A. mellifera* antennae to Z-3-hexenol standards

Z-3-hexenyl acetate

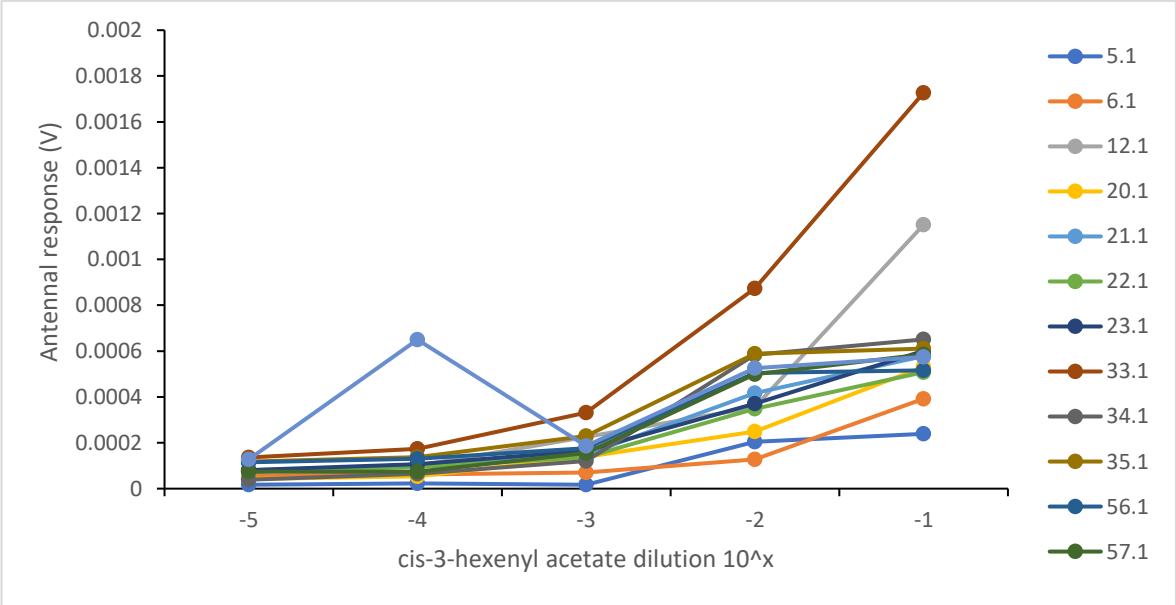

Figure AP2- Raw EAG responses of various *A. mellifera* antennae to Z-3-hexenyl acetate standards

3-Carene

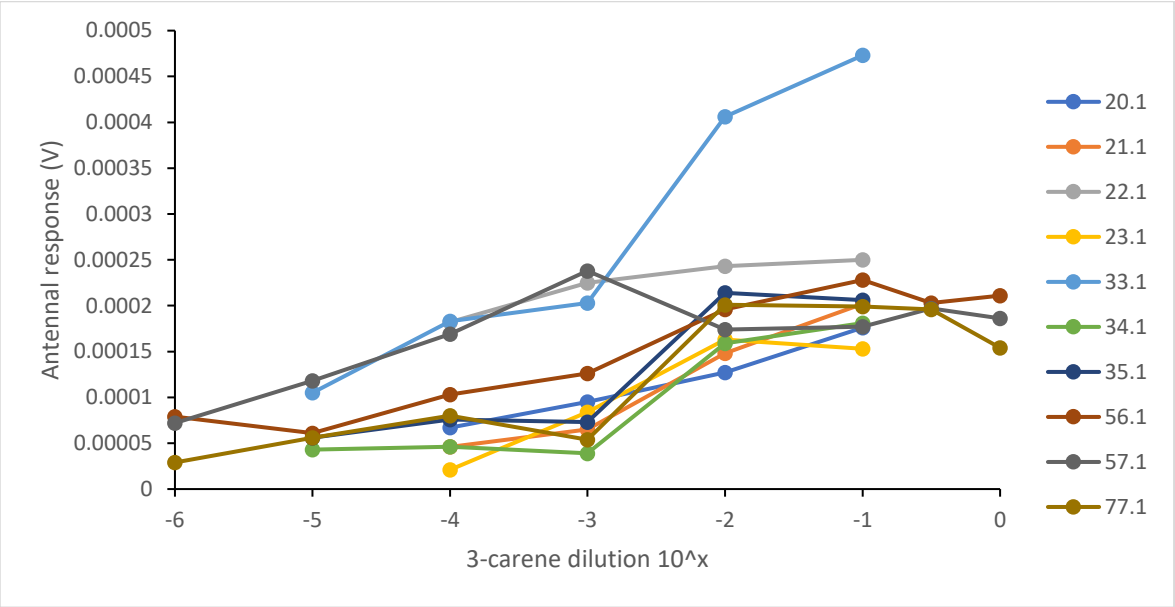

Figure AP3- Raw EAG responses of various *A. mellifera* antennae to 3-carene standards

1-dodecene

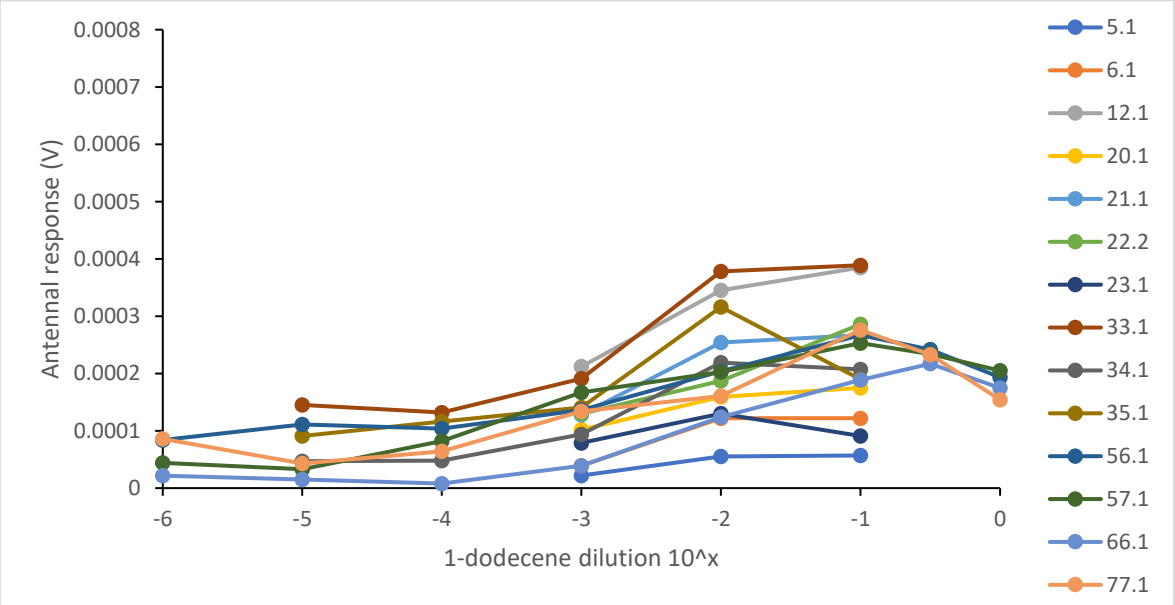

Figure AP4- Raw EAG responses of various *A.mellifera* antennae to 1-dodecene standards

1-undecene

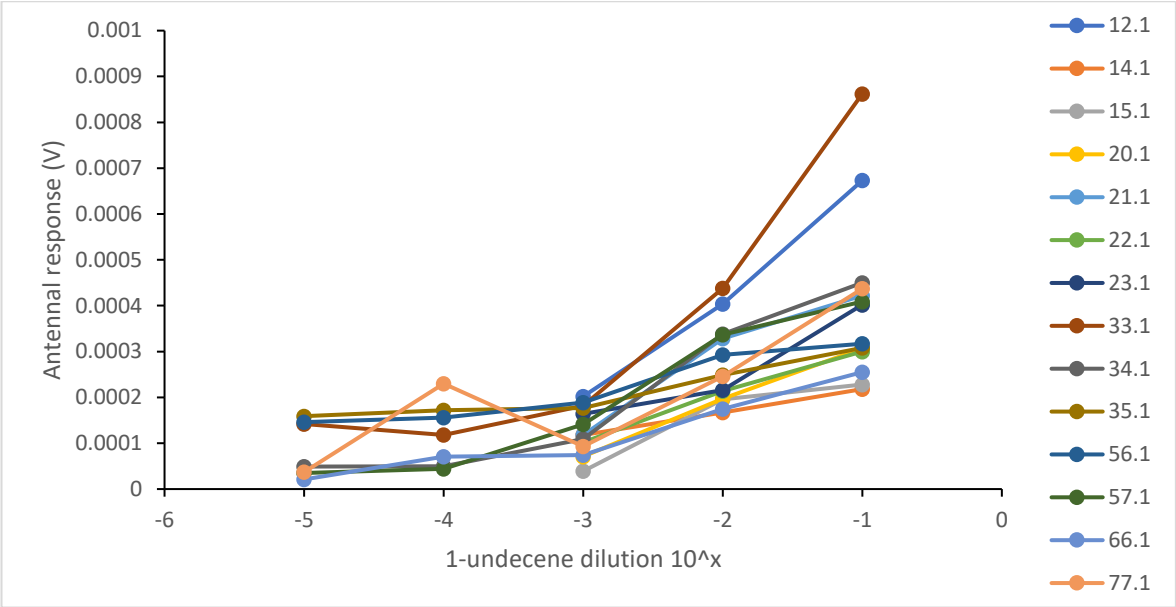

Figure AP5- Raw EAG responses of various *A.mellifera* antennae to 1-undecene standards

AP3 – SPME GC-MS reproducibility

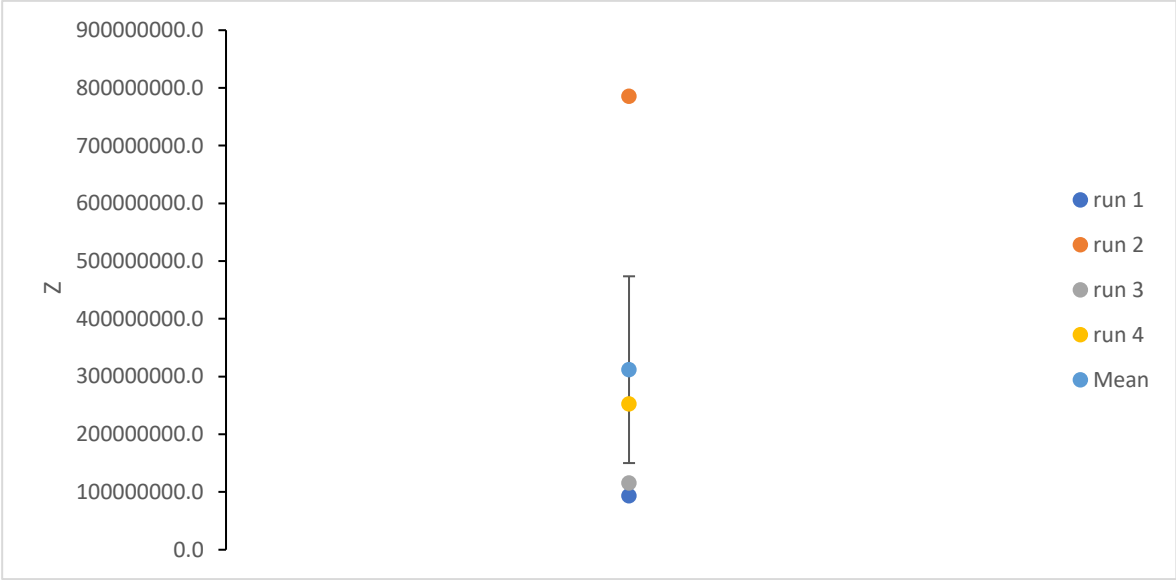

Figure AP6 – Scatter graph showing individual recoveries of Z-3-hexenol (1ppm) using SPME GC-MS. Mean is plotted ± SE.

AP4 – Raw product recognition response values

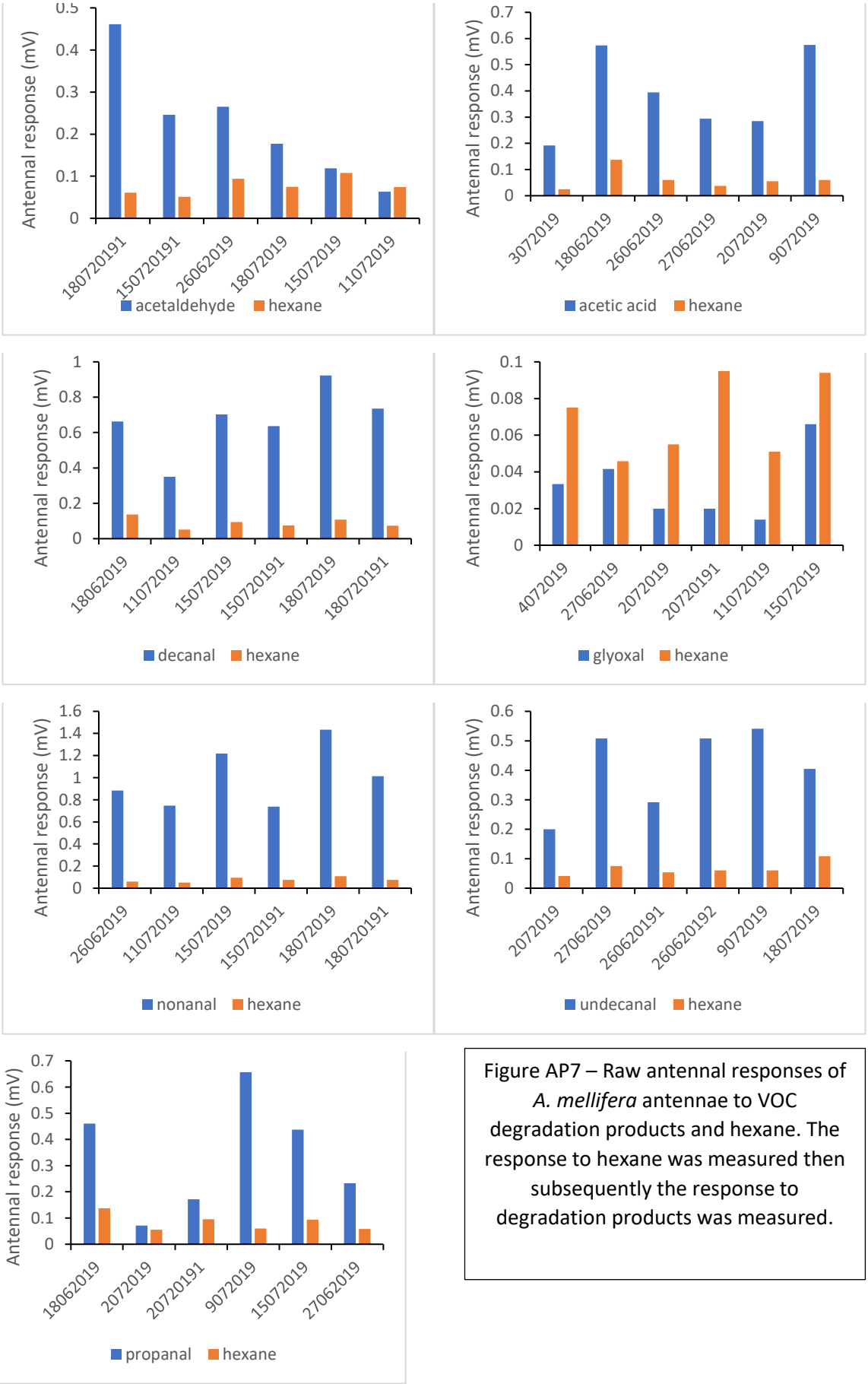

Figure AP7 – Raw antennal responses of *A. mellifera* antennae to VOC degradation products and hexane. The response to hexane was measured then subsequently the response to degradation products was measured.

AP5 – Effect of altering reactant introduction order on SOA yield over time

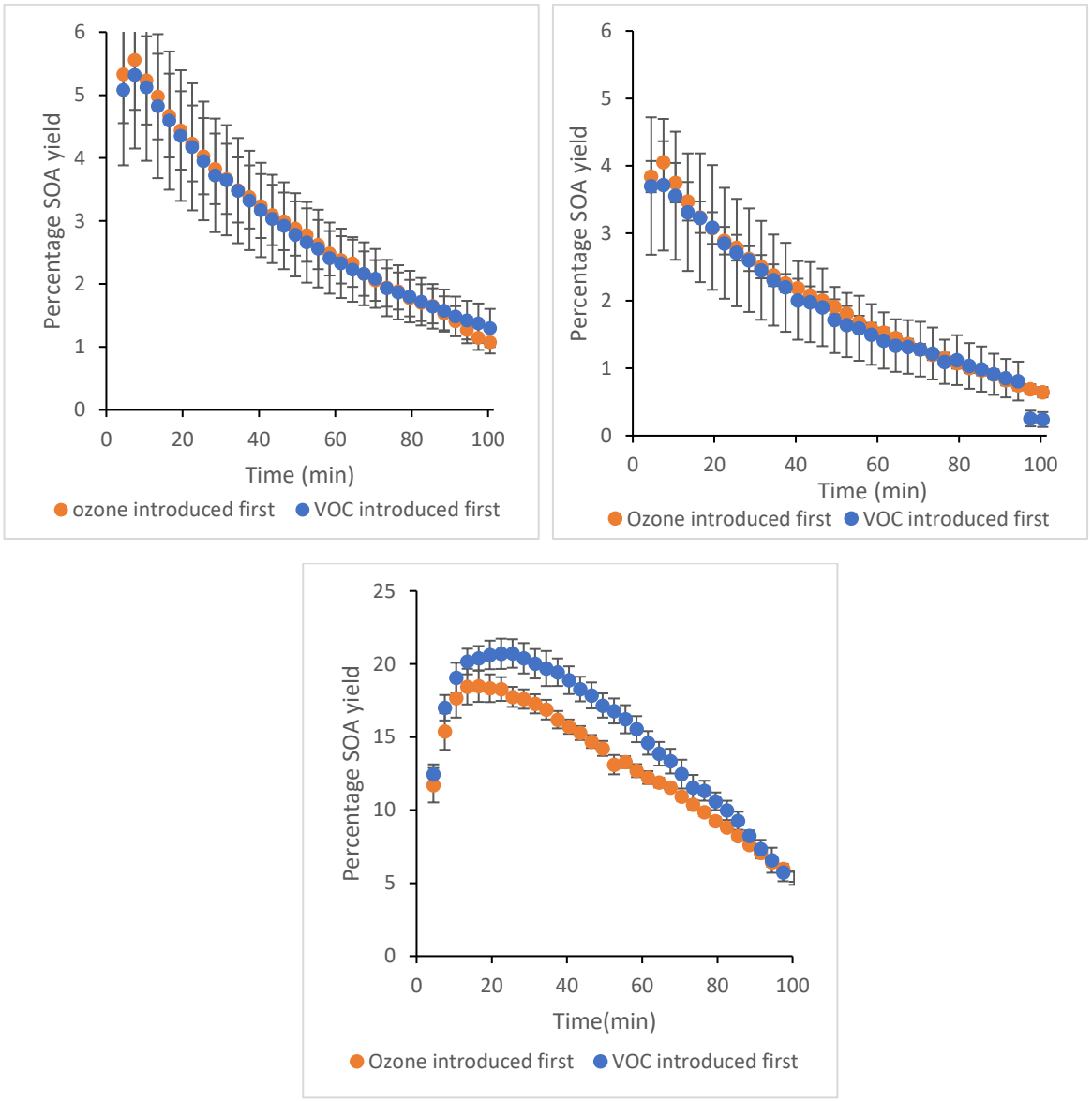

Figure AP9 – Percentage SOA yields over time for Z-3-hexenol (top left) and Z-3-hexenyl acetate (top right) comparing introducing VOC into the static chamber first vs introducing ozone first into the static chamber [O_3] = 4ppm, [VOC]=1ppm. Percentage SOA yields over time for 3-carene(bottom centre) comparing introducing VOC into the static chamber first vs introducing ozone first into the static chamber [O_3] = 1ppm, [VOC]=3ppm.

Table AP2 – summary of LMER statistical test results comparing percentage yield over time data as a result of introducing VOC into the static chamber first vs introducing ozone first into the static chamber for both Z-3-hexenol and Z-3-hexenyl acetate. Df=degrees of freedom, t= T statistic ,p=significance value

compound	Z-3-hexenol	Z-3-hexenyl acetate	3-carene
LMER comparing the effect of altering reactant introduction order on SOA yield	df=8.999, t=-0.042, p=0.967	df=8.982, t=-0.029, p=0.978	df=8.987, t=-0.029, p=0.978

AP6 - Effect of altering the order of static chamber construction on SOA yield

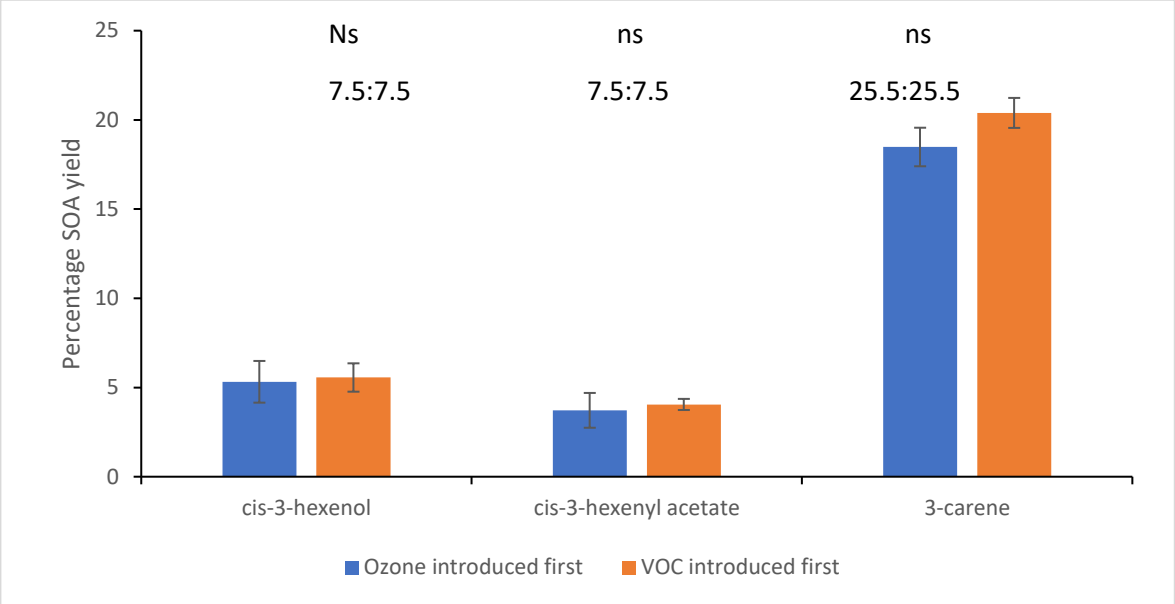

Figure AP10 - Maximum SOA yields for Z-3-hexenol, Z-3-hexenyl acetate and 3-carene comparing introducing VOC into the static chamber first vs introducing ozone first into the static chamber. Z-3-hexenyl acetate/Z-3-hexenol, Ozone excess, [O_3] = 4ppm, [VOC]=1ppm. 3-carene, VOC excess, [O_3] = 1ppm, [VOC]=3ppm.

From statistical comparison of maximum yield under VOC first and Ozone first conditions, Z-3-hexenol shows no statistically significant difference in maximum yield for Z-3-hexenol (W = 19 , N = 11, p = 0.5368), 3-carene (W=16, N=14, p=0.345) or Z-3-hexenyl acetate (W=18, N= 11, p=0.6623).

AP7 – SOA yield raw data

Removed data sets

The following replicates were excluded from the mean due to a physical condition abnormality seeming to cause these to be “outliers”. They are still plotted however as future work may show that these replicates are indeed valid.

Table AP3 – list of removed data sets from raw SOA yield experiments using SMPS

Date	Compound	condition	Reasoning
03/12/2018	1-undecene	VOC excess	A large room temperature gradient was noticed and this is likely to cause VOC deposition and is seemingly reflected in the lower yield
26/10/2018	3-carene	ozone excess	Change in sampling flow rate mid experiment
15/05/2018am	3-carene	ozone Excess	The last few points only removed due to increased sampling flow rate

1-undecene 4:1 ozone excess

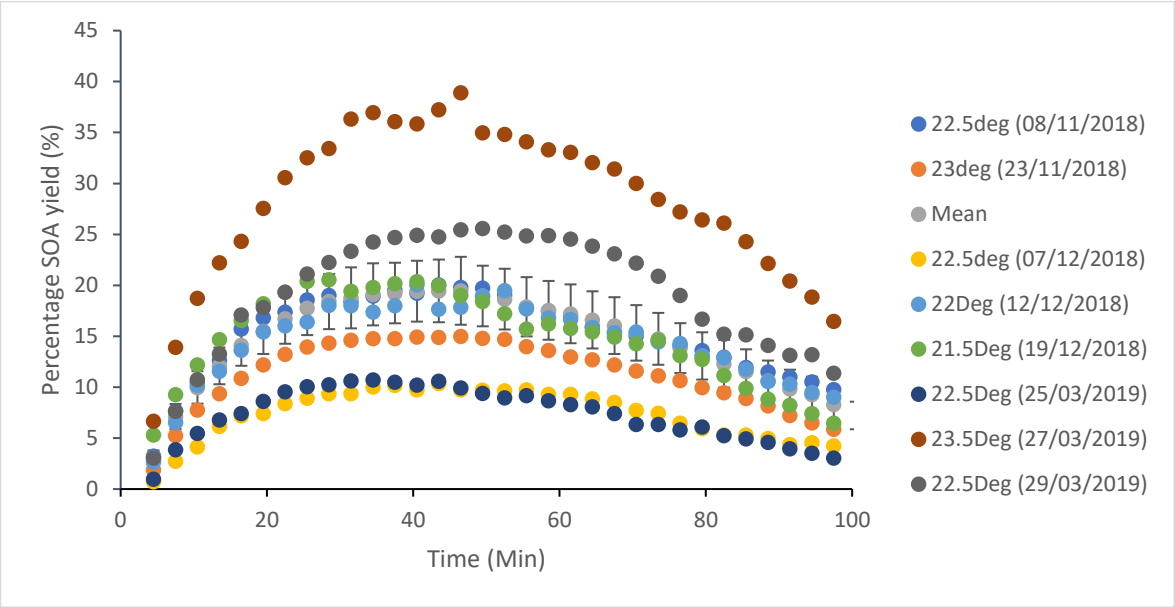

Figure AP11 – Raw SMPS measurements of 1-undecene SOA yield produced under ozone excess conditions ([VOC]=0.25ppm, O_3 = 1ppm)

1-undecene 1:3 VOC excess

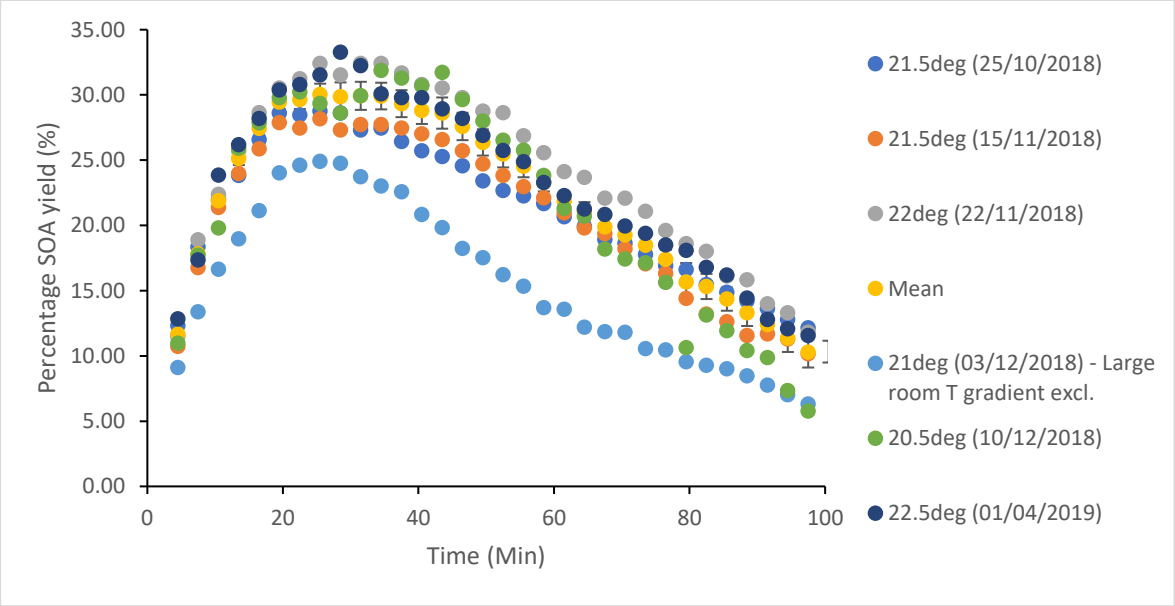

Figure AP12 – Raw SMPS measurements of 1-undecene SOA yield produced under VOC excess conditions ([VOC]=3ppm, O_3 = 1ppm)

1-dodecene 4:1 Ozone excess

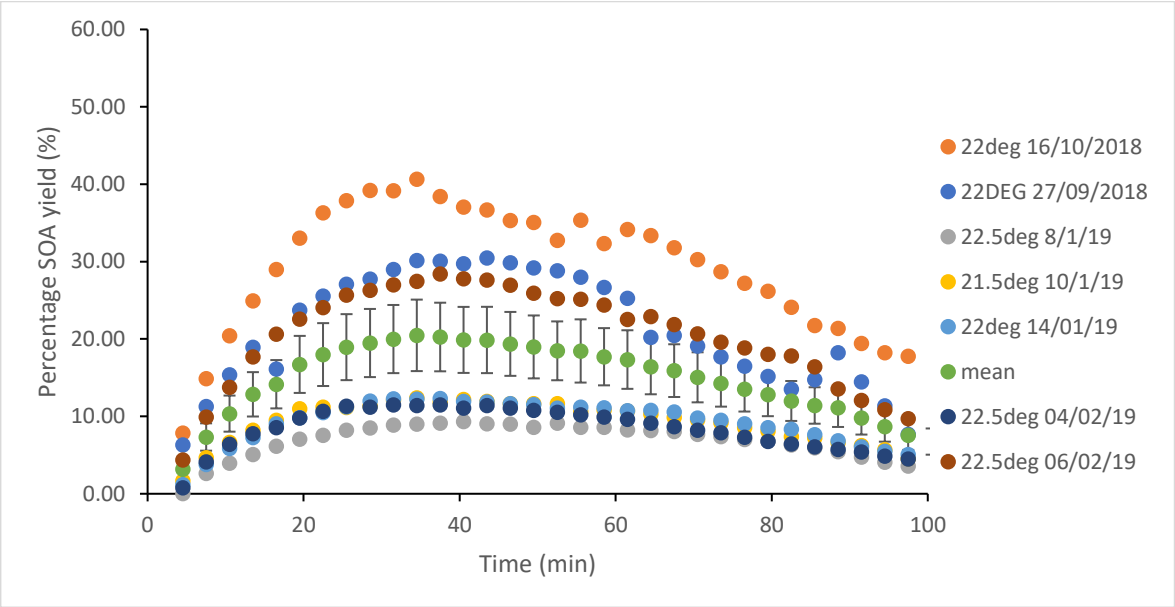

Figure AP13 – Raw SMPS measurements of 1-dodecene SOA yield produced under ozone excess conditions ([VOC]=0.25ppm, O_3 = 1ppm)

1-dodecene 1:3 VOC excess

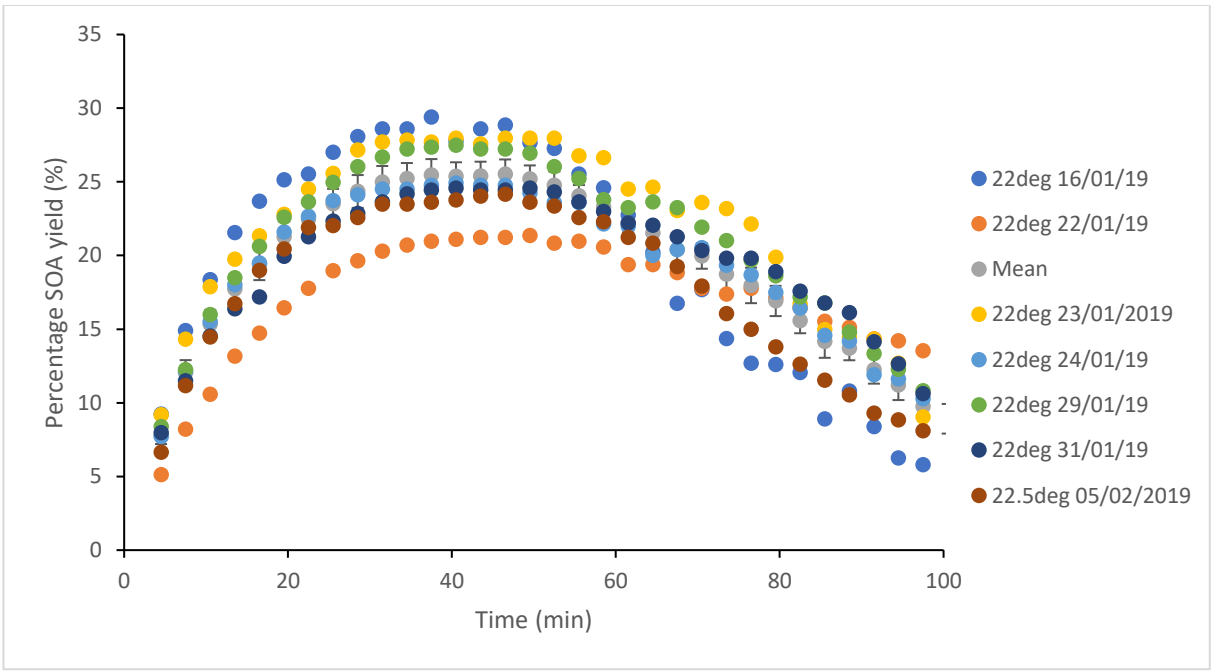

Figure AP14 – Raw SMPS measurements of 1-dodecene SOA yield produced under VOC excess conditions ([VOC]=3ppm, O_3 = 1ppm)

3-carene 4:1 ozone excess

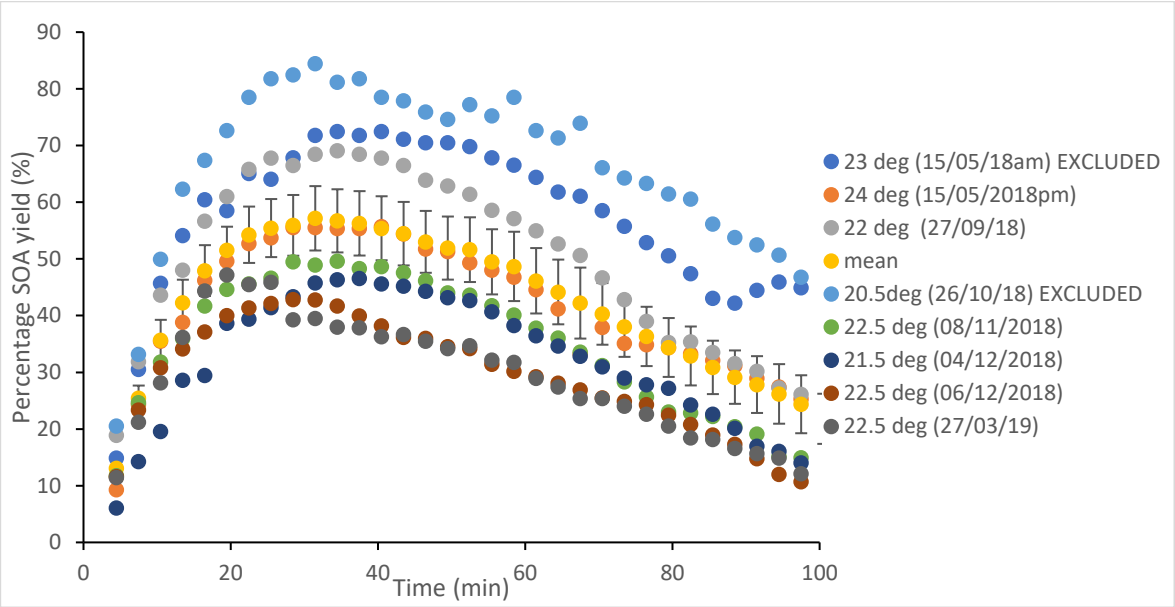

Figure AP15 – Raw SMPS measurements of 3-carene SOA yield produced under VOC excess conditions ([VOC]=3ppm, O_3 = 1ppm)

3-carene 1:3 VOC excess

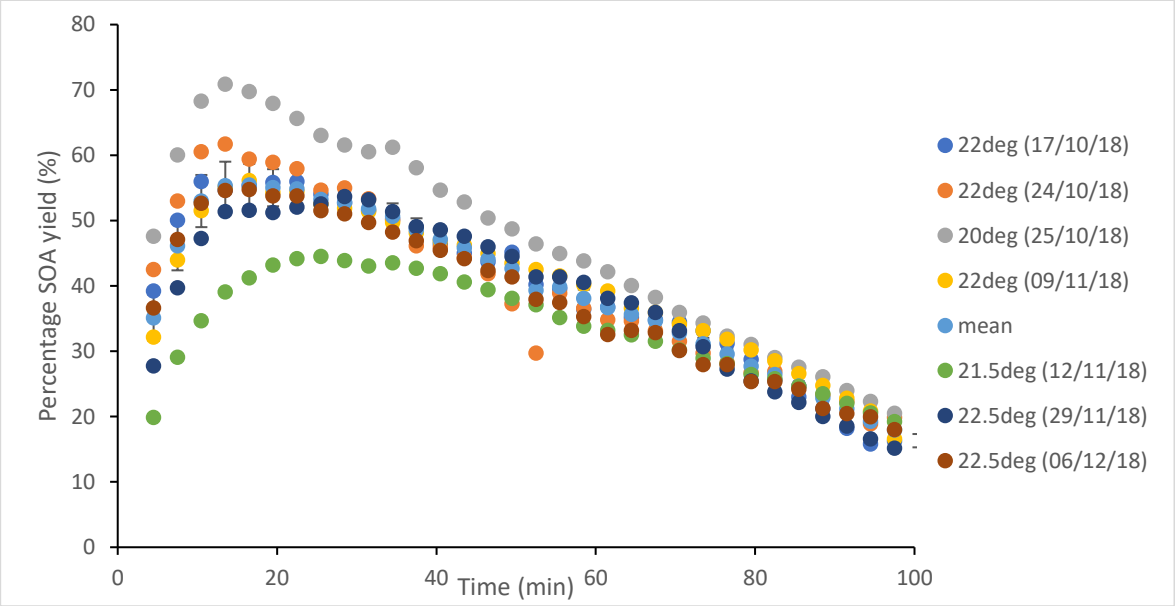

Figure AP16 – Raw SMPS measurements of 3-carene SOA yield produced under VOC excess conditions ([VOC]=3ppm, O_3 = 1ppm)

Z-3-hexenol 4:1 ozone excess

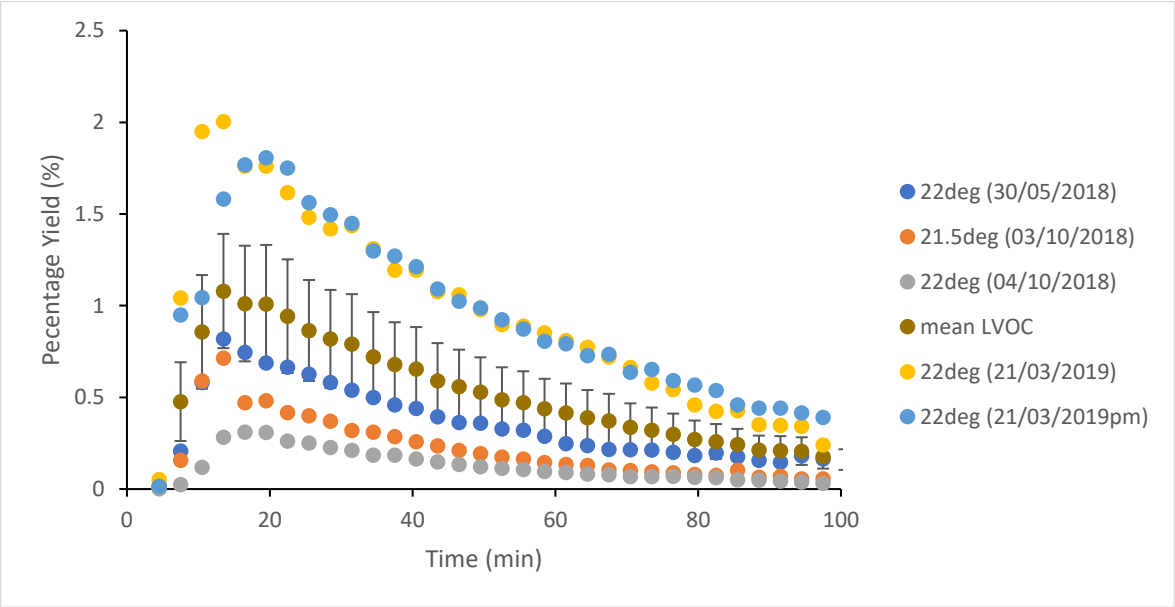

Figure AP17 – Raw SMPS measurements of Z-3-hexenol SOA yield produced under ozone excess conditions ([VOC]=0.25ppm, O_3 = 1ppm)

Z-3-hexenol 1:3 VOC excess

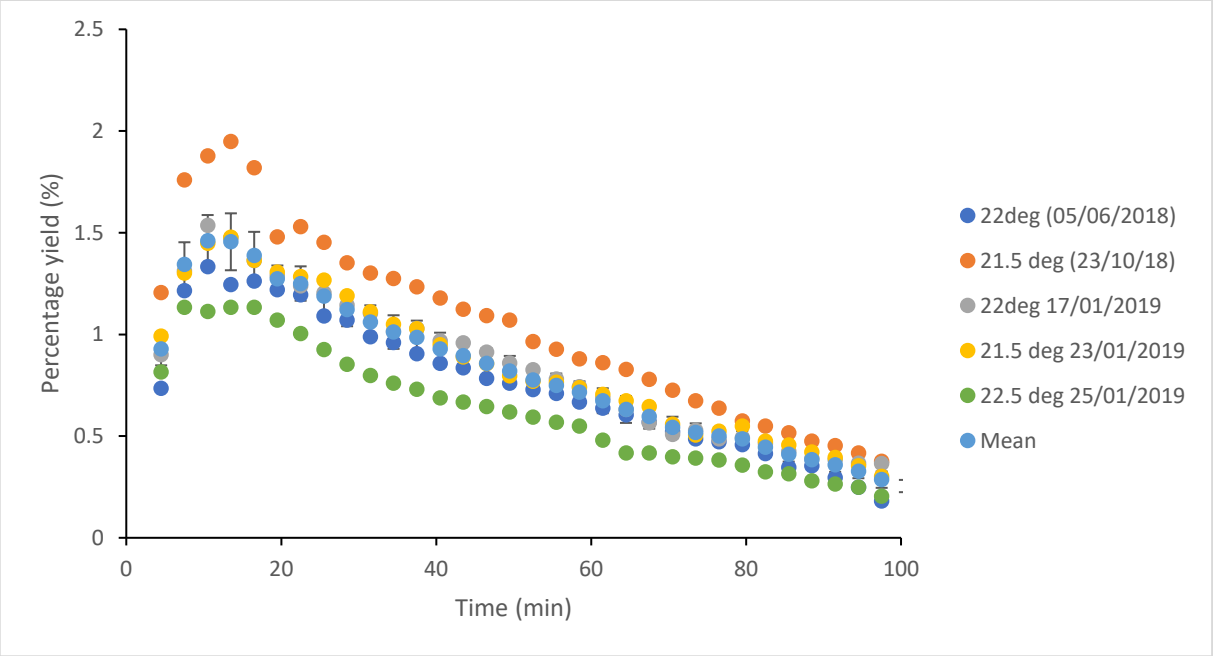

Figure AP18 – Raw SMPS measurements of Z-3-hexenol SOA yield produced under VOC excess conditions ([VOC]=3ppm, O_3 = 1ppm)

Z-3-hexenyl acetate 4:1 ozone excess

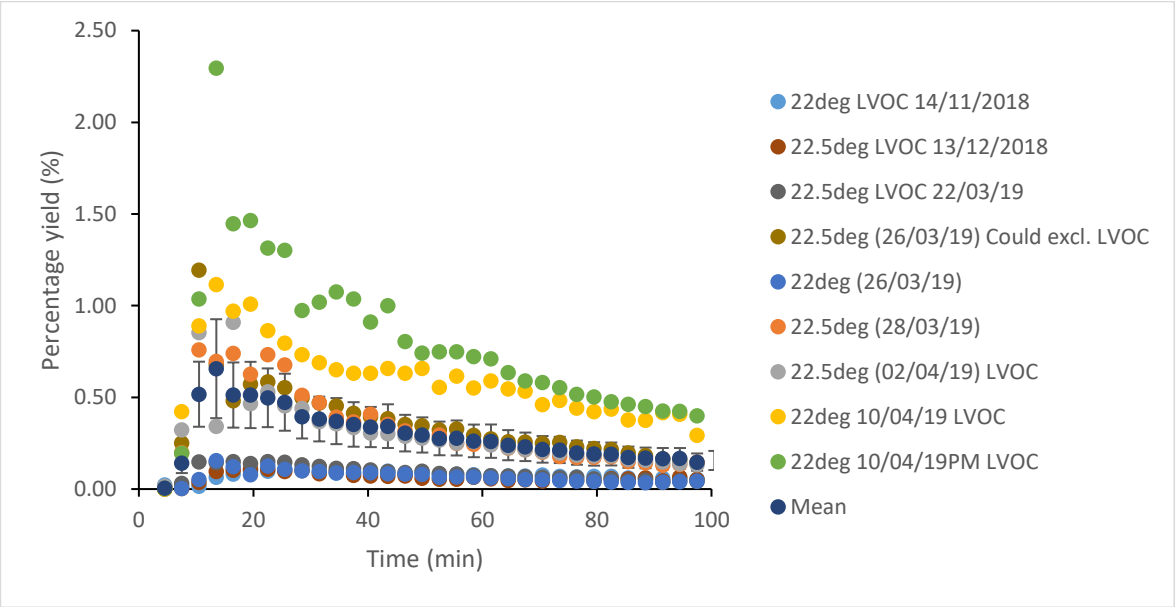

Figure AP19 – Raw SMPS measurements of Z-3-hexenyl acetate SOA yield produced under ozone excess conditions ([VOC]=0.25ppm, O_3 = 1ppm)

Z-3-hexenyl acetate 1:3 VOC excess

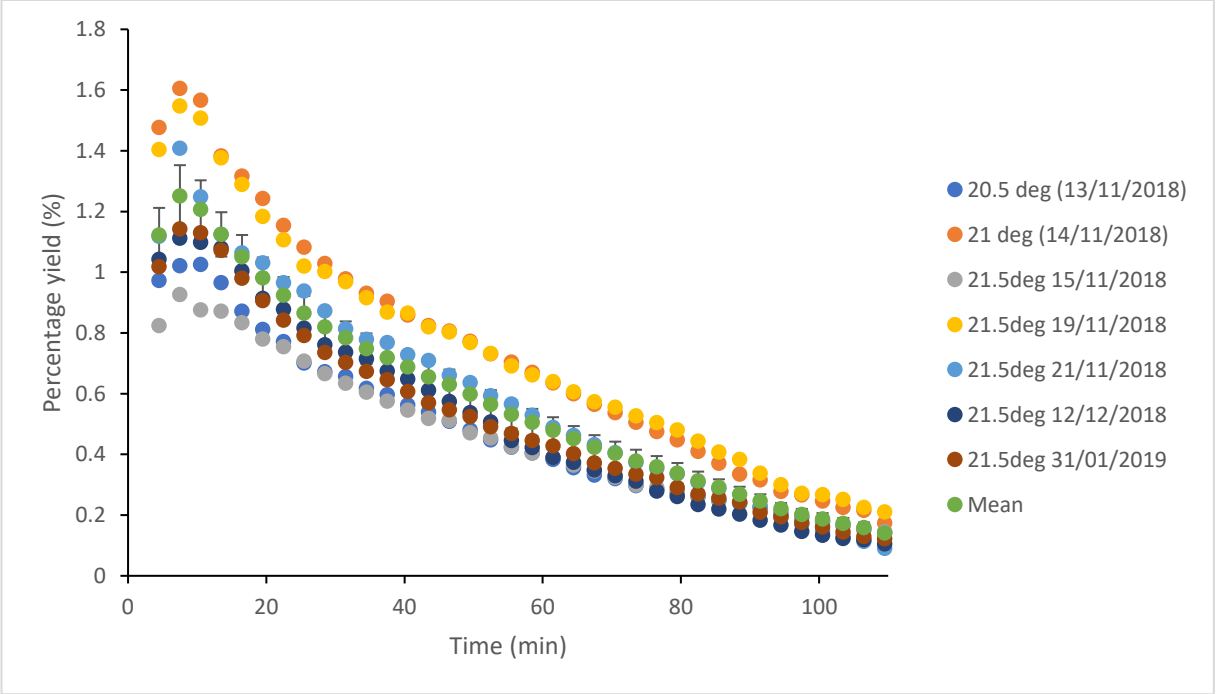

Figure AP20 – Raw SMPS measurements of Z-3-hexenyl acetate SOA yield produced under VOC excess conditions ([VOC]=3ppm, O_3 = 1ppm)

AP8 – SOA yield mean data

Mean ozone excess SOA yield over time

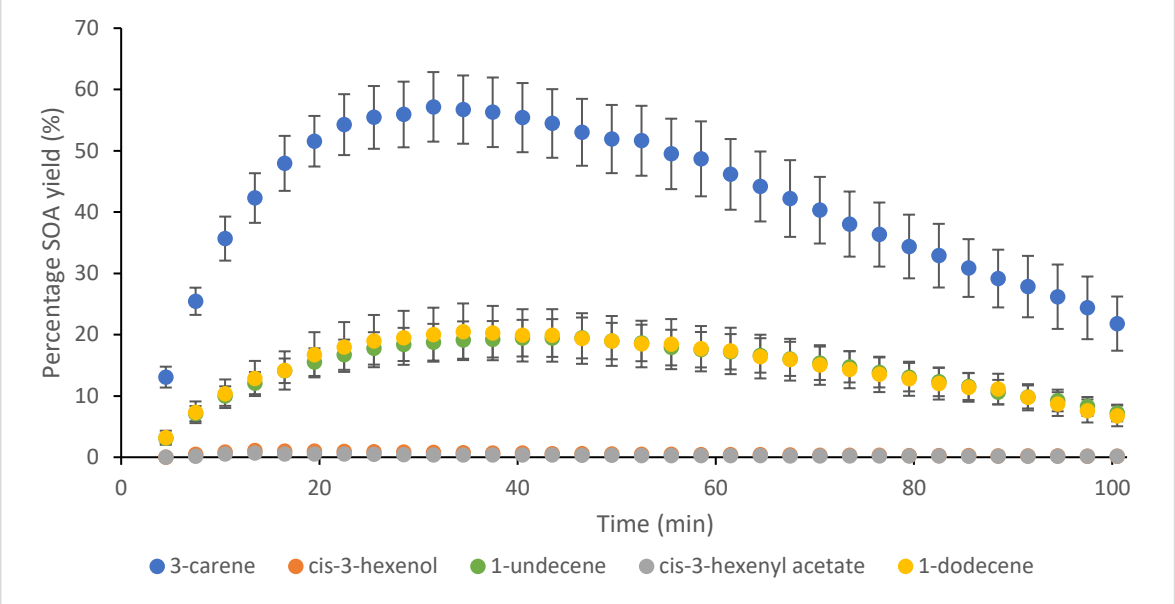

Figure AP21 – Mean SOA yield over time for the 5 study compounds under a 4x ozone excess. [VOC] = 0.25ppm, [O_3]= 1ppm. Error = ± standard error (SE).

Mean VOC excess SOA yield over time

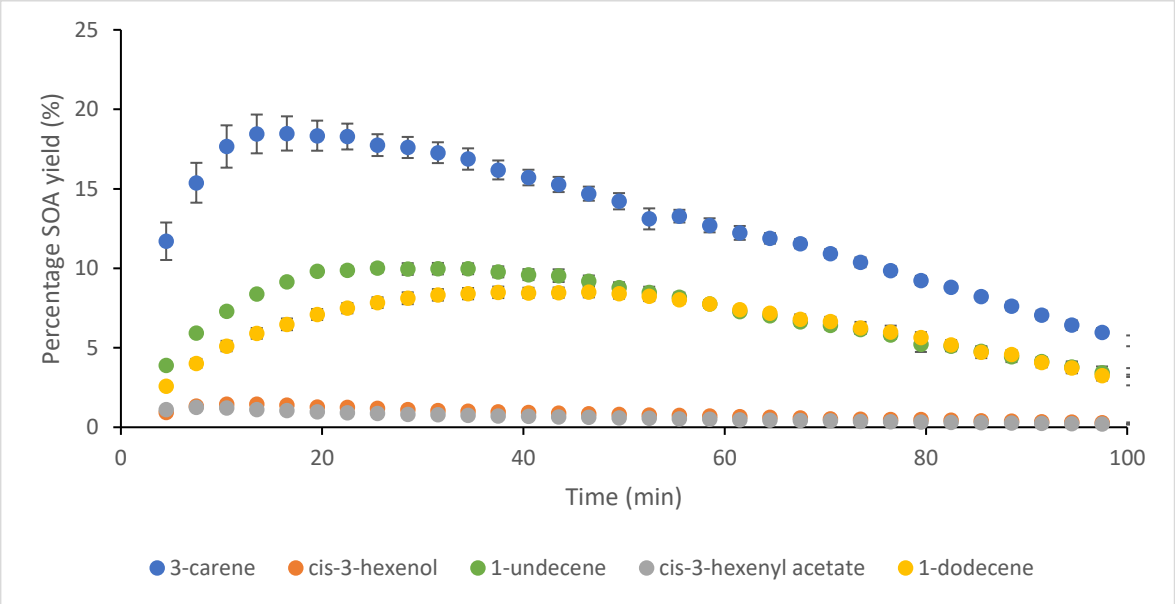

Figure AP22 – Mean SOA yield over time for the 5 study compounds under a 3x VOC excess. [VOC] = 3ppm, [O_3]= 1ppm. Error = ± standard error (SE).

AP9 - SOA yield with increased reactant concentration for Z-3-hexenol, 3-carene and Z-3-hexenyl acetate

Mean SOA particle yield over time

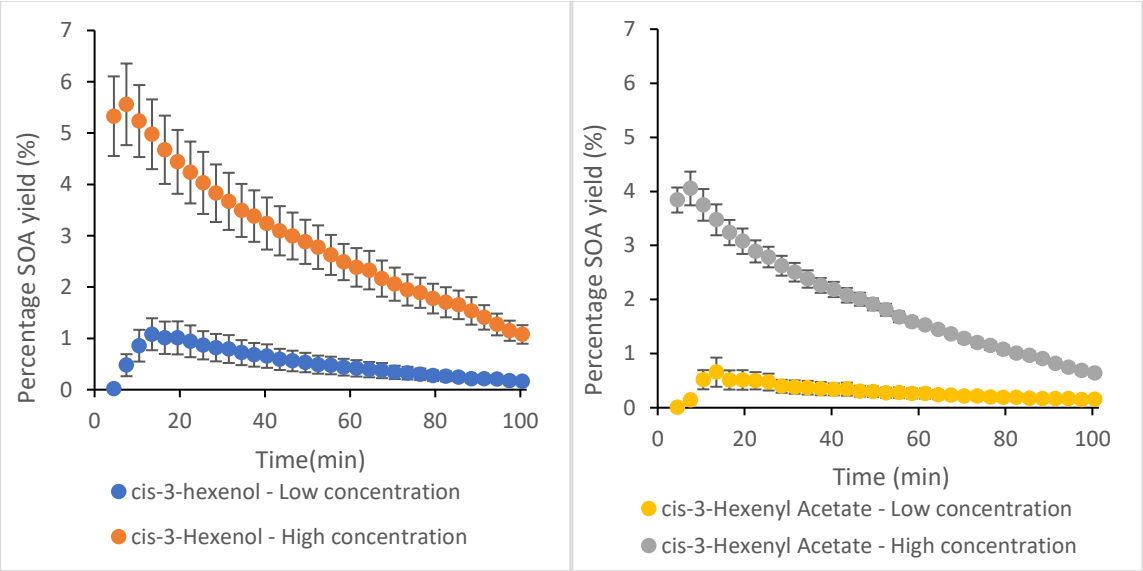

Figure AP23 – Mean SOA yield over time for Z-3-hexenol (Left) and Z-3-hexenyl acetate (right) under ozone excess conditions using both high and low concentration reactants. low concentration (0.25ppm VOC, 1ppm O_3) and high concentration (1ppm VOC, 4ppm O_3).

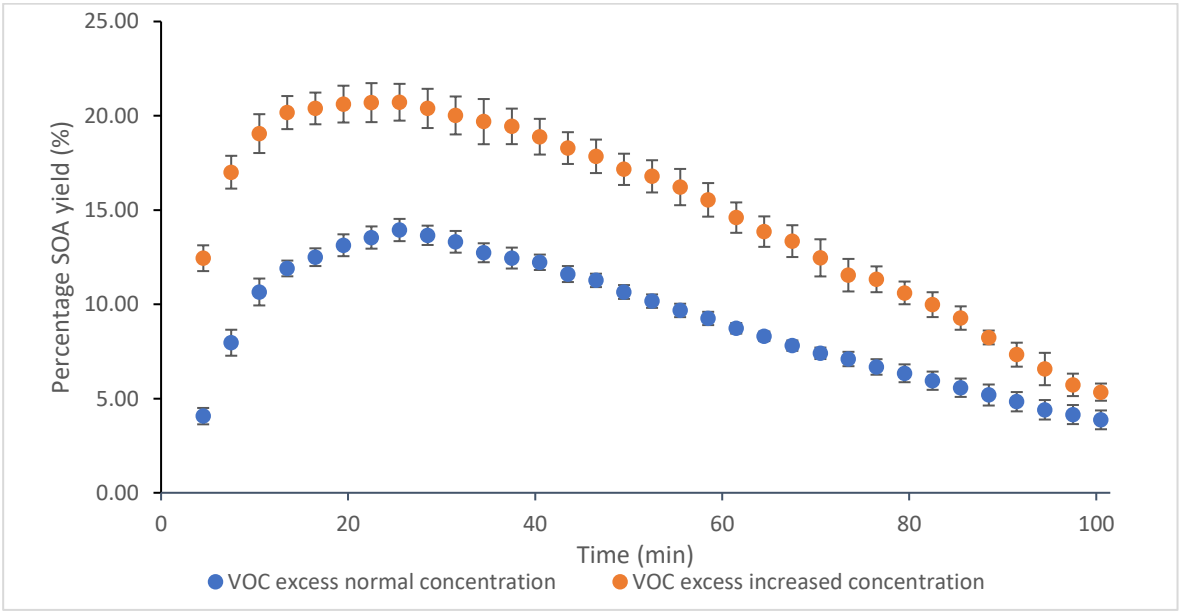

Figure AP24 – SOA yield over time for 3-carene under a VOC excess High (VOC=3ppm, O_3=1ppm) and low (VOC=1ppm, O_3=0.33ppm) concentration conditions. S = significant.

Table AP4 – summary of test results produced from the LMER of ozone excess particle yield over time data at both low concentration (0.25ppm VOC, 1ppm O_3) and high concentration (1ppm VOC, 4ppm O_3). Df=degrees of freedom, t= T statistic ,p=significance value

compound	Z-3-hexenol	Z-3-hexenyl acetate
LMER comparing increases in reactant concentration on observed yield	df=7.99, t=5.202, p=<0.001	df=10.99, t=10.436, p=<0.001

It can be seen from Figure AP24 that SOA yield seems to increase for both Z-3-hexenol and Z-3-hexenyl acetate under ozone excess conditions when increased concentrations of reactants are used. This difference was only borderline statistically significant for Z-3-hexenyl acetate.

Mean maximum SOA yield

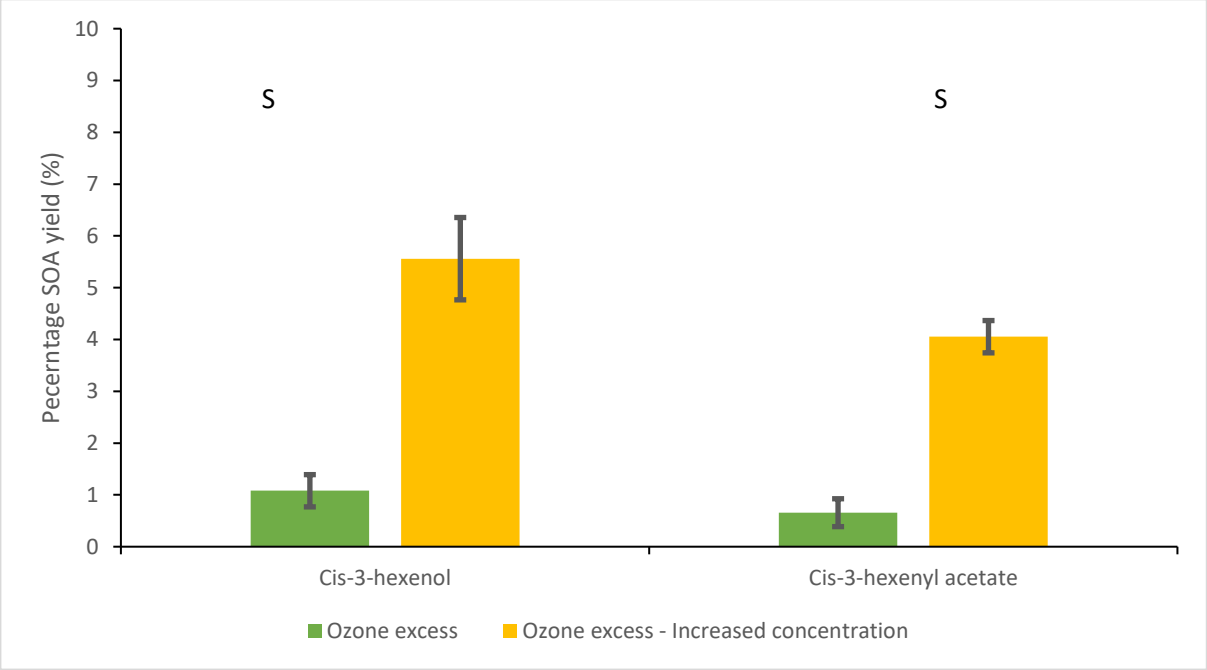

Figure AP25 – Maximum SOA yield for the Z-3-Hexnenol and Z-3-hexenyl acetate under ozone excess High (VOC=1ppm, O_3=4ppm) and low (VOC=0.25ppm, O_3=1ppm) concentration conditions. S = significant.

There was a statistically significant difference between treatments for Z-3-hexenol (W = 0, N = 10 p = 0.008) and for Z-3-hexenyl acetate (W = 0, N = 15 p = 0.002).

AP10 – Effect of altering reactant introduction order on SOA size over time

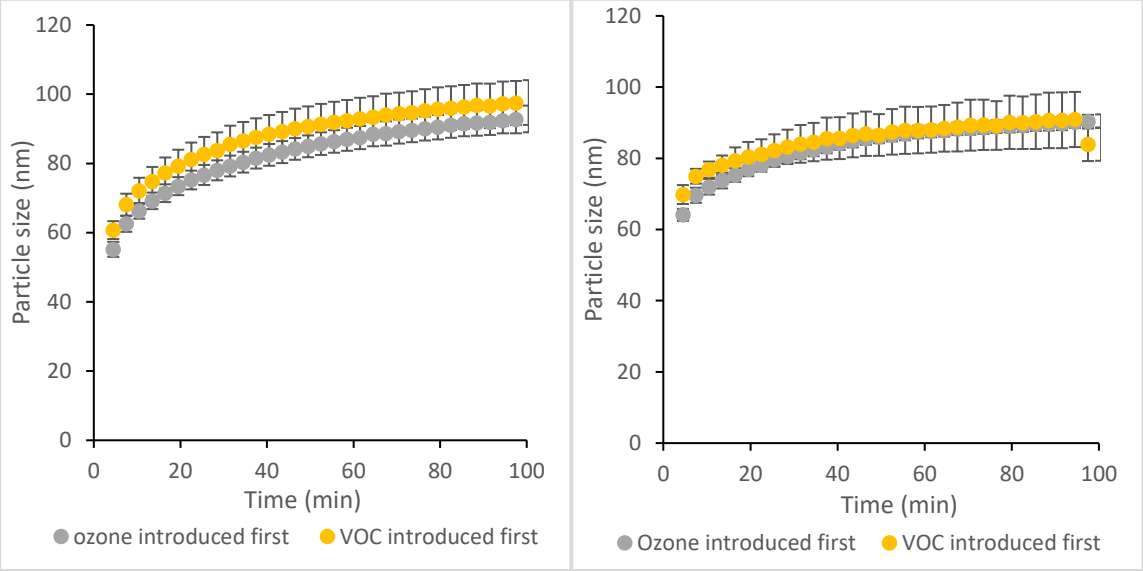

Figure AP26 – Comparison of SOA particle size over time for Z-3-hexenol (left) and Z-3-hexenyl acetate (right) under ozone excess conditions comparing VOC introduction into ozone vs ozone into VOC static chamber preparation methodologies. The latter points of the Z-3-hexenyl acetate are a result of the early termination of the experiment for one run.

Table AP5 – summary of test results produced from the LMER of ozone excess particle size over time data for both ozone first and VOC first experiments. Df=degrees of freedom, t= T statistic ,p=significance value.

compound	Z-3-hexenol	Z-3-hexenyl acetate
LMER comparing the effect of reactant introduction order on SOA particle size	df=9.0, t=0.80 p=0.444	df=6.991, t=-0.286, p=0.783

It can be seen from Figure AP26 that for both Z-3-hexenol and Z-3-hexenyl acetate, a partial overlap of the data set is seen. Table AP5 suggests no statistically significant differences between preparation methodologies for either compound.

AP11- effect of altering reactant introduction order on SOA particle size at maximum yield

Effect of altering the order of static chamber construction on SOA particle size

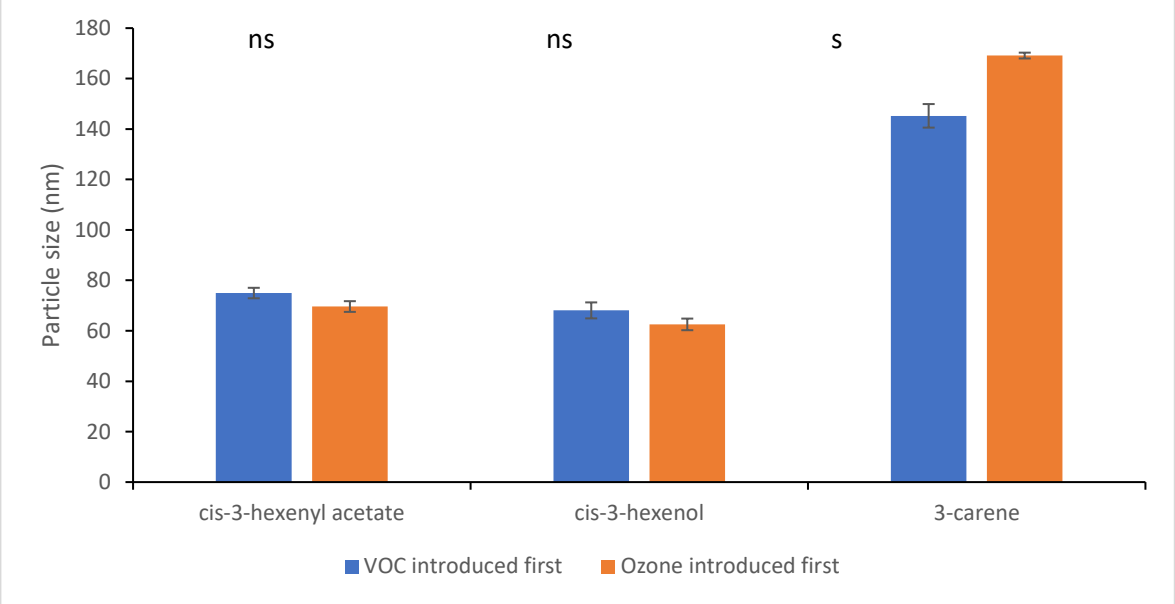

Figure AP27 – Comparison of SOA particle size at maximum yield for Z-3-hexenol (left) and Z-3-hexenyl acetate (right) under ozone excess conditions comparing VOC introduction into ozone vs ozone into VOC static chamber preparation methodologies.

Statistical comparison of particle size at maximum yield for VOC first and Ozone first preparation conditions shows no statistically significant difference for Z-3-hexenyl acetate (t=-1.872, df=6.976, p=0.104) or Z-3-hexenol (t=-1.417,df=8.648,p=0.191). For 3-carene experiments, a statistically difference in SOA particle size at maximum yield is seen (W=28,N=11,p=0.006).

AP12 – raw SOA particle size over time data

1-Undecene 4:1 ozone excess

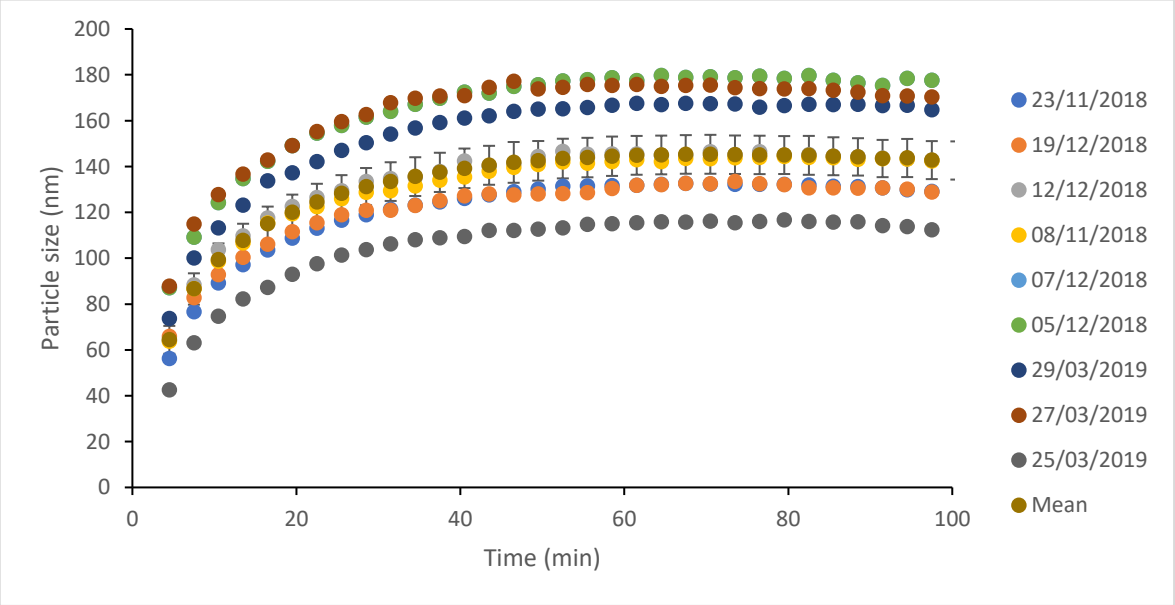

Figure AP28 – Raw SMPS measurements of 1-undecene SOA particle size produced under ozone excess conditions ([VOC]=0.25ppm, O_3 = 1ppm)

1-Undecene 1:3 VOC excess

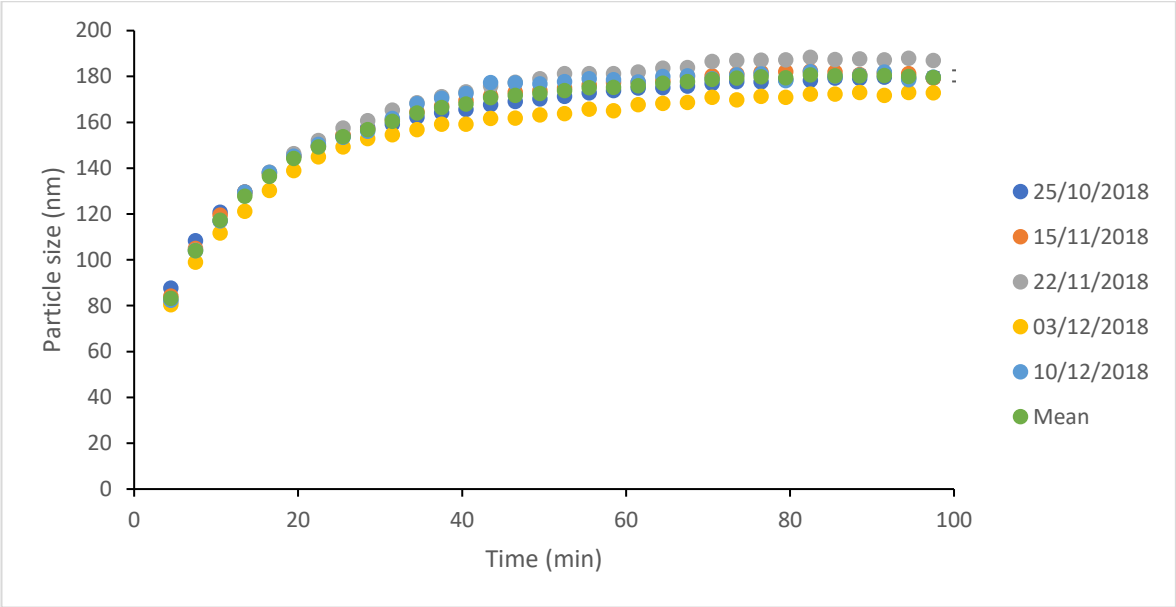

Figure AP29 – Raw SMPS measurements of 1-undecene SOA particle size produced under VOC excess conditions ([VOC]=3ppm, O_3 = 1ppm)

1-Dodecene 4:1 ozone excess

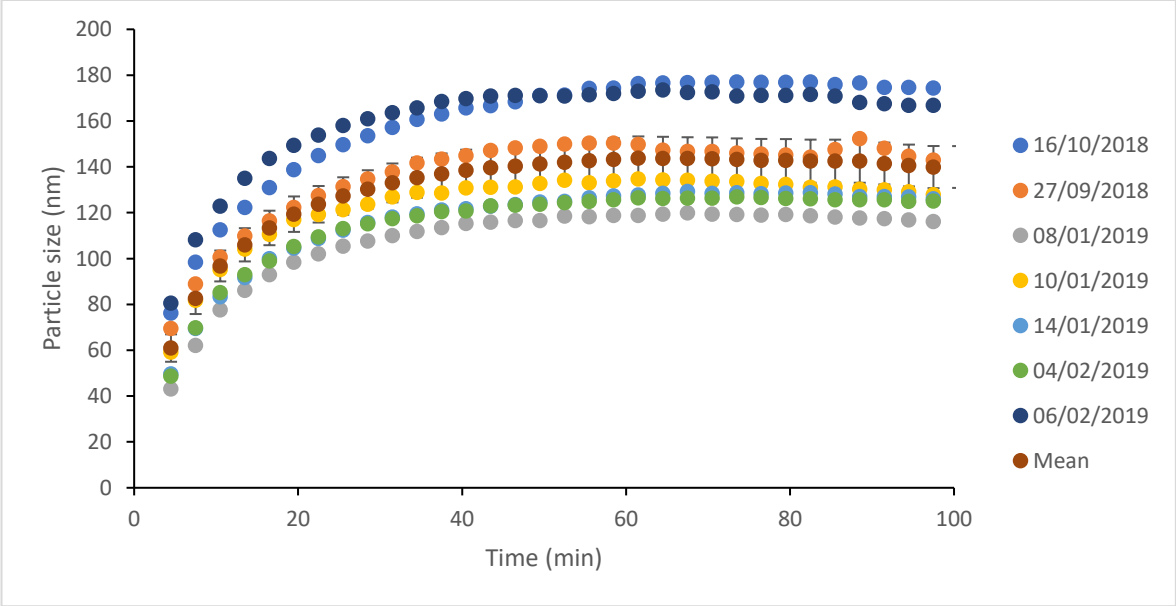

Figure AP30 – Raw SMPS measurements of 1-dodecene SOA particle size produced under ozone excess conditions ([VOC]=0.25ppm, O_3 = 1ppm)

1-Dodecene 1:3 VOC excess

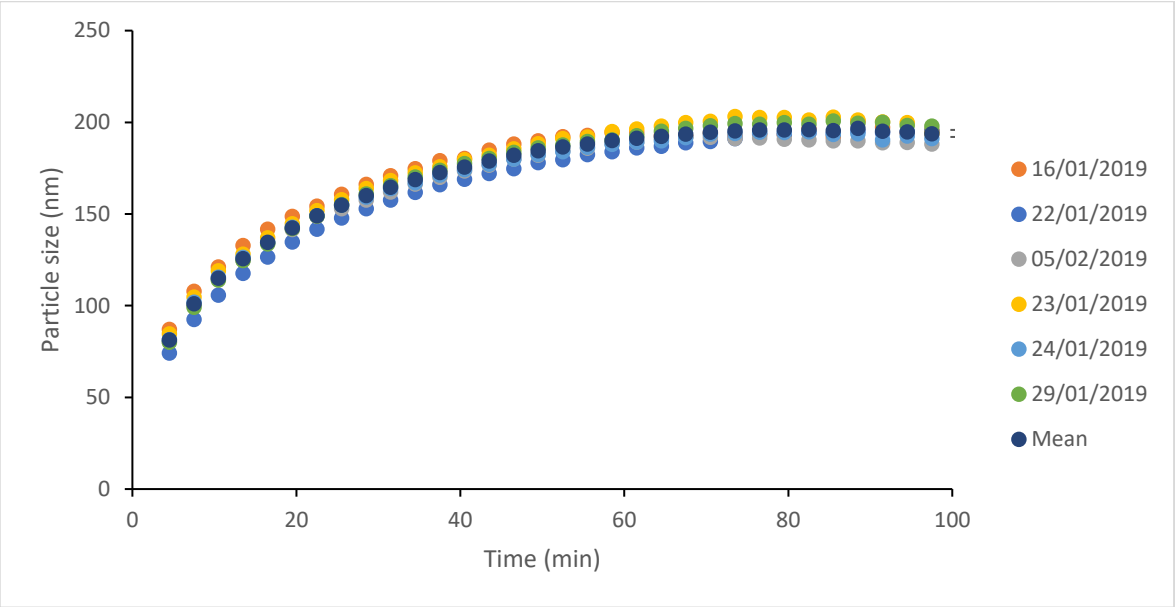

Figure AP31 – Raw SMPS measurements of 1-dodecene SOA particle size produced under VOC excess conditions ([VOC]=3ppm, O_3 = 1ppm)

3-Carene 4:1 ozone excess

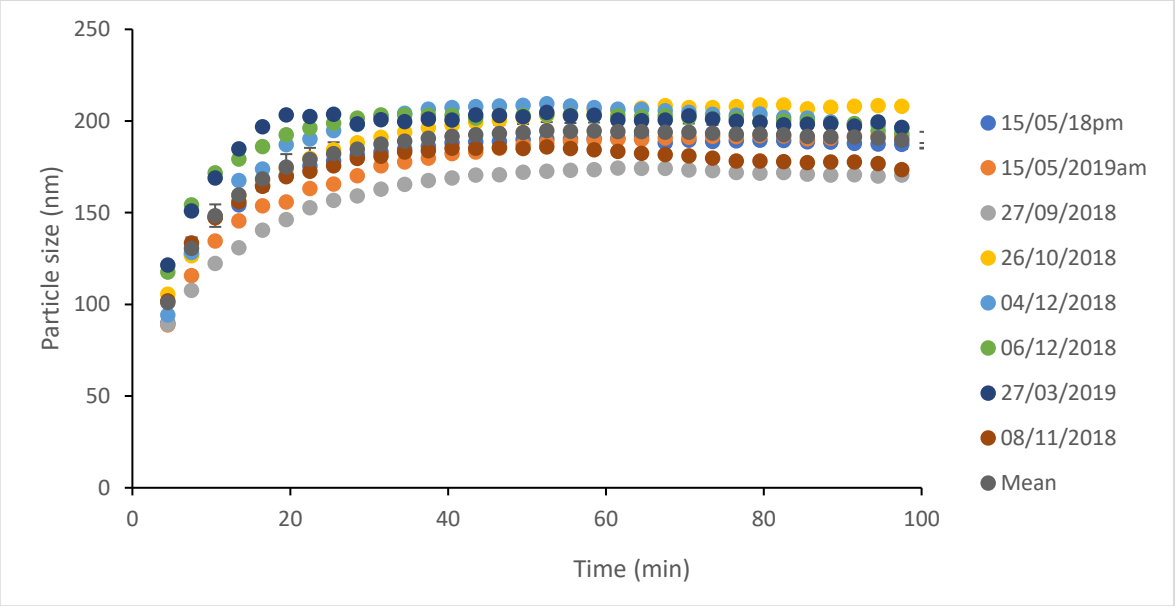

Figure AP32 – Raw SMPS measurements of 3-carene SOA particle size produced under ozone excess conditions ([VOC]=0.25ppm, O_3 = 1ppm)

3-Carene 1:3 VOC excess

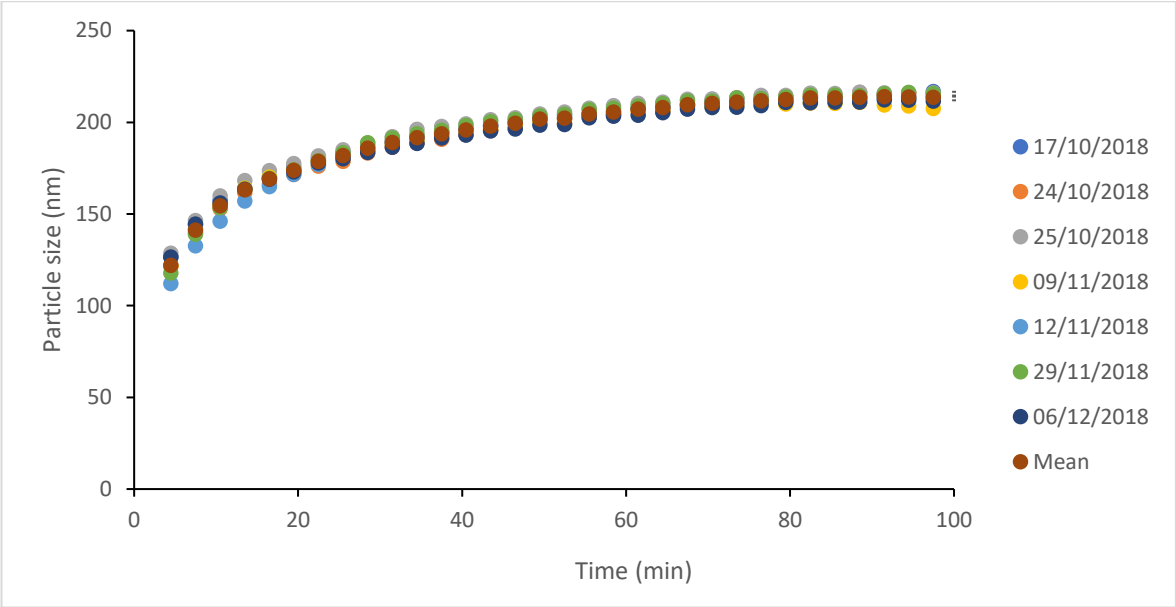

Figure AP33 – Raw SMPS measurements of 3-carene SOA particle size produced under VOC excess conditions ([VOC]=3ppm, O_3 = 1ppm)

Z-3-hexenol 4:1 ozone excess

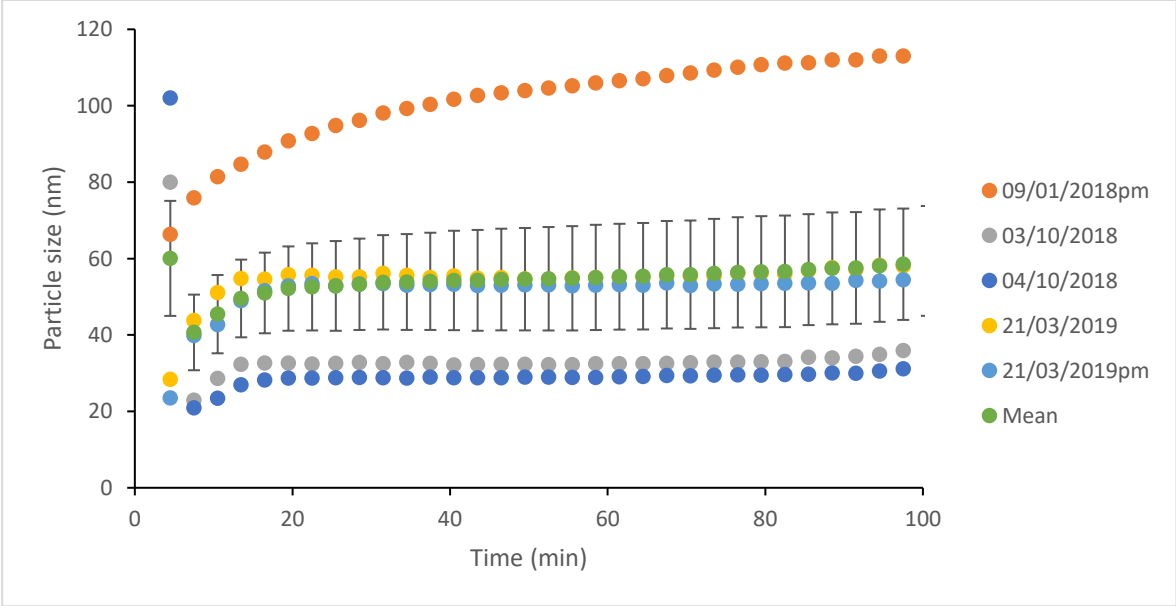

Figure AP34 – Raw SMPS measurements of Z-3-hexenol SOA particle size produced under ozone excess conditions ([VOC]=0.25ppm, O_3 = 1ppm)

Z-3-hexenol 1:3 VOC excess

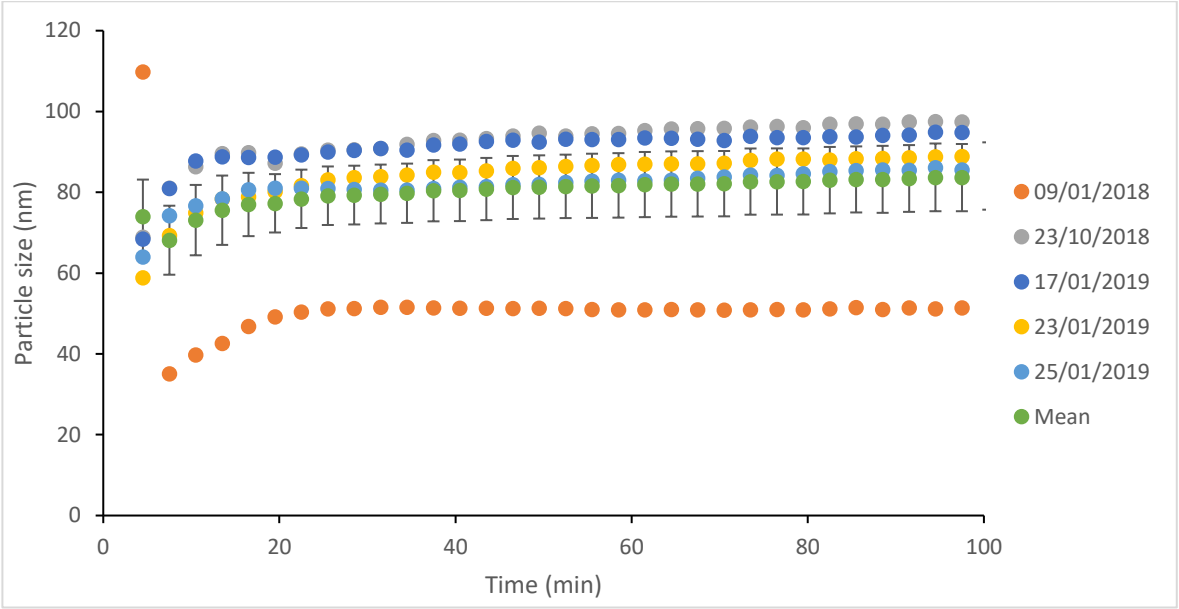

Figure AP35 – Raw SMPS measurements of Z-3-hexenol SOA particle size produced under VOC excess conditions ([VOC]=3ppm, O_3 = 1ppm)

Z-3-hexenyl acetate 4:1 ozone excess

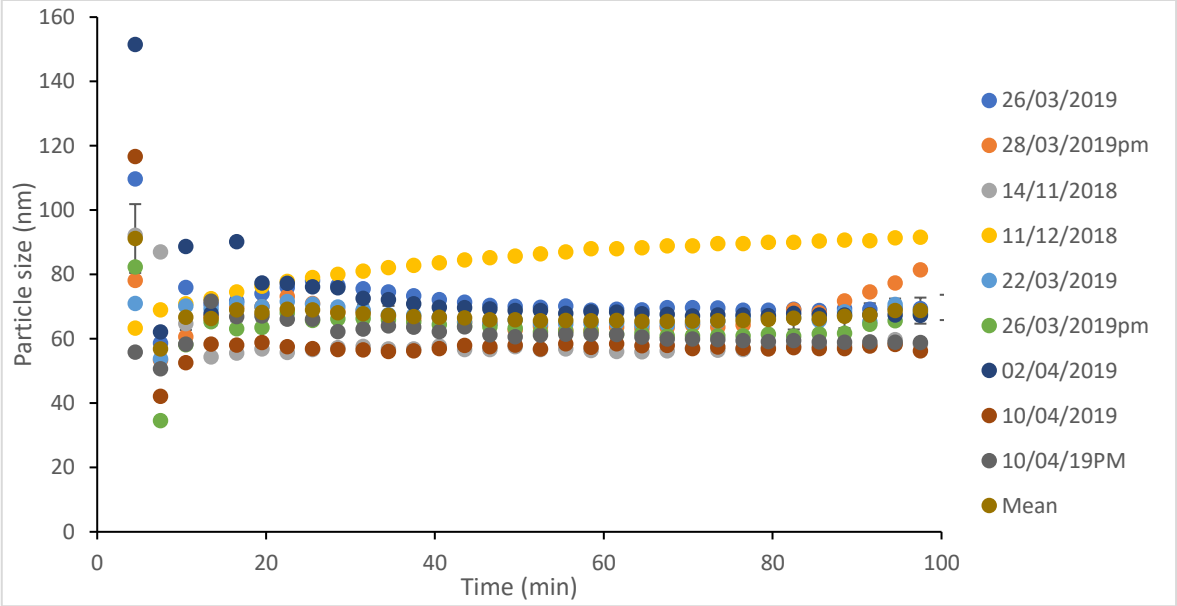

Figure AP36 – Raw SMPS measurements of Z-3-hexenyl acetate SOA particle size produced under ozone excess conditions ([VOC]=0.25ppm, O_3 = 1ppm)

Z-3-hexenyl acetate 1:3 VOC excess

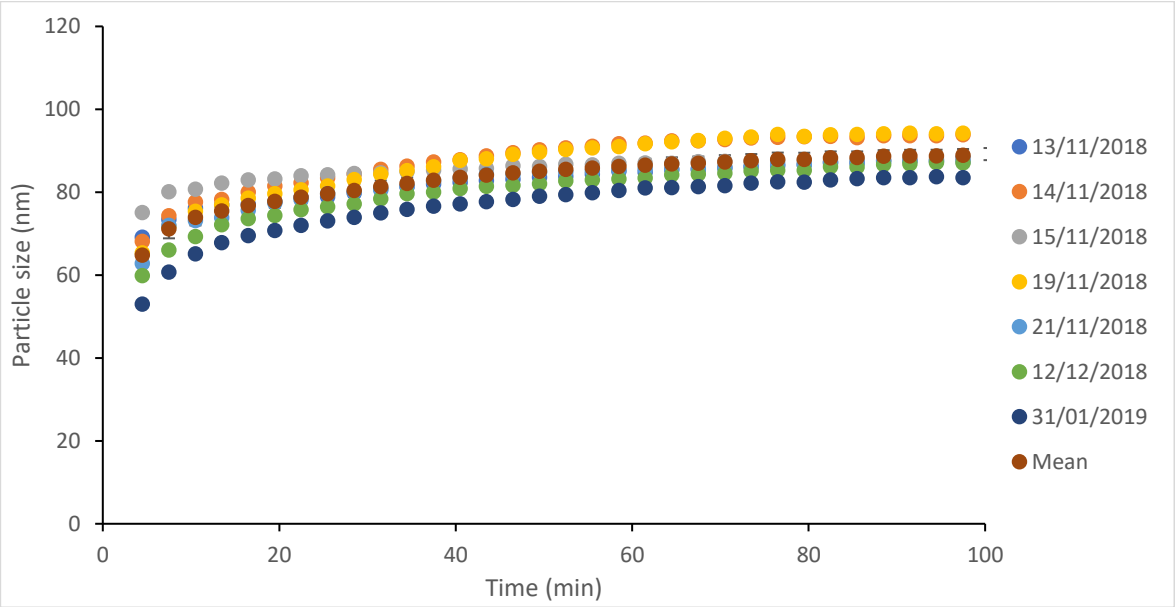

Figure AP37 – Raw SMPS measurements of Z-3-hexenyl acetate SOA particle size produced under VOC excess conditions ([VOC]=3ppm, O_3 = 1ppm)

AP13 – mean SOA size over time traces

Ozone excess

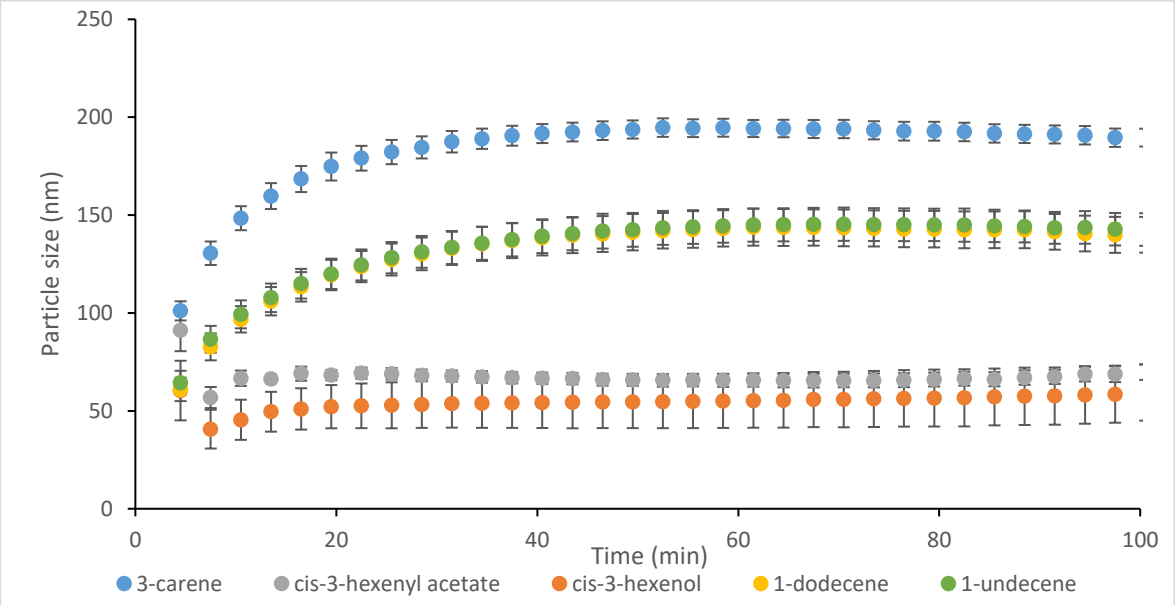

Figure AP38 – Mean SOA size over time for the 5 study compounds (0.25ppm) under excess ozone (1ppm) conditions

VOC excess

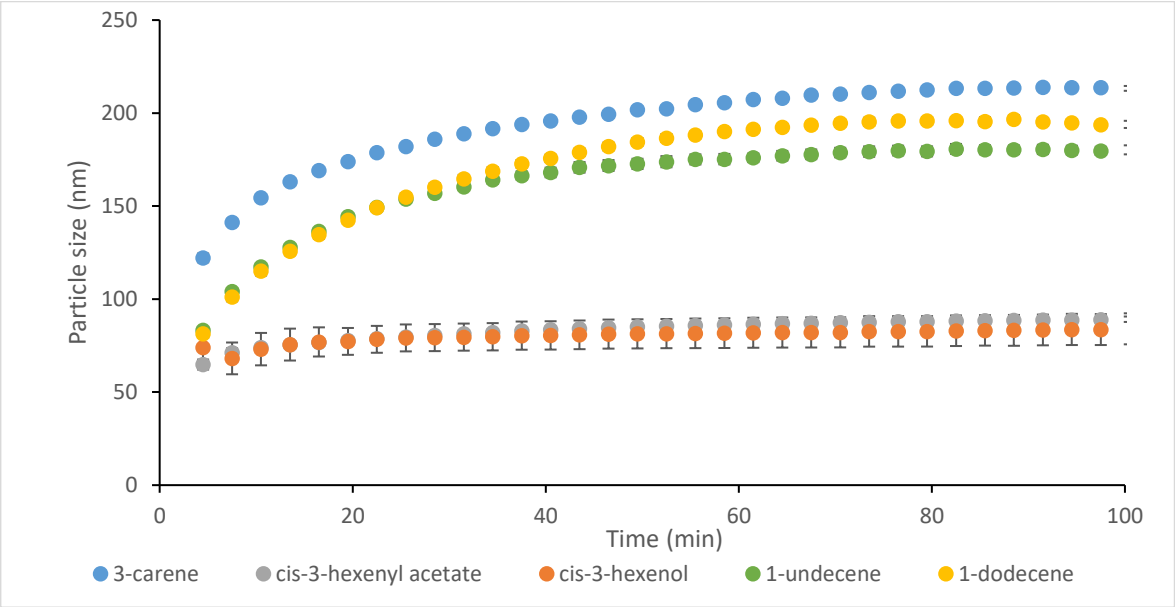

Figure AP39 – Mean SOA size over time for the 5 study compounds under excess VOC conditions. Ozone (1ppm) VOC (3ppm)

From both Figures (AP38/AP39) it can be seen that particle size increased with time until a maximum was reached at which point the particles no longer increased in size and size stayed broadly constant. The size peak was reached more quickly under ozone excess conditions than under VOC excess conditions.

AP14 – Mean SOA particle size over time for Z-3-hexenol and Z-3-hexenyl acetate at both base and increased reactant concentration

Mean SOA particle size over time

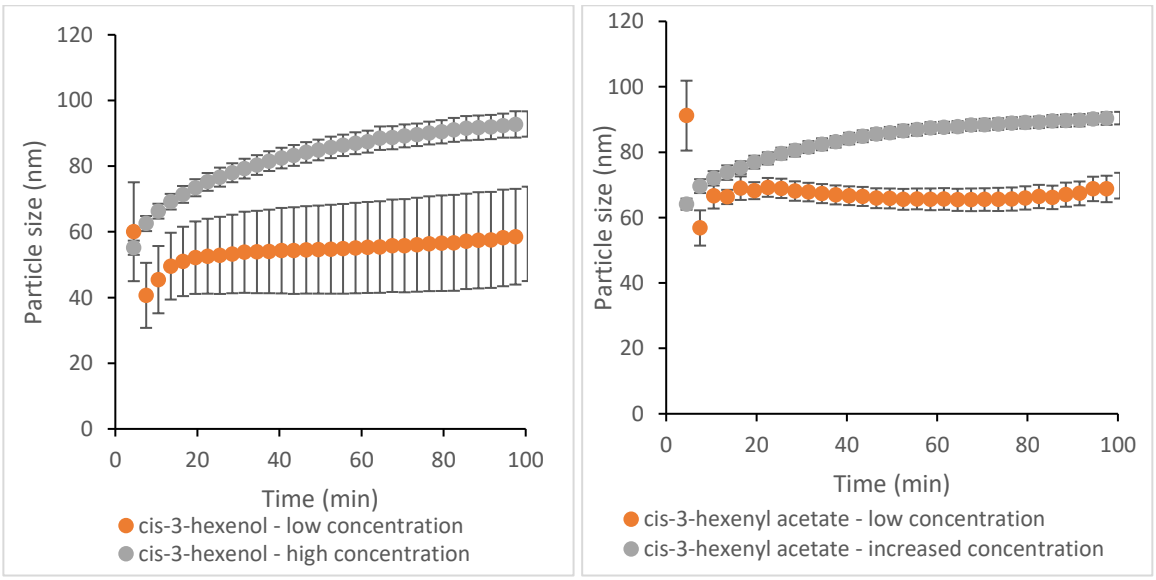

Figure AP40 – Mean SOA particle size over time for Z-3-hexenol (Left) and Z-3-hexenyl acetate (right) under ozone excess conditions using both high and low concentration reactants. The initial scan for low concentration highlights the error in SOA concentration measurement at low reactant concentrations and thus was retained for completeness.

Table AP6 – summary of test results produced from the LMER of ozone excess particle size over time data for both low concentration and high concentration experiments. Df=degrees of freedom, t= T statistic ,p=significance value.

compound	Z-3-hexenol	Z-3-hexenyl acetate
LMER comparing increased reactant concentration on SOA yield	df=8.00, t=2.188 p=0.06	df=12.00, t=4.235, p=0.001

Mean SOA particle size at maximum yield

Figure AP41 shows an increase in SOA particle size as a result of increases in reactant concentration for both Z-3-hexenol and Z-3-hexenyl acetate.

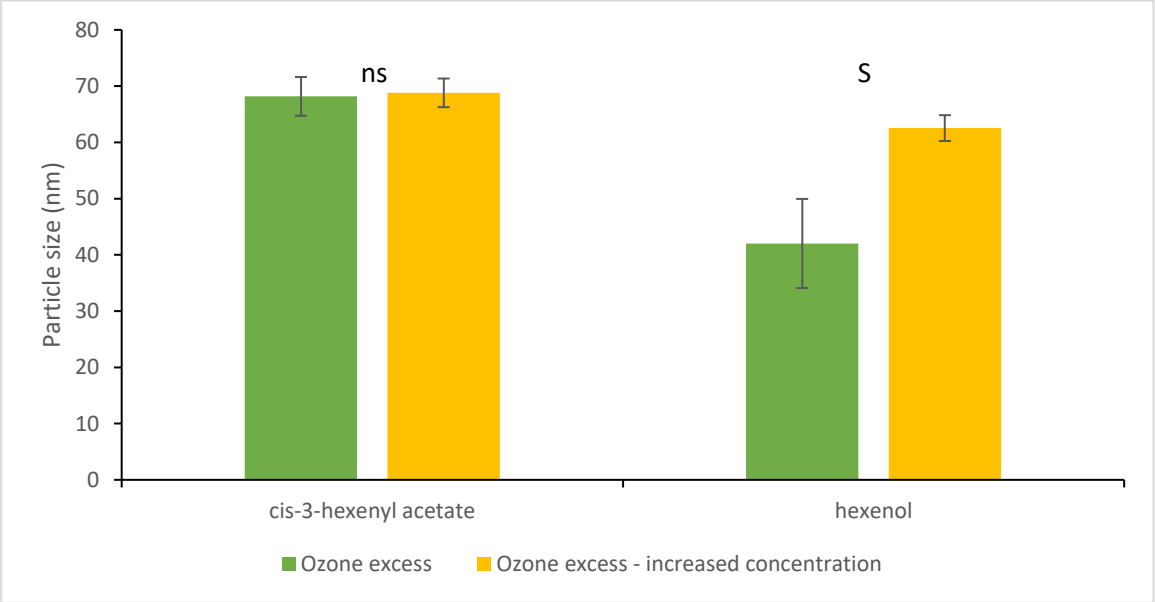

Figure AP41 – Peak SOA size for the Z-3-Hexnenol and Z-3-hexenyl acetate under ozone excess High (VOC=1ppm, O_3=4ppm) and low (VOC=0.25ppm, O_3=1ppm) concentration and VOC excess (VOC=3ppm, O_3=1ppm) conditions. S=Significant, ns = not significant.

There was also no statistically significant difference between reaction conditions for Z-3-hexenyl acetate (H = 1.098, df=2, p = 0.578). There was a statistical significant difference between reactant conditions for Z-3-hexenol (H = 10.68, df=2, p = 0.005), with pairwise differences between the ozone excess and increased concentration ozone excess conditions (W = 25, N = 9 p = 0.016), the ozone excess and VOC excess conditions ((W = 16, N = 8, p = 0.029), and the increased concentration ozone excess and VOC excess conditions (W = 20,N = 9, p = 0.016).

AP15 – Comparison of SOA parameters at 400m and maximum yield

SOA particle yield

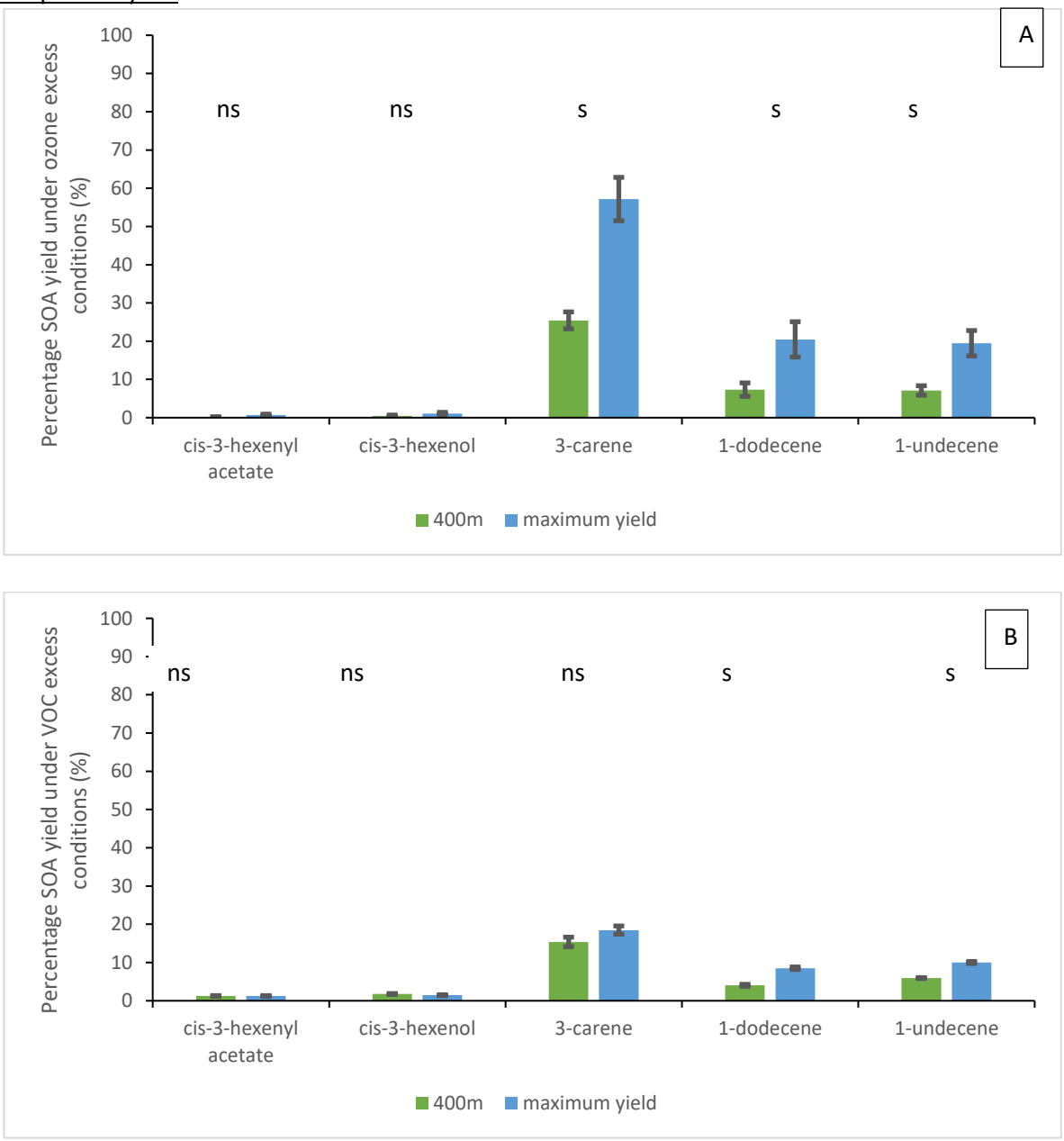

Figure AP42 – Maximum SOA yield and SOA yield at 400m for the five study VOCs under both ozone excess (A, 1ppm O_3,0.25ppm VOC) and VOC excess (B, 1ppm O_3,3ppm VOC). S=statistically significant, ns= not statistically significant at the 95% confidence interval. For ozone excess conditions (A), there are statistically significant differences for 3-carene (W = 0, N = 15, p = <0.001), 1-dodecene (W = 6, N = 14, p = 0.017) and 1-undecene (W = 2, N = 16, p<0.001). For VOC excess conditions (B), A statistically significant difference in SOA yield between treatments is seen for 1-dodecene (W=0,n=15,p=0.003) and 1-undecene (W=0,n=10,p=0.007). All data are mean ± SE.

Under both VOC excess and ozone excess conditions, yield at maximum yield is generally larger than at 400m with this difference being less pronounced for VOC excess conditions. The lower significance

seen for VOC excess conditions is hypothesised to be as a result of the small differences in the rate of reaction experienced between 400m and the maximum yield time points. Lower levels of significance are seen for faster reacting compounds as the time to maximum yield is far closer to the time equivalent of 400m at 1m/s wind speed.

SOA particle size

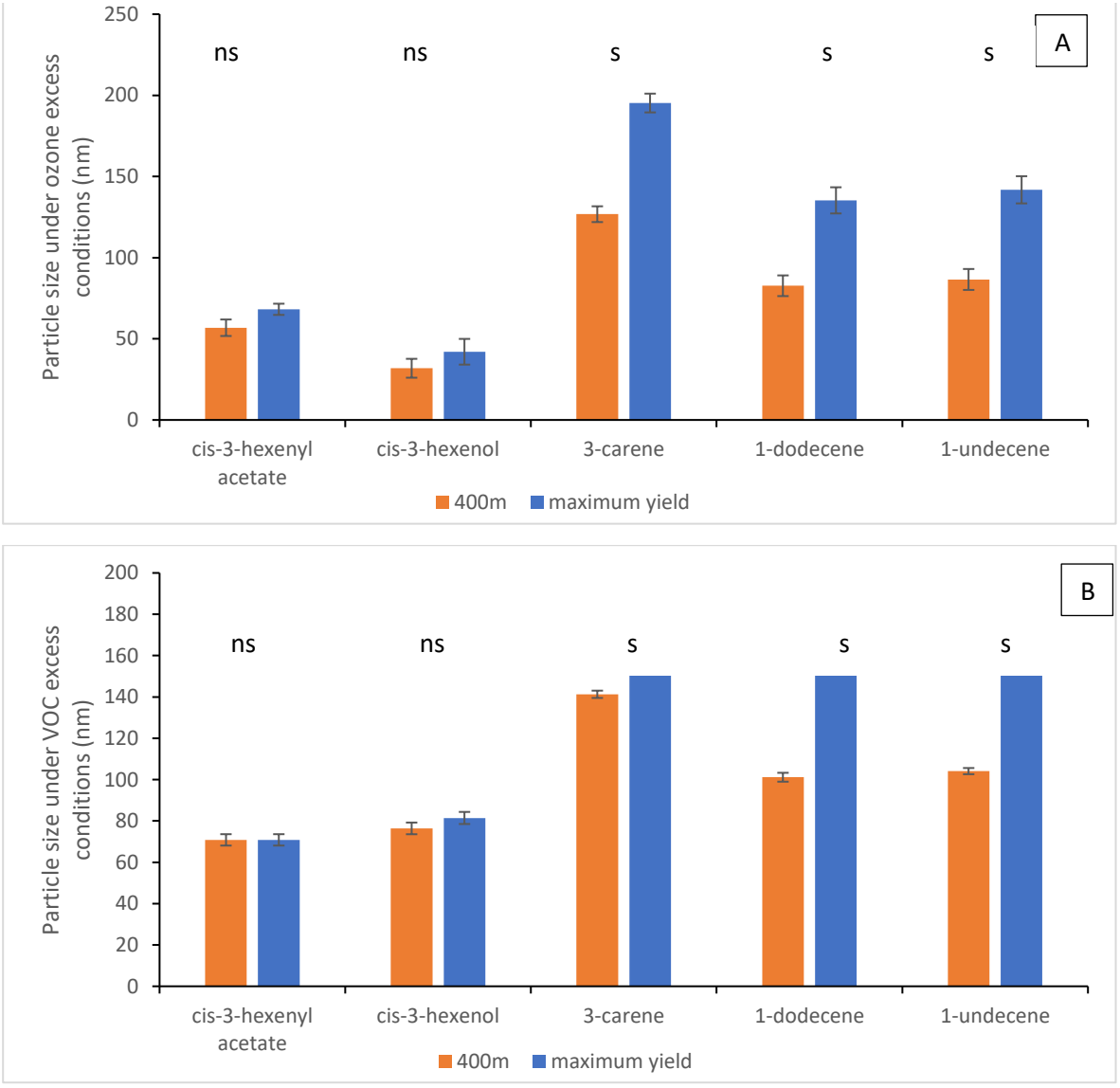

Figure AP43 – SOA particle size at maximum yield and at 400m (B) for the five study VOCs under both ozone excess (A, 1ppm O_3,0.25ppm VOC) and VOC excess (B, 1ppm O_3,3ppm VOC). S=statistically significant, ns= not statistically significant at the 95% confidence interval. For SOA particle size under ozone excess conditions (A), there was a statistically significant difference between distances for 3-carene (W=0,n=16,p<0.001), 1-undcene (W=2,n=18,p<0.001) and 1-dodecene (W=0,n=14,p<0.001). For SOA particle size under VOC excess conditions (B), A statistically significant difference in SOA particle size between distances is seen for 3-carene (W=0,n=14,p<0.001), 1-undcene (W=0,n=12,p=0.002) and 1-dodecene (W=0,n=10,p=0.007). All data are mean ± SE.

Under both ozone excess and VOC excess conditions, a statistically significant difference in mean particle diameter was seen for 3-carene, 1-dodecene and 1-undecene with mean particle diameter being observed to be smaller at 400m. Lower levels of significance are seen for faster reacting compounds as the time to maximum yield is far closer to the time equivalent of 400m at 1m/s wind speed.

AP16 – Raw treatment-EAG responses of *A. mellifera antennae* to stimuli during treatments

Air – With bubbler

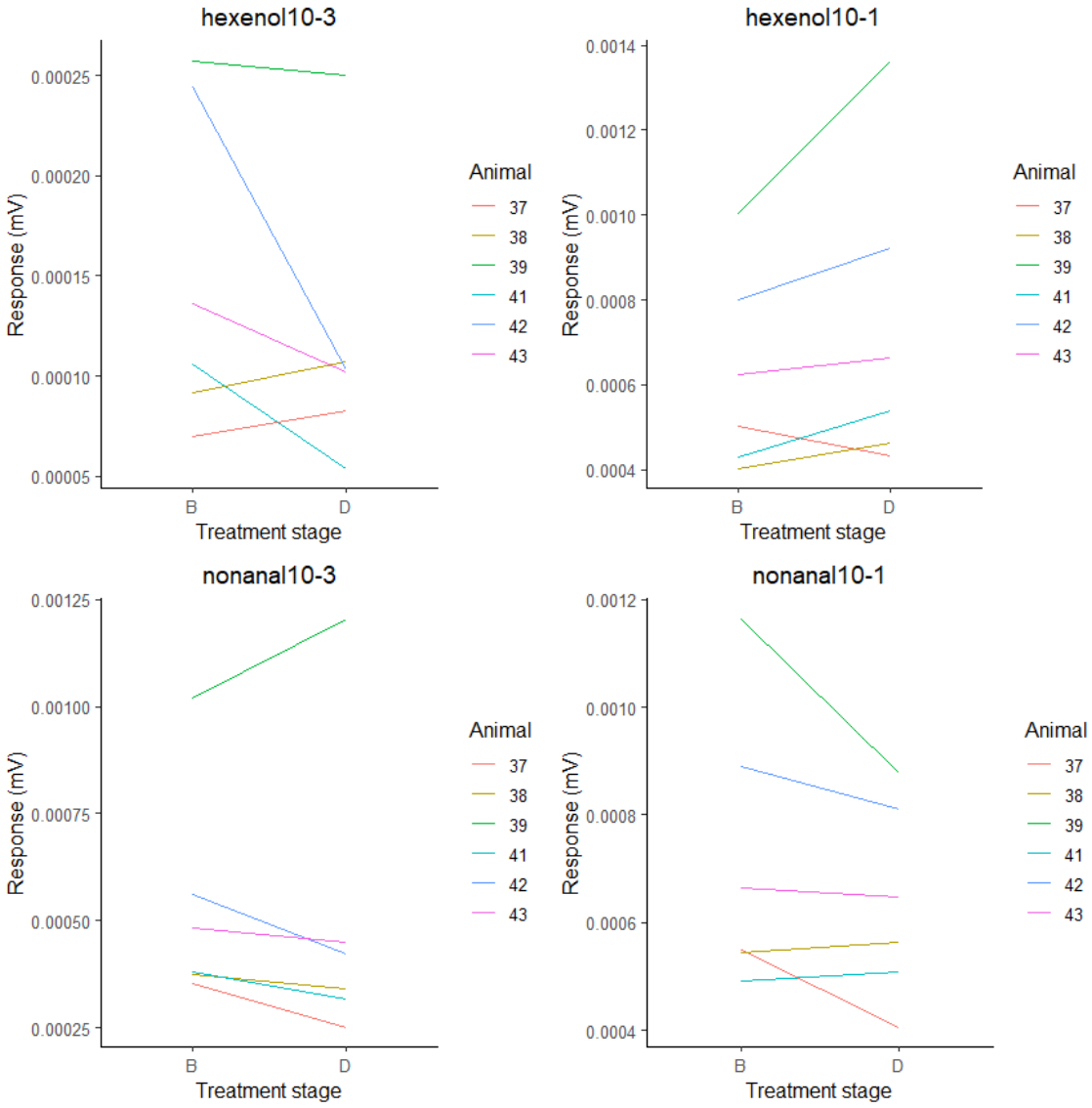

Figure AP44 – Raw EAG responses for each of the four stimuli before (B) and during (D) treatment with a water bubbler

Air – Without bubbler

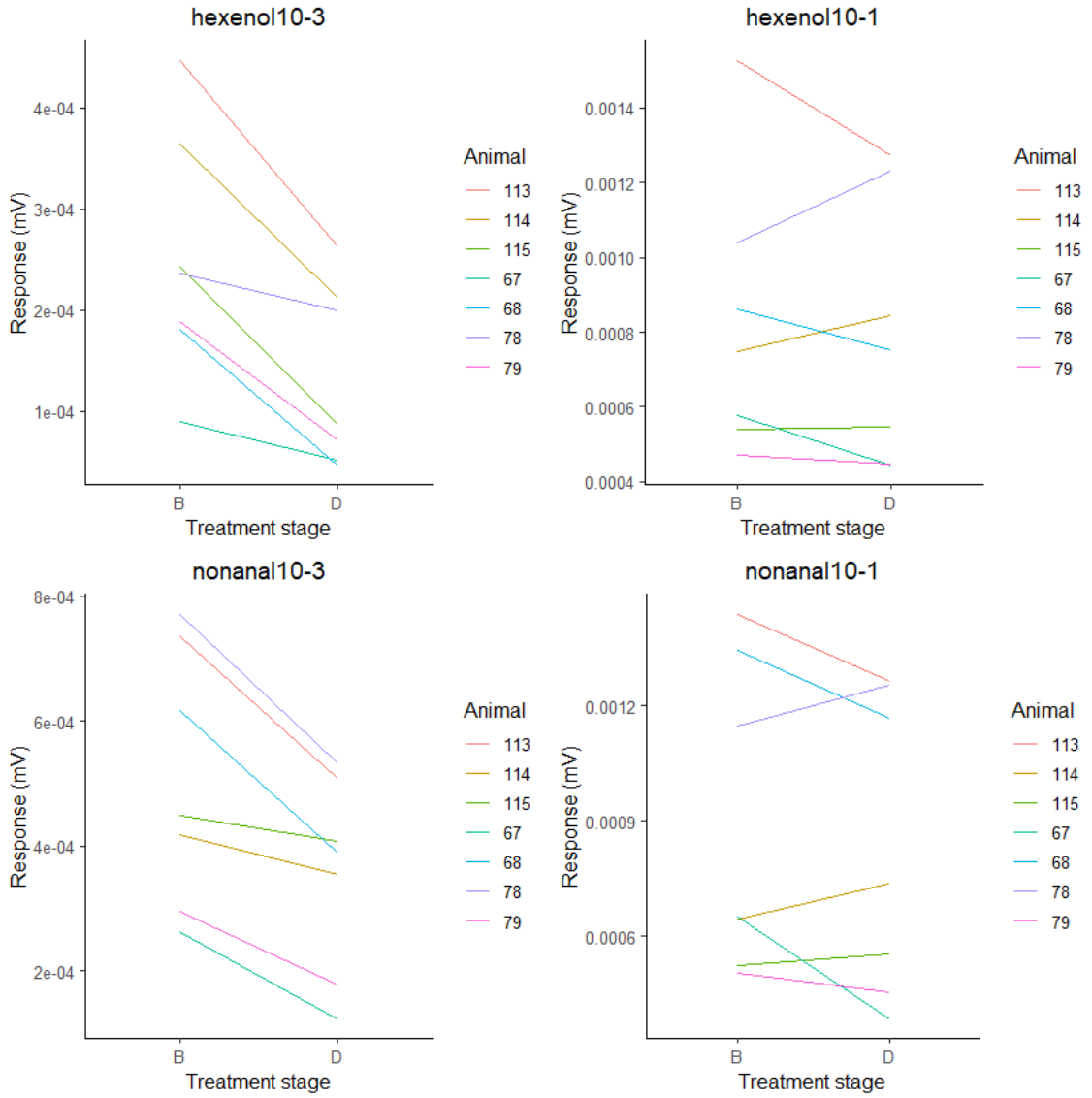

Figure AP45 – Raw EAG responses for each of the four stimuli before (B) and during (D) treatment with the water bubbler removed during the treatment phase.

Air

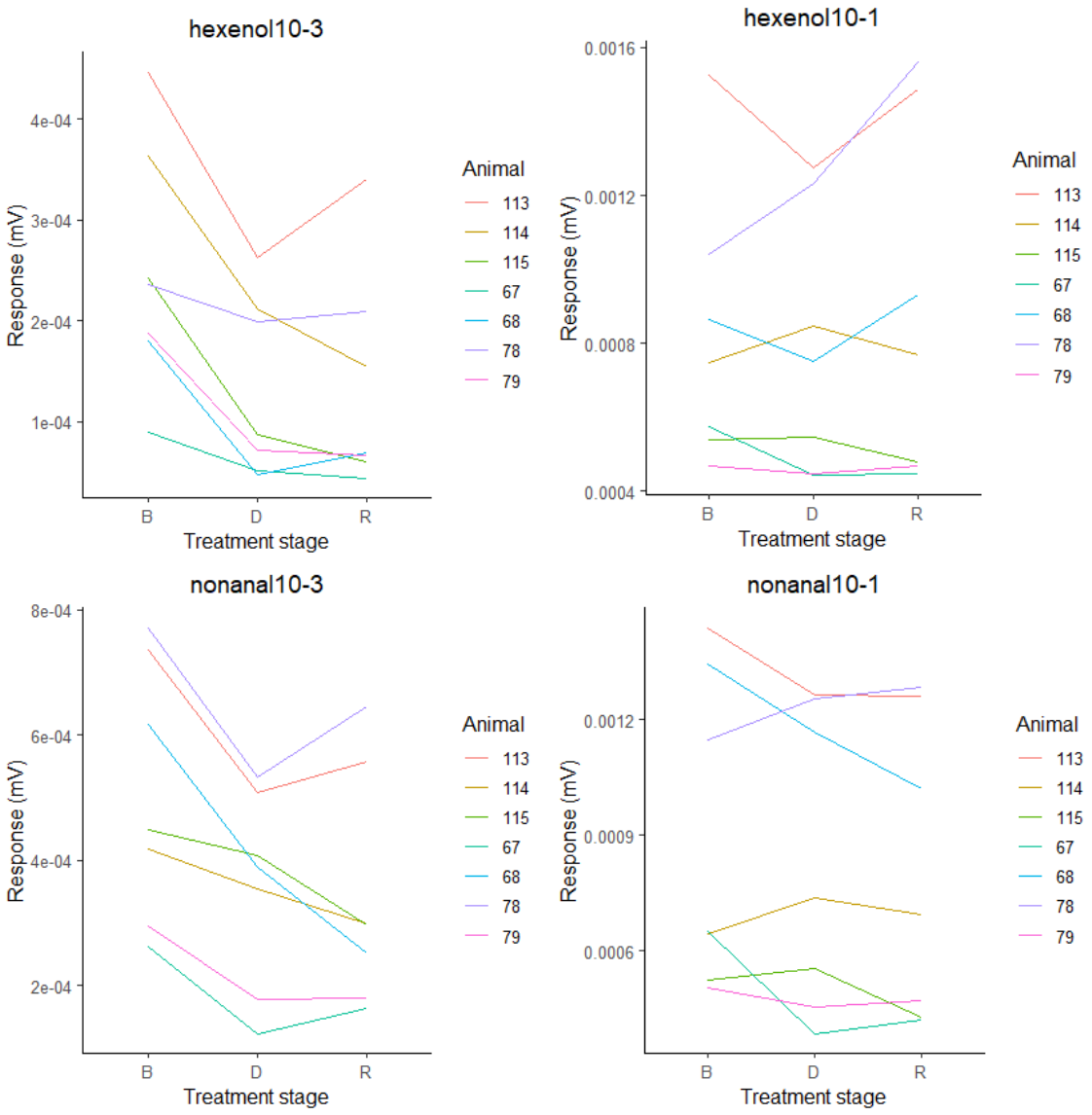

Figure AP46 – Raw EAG responses for each of the four stimuli before (B), during (D) and after recovery (R) from treatment with air and the water bubbler removed during the treatment phase.

VOC low

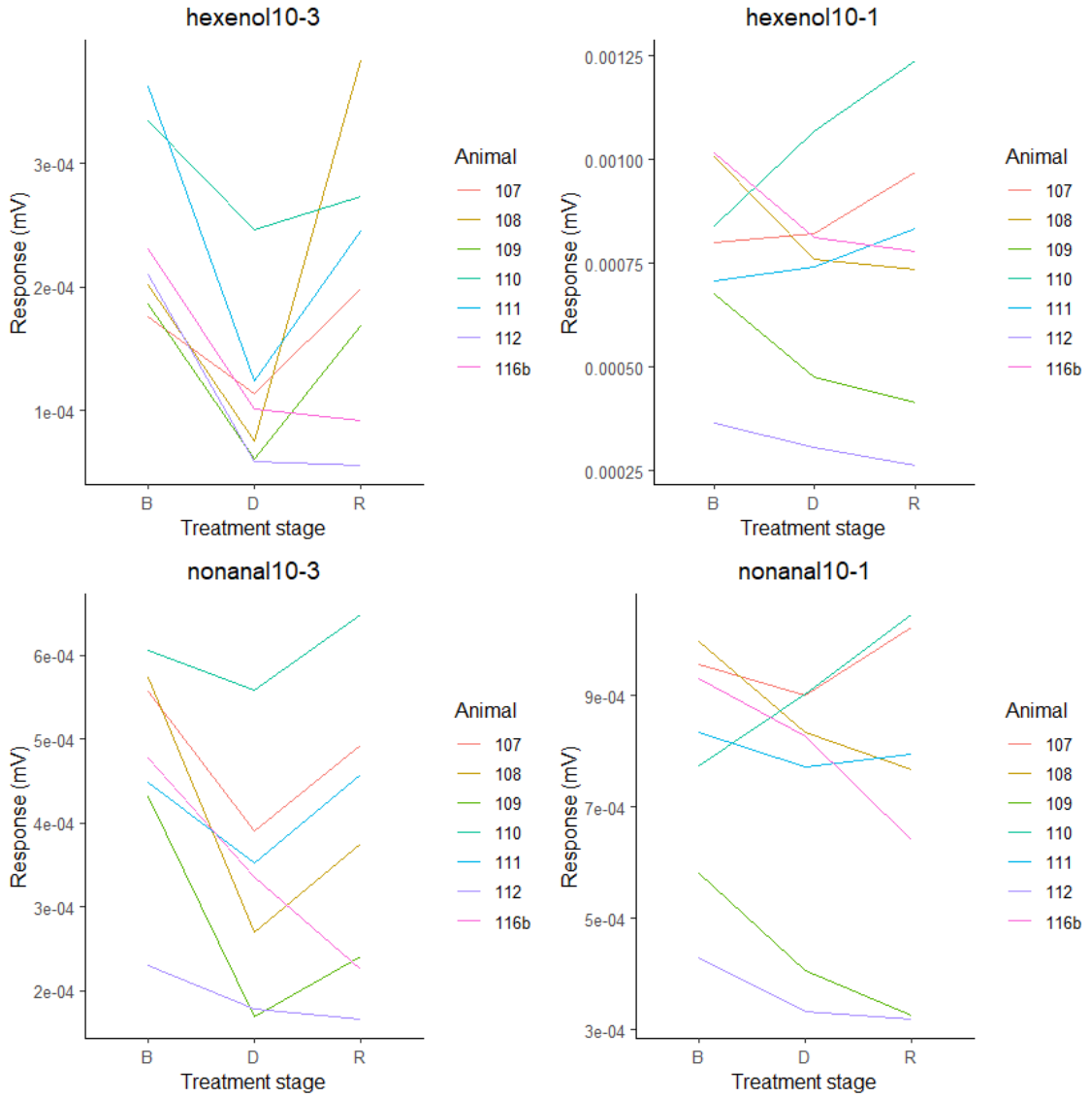

Figure AP47 – Raw EAG responses for each of the four stimuli before (B), during (D) and after recovery (R) from treatment with low concentration VOC (3-carene,1ppm) and the water bubbler removed during the treatment phase.

VOC high

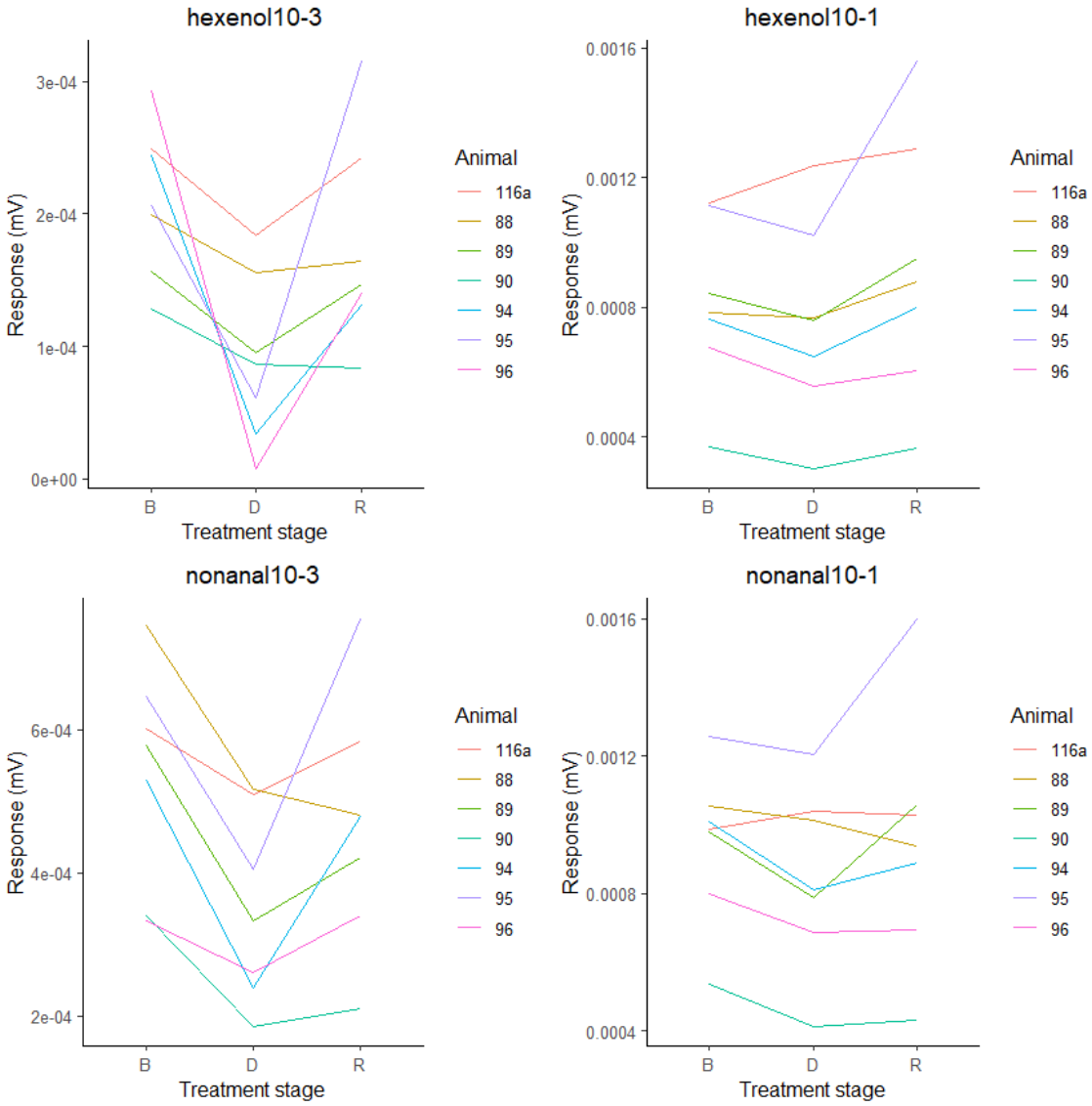

Figure AP48 – Raw EAG responses for each of the four stimuli before (B), during (D) and after recovery (R) from treatment with high concentration VOC (3-carene, 4ppm) and the water bubbler removed during the treatment phase.

Ozone low

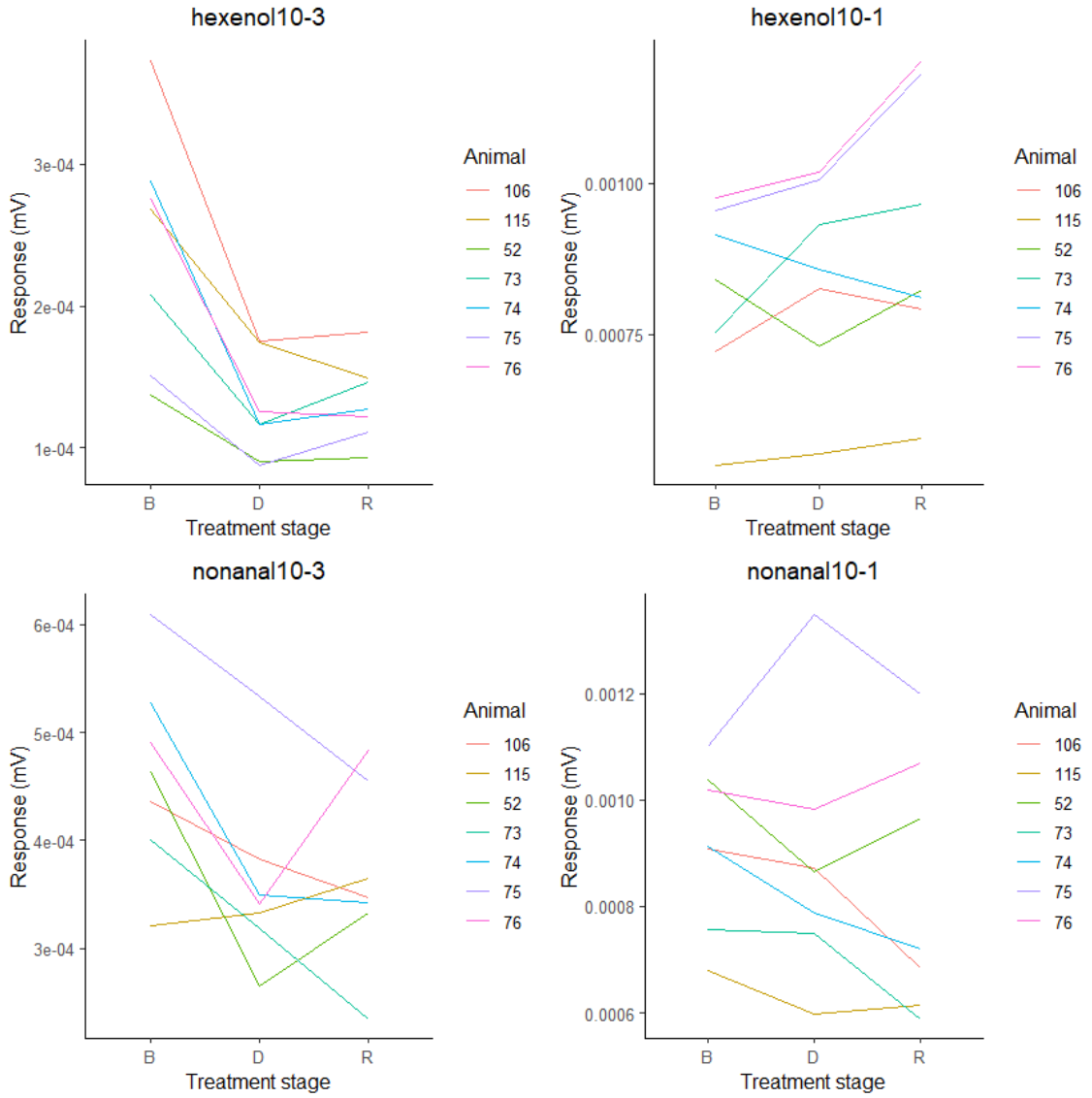

Figure AP49 – Raw EAG responses for each of the four stimuli before (B), during (D) and after recovery (R) from treatment with low concentration ozone (1ppm) and the water bubbler removed during the treatment phase.

Ozone high

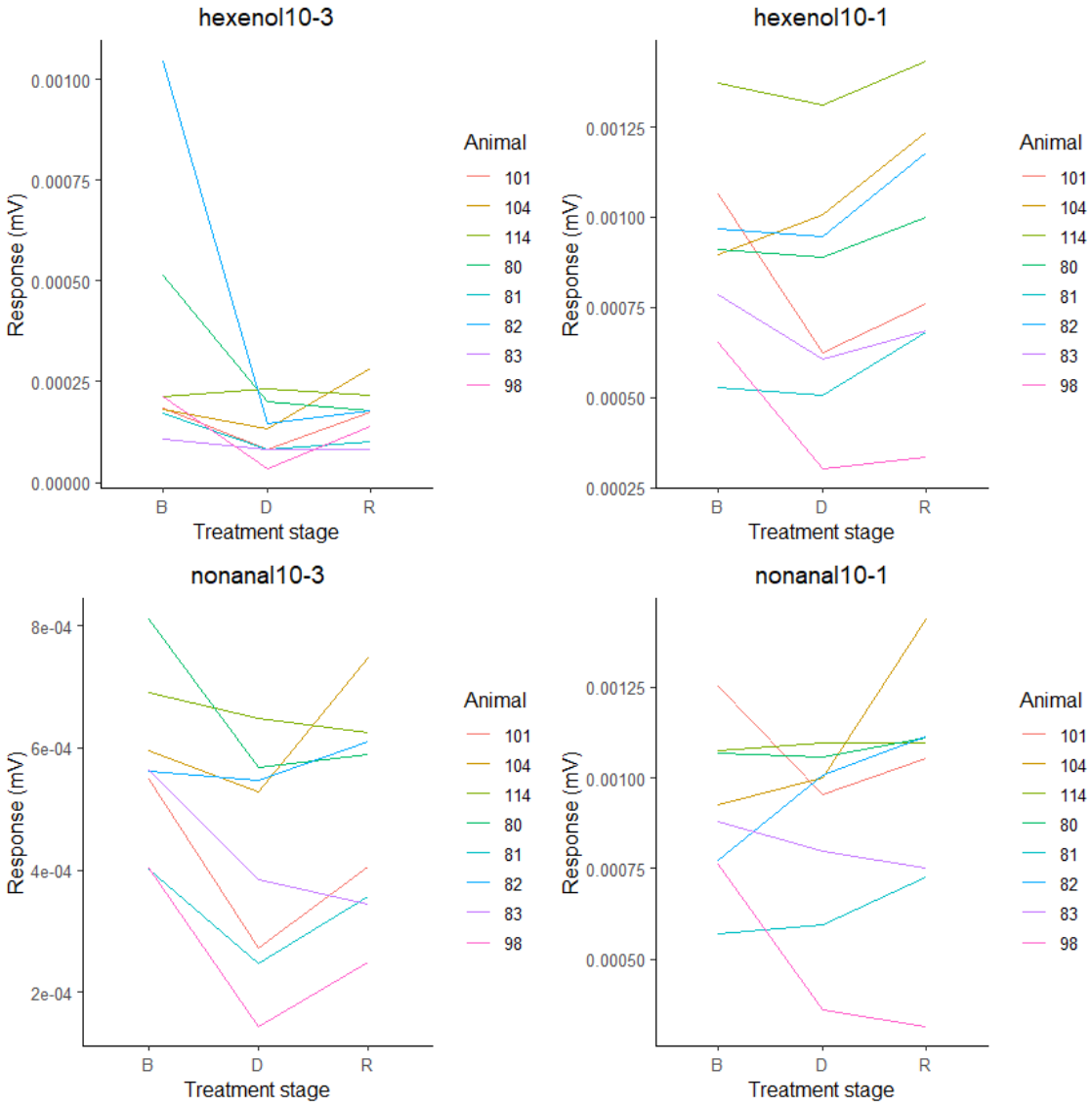

Figure AP50 – Raw EAG responses for each of the four stimuli before (B), during (D) and after recovery (R) from treatment with high concentration ozone (4ppm) and the water bubbler removed during the treatment phase.

SOA low

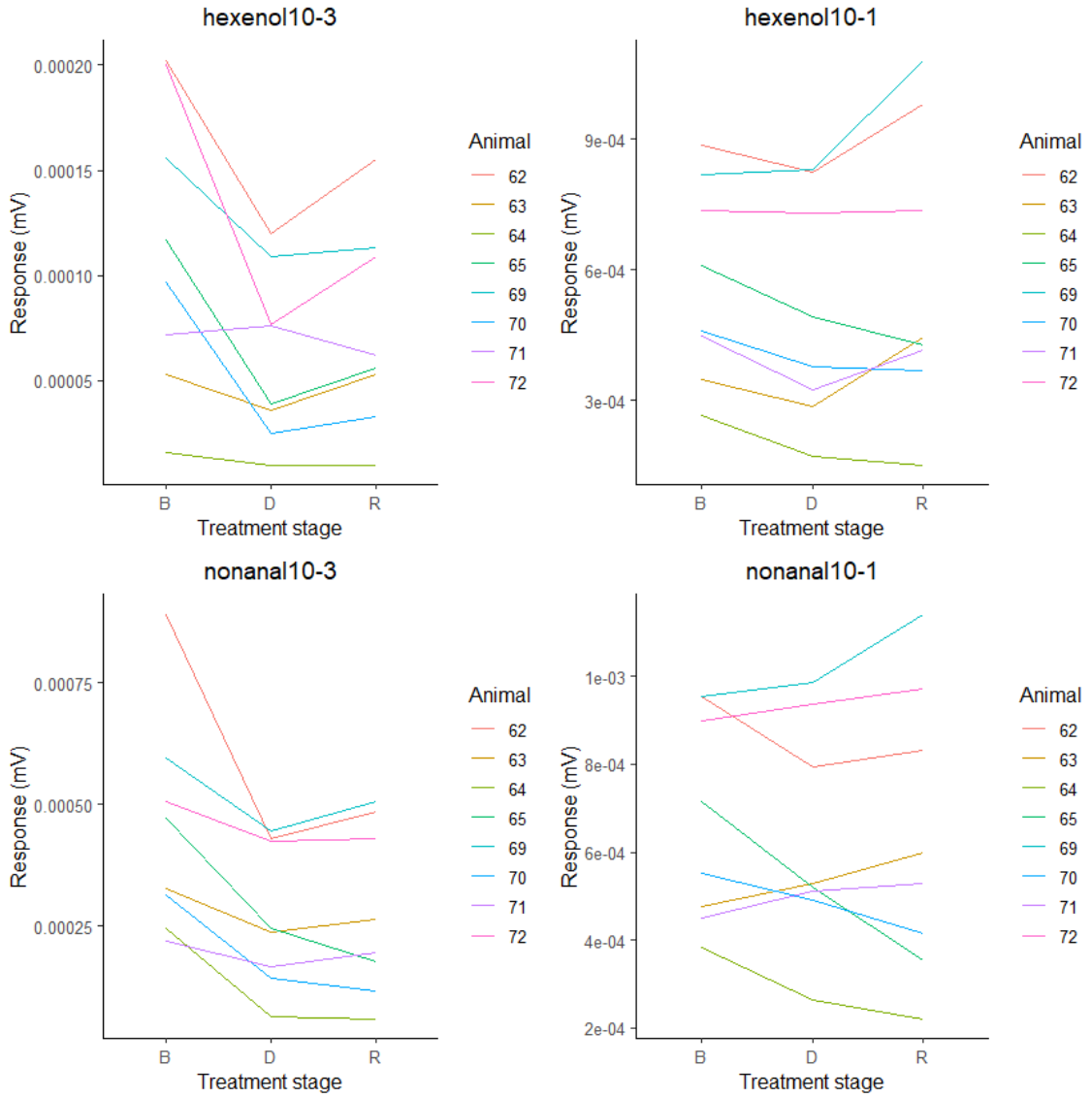

Figure AP51 – Raw EAG responses for each of the four stimuli before (B), during (D) and after recovery (R) from treatment with low concentration SOA ([O_3]=1ppm, [3-carene]= 0.25ppm) and the water bubbler removed during the treatment phase.

SOA high

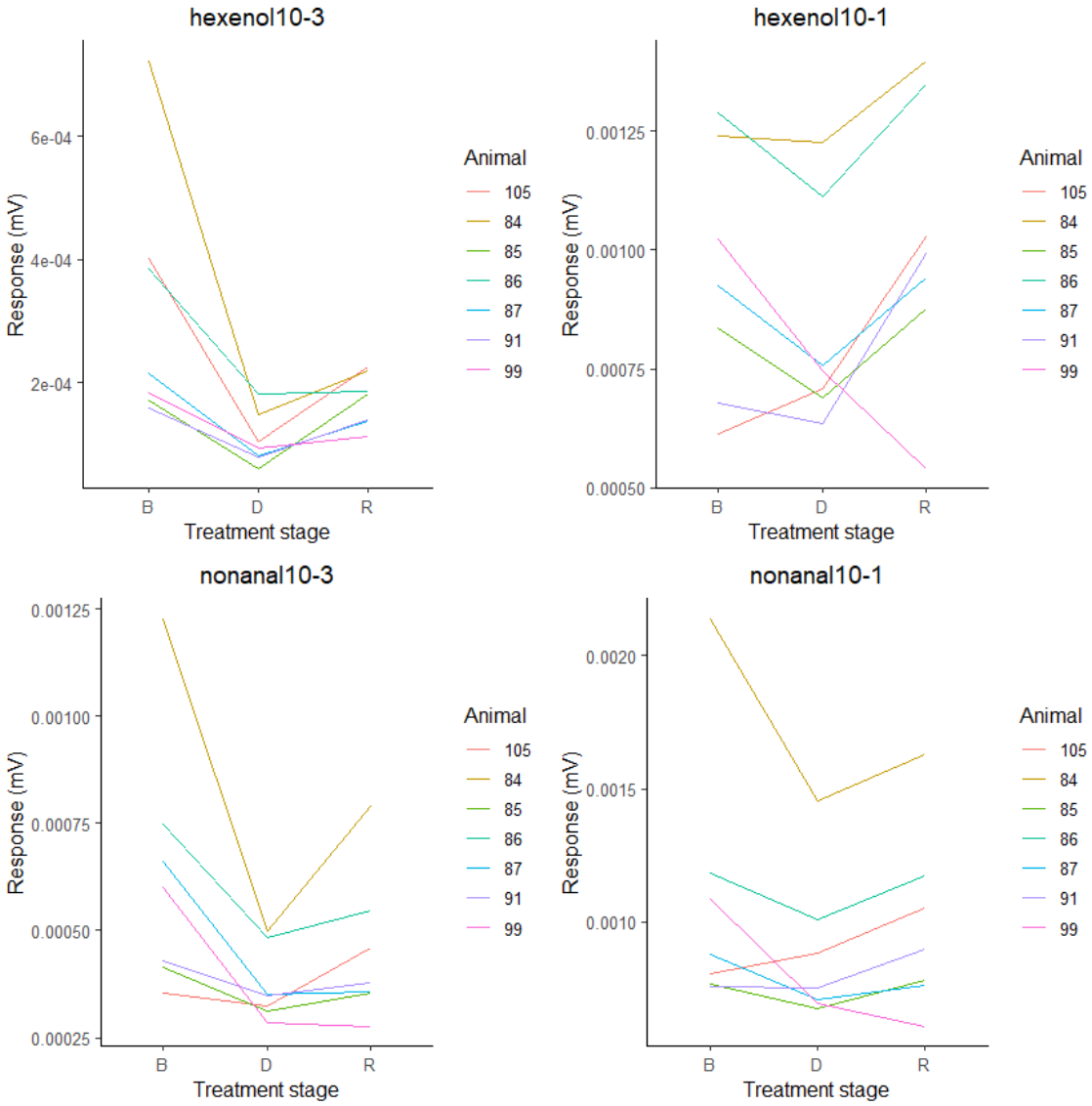

Figure AP52 – Raw EAG responses for each of the four stimuli before (B), during (D) and after recovery (R) from treatment with high concentration SOA ([O_3]=4ppm, [3-carene]= 1ppm) and the water bubbler removed during the treatment phase.

AP17 – Raw data sets (DOI)

Raw data files for all experiments and modelling conducted in the formation of this thesis are openly accessible in compliance with terms set out by the national environmental research council (NERC). Data is hosted by the University of Reading Research Data Archive and may be reached at https://doi.org/10.17864/1947.000337 for further inspection.